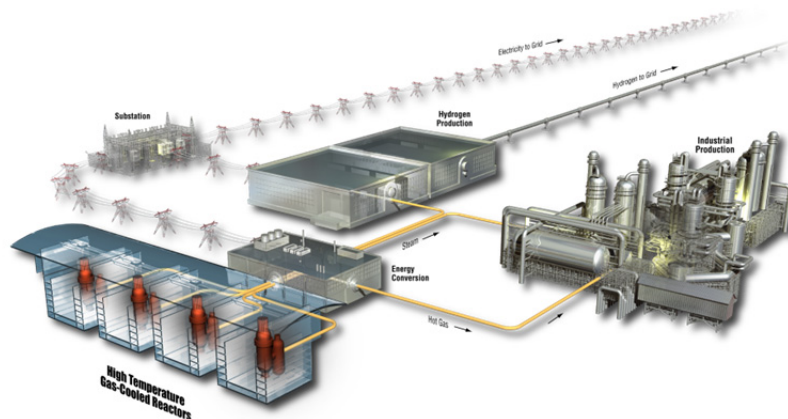


AGC-4 Graphite Preirradiation Data Analysis Report

David Rohrbaugh, William Windes,
W. David Swank

May 2016

The INL is a
U.S. Department of Energy
National Laboratory
operated by
Battelle Energy Alliance



DISCLAIMER

This information was prepared as an account of work sponsored by an agency of the U.S. Government. Neither the U.S. Government nor any agency thereof, nor any of their employees, makes any warranty, expressed or implied, or assumes any legal liability or responsibility for the accuracy, completeness, or usefulness, of any information, apparatus, product, or process disclosed, or represents that its use would not infringe privately owned rights. References herein to any specific commercial product, process, or service by trade name, trade mark, manufacturer, or otherwise, does not necessarily constitute or imply its endorsement, recommendation, or favoring by the U.S. Government or any agency thereof. The views and opinions of authors expressed herein do not necessarily state or reflect those of the U.S. Government or any agency thereof.

AGC-4 Graphite Preirradiation Data Analysis Report

David Rohrbaugh, William Windes, W. David Swank

May 2016

**Idaho National Laboratory
INL ART TDO Program
Idaho Falls, Idaho 83415
<http://www.inl.gov>**

**Prepared for the
U.S. Department of Energy
Office of Nuclear Energy
Under DOE Idaho Operations Office
Contract DE-AC07-05ID14517**

INL ART TDO Program

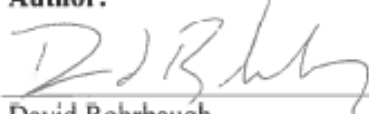
AGC-4 Graphite Preirradiation Data Analysis Report

INL/EXT-16-38044

Revision 0

May 2016

Author:

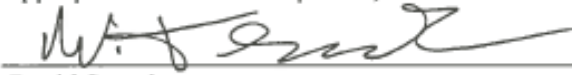


David Rohrbaugh
INL ART Graphite Researcher

5/25/16

Date

Technical Reviewer: (Confirmation of mathematical accuracy, and correctness of data and appropriateness of assumptions.)

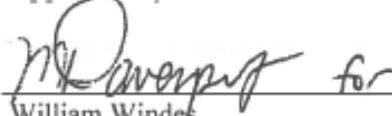


David Swank
INL ART Graphite Researcher

5/25/16

Date

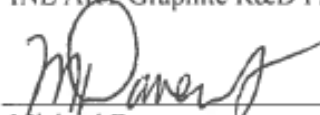
Approved by:



William Windes
INL ART Graphite R&D Program Technical Lead

5/25/16

Date



Michael Davenport
INL ART Program Manager

5/25/16

Date



Michelle T. Sharp
INL ART TDO Quality Assurance

5/25/16

Date

SUMMARY

This report describes the specimen loading order and documents all preirradiation examination material property measurement data for the graphite specimens contained within the fourth Advanced Graphite Capsule (AGC-4) irradiation capsule. The AGC-4 capsule is fourth in six planned irradiation capsules in the AGC test series. The AGC test series is used to irradiate graphite specimens allowing quantitative data necessary for predicting the irradiation behavior and operating performance of new nuclear graphite grades to be generated. This will ascertain the in-service behavior of the graphite for pebble bed and prismatic Very High Temperature Reactor designs. The general design of the AGC-4 test capsule is similar to the AGC-3 test capsule. The major grades of the graphite in AGC-4 remained the same as AGC-3 (IG-110, NBG-17, NBG-18, PCEA and 2114). In addition to the major grades, small specimens of experimental carbonaceous material were also added to AGC-4. These include Highly Oriented Pyrolytic Graphite (HOPG), Silicon-Carbide (SiC) coated graphite specimens, and Carbon-Carbon (C/C) composites. Material property tests were conducted on graphite specimens prior to loading into the AGC-4 irradiation assembly. Specimen testing of three graphite grades (PCEA, 2114, and NBG-17) was conducted at Idaho National Laboratory (INL) and specimen testing for two grades (IG-110 and NBG-18) was conducted at Oak Ridge National Laboratory (ORNL) from April 2012 to May 2014.

This report also details the specimen loading methodology for the graphite specimens inside the AGC-4 irradiation capsule. To determine the creep behavior of the different grades of graphite, it is necessary for all AGC experiments to have “matched pairs” of creep specimens: one specimen that has experienced compressive stress during irradiation and one that has not. The experiment design utilized the neutron flux profile, capsule dimensions, size (length) of the graphite specimens, and graphite grade to create a stacking order that will produce these “matched pairs” of stressed and unstressed specimens with similar neutron dose levels.

CONTENTS

SUMMARY	v
ACRONYMS	xiii
1. INTRODUCTION	1
2. AGC EXPERIMENT DESCRIPTION	2
2.1 Background Information for the AGC Experiment.....	2
2.2 Description of AGC-4 Test	4
2.2.1 Establishing the Capsule Physical Centerline to the Core Neutron Flux Mid-plane	5
2.2.2 Establishing the Dose Levels as a Function of Position within the Capsule	6
2.2.3 Determining the Physical Positions of Irradiation Creep Specimens in the Stacks	7
2.2.4 Determining the Physical Positions of Piggy-Back Specimens in the Central Stack.....	9
3. PREIRRADIATION MATERIAL PROPERTY MEASUREMENTS	9
3.1 General Provisions.....	11
3.2 Specimen Description and Preparation	11
3.3 Personnel and Training	12
3.4 Variations, Exceptions and Discrepancies.....	12
3.5 Calibration and Functional Validation	13
4. TEST METHODS	13
4.1 Mass, Dimensions, and Bulk Density	13
4.2 Electrical Resistivity	14
4.3 Approximation of Elastic Modulus from the Measurement of Sonic Velocity	15
4.4 Modulus of Elasticity by Measurement of Fundamental Frequency	17
4.5 Thermal Expansion	18
4.6 Thermal Diffusivity.....	20
5. DATA ANALYSIS.....	21
5.1 Mass, Dimensions and Density Data Analysis	21
5.2 Electrical Resistivity	22
5.3 Approximation of Elastic Modulus from the Measurement of Sonic Velocity	23
5.4 Modulus of Elasticity by Measurement of Fundamental Frequency	24
5.5 Thermal Expansion	25
5.6 Thermal Diffusivity.....	27
6. REFERENCES	29
Appendix A AGC-4 Post-Irradiation Data.....	31

Appendix B Summary of Statistical Parameters.....	91
Appendix C Final Loading Configuration for AGC-4 Specimens.....	113
Appendix D Analytical Report	129

FIGURES

Figure 1. Design of AGC experiment illustrating planned dose levels and irradiation temperatures for all six test irradiation capsules.....	3
Figure 2. AGC-4 specimen and capsule elevation locations (from DWG 604553, “AGC-4 Specimen Stack-up Arrangements”).....	6
Figure 3. Typical AGC-4 dose profile for creep graphite specimens utilizing similar applied stress in matched stacks.	7
Figure 4. Estimated creep specimen dose profiles for each major graphite type.	8
Figure 5. Electrical resistivity measurement station.	14
Figure 6. Sonic velocity measurement station.	16
Figure 7. Sonic velocity measurement user interface.	17
Figure 8. Fundamental frequency measurement station.	18
Figure 9. Commercial push rod dilatometer for measurement of CTE.....	19
Figure 10. LFA measurement station for determination of thermal diffusivity.	21
Figure 11. Electrical resistivity for the major graphite grades. The anisotropy ratio is above each set of data bars. The error bars represent ± 1 standard deviation.....	23
Figure 12. Young’s modulus using the sonic velocity technique versus density for each major graphite grade. The error bars represent ± 1 standard deviation.....	23
Figure 13. Young’s modulus by sonic velocity for the major graphite grades. The anisotropy ratio is above each set of data bars. The error bars represent ± 1 standard deviation.....	24
Figure 14. Young’s modulus calculated by the fundamental frequency method for the major graphite grades. The anisotropy ratio is above each set of data bars. The error bars represent ± 1 standard deviation.	25
Figure 15. Coefficient of variance for mean CTE at three discrete temperatures for each major graphite grade and grain orientation.	26
Figure 16. Mean CTE for the major grades of graphite as a function of temperature. The error bars represent ± 1 standard deviation.	26
Figure 17. CTE anisotropy ratio for nuclear grade graphite as a function of temperature.	27
Figure 18. Coefficient of variance for diffusivity at three discrete temperatures for each major graphite grade and grain orientation.	28
Figure 19. Thermal diffusivity for various graphite types as a function of temperature. Error bars represent ± 1 standard deviation.	28

Figure 20. Thermal diffusivity anisotropy ratio for several types of nuclear grade graphite as a function of temperature.	29
Figure A-1. 2114 Creep specimen density.	33
Figure A-2. IG-110 Creep specimen density.	33
Figure A-3. NBG-17 creep specimen density.	34
Figure A-4. NBG-18 creep specimen density.	34
Figure A-5. PCEA creep specimen density.	35
Figure A-6. 2114 piggyback specimen density.	35
Figure A-7. IG-110 piggyback specimen density.	36
Figure A-8. NBG-17 piggyback specimen density.	36
Figure A-9. NBG-18 piggyback specimen density.	37
Figure A-10. PCEA piggyback specimen density.	37
Figure A-11. IG-430 piggyback specimen density.	38
Figure A-12. NBG-25 piggyback specimen density.	38
Figure A-13. 2114 creep specimen length.	39
Figure A-14. IG-110 creep specimen length.	39
Figure A-15. NBG-17 creep specimen length.	40
Figure A-16. NBG-18 creep specimen length.	40
Figure A-17. PCEA creep specimen length.	41
Figure A-18. 2114 piggyback specimen length.	41
Figure A-19. IG-110 piggyback specimen length.	42
Figure A-20. NBG-17 piggyback specimen length.	42
Figure A-21. NBG-18 piggyback specimen length.	43
Figure A-22. PCEA piggyback specimen length.	43
Figure A-23. IG-430 piggyback specimen length.	44
Figure A-24. NBG-25 piggyback specimen length.	44
Figure A-25. 2114 creep specimen diameter.	45
Figure A-26. IG-110 creep specimen diameter.	45
Figure A-27. NBG-17 creep specimen diameter.	46
Figure A-28. NBG-18 creep specimen diameter.	46
Figure A-29. PCEA creep specimen diameter.	47
Figure A-30. 2114 piggyback specimen diameter.	47
Figure A-31. IG-110 piggyback specimen diameter.	48
Figure A-32. NBG-17 piggyback specimen diameter.	48
Figure A-33. NBG-18 piggyback specimen diameter.	49

Figure A-34. PCEA piggyback specimen diameter.....	49
Figure A-35. IG-430 piggyback specimen diameter.....	50
Figure A-36. NBG-25 piggyback specimen diameter.....	50
Figure A-37. 2114 creep specimen mass.	51
Figure A-38. IG-110 creep specimen mass.....	51
Figure A-39. NBG-17 creep specimen mass.	52
Figure A-40. NBG-18 creep specimen mass.	52
Figure A-41. PCEA creep specimen mass.	53
Figure A-42. 2114 piggyback specimen mass.	53
Figure A-43. IG-110 piggyback specimen mass.....	54
Figure A-44. NBG-17 piggyback specimen mass.....	54
Figure A-45. NBG-18 piggyback specimen mass.....	55
Figure A-46. PCEA piggyback specimen mass.	55
Figure A-47. IG-430 piggyback specimen mass.....	56
Figure A-48. NBG-25 piggyback specimen mass.....	56
Figure A-49. 2114 Creep Specimen Coefficient of Thermal Expansion.	57
Figure A-50. 2114 creep specimen coefficient of thermal expansion @ 100°C.....	57
Figure A-51. 2114 creep specimen coefficient of thermal expansion @ 500°C.....	58
Figure A-52. 2114 creep specimen coefficient of thermal expansion @ 900°C.....	58
Figure A-53. IG-110 creep specimen coefficient of thermal expansion.	59
Figure A-54. IG-110 creep specimen coefficient of thermal expansion @ 100°C.	59
Figure A-55. IG-110 creep specimen coefficient of thermal expansion @ 500°C.	60
Figure A-56. IG-110 creep specimen coefficient of thermal expansion @ 900°C.	60
Figure A-57. NBG-17 creep specimen coefficient of thermal expansion.....	61
Figure A-58. NBG-17 creep specimen coefficient of thermal expansion @ 100°C.	61
Figure A-59. NBG-17 creep specimen coefficient of thermal expansion @ 500°C.....	62
Figure A-60. NBG-17 creep specimen coefficient of thermal expansion @ 900°C.....	62
Figure A-61. NBG-18 creep specimen coefficient of thermal expansion.....	63
Figure A-62. NBG-18 creep specimen coefficient of thermal expansion @ 100°C.....	63
Figure A-63. NBG-18 creep specimen coefficient of thermal expansion @ 500°C.....	64
Figure A-64. NBG-18 creep specimen coefficient of thermal expansion @ 900°C.....	64
Figure A-65. PCEA creep specimen coefficient of thermal expansion.	65
Figure A-66. PCEA creep specimen coefficient of thermal expansion @ 100°C.	65
Figure A-67. PCEA creep specimen coefficient of thermal expansion @ 500°C.	66
Figure A-68. PCEA creep specimen coefficient of thermal expansion @ 900°C.	66

Figure A-69. 2114 creep specimen modulus by sonic resonance.	67
Figure A-70. IG-110 creep specimen modulus by sonic resonance.....	67
Figure A-71. NBG-17 creep specimen modulus by sonic resonance.	68
Figure A-72. NBG-18 creep specimen modulus by sonic resonance.	68
Figure A-73. PCEA creep specimen modulus by sonic resonance.	69
Figure A-74. 2114 creep specimen resistivity.	69
Figure A-75. IG-110 creep specimen resistivity.....	70
Figure A-76. NBG-17 creep specimen resistivity.....	70
Figure A-77. NBG-18 creep specimen resistivity.....	71
Figure A-78. PCEA creep specimen resistivity.	71
Figure A-79. 2114 creep specimen Young’s Modulus by sonic velocity.	72
Figure A-80. IG-110 creep specimen Young’s Modulus by sonic velocity.....	72
Figure A-81. NBG-17 creep specimen Young’s Modulus by sonic velocity.	73
Figure A-82. NBG-18 creep specimen Young’s Modulus by sonic velocity.	73
Figure A-83. PCEA creep specimen Young’s Modulus by sonic velocity.....	74
Figure A-84. 2114 creep specimen shear modulus by sonic velocity.....	74
Figure A-85. IG-110 creep specimen shear modulus by sonic velocity.	75
Figure A-86. NBG-17 creep specimen shear modulus by sonic velocity.	75
Figure A-87. NBG-18 creep specimen shear modulus by sonic velocity.	76
Figure A-88. PCEA creep specimen shear modulus by sonic velocity.....	76
Figure A-89. 2114 piggyback specimen diffusivity.....	77
Figure A-90. 2114 piggyback specimen diffusivity @ 100°C.....	77
Figure A-91. 2114 piggyback specimen diffusivity @ 500°C.....	78
Figure A-92. 2114 piggyback specimen diffusivity @ 900°C.....	78
Figure A-93. IG-110 piggyback specimen diffusivity.	79
Figure A-94. IG-110 piggyback specimen diffusivity @ 100°C.	79
Figure A-95. IG-110 piggyback specimen diffusivity @ 500°C.	80
Figure A-96. IG-110 piggyback specimen diffusivity @ 900°C.	80
Figure A-97. NBG-17 piggyback specimen diffusivity.....	81
Figure A-98. NBG-17 piggyback specimen diffusivity @ 100°C.....	81
Figure A-99. NBG-17 piggyback specimen diffusivity @ 500°C.....	82
Figure A-100. NBG-17 piggyback specimen diffusivity @ 900°C.....	82
Figure A-101. NBG-18 piggyback specimen diffusivity.....	83
Figure A-102. NBG-18 piggyback specimen diffusivity @ 100°C.....	83
Figure A-103. NBG-18 piggyback specimen diffusivity @ 500°C.....	84

Figure A-104. NBG-18 piggyback specimen diffusivity @ 900°C.....	84
Figure A-105. PCEA piggyback specimen diffusivity.	85
Figure A-106. PCEA piggyback specimen diffusivity @ 100°C.....	85
Figure A-107. PCEA piggyback specimen diffusivity @ 500°C.....	86
Figure A-108. PCEA piggyback specimen diffusivity @ 900°C.....	86
Figure A-109. IG-430 piggyback specimen diffusivity.	87
Figure A-110. IG-430 piggyback specimen diffusivity @ 100°C.	87
Figure A-111. IG-430 piggyback diffusivity @ 500°C.	88
Figure A-112. IG-430 piggyback specimen diffusivity @ 900°C.	88
Figure A-113. NBG-25 piggyback specimen diffusivity.....	89
Figure A-114. NBG-25 piggyback specimen diffusivity @ 100°C.....	89
Figure A-115. NBG-25 piggyback specimen diffusivity @ 500°C.....	90
Figure A-116. NBG-25 piggyback specimen diffusivity @ 900°C.....	90

TABLES

Table 1. Graphite grades and grain orientations within AGC-4 capsule.	5
Table 2. Total number of irradiated creep and piggyback specimens for the major grades in AGC-4 capsule.	7
Table 3. Graphite measurement and test equipment.....	9
Table 4. Creep specimen length outliers.	22

ACRONYMS

AGC	Advanced Graphite Creep
AGC-1	First Advanced Graphite Capsule
AGC-3	Third Advanced Graphite Capsule
ART	Advanced Reactor Technology
ASTM	American Society for Testing and Materials
ATR	Advanced Test Reactor
C/C	carbon-carbon
COV	coefficient of variation
CTE	coefficient of thermal expansion
HOPG	Highly Oriented Pyrolytic Graphite
HTGR	high temperature gas-cooled reactor
HTR	high-temperature reactor
INL	Idaho National Laboratory
IQR	interquartile range
LFA	laser flash apparatus
LWP	Laboratory-wide Procedure
MCP	Management Control Procedure
NDMAS	Data Management and Analysis
NGNP	Next Generation Nuclear Plant
ORNL	Oak Ridge National Laboratory
PB	piggy-back specimen
PI	principal investigator
PIE	post-irradiation examination
PLN	plan
Pre-IE	preirradiation examination
R&D	research and development

AGC-4 Graphite Preirradiation Data Analysis Report

1. INTRODUCTION

The Advanced Reactor Technology (ART) Graphite research and development (R&D) program is conducting an extensive graphite irradiation program to provide data for licensing of a high-temperature reactor (HTR) design. In past applications, graphite has been used effectively as a structural and moderator material in both research and commercial high temperature gas-cooled reactor (HTGR) designs.¹ Nuclear graphite H-451, used previously in the United States for nuclear reactor graphite components, is no longer available. New nuclear graphite grades have been developed and are considered suitable candidates for new HTR reactor designs. To support the design and licensing of new HTR core components within a commercial reactor, a complete properties database must be developed for these current grades of graphite. Quantitative data on in-service material performance is required for the physical, mechanical, and thermal properties of each major graphite grade with a specific emphasis on data accounting for the life-limiting effects of irradiation creep on key physical properties of the HTR candidate graphite grades. Further details on the R&D activities and associated rationale required to qualify nuclear-grade graphite for use within the HTR are documented in the *Graphite Technology Development Plan*.^{2,3}

Based on experience with previous graphite-core components, the phenomenon of irradiation-induced creep within the graphite has been shown to be critical to the total useful lifetime of graphite components. Irradiation-induced creep occurs under the simultaneous application of high temperatures, neutron irradiation, *and* applied stresses within the graphite components. Significant internal stresses within the graphite components can result from a second phenomenon—irradiation-induced dimensional change—where the graphite physically changes (i.e., first shrinking and then expanding with increasing neutron dose). This disparity in material volume change can produce significant internal stresses within graphite components. Irradiation-induced creep relaxes these large internal stresses, thus reducing the risk of crack formation and component failure. Obviously, higher irradiation-creep levels tend to relieve more internal stress, thus allowing the components longer useful lifetimes within the core. Determining the irradiation-creep rates of nuclear-grade graphite is critical for determining the useful lifetime of graphite components and is a major component of the Advanced Graphite Creep (AGC) experiment.

The AGC experiment is currently underway to determine the in-service behavior of these new graphite grades for HTR and molten salt reactor designs. This experiment will examine properties and behavior of nuclear grade graphite over a large spectrum of temperatures, irradiation fluencies, and applied stress levels that are expected to cause irradiation creep strains within a HTR graphite component. Irradiation data are provided through the AGC test series, which is comprised of six planned capsules irradiated in the Advanced Test Reactor (ATR) in a large flux trap located at Idaho National Laboratory (INL). Each irradiation capsule consists of over 400 graphite specimens that are characterized before and after irradiation to determine the irradiation induced material properties changes and life-limiting irradiation creep rate for each graphite grade.

To achieve the proper irradiation conditions and applied loads to the creep specimens, an exact specimen loading order is critical. Since irradiation creep is usually determined by the difference in dimensional change occurring within specimens that have an applied load and those that do not, it is assumed that the specimens must have the same irradiation dose and irradiation temperature values. To achieve these similar irradiation conditions for “matched pairs,” a careful map of where each specimen resides within the irradiation capsule is required. A detailed analysis of the reactor flux profile to ascertain

the dose levels for each specimen, as well as the designed loading configurations within the capsule, are all required to guarantee that the matched pairs have the same temperature and dose levels. Details of the specimen loading order, the capsule loading design, the flux profile within the ATR, and the resulting estimated dose profiles for each graphite specimen are discussed within this preirradiation data analysis report.

2. AGC EXPERIMENT DESCRIPTION

The AGC experiment is designed to establish the data necessary to determine the safe operating envelope of graphite core components for a HTR by measuring the irradiated material property changes and behavior of several new nuclear graphite grades over a large range of temperatures, neutron fluence levels, and mechanical compressive loads. The experiment consists of three interrelated stages: preirradiation characterization of the graphite specimens, the irradiation test series (designated as six separate irradiation test train capsules), and post-irradiation examination (PIE) and analysis of the graphite specimens after irradiation. Separate reports for each distinct stage are prepared after each individual activity is completed.

The preirradiation examination (pre-IE) reports detail the total number of graphite types and specimens, the specimen loading configuration to expose all specimens to the entire range of irradiation conditions and the pre-irradiation material property testing results. The test series as-run irradiation reports detail the irradiation history of each capsule while in the reactor, noting any changes from the technical and function specifications for each specific test series capsule and identifying the possible improvements to the next test series capsule design. The PIE reports detail the changes in the specimen material property measurements, compare the results to the pre-IE material property measurements, and analyze the data to assist in determining credible safe operating limits for graphite core components in a HTR design and licensing application.

2.1 Background Information for the AGC Experiment

The AGC experiment will provide irradiated material property data for current graphite types available for use within a HTR design. Due to volume limitations within typical material test reactors (i.e., ATR), only a limited number of specimens can be irradiated—far fewer than can be used in an accurate statistical specimen population analysis. Therefore, the AGC only measures the irradiated material property changes and behavior of relatively few specimens of new nuclear graphite grades over the anticipated operating temperature range, neutron fluencies, and mechanical loads. The experiment does generate quantitative material property change data (and limited irradiation creep data), which will be used in conjunction with the as-fabricated material property measurement program (Baseline program) to predict the in-service behavior and operating performance of these new nuclear graphite grades for pebble bed and prismatic reactor designs. Changes to key thermal, physical, and mechanical material properties are determined by comparing the material properties of each specimen before irradiation and after irradiation. Differences measured from the irradiation conditions will provide irradiation behavior data in graphite with a specific emphasis on data accounting for the life-limiting effects of irradiation creep on key physical properties of several candidate graphite grades for HTR.

The critical component of the AGC experiment is the irradiation test series, which irradiates the graphite specimens after pre-IE characterization has been completed. The AGC test series is comprised of six planned irradiation capsules that are irradiated in the ATR in a large flux trap as described in the *Graphite Technology Development Plan*.² The test series exposes test specimens of the selected nuclear grade graphite types to temperatures and a range of doses that are expected within a HTR design. Specifically, graphite specimens will be exposed to a fast neutron dose ($E > 0.1$ MeV) ranging from 1 to 7 dpa and temperatures of 600°C, 800°C, and 1100°C (Figure 1). AGC-4 was designed to be irradiated within the ATR's East Flux Trap rather than the South Flux Trap as previously used with AGC-1 and

AGC-2.⁴ AGC-4 was irradiated 12,255 MWd or about 1.7 times longer than the AGC-3 irradiation period (7418 MWd).⁵

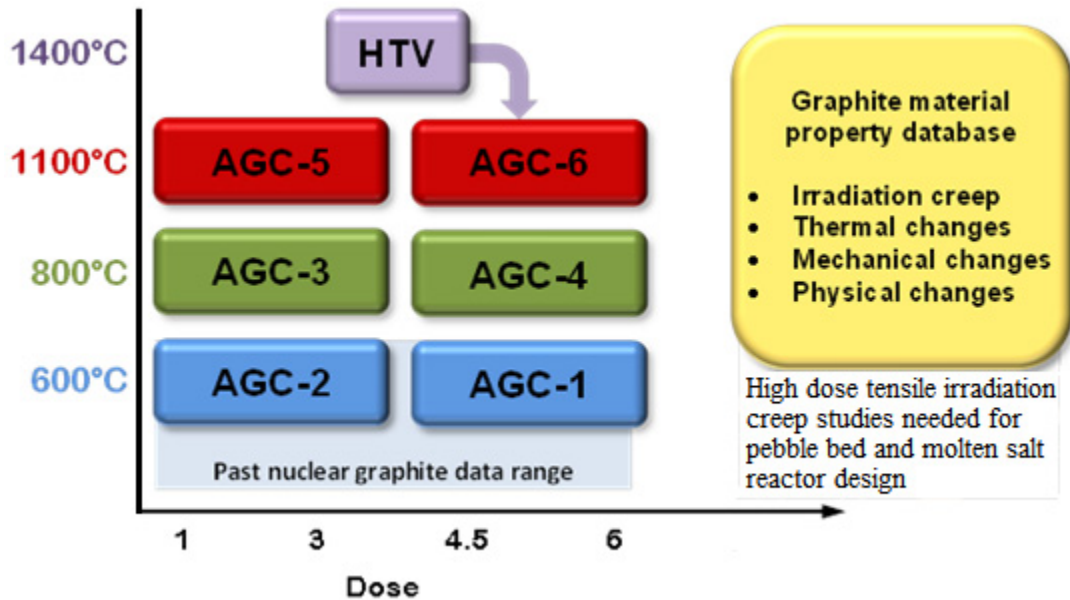


Figure 1. Design of AGC experiment illustrating planned dose levels and irradiation temperatures for all six test irradiation capsules.

Significant scope is dedicated to determining the irradiation-induced creep rates of the different types of nuclear graphite within the AGC experiment. The traditional method for measuring irradiation-induced creep is to apply a significant load to half the specimens during irradiation while leaving the remaining half of the specimens unloaded. The resulting difference in dimensional change between the loaded and unloaded specimens (assuming the temperature and dose levels are the same) provides the amount of irradiation-induced strain for each “matched pair” of graphite specimens at a specified dose level. From this strain level, a creep rate for each graphite type can be calculated as a function of dose if both specimens were irradiated at the same temperature. Thus, each capsule is designed to be irradiated at a constant temperature allowing only the dose and applied mechanical load to vary inside each test series capsule. The creep rate of graphite types is therefore measured as only a function of load and dose within each capsule. To ascertain the temperature dependency of irradiation induced material property changes, the property changes for similar graphite types, at similar dose and load levels, must be compared between capsules. This implies that similar graphite types must be in the same locations in every capsule to receive similar dose and load levels at different temperatures.

Each test series capsule contains two primary specimen types: creep specimens providing irradiation creep rate values as well as mechanical properties and “piggyback” specimens providing thermal material property changes to the graphite. The creep specimens are 25.4 mm tall by 12.5 mm in diameter and are irradiated in the mechanically loaded outer stack positions of the capsule body where an applied load can be imposed upon half of the specimens. Piggyback specimens are short (6.3 mm tall by 12.5 mm in diameter) button specimens that reside in the axial spine of the capsule receiving no applied load and are subjected only to neutron irradiation to assess the effects of a reactor environment on the specific graphite grade. Together, both types of specimens provide the material property changes for stressed and unstressed graphite types. The physical dimensions for both creep and piggyback specimens are shown in INL Drawing 778033.⁶

The creep specimens are best suited for physical and mechanical testing techniques, such as dimensional change, irradiation creep, elastic modulus, density, and thermal expansion. The piggyback specimens are best suited for thermal and physical testing, such as thermal diffusivity, mass measurements, and density. Because piggyback specimens are not stressed during irradiation, new “experimental” types of graphite and carbon-based material were allowed to be tested for irradiation stability only. These experimental graphite grades are sufficiently stable to be machined into piggyback specimen dimensions, but the carbon-based materials are located in small, hollow graphite cans with dimensions similar to the piggyback specimens (either 6.3 mm tall or 12 mm tall by 12.5 mm in diameter). These cans are designed to hold specimens of Highly Oriented Pyrolytic Graphite (HOPG) and other experimental carbon-based materials of interest to HTR designs. These newer experimental types of carbon-based materials may provide superior irradiation performance and could be used in future reactor designs.

2.2 Description of AGC-4 Test

The Advanced Graphite Creep experiment consists of six irradiation capsules irradiating approximately 500 graphite specimens in each capsule. The first two capsules are intended to be irradiated at 600°C, the next two capsules at 800°C, and the final two at 1100°C. The design of these capsules makes use of the symmetric neutron flux profile of the ATR to irradiate “matched pairs” of graphite specimens. Graphite specimens above the reactor mid-point elevation that are mechanically loaded match graphite specimens below the reactor mid-point line that are not mechanically loaded during irradiation. The design of the capsule ensures a constant temperature for all specimens throughout the capsule; however, to ensure that specimen “matched pairs” are similar in dose, the specimen stacking order must be matched to the ATR flux profile so that similar specimens on the top portion of the capsule match the dose received in the bottom of the capsule.

To achieve this similar dose level in the AGC-4 test capsule, the ATR flux profile is compared to the specimen capsule elevation specifications. By taking into account the flux profile, the AGC-4 specimens can be stacked so that matched pairs will receive similar dose levels on the bottom and top sections of the capsule. This is not so straight forward since the axial ATR neutron flux profile is not completely symmetric due to core components altering the profile. This requires a small offset in the specimen stacking order in the bottom half of the capsule to line up specimens to the correct dose level. This is usually achieved by the addition of spare piggyback specimens until the correct dose level is achieved for the first creep specimen.

In addition, due to the limited volume in the capsules and the large number of graphite grades being investigated, the stacking order must ensure an equal distribution of specimens over the entire dose range in the irradiation capsule. With five graphite grades, three different mechanical load levels, and specimens 25.4 mm long being investigated, this requires a careful plan to evenly distribute as many specimens as possible over the entire dose range. For this study, some graphite grades were allowed more specimens than other types. This skewed the number of specimens slightly from grade to grade. To further complicate the stacking order, the microstructural orientation of the graphite specimens to the applied load during irradiation must also be considered since it is anticipated that “with-grain” creep rates will differ from “against-grain” creep rates.

AGC-4 was designed to be irradiated for a longer time than AGC-3 to obtain the 3.5 to 7.0 dpa irradiation levels and nominal temperature of 800°C (Figure 1). This allows for a direct comparison between AGC-1 and AGC-4 since the stress and dose levels will be constant but the temperatures differ (AGC-1 at a nominal 600°C and AGC-4 at a nominal 800°C).

The five major grades of graphite that were used in AGC-3 are also used in AGC-4. These major grades are PCEA, NBG-17, NBG-18, IG-110, and 2114. These are the grades that will be used for all of the remaining AGC capsules (AGC-5 and AGC-6).

The piggyback specimens in the AGC-4 capsule are smaller button-sized specimens that are approximately 6.3 mm (1/4 inch) tall \times 12.5 mm (1/2 inch) diameter. They are made with all of the major grades of graphite. There are also two graphite container-type specimens: One is 12.5 mm tall and the other is 6.3 mm tall. The 6.3-mm-tall containers each held one HOPG specimen. The 12.5-mm (1/2 inch) tall containers contained two types of experimental carbon-based materials. One set of 12.5-mm-tall containers each held a silicon carbide-coated graphite specimen fabricated at the Korean Atomic Energy Research Institution to test for irradiation performance of oxidation-resistant SiC-coated graphite. A second set of 12.5-mm-tall graphite containers each held a chopped fiber carbon-carbon (C/C) composite specimen fabricated at Carlisle Composites, Inc. Similar to the previous AGC experimental designs (AGC-1, AGC-2, and AGC-3); most of the piggyback graphite specimens were irradiated in the unloaded center stack of AGC-4. A list of all major graphite grades, piggyback grades, and experimental graphite grades is in Table 1.

Table 1. Graphite grades and grain orientations within AGC-4 capsule.

Grade	Specimen Type	Dimension	With-Grain (WG)/ Against-Grain (AG)
2114	Creep	$\text{Ø}12.5 \times 25.4 \text{ mm}$	48 WG/0 AG
NBG-17	Creep	$\text{Ø}12.5 \times 25.4 \text{ mm}$	18 WG/18 AG
NBG-18	Creep	$\text{Ø}12.5 \times 25.4 \text{ mm}$	24 WG/24 AG
IG-110	Creep	$\text{Ø}12.5 \times 25.4 \text{ mm}$	30 WG/12 AG
PCEA	Creep	$\text{Ø}12.5 \times 25.4 \text{ mm}$	36 WG/12 AG
2114	Piggyback	$\text{Ø}12.5 \times 6.3 \text{ mm}$	26 WG/0 AG
NBG-17	Piggyback	$\text{Ø}12.5 \times 6.3 \text{ mm}$	20 WG/6 AG
NBG-18	Piggyback	$\text{Ø}12.5 \times 6.3 \text{ mm}$	15 WG/11 AG
IG-110	Piggyback	$\text{Ø}12.5 \times 6.3 \text{ mm}$	16 WG/10 AG
PCEA	Piggyback	$\text{Ø}12.5 \times 6.3 \text{ mm}$	13 WG/10 AG
IG-430	Piggyback	$\text{Ø}12.5 \times 6.3 \text{ mm}$	9 WG/0 AG
NBG-25	Piggyback	$\text{Ø}12.5 \times 6.3 \text{ mm}$	22
A3-27	Piggyback	$\text{Ø}12.5 \times 6.3 \text{ mm}$	18
HOPG	Experimental	$\text{Ø}12.5 \times 6.3 \text{ mm}$	20
SiC coated	Experimental	$\text{Ø}12.5 \times 12 \text{ mm}$	10
C/C comp.	Experimental	$\text{Ø}12.5 \times 12 \text{ mm}$	12

2.2.1 Establishing the Capsule Physical Centerline to the Core Neutron Flux Mid-plane

The core flux mid-plane in relation to the capsule arrangement was established so that the reactor neutron flux field could be correlated to the physical elevations/positions in the capsule. The dose levels through all elevations in the ATR are calculated based upon the core mid-plane flux levels. Capsule arrangement drawings were used to determine the position of each specimen in the capsule as a function of height above and below the mid-plane of the core neutron flux profile (Figure 2).^{7,8,9} By establishing the specimen locations to the core mid-plane elevation, each specimen dose below and above the core mid-plane can be estimated.

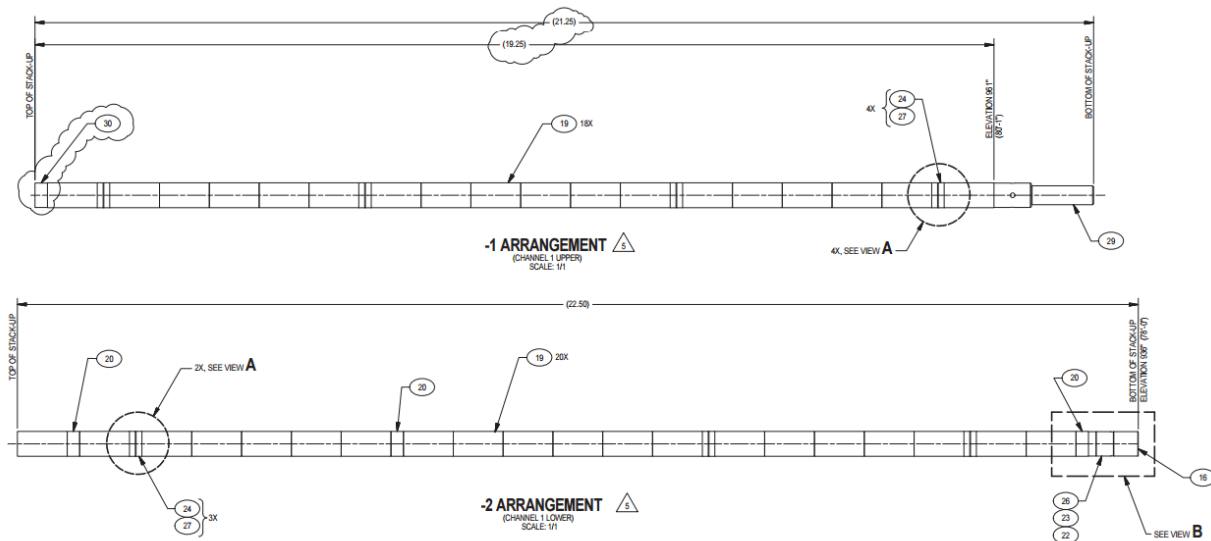


Figure 2. AGC-4 specimen and capsule elevation locations (from DWG 604553, “AGC-4 Specimen Stack-up Arrangements”).

Two important points were learned from AGC-1 irradiations: (1) the lower half of the capsule crept under irradiation and produced a slightly smaller gap between the lower stack and the shuttle piston at the end of irradiations, and (2) the loaded specimens in the upper stacks shrink under irradiation substantially more than expected requiring longer push rods for the expected higher levels of shrinkage for this higher temperature capsule. The shuttle piston is used to upset the upper specimens in each of the loaded upper stacks to make sure they do not become bound within the stack during loading. The gap between the shuttle piston and the top of the lower stack is needed to allow free movement of the shuttle piston when it is not engaged. If this gap had been reduced completely, AGC-1 might have transferred the load in the upper stacks to the specimens in the lower stacks. This did not occur, but design changes to the specimen loading to increase the gap were made in the subsequent experiments, including AGC-4. Because the AGC-1 specimens in the upper stacks did not volumetrically shrink the same amount as the specimens in the lower stacks, the received dose levels did not match the expected values established at the start of the irradiation. The changes are slight but this was considered when the final specimen offset distance was established at the beginning of the AGC-4 experiment.

These irradiation lessons learned have a bearing on the final positions of both the upper specimen position and the lower specimen position since the centerlines for all specimens will change over time and irradiation. The centerline movement of the specimens cannot be adjusted during irradiations. Any final differences between the matched pairs will be accounted for in the post-irradiation analysis of this test series.

2.2.2 Establishing the Dose Levels as a Function of Position within the Capsule

Once the physical elevation dimensions were established and correlated to the reactor core centerline, the estimated dose as a function of distance from the core centerline was calculated for each specimen in the AGC-4 capsule. AGC-4 is essentially a duplicate of AGC-3 (the same reactor position, operating temperatures, and power levels), the only difference being that AGC-4 will have an increased irradiation time. Therefore, it was determined that AGC-4 fluence profiles could be estimated by simply multiplying the AGC-3 profiles by a factor of 1.7.⁵ As with AGC-3, offsets were needed in AGC-4 to allow matched pair specimens to have similar dose profiles both above and below the core mid-plane. More details about the AGC-3 dose profiles and specimen offsets used can be found in the *AGC-3 Graphite Preirradiation Data Analysis Report*.¹⁰

2.2.3 Determining the Physical Positions of Irradiation Creep Specimens in the Stacks

After establishing the specimen position offsets for the bottom half of the specimens, the number of matched creep specimens for each type of graphite was determined. To provide consistency, the same number of matched pair creep specimens that were used in AGC-3 were used in AGC-4. There were six additional unstressed creep 2114 specimens that were used for spacing in the bottom half of each stack. The total number of creep and piggyback specimens irradiated per major graphite grade is shown in Table 2.

Table 2. Total number of irradiated creep and piggyback specimens for the major grades in AGC-4 capsule.

Graphite Grade	Stressed Creep	Unstressed Creep	Piggyback
2114	21	27	26
IG-110	21	21	26
NBG-17	18	18	26
NBG-18	24	24	26
PCEA	24	24	23

A number of other factors were considered before the stacking order for each stack could be finalized. First, there are three load levels applied to the specimens in the loaded upper parts of the stacks (loads of 13.8, 17, and 21 MPa). There are six outer stacks in the capsule allowing the specimens in two of the stacks to be loaded at 13.8 MPa, with specimens loaded at 17 and 21 MPa, respectively, in the other two pairs of stacks. Since there are two stacks at similar applied stress levels, the specimen loading order can be shifted between the two stacks allowing the same type of graphite loaded at the specimen stress levels to be exposed over a broader neutron dose range (Figure 3). It is assumed that both stacks are at a constant temperature and will be exposed to the same applied stress. Since the radial flux profile is constant through the capsule diameter, the specimens will receive similar dose levels per position, which account for the shifting of the specimens and more uniform, smoother dose profile for each graphite type.

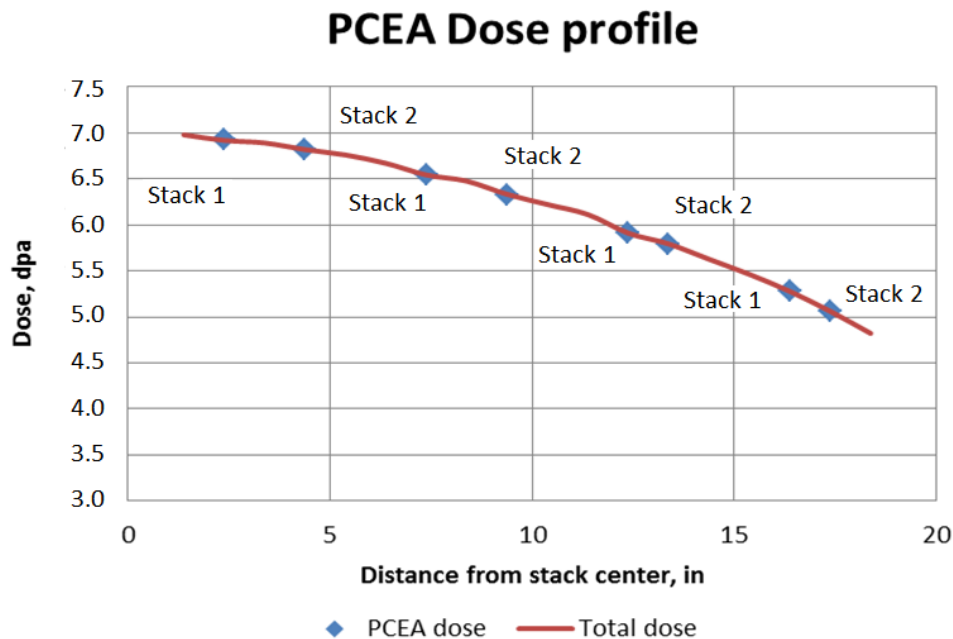


Figure 3. Typical AGC-4 dose profile for creep graphite specimens utilizing similar applied stress in matched stacks.

The second consideration is the grain orientation of the specimens. A decision was made to have approximately 70% of the specimens be orientated in the “with-grain” direction and 30% of the specimens be “against-grain.” However, in the case of the vibration-molded graphite types (NBG-17 and NBG-18), there are actually two with-grain directions and one against-grain direction because of the fabrication process.⁶ As such, it was logical to split the with-grain and against-grain specimens evenly rather than the 70/30 ratio established for the other specimens.

Once these considerations were accounted for, the dose level profiles were determined for each graphite type and within each stack. The estimated creep specimen dose profiles for each graphite type at each stress level are illustrated in the charts for Figure 4.

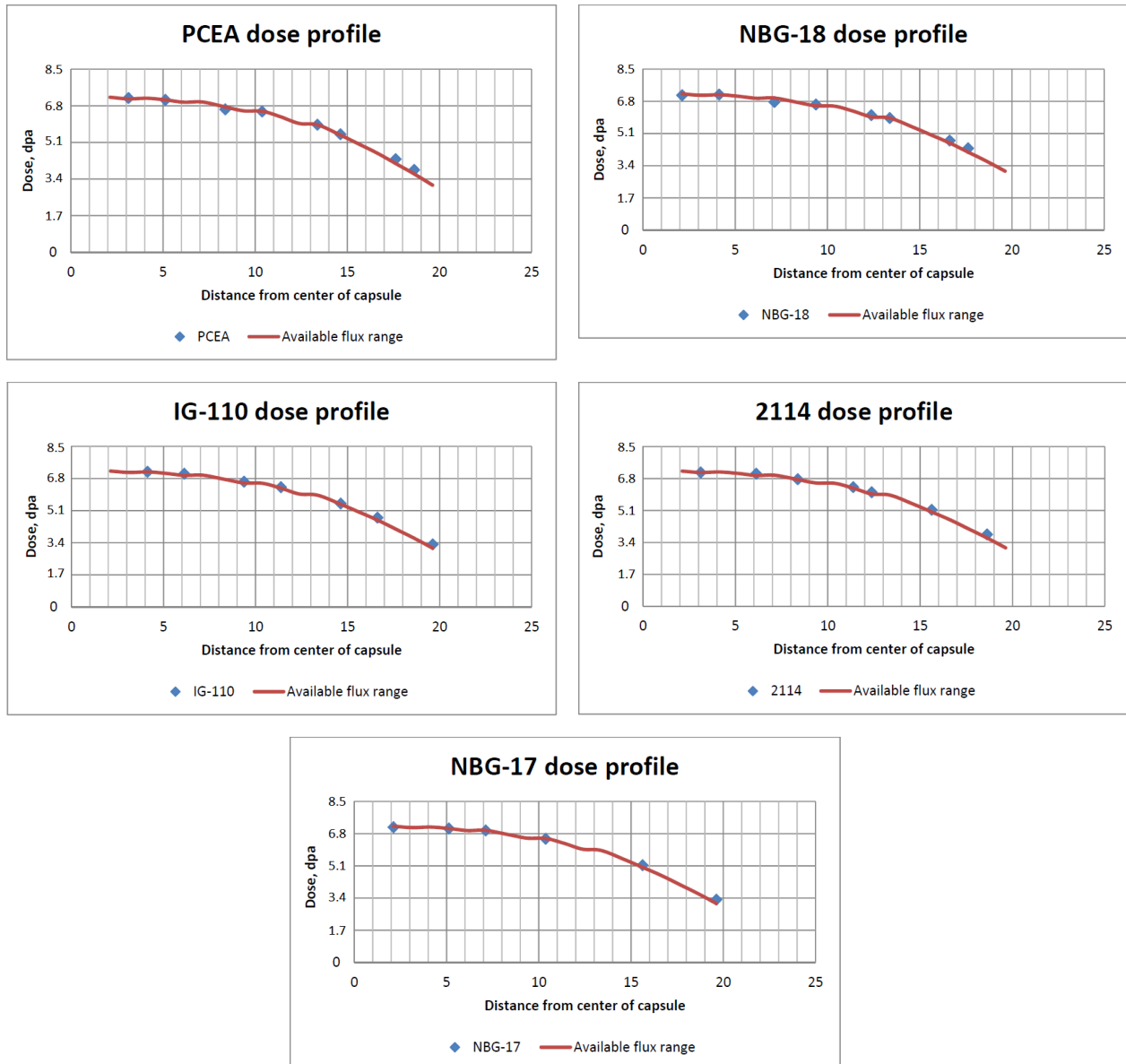


Figure 4. Estimated creep specimen dose profiles for each major graphite type.

The final loading configuration for the outer stacks was established once a smooth dose profile was achieved for each graphite type (Appendix C Table C-1). The lower stack offset, the flux wire spacers, creep specimens, and specimen symmetry above and below the capsule mid-plane were mapped for each graphite specimen.

2.2.4 Determining the Physical Positions of Piggy-Back Specimens in the Central Stack

Similar to the AGC-1, AGC-2, and AGC-3 designs, most of the AGC-4 piggyback specimens are contained within the central stack and did not have a designed applied stress imposed. Like the AGC-2 and AGC-3 design, AGC-4 piggyback specimens did not have a central hole machined in the center of the specimens. This allowed them to be tested for high-temperature thermal diffusivity.

3. PREIRRADIATION MATERIAL PROPERTY MEASUREMENTS

The objective of the AGC-4 experiment is to determine the material property changes induced in nuclear grade graphite during exposure to a high-temperature neutron environment. The approach is to perform extensive preirradiation characterization testing on each specimen before exposing the graphite specimens to various neutron doses. After irradiation, the same characterization tests will be performed on each irradiated specimen to quantify changes to the material properties of the graphite.

A brief summary of the material testing is in Table 3. These measurements include dimensional and non-destructive characterization of the physical properties. The properties measured were bulk density, electrical resistivity, elastic constants (flexural dynamic Young's modulus) by resonant fundamental frequency method, sonic elastic constants (Young's modulus and shear modulus), high-temperature thermal diffusivity (room temperature-1000°C), and thermal expansion (100–1000°C).

Table 3. Graphite measurement and test equipment.

Measurement	Standard	Instrumentation	Calibration Method	Result
Physical Dimensions and Mass	ASTM C559-90 (Reapproved 2010)	Mitutoyo Micrometer 121-155 INL ID: 725884 INL ID: 727312 Mitutoyo Caliper CD-6-in. CSX INL ID: 725813 INL ID: 726607 INL ID: 727194 Sartorius Scale ME235P INL ID: 412642 INL ID: 415907	INL Standards and Calibration Laboratory	Bulk density
Fundamental Frequency	ASTM C747-93 (Reapproved 2010) ASTM C1259-08	J. W. Lemmens Grindosonic INL ID: 412850	No calibration required per instrument manufacturer	Elastic modulus (flexural mode)
Sonic Velocity	ASTM C769-98 (reapproved 2005)	Olympus NDT Sq. Wave Pulser/Receiver 5077PR INL ID: 728024 National Instruments Digitizer USB 5133 INL ID: 726725 INL ID: 415868	INL Standards and Calibration Laboratory	Young's modulus, Shear modulus, Poisson ratio

Table 3. (continued).

Measurement	Standard	Instrumentation	Calibration Method	Result
4-point Electrical Resistivity	ASTM C611-98 (Reapproved 2010)	Keithly 6220 Precision Current Source INL ID: 725865 INL ID: 727290 Keithly 2182A Nano Voltmeter INL ID: 725866 INL ID: 727289	INL Standards and Calibration Laboratory	Electrical resistivity
Laser Flash Diffusivity	ASTM E1461-07	Netzsch LFA 457 2 ea. INL ID: 412855 INL ID: 412864	Calibration by user per manufacturer's instructions	Thermal diffusivity
Push Rod Dilatometry	ASTM E228-06	Netzsch DIL 402 C 2 ea. INL ID: 412860 INL ID: 412861	Calibration by user per manufacturer's instructions	Coefficient of thermal expansion
Environmental Monitoring	ALL	Vaisala Pressure, Humidity and Temperature PTU301 INL ID: 726912 INL ID: 727884 INL ID: 727502	INL Standards and Calibration Laboratory	Laboratory environmental conditions

The measurements listed in Table 3 are segregated into individual stations that consist of the instrumentation necessary, a computer for automated data acquisition, and a bar code reader. The bar code of the individual specimen container is read and the file for that specimen is automatically opened for data input prior to each measurement. Associated with each measurement type is a unique laboratory notebook maintained to INL Management Control Procedure (MCP)-2875, Rev. 11, "Proper Use and Maintenance of Laboratory Notebooks," and Plan (PLN)-2690, Rev. 14, "Idaho National Laboratory Advanced Reactor Technologies Technology Development Office Quality Assurance Program Plan," Subsection 3.3.^{11,12} Accepted data will be stored in the Next Generation Nuclear Plant (NGNP) Data Management and Analysis System (NDMAS), a satellite file location for ART. Data in a standardized Excel file format will be transmitted to NDMAS using Form 241.21, Rev. 6, "Records Transmittal" following PLN-3319, Rev 4, "Records Management Plan for the INL Advanced Reactor Technologies Technology Development Office Program."^{13,14}

In addition to laboratory notebooks, the specific measuring instruments are networked to a server computer where the measurement data is automatically stored. This has been implemented in the INL Carbon Characterization Laboratory where custom LabVIEW software was written to facilitate automated data acquisition. This software is comprised of five main programs: Manufacturers Data, Physical and Dimensional Measurements, Electrical Resistivity Measurements, Sonic Resonance (Fundamental Frequency) Measurements, and Sonic Velocity Measurements. These five programs acquire data from instrumentation and user input. The programs then record the results in an Excel spreadsheet located on a server computer. In the case of thermal expansion and thermal diffusivity measurements, two other LabVIEW programs have also been written to parse vendor software acquired data into Excel spreadsheets. Laboratory-wide procedure (LWP)-20000-01, "Conduct of Research Plan," is used to govern the development, accuracy and configuration control of this software.¹⁵

Following is the sequence in which the measurements are made:

1. Wash and dry – All specimens.
2. Mass and dimensional measurements – All specimens.
3. Thermal diffusivity – Piggy Back specimens.
4. Elastic modulus by sonic resonance – Creep specimens.
5. Electrical resistivity – Creep specimens.
6. Elastic modulus by measurement of sonic velocity – Creep specimens.
7. Wash and dry to remove couplant – Creep specimens.
8. Coefficient of thermal expansion – Creep specimens.

3.1 General Provisions

The AGC-4 specimens have been characterized per PLN-4239, “AGC-4 Graphite Specimen Preirradiation Characterization Plan,” which describes the thermal, physical, and mechanical measurement techniques that were used to characterize the different graphite types being tested in the AGC-4 experiment.¹⁶ It is intended to meet the requirements of MCP-1380, “Research and Development Test Control,” and NQA-1-2008; 1a-2009, “Quality Assurance Requirements for Nuclear Facility Applications,” Requirement 11, “Test Control.”^{17,18} Described within the plan are the instruments, fixtures, and methods used for preirradiation material property measurements of bulk density, thermal diffusivity, coefficient of thermal expansion, elastic modulus, and electrical resistivity.

All work was performed in accordance with LWP-21220, “Work Management.”¹⁹ All records designated in implementing documents as quality assurance records were controlled in accordance with PLN-3319, “Records Management Plan for the INL Advanced Reactor Technologies Technology Development Office Program.”²⁰

The data resulting from the preirradiation characterization are plotted in Appendix A. A statistical evaluation has been performed using an inner quartile range analysis to identify levels of precision and outliers in the data.

3.2 Specimen Description and Preparation

The major nuclear-grade graphite types to be tested in AGC-4 are NBG-17, NBG-18, PCEA, 2114, and IG-110. Minor grades of graphite include NBG-25 and IG-430. All major grades have been characterized fully per PLN-4239 and the minor grades have only had dimensional, density, and thermal diffusivity measurements performed on them. Of the experimental grades, the HOPG specimens were the only specimens in which dimensional and mass measurements were made. The SiC-coated graphite and C/C composites were only visually inspected.

The two primary specimen types in the AGC experiments are creep specimens and piggyback specimens. Creep specimens from major grade graphite types are shown in INL Drawing 778033, Rev. 1, and will be subjected to a mechanical load during irradiation to induce irradiation creep within the specimens. Piggyback specimens from both major and minor grade graphite types are also shown in INL Drawing 778033, Rev. 1.⁶ These specimens are not subjected to a mechanical load and are subjected only to neutron irradiation at high-operating temperatures to assess the effects of a reactor environment on the specific graphite grade. The containers that hold the experimental carbon-based material specimens are shown in INL Drawing 604553, Rev 2.

All specimens are 12.5 mm in diameter, with the creep specimens being 25.4 mm long and the piggyback specimens being 6.3 mm long. Details of how specimens were cut from the graphite blocks are also contained in INL Drawing 778033, Rev. 1, “ATR Advance Graphite Capsule (AGC) AGC-4 Graphite Specimen Cutout Diagrams.” The chemical analysis for all graphite in the AGC-4 experiment is attached in Appendix D.

Immediately after being machined, each specimen is placed in an individual container that is bar coded with a unique identification number per INL Drawing 778033, Rev. 1. Each graphite specimen is then laser engraved with that same unique identification number around the circumference at one end. Prior to any material property measurement, each specific specimen is identified by its unique identification number and the data is recorded/stored under this identification number. After the specimens have been laser engraved, they are ultrasonically cleaned as follows:

1. Handle the specimens only while wearing cotton or powder-free nitrile gloves.
2. Remove all dust and debris using an aerosol pressurized dust-off product.
3. Ultrasonically clean specimens for 20 minutes in deionized water.
4. Rinse specimens in ethyl alcohol to help displace water.
5. Allow to air dry.
6. Place specimens in a laboratory oven at 130°C for 2 hours.
7. Allow specimens to cool in a desiccator and retain there in storage until resistivity or bulk density measurements are taken.

It should be noted that irradiated specimens are not washed again prior to characterization measurements. However, for measurements of density and resistivity, Steps 6 and 7 above are followed.

3.3 Personnel and Training

Personnel who perform measurements identified in this plan are qualified in accordance with LWP-12033, “Personnel Qualification and Certification.”²¹ Their ability to adequately perform measurements described in this plan is demonstrated by instrument manufacturers’ training and certification and/or performance of an instrument/measurement operational validation. Personnel qualifications are reviewed by the Graphite R&D lead and documented in laboratory notebooks.

3.4 Variations, Exceptions and Discrepancies

There are several variations, exceptions, and discrepancies that may occur. The first is a known departure from the applicable American Society for Testing and Materials (ASTM) standard. These departures are typically related to geometrical constraints. All currently known departures or exceptions taken to the ASTM standard are described in detail in Section 4 of this plan. Any departure not captured in this plan will be recorded in laboratory notebooks associated with the measurement. When possible, sensitivity studies will be performed and documented in laboratory notebooks to understand the impact of these exceptions and departures.

It is likely that the ASTM standards and/or test methods will be revised and improved during the more than 10-year-long AGC experiment cycle. Each revision or development will be evaluated for how it could impact future measurements and their consistency with measurements made under previous revisions or techniques. A programmatic determination will be made whether to continue with the current version of the ASTM/method or use the updated version. This determination will be documented in laboratory notebooks associated with the affected measurement.

While measurements are being made, it is possible that something out of the ordinary may occur. Any unusual event that occurs during a measurement will be documented in the laboratory notebook associated with that specific measurement and duly noted within the database associated with the data generated for this program. The principal investigator (PI) will be notified of the event and will determine what impact it has on the data. The significance of the result will be documented in the laboratory notebook by the PI.

3.5 Calibration and Functional Validation

The measurement protocol consists of calibration, functional validation, and data acquisition. Functional validations established for each measurement in collaboration with the instrument manufacturer are performed periodically to ensure that accurate and consistent data is acquired. All validations are performed on traceable standards and documented in retrievable laboratory notebooks associated with each measurement. In the event of an instrument functional validation failure, the reason for the failure is investigated and resolved prior to that measurement being used for further characterization. Upon resolution, a determination is made as to the impact of the failure on data taken prior to the failure and back to the last valid measurement. If it is determined the data captured during this interval is suspect, the impacted data will be evaluated for accuracy.

LWP-13455, "Control of Measuring and Test Equipment,"²² is followed for calibration standards, methods, and frequencies that have been established for each measurement. Where it is not possible to use the INL Standards and Calibration Laboratory, calibration by user procedures are established based on ASTM standards and manufacturers' instructions and performed against international standards. These procedures are documented in laboratory notebooks associated with each measurement.

4. TEST METHODS

Before any measurements are made, specimen numbers and basic information about each type of graphite are entered into the manufacturer's data program. Once basic information about the graphite type has been recorded, it is automatically saved to an Excel spreadsheet file and the individual specimen numbers are entered using a bar code reader. Following the initial input of general information, individual material property measurements are made starting with mass and dimensional measurements for determining bulk density.

4.1 Mass, Dimensions, and Bulk Density

Dimensional change is one of the key parameters affecting the performance of graphite in a neutron environment. Determining volumetric and linear dimension as a function of temperature and radiological dose is necessary to understand critical performance measures such as dimensional change turnaround, irradiation creep, and internal stresses imposed upon graphite components. Dimensional and mass measurements are performed to ASTM Standard C559-90 (Reapproved 2010), which describes in detail the procedure for making dimensional measurements and calculating bulk density.

The accuracy of the dial micrometers used here is stated by the manufacturer to be 2 μm . This is a 0.008% accuracy on a 25.4-mm measurement. However, when evaluating the uncertainty of the density determination, other factors must be considered, such as the hardness of the material and the force with which the micrometer blade is engaged with the material, specimen temperature variation, technician skill, etc. These and other factors were considered in a propagation of error analysis to arrive at an uncertainty of 0.08% with the measurement of the diameter being the largest contributor to the error.

4.2 Electrical Resistivity

Electrical resistivity is used as a rapid, simple means to determine grain orientation, structure, and crystallinity of graphite. In conjunction with optical microscopy, it can be used to determine the microstructural texture of graphite components without much specimen preparation work. Resistivity is measured following ASTM C611-98 (Reapproved 2010), “Standard Test Method for Electrical Resistivity of Manufactured Carbon and Graphite Articles at Room Temperature.”²³ The measurement technique is commonly referred to as a 4-point probe. It consists of passing a known current through the specimen and measuring the voltage across the specimen at known locations.

Based on Ohms Law, the resistance is determined and the resistivity is calculated from:

$$\rho = R \cdot A / L$$

where

R = the measured resistance

A = the cross sectional area

L = the length over which the voltage is measured.

Figure 5 shows a test fixture fabricated at INL that allows a specimen to be rotated for multiple measurements of voltage around its periphery.

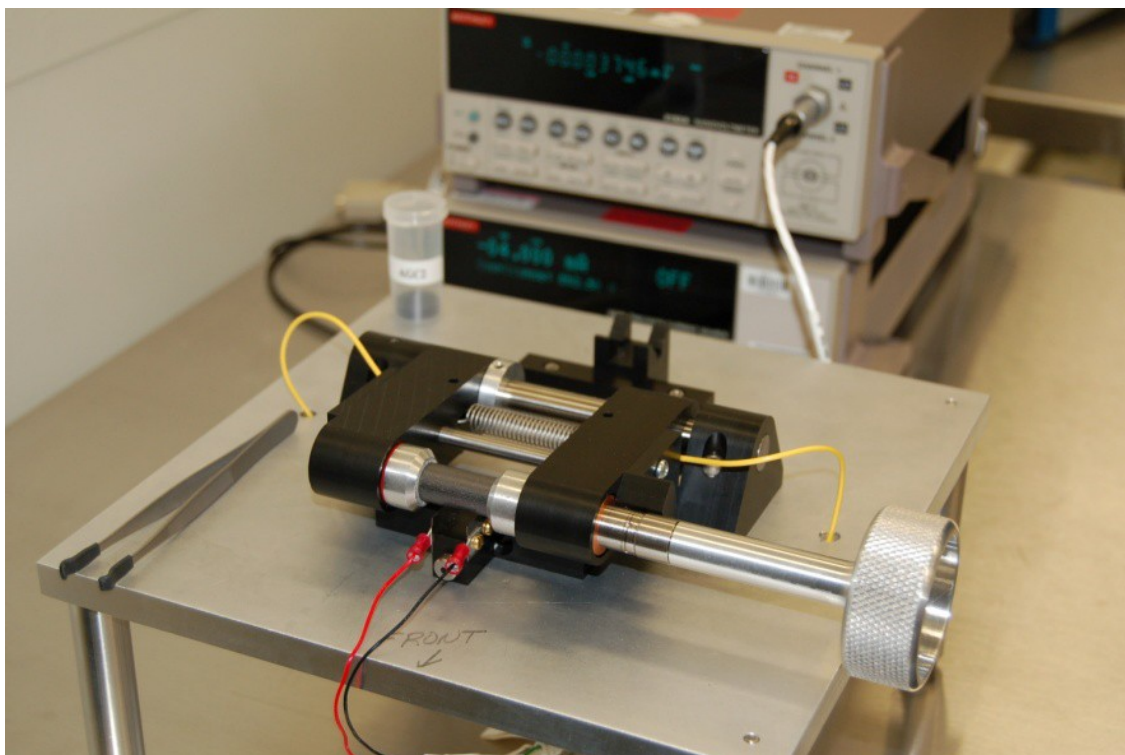


Figure 5. Electrical resistivity measurement station.

Uncertainty in the resistivity measurement is mainly comprised of the contact resistance between the specimen and the contacting blades for the voltage measurement. Specimen temperature and the temperature of other bimetal junctions in the voltage measuring leads are also factors. These effects are minimized by passing the current through the specimen in two directions and averaging the measured voltage for each direction. In this way, any thermoelectric or small differences in junction resistances will

cancel. A round robin test series reported in ASTM C611-98 precision and bias section states a lab-to-lab variability of 2.5%. A round robin test series such as this would take into account the variables discussed above and is considered a good estimate of the measurement uncertainty.

4.3 Approximation of Elastic Modulus from the Measurement of Sonic Velocity

The mechanical properties of graphite are necessary to determine the structural integrity of graphite components. These properties are vital to determining the viability of the structural strength and integrity of the reactor core. The as-received and irradiated values are needed for whole-core models, which will be used for the graphite design code. This test is carried out in accordance with ASTM C769-98 (reapproved 2005), “Standard Test Method for Sonic Velocity in Manufactured Carbon and Graphite Materials for Use in Obtaining an Approximate Value of Young’s Modulus.”²⁴ In this measurement, the transmitting piezoelectric transducer sends a 2.25 MHz sound wave through the specimen. At the opposite end of the specimen, the acoustic wave is received by another piezoelectric transducer. The sonic velocity of the specimen is the ratio of specimen length to the signal time lapse between transducers.

An approximate value for Young’s modulus, E , can be obtained from:

$$E = \rho V^2$$

where

ρ = the specimen density

V = the sonic velocity.

Figure 6 shows the sonic velocity measurement station. In the foreground are the fixtures for clamping the specimen between the transducer and receiver that were specifically designed and fabricated at INL for this application. They have unique features that improve measurement accuracy, precision, and efficiency. For example, measurement precision is improved because the spring-loaded clamp applies consistent pressure between the transducers and specimen resulting in repeatable couplant thickness. The specimens are easily and rapidly loaded into the fixture using the cam-operated clamp.

As specified in Paragraphs 8.1 and 8.5.1 of ASTM C769-98, a suitable coupling medium should be used and reported with the data. Here, Shear Gel[®], manufactured by Sonotech, Inc., is used for a shear wave couplant and Ultragel II[®], also manufactured by Sonotech, Inc., is used for the transverse wave couplant.

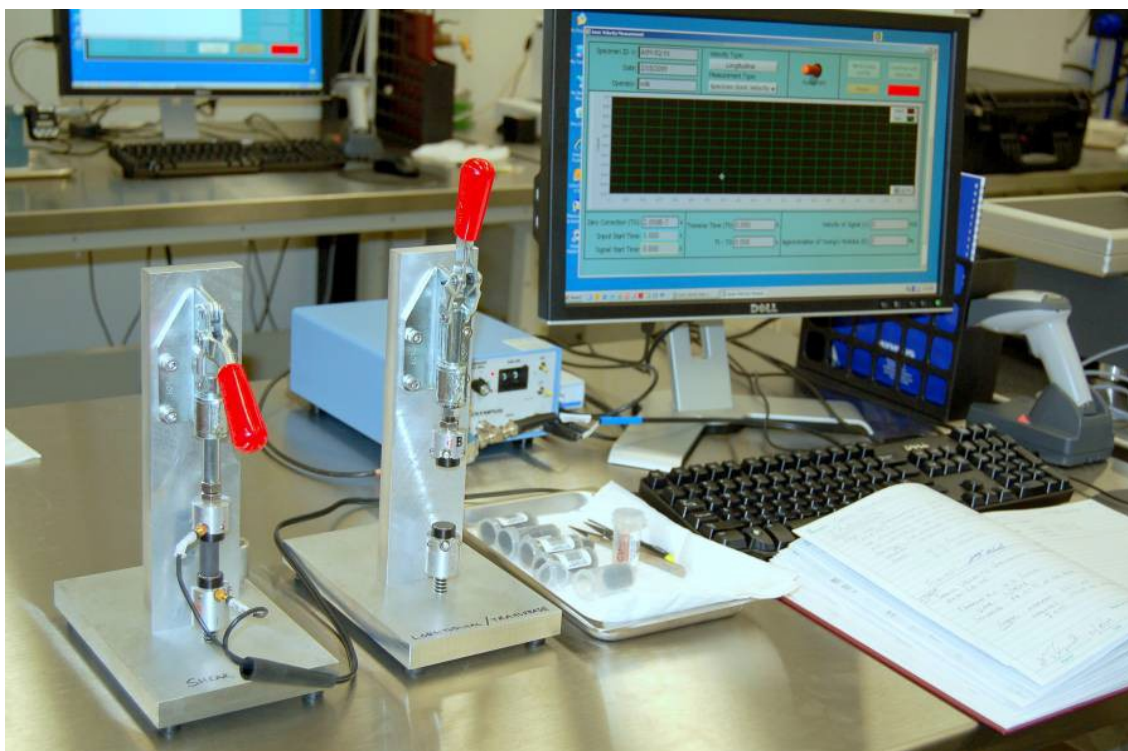


Figure 6. Sonic velocity measurement station.

Figure 7 shows the LabVIEW software user interface display for sonic velocity measurements after scanning the bar code of the specimen to be tested. This screen is used to acquire sonic velocity measurements of a specimen in both the longitudinal and shear directions. Operating much like an oscilloscope, the cursors automatically mark the time between the transmitted wave and the received wave. Also shown in Figure 7 are two examples of the shear wave and transverse wave timing locations for properly coupled specimens. The specimen length divided by this transit time is the sonic velocity.

The uncertainty in determining elastic moduli from the measurement of sonic velocity comes from several sources. First there is the effect of material and geometry related dispersion of the transmitted wave. ASTM C769-98 provides guidance to minimize this problem by choosing the correct frequency. This technique also assumes linear elastic behavior, but graphite is not completely linearly elastic. And finally, the operator's judgment on the placement of the timing cursors is somewhat subjective. Clean wave forms to base these judgments on are highly dependent on the quality of the transducer-material coupling. These sources of error are difficult to quantify; therefore, they are difficult to combine in a propagation of error analysis. However, ASTM C769-98 describes in some detail a round robin test series between different laboratories. Using round robin test data to determine a coefficient of variation (COV) provides a good means of estimating the measurement uncertainty. With caution, the COV of 3.8% reported in ASTM C769-98 is taken here to be representative of the uncertainty of these measurements. When considering a single material and making comparisons between the pre and post-irradiation values, the precision of these measurements is good enough to consider differences greater than 4% significant. However, one is cautioned to refrain from using the values here as absolute, or better than $\pm 10\%$ accurate.

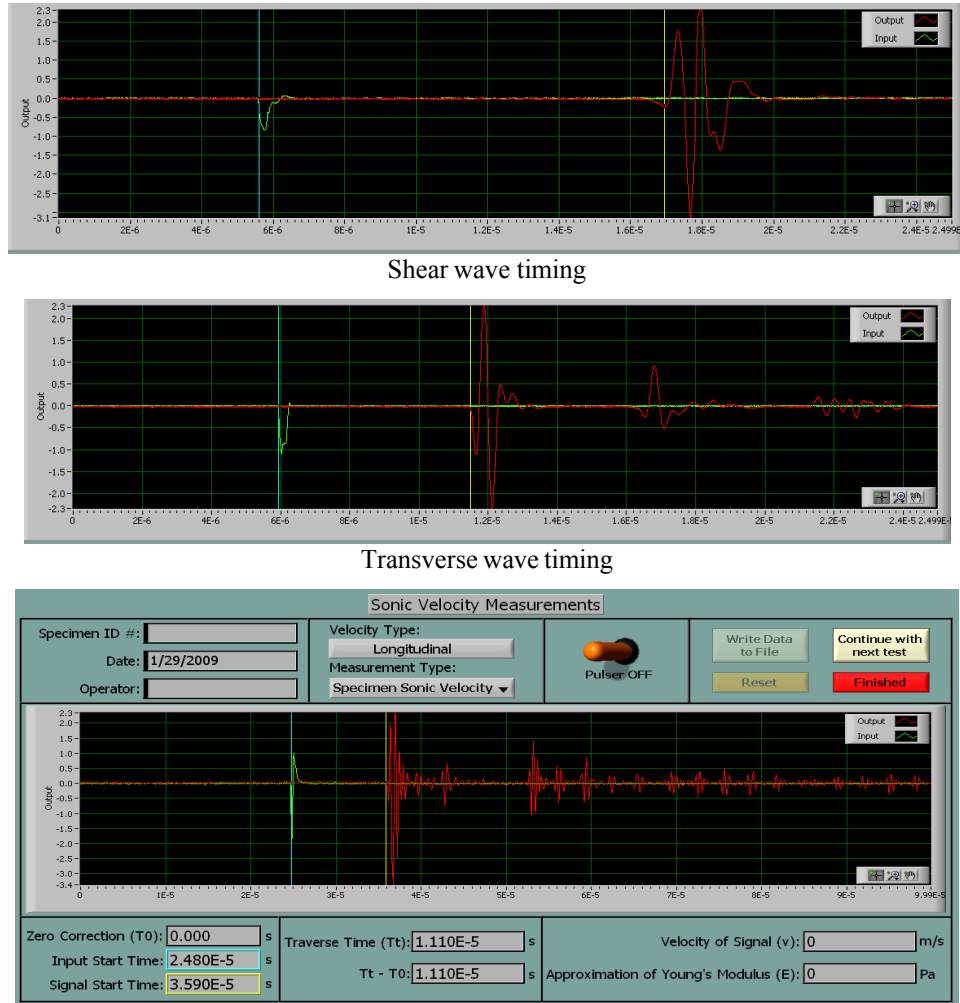


Figure 7. Sonic velocity measurement user interface.

4.4 Modulus of Elasticity by Measurement of Fundamental Frequency

The mechanical properties of graphite are necessary to determine the structural integrity of graphitic components. These properties are vital to determining the viability of the structural strength and integrity of the reactor core. This test method measures the fundamental resonant frequency of test specimens of suitable geometry by exciting them mechanically with a singular elastic strike. Specimen supports, impulse locations, and signal pick-up points are selected to induce and measure specific modes of the transient vibration of the specimen. The transient signals are analyzed, and the fundamental resonant frequency is isolated and measured by the signal analyzer. The measured fundamental resonant frequency, specimen dimensions, and mass are used to calculate the dynamic Young's modulus, shear modulus, and Poisson's ratio per ASTM C747-93 (Reapproved 2010), "Standard Test Method for Moduli of Elasticity and Fundamental Frequencies of Carbon and Graphite Materials by Sonic Resonance," in combination with apparatus and calculations described in ASTM C1259-08, "Standard Test Method for Dynamic Young's Modulus, Shear Modulus, and Poisson's Ratio for Advanced Ceramics by Impulse Excitation of Vibration." ^{25,26} The fundamental frequency measurement station is shown in Figure 8.



Figure 8. Fundamental frequency measurement station.

After placing a specimen in the test fixture, the user excites it by lightly tapping it with a small mechanical impulse. A consistent impulse is achieved by placing the ball hammer onto a lever that rotates out from under the hammer as it is raised. The specimen is supported in such a way that it vibrates at its natural frequency. A microphone placed underneath one end of the specimen in combination with the Grindosonic electronics measure this frequency, which is recorded and displayed by the computer. The modulus of elasticity is calculated and displayed next to the newly acquired frequency. If the results are satisfactory, the user can press the “Save 1st Frequency” button and go on to the next measurement. Following the recommendations of ASTM C-1259-08, 10 readings of the fundamental frequency are measured before the results of the test are written to the applicable Excel spreadsheet.

ASTM C-1259-08 describes in detail a round robin test series using ceramic materials along with an analysis of the propagation of errors in the calculation of moduli from the measurement of resonant frequency, geometry, and mass of the specimen. This error analysis shows the major sources of experimental variation are the measurement of the fundamental frequency and the smallest dimension (diameter) of the specimens due to their higher exponent in the modulus calculations. Both the propagation of error analysis and round robin data indicated an uncertainty of less than 2%. However, the creep specimens tested here do not meet the geometry requirements of C-1259-08. With a length-to-diameter ratio of only 2, these specimens are, at times, difficult to excite consistently and in a single mode of vibration. Once a resonant frequency is determined by an experienced operator for the flexural mode of vibration, it was easily repeated with accuracy within 2% uncertainty.

4.5 Thermal Expansion

Understanding the coefficient of thermal expansion (CTE) for graphite components is critical for determining the dimensional changes that occur as a result of temperature cycles. Localized external stresses can be imposed upon mechanically interlocked graphite core components as the individual pieces experience differential thermal expansion. Internal stresses can occur within larger graphite components if there is a temperature gradient causing differential expansion within the piece (one side has a higher temperature than the other). Finally, the thermal expansion is highly dependent upon the graphite microstructure, such as orientation/anisotropy, pore size and distribution, and crystallinity. Irradiation

damage can significantly alter graphite microstructure, and thus the CTE values. Determining the extent of the changes as a function of irradiation dose and temperature will be a key parameter for reliable calculation of stress states within graphite components, volumetric changes, and irradiation creep rates.

The CTE measured here follows ASTM E228-06.²⁷ This test method uses a push-rod-type dilatometer to determine the change in length of a graphite specimen relative to that of the holder as a function of temperature. The temperature is varied over the desired range at a slow constant heating or cooling rate. The linear thermal expansion and mean coefficient of thermal expansion, α , are calculated from the recorded data using:

$$\alpha = \frac{1}{L_0} \frac{\Delta L}{\Delta T}$$

where

L_0 = the specimen initial length

ΔL = the change in length

ΔT = the temperature difference between a specified reference temperature and the temperature at which the change in length was measured.

The Netzsch DIL 402 C commercial system (Figure 9) currently used at INL does not have the capability to cool the specimen below ambient temperature. Therefore, the initial length at 20°C is linearly extrapolated from expansion data between 100°C and 150°C and the mean CTE is calculated from a 20°C reference temperature.

The greatest source of experimental error in the dilatometry method described here is the correction made for the expansion of the specimen holder and push rod/LVDT mechanism. This differential between the specimen and the apparatus must be accounted for to isolate the specimen expansion only. Studies reported in the precision and bias section of ASTM E228 have indicated that this type of dilatometry can be accurate to 4% when calibrations are performed carefully.

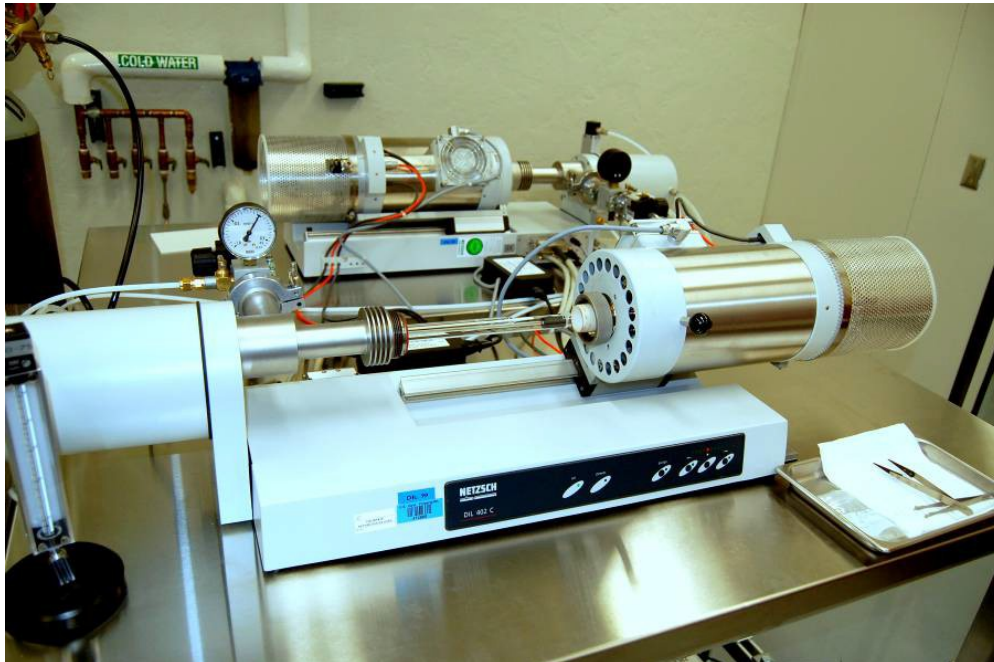


Figure 9. Commercial push rod dilatometer for measurement of CTE.

4.6 Thermal Diffusivity

The ability to conduct heat through the graphite core is critical to the passive removal of decay heat. Reduction of the thermal conductivity within graphite can have a significant effect on the passive heat removal rate and thus the peak temperature that the core and, subsequently the fuel particles, will experience during off-normal events. Determining changes to the conductivity as a function of irradiation dose and temperature is important for the HTGR safety analysis. Here, ASTM E1461-07 is followed for the calculation of thermal diffusivity and conductivity. Thermal diffusivity (δ) is measured and defined as the ratio of thermal conductivity to volumetric heat capacity by:

$$\delta = \frac{k}{\rho C_p}$$

where

k = thermal conductivity

ρ = density

C_p = specific heat.

The measurement is performed on piggyback specimens. A pulsed laser is used to subject one surface of the specimen to a high-intensity, short-duration energy pulse. The energy of this pulse is absorbed on the front surface of the specimen and the resulting rise in rear-face temperature is recorded. The thermal diffusivity is calculated from the specimen thickness and the time required for the rear-face temperature to reach 50% of its maximum value. A commercially available laser flash apparatus (LFA), complete with vendor-developed software for instrument control and data acquisition, is used as shown in Figure 10.

Uncertainty in the measurement of thermal diffusivity comes about from specimen heat loss and temperature measurement. Specimen temperature measurement is performed with a calibrated type-S thermocouple in the near vicinity of the specimen. Being relatively straight forward, the specimen temperature measurement is typically a small contribution to the overall measurement error or uncertainty.

The main contributor to the measurement uncertainty is heat loss from the specimen. Because this measurement technique depends on the assumption of one-dimensional heat transfer from the flat face receiving the laser pulse to the flat face radiating to the detector, heat loss errors are mainly attributed to radiative heat loss from the circumference of the specimen at temperatures above 300°C. Typically, several correction models are provided with the instrument software to account for this heat loss. As the specimen diameter to thickness ratio decreases, the heat loss increases to the point that the correction models no longer can account for the error. A study was performed to gain a fuller understanding of the limits of the models made available with the NETZSCH LFA and the dependence of the diameter to thickness ratio on measurement error. In this study, the heat loss models were applied to data taken on specimens with various diameter-to-thickness ratios and at specimen temperatures between 25°C and 1000°C. It was determined that the Cowan model along with diameter to thickness ratios greater than or equal to 2 resulted in determination of the diffusivity within ASTM E1461 and the manufactures specified uncertainties of 4% and 3%, respectively.²⁸ This was further verified by instrument functional tests performed monthly on a pure iron validation specimen for which the diffusivity was determined to be within 3% of the Touloukian values between 100°C and 700°C.²⁹



Figure 10. LFA measurement station for determination of thermal diffusivity.

5. DATA ANALYSIS

Data gathered for the characterization of AGC-4 specimens are contained in the appendices of this report. Appendix A contains plots of the individual data points for each specimen. Shown by the dashed lines in each plot are the upper and lower limits of the interquartile range. These limits are established by the lesser of either the least or greatest value in the data or by multiplying the interquartile range (IQR) by 1.5 and adding or subtracting this value from the third and first quartile. Any data value outside of these limits is a suspected outlier of the established pattern. However, it is important to note that these outlying values are subject to not only measurement variability, but also material variability; therefore, the values cannot necessarily be discarded. These outlying values are examined in the context of the entire data set and will be evaluated further following irradiation. Other statistical parameters are calculated and presented in the tables of Appendix B. The mean, standard deviation, and coefficient of variance are all calculated for the different measurement data sets and graphite types. Upper and lower limits are presented in the tables of Appendix B are the IQR limits described above.

There are many ways to combine and compare the data presented here. In doing so, the validity of the data is exercised and scrutinized. First the data sets are considered independently with the statistical analysis described above. Additionally, a limited comparison of the absolute property values is performed between different graphite types and grades. The degree of isotropy is also evaluated for a limited number of grades by calculating the anisotropy ratio.

$$\text{Anisotropy Ratio} = \frac{\text{Value of the Property in the Against-Grain Direction}}{\text{Value of the Property in the With-Grain Direction}}$$

Note that in the case of isostatically molded graphite with-grain and against-grain indicate specimens taken from orthogonal planes in the billet.

5.1 Mass, Dimensions and Density Data Analysis

Plots of the measured mass, dimensions and density for all AGC-4 specimens along with their IQR limits are shown in Figure A-1 through Figure A-48 (Appendix A). The HOPG specimen data is shown in Table B-19. Analyzing the dimensional and mass measurements of the creep specimens for combined

grain orientations, the data shows that the COVs are all at or below 0.5% with the exception being the PCEA creep specimens. Upon further review, the mass measurements for these specimens revealed that there are two distinct modes: one associated with the against-grain specimens and one associated with the with-grain specimens (Figure A-41). These two modes in the mass measurements led to a higher combined COV for both the density and the mass. The degree of bimodality for mass and density was not as great for the PCEA piggyback specimens as it was for the creep specimens, but it still existed (Figure A-10 and Figure A-46). This bimodal difference in mass, and therefore density is most likely due to material variability in the billet from which the specimens were taken. As shown in INL Drawing 778033, the with-grain (wg) specimens were taken from a different block than the against-grain (ag) specimens, but no measurement error or mistake was suspected here. Following the irradiation of the specimens, this difference between with-grain and against-grain specimen mass should remain the same and the change in volume of individual specimens will be evaluated to understand irradiation induced densification.

One of the most important parameters in the AGC experiment is the dimensional change of the specimens due to irradiation and stress. Therefore, particular care needs to be taken when evaluating the dimensional measurements. The scatter in the dimensional data is reasonable with the length measurements having a COV of 0.18% or less and the diameter measurements having a COV of 0.11% or less. This is both a function of machining consistency and measurement precision. However, 13 specimens throughout the different grades fall outside of their respective IQR. This does not necessarily indicate a measurement error. It is possible that the specimen dimensions are simply different than the majority. It is also possible that there is some material variability between the specimens. Either way, it is suspected, but not necessarily concluded, that the dimensional measurement is not accurate. The specimens that have suspect dimensional values are listed in Table 4 and will be closely evaluated following irradiation.

Table 4. Creep specimen length outliers.

Grade	Specimen ID No.	Grade	Specimen ID No.
NBG-17	AP5004	PCEA	DA3801
NBG-17	AW4801	PCEA	DA3804
NBG-17	AW4803	PCEA	DA3902
NBG-17	AW4804	NBG-18	BP4303
2114	TW4001	NBG-18	BP4503
2114	TW4102	NBG-18	BW4301
2114	TW4501	—	—

5.2 Electrical Resistivity

Plots of electrical resistivity are shown in Figures A-74 through A-78 for graphite grades 2114, IG-110, NBG-17, NBG-18, and PCEA. The resistivity measurements were performed on the creep specimens only. The COVs for the combined orientation specimens varies by the grade. NBG-17 had the lowest at 2.2%, and IG-110 had the highest at 5.0%. After performing the IQR analysis for each grade, there were only five specimens whose resistivity values were outside the IQR limits. NBG-18 had four against-grain specimens that were outside of the IQR limits (three were low and one was high) and one 2114 specimen had a high resistivity value.

In Figure 11, the mean resistivity values of several grades of graphite are plotted for both specimen grain orientations. The anisotropy ratio is displayed above each mean value. NBG-17 exhibited the best isotropy ratio, while PCEA had the largest resistivity difference between the two-grain orientations.

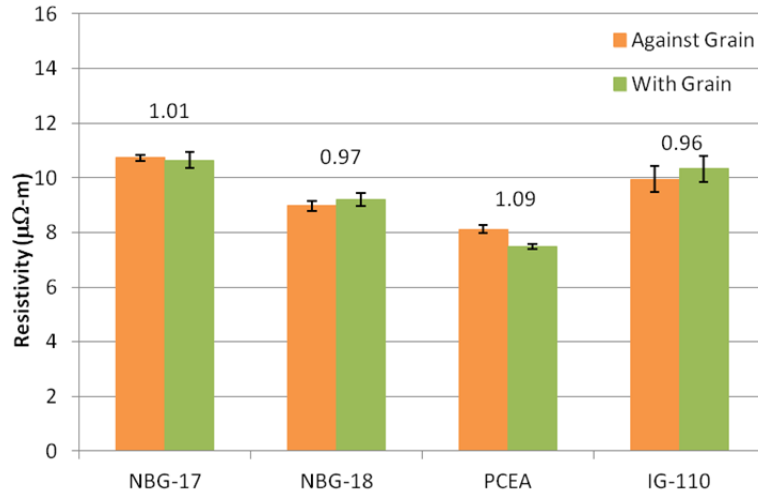


Figure 11. Electrical resistivity for the major graphite grades. The anisotropy ratio is above each set of data bars. The error bars represent ± 1 standard deviation.

5.3 Approximation of Elastic Modulus from the Measurement of Sonic Velocity

Figure A-79 through Figure A-88 are plots of Young's and shear modulus that were calculated from the measurement of sonic velocity through the graphite specimens. Young's and shear moduli statistics are shown for each graphite grade in Table B-10 and Table B-11, respectively. The IQR analysis showed there were three Young's modulus outliers and four shear modulus outliers. The COVs calculated for both the with-grain orientation and the against-grain orientation agree with the COV reported in the precision and bias section of ASTM C769 (3.8%).

Figure 12 shows the relationship between Young's modulus measured using the sonic velocity technique and the density for each graphite grade. In general, as the density of a material increases, so does the modulus of elasticity. Consistent with this, Figure 17 shows that the highest density graphite (NGB-17 and NGB-18) had the highest modulus of elasticity.

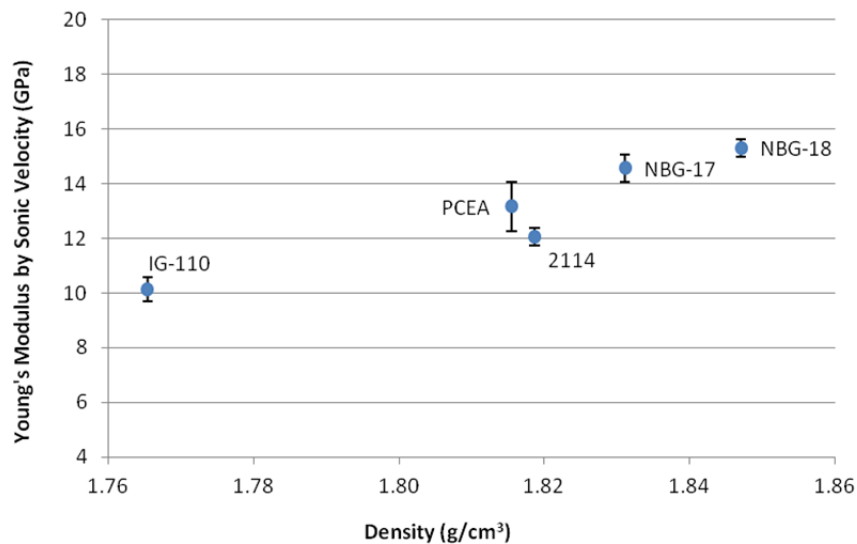


Figure 12. Young's modulus using the sonic velocity technique versus density for each major graphite grade. The error bars represent ± 1 standard deviation.

The COVs for all of the different graphite grades by grain orientation (Table B-10) were in agreement with the value (3.8%) reported in the ASTM C769 precision and bias section. However, the IG-110 with-grain specimens had a slightly higher COV of 4.4%. Figure 13 shows Young's modulus by sonic velocity method for each grade of graphite by grain orientation with the anisotropy ratio.

Prior AGC specimen testing was performed under the previous ASTM sonic velocity standard, ASTM-769-98 (reapproved 2005), which does not use the Poisson Factor to calculate the modulus values. To avoid confusion when comparing AGC-4 data to previous AGC data, it was decided to continue using ASTM-769-98 and when necessary the correction can be applied. Using the same ASTM test method version assures the unirradiated and irradiated measurements will be consistent and comparable without testing method bias.

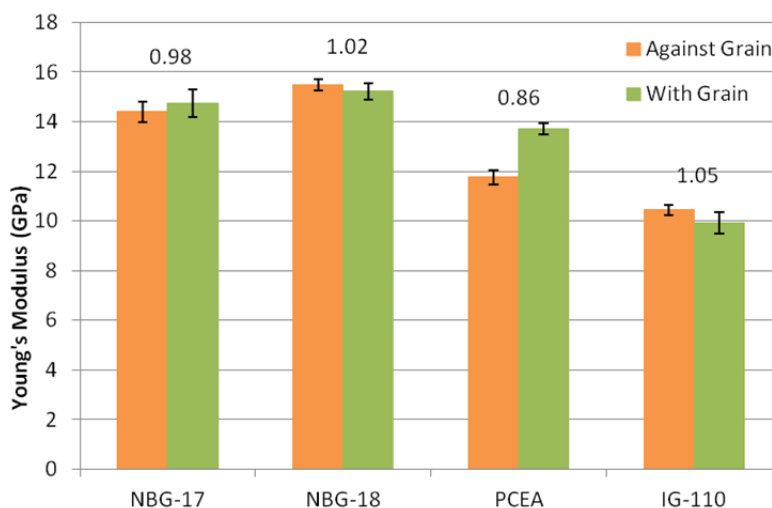


Figure 13. Young's modulus by sonic velocity for the major graphite grades. The anisotropy ratio is above each set of data bars. The error bars represent ± 1 standard deviation.

5.4 Modulus of Elasticity by Measurement of Fundamental Frequency

Young's modulus of each specimen was also calculated using the fundamental frequency technique. The results are plotted in Figure A-69 through Figure A-73 and the statistical data is contained in Table B-8. Statistically this data is well behaved with the IQR analysis showing only two PCEA specimens that were outliers (Figure A-73).

It should be noted that for AGC-4 specimens, the dynamic Young's modulus values determined by sonic velocity testing techniques are generally 2–3 GPa higher than the measurements obtained by the fundamental frequency testing technique. Figure A-71 and Figure A-81 demonstrate this for the NBG-17 specimens. The difference between the two standards has been noted for a number of years and was finally addressed in the latest version of the sonic velocity standard (ASTM-769-09). In this latest version, the Young's modulus value is calculated from the time-of-flight measurement utilizing a correction factor designated as the Poisson's Factor (C_v). This factor is a function of Poisson's ratio and normally has a value between ~ 0.8 and 0.9 . Calculating the modulus using the Poisson's Factor effectively lowers the value by 10% to 20%, bringing the Young's modulus values measured by the sonic velocity technique nearly equal to values arrived at by the fundamental frequency test method.

While the absolute Young's modulus values between the sonic velocity technique and the fundamental frequency technique may differ for the AGC-4 measurements, relative trends of specimen groups and individual specimens can be compared to identify gross measurement error. For example, the outliers in Figure A-73 also have a relative high value in the group of against-grain specimens measured using the sonic velocity technique (Figure A-83). The trend of against-grain specimens having a lower Young's modulus than the with-grain specimens is also consistent between the two techniques. Similar consistencies can be seen throughout the other graphite grades. Figure 14 shows a comparison of Young's modulus from the measurement of fundamental frequency for the primary grades of graphite by grain orientation. Again, all except one of the COVs for the different graphite grades and grain orientation compare favorably with the 3% uncertainty that is reported in the ASTM for this measurement technique. The IG-110 with-grain specimens had the highest COV of 4.1%. PCEA showed the biggest discrepancy between grain orientations. Its anisotropy ratio was 0.85. The other grades all exhibited very good isotropy ratios.

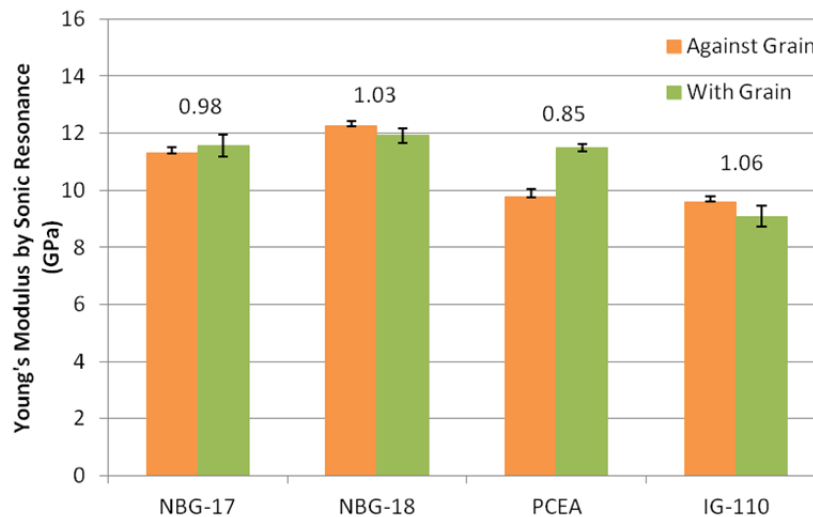


Figure 14. Young's modulus calculated by the fundamental frequency method for the major graphite grades. The anisotropy ratio is above each set of data bars. The error bars represent ± 1 standard deviation.

5.5 Thermal Expansion

Mean coefficient of thermal expansion data is plotted in Figure A-49 through Figure A-68. A statistical evaluation of the CTE data was performed at three discrete temperatures for each graphite type: 100°C, 500°C, and 900°C. The dashed lines in these plots indicate the upper and lower IQR limits. Table B-5 through Table B-7 contain the mean, standard deviation, COV, median, and the values of the upper and lower IQR limits for the data evaluated at the discrete temperatures.

Figure 15 shows the CTE COVs for the discrete temperatures listed above by graphite grade and grain orientation. With exception of measurements at low temperature for IG-110 and NBG-18, the CTE data is well behaved with the COV less than 5%. When compared to other materials, the coefficient of thermal expansion of graphite is relatively low. Combining this low thermal expansion with small temperature changes results in a length change of approximately 10 μm for a 25.4-mm-long creep specimen. This is arguably a difficult measurement to make consistently and should be considered when using CTE data below $\sim 200^\circ\text{C}$.

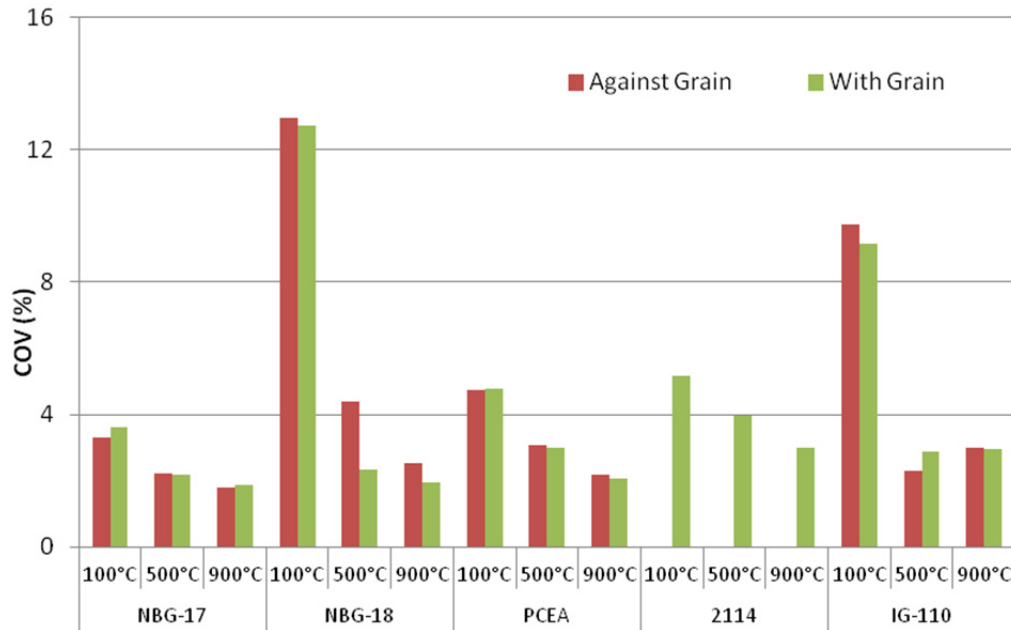


Figure 15. Coefficient of variance for mean CTE at three discrete temperatures for each major graphite grade and grain orientation.

Figure 16 shows the average of all specimens for the primary grades of graphite with error bars indicating ± 1 standard deviation. All of the grades show an increase with temperature in a near linear fashion between 300°C and 1000°C.

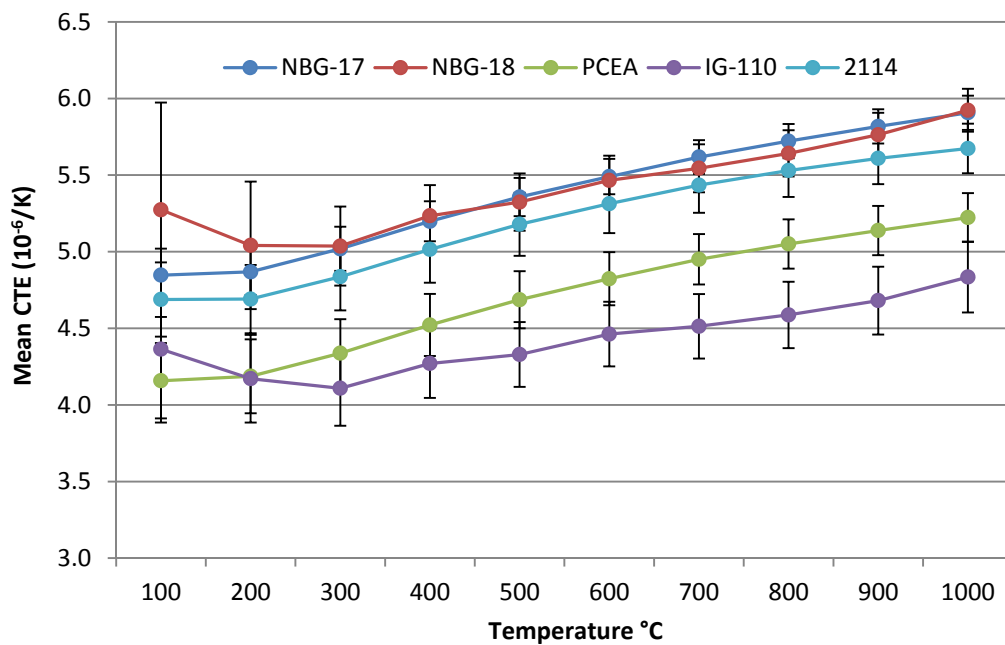


Figure 16. Mean CTE for the major grades of graphite as a function of temperature. The error bars represent ± 1 standard deviation.

Measurements of CTE were performed on both with-grain and against-grain specimens. Figure 17 shows the CTE anisotropy ratio for the same primary grades of graphite as a function of temperature. As expected the ratios are fairly constant across all measurement temperatures. The graphite grade 2114 is not shown because it is isotropic; therefore, there is only one grain orientation.

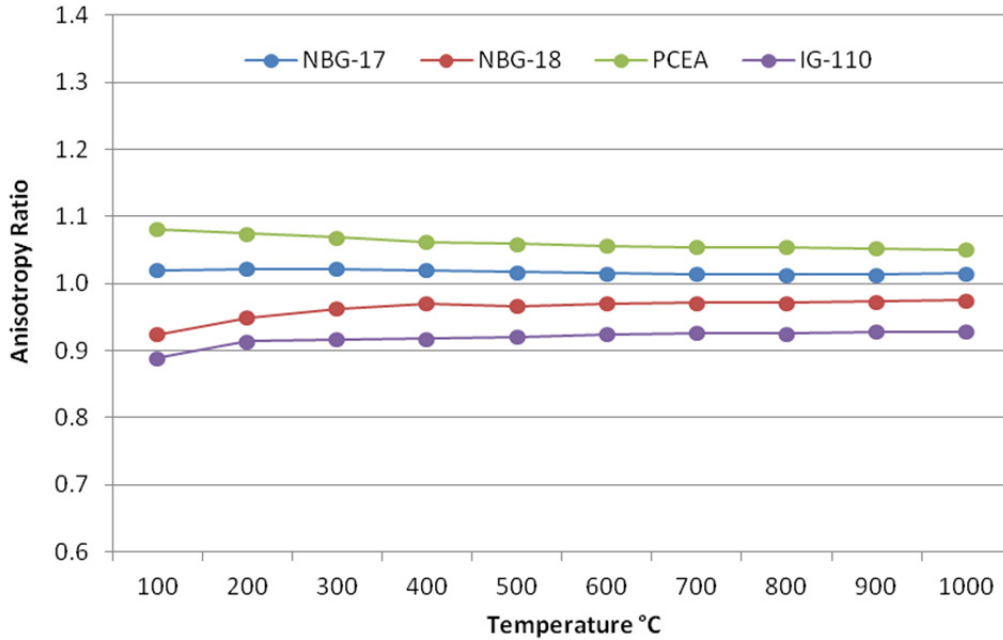


Figure 17. CTE anisotropy ratio for nuclear grade graphite as a function of temperature.

5.6 Thermal Diffusivity

Plots of thermal diffusivity are shown in Figure A-89 through Figure A-116. As with the CTE data, discrete temperatures of 100°C, 500°C, and 900°C were statistically evaluated. Table B-16 through Table B-18 contain values of the mean, standard deviation, COV, median, and the lower and upper IQR limits. With exception of IG-110, the COVs for all the graphite grades within a specific grain orientation are below 2%. Thirteen outliers were found after performing the IQR analysis. Seven of these specimens were PCEA specimens (Figure A-106 through Figure A-108). Three of the outlying specimens were IG-110 (all three of these outliers were the same specimen for temperatures 100°C, 500°C, and 900° [Figure A-94 through Figure A-96]). The remaining specimens were one each of NBG-25, NBG-17, and 2114. None of these specimens were gross outliers with respect to the IQR limits. Material variability is likely the reason for these specimens to exceed the IQR limits.

Figure 18 shows the diffusivity COVs for the discrete temperatures listed above by graphite grade and grain orientation. Here, the scatter in the data for the with-grain specimens of IG-110 is significantly higher than the other grades, but is still within the estimated measurement precision. Again, material variability is thought to be the cause.

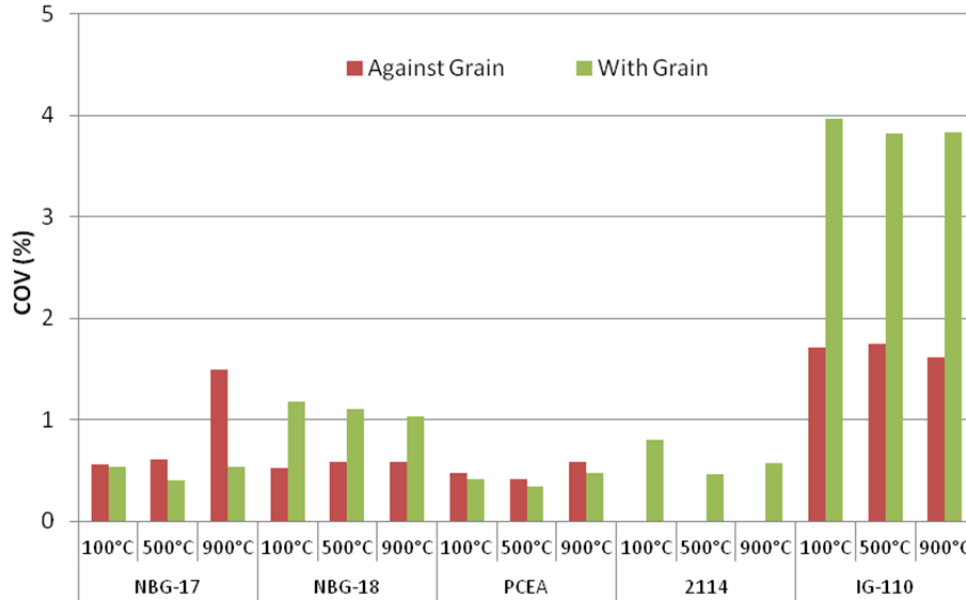


Figure 18. Coefficient of variance for diffusivity at three discrete temperatures for each major graphite grade and grain orientation.

Figure 19 shows the average thermal diffusivity for the five primary graphite grades of interest. Error bars are ± 1 standard deviation and in some cases cannot be seen because they are smaller than the plotted symbol. The diffusivity between different grades of graphite varies as much as 40% at room temperature (2114 and PCEA). However, this percentage is reduced to 20% at 1000°C.

Shown in Figure 20 is the anisotropy ratio for the same graphite grades. As expected this ratio is constant as a function of temperature for all grades.

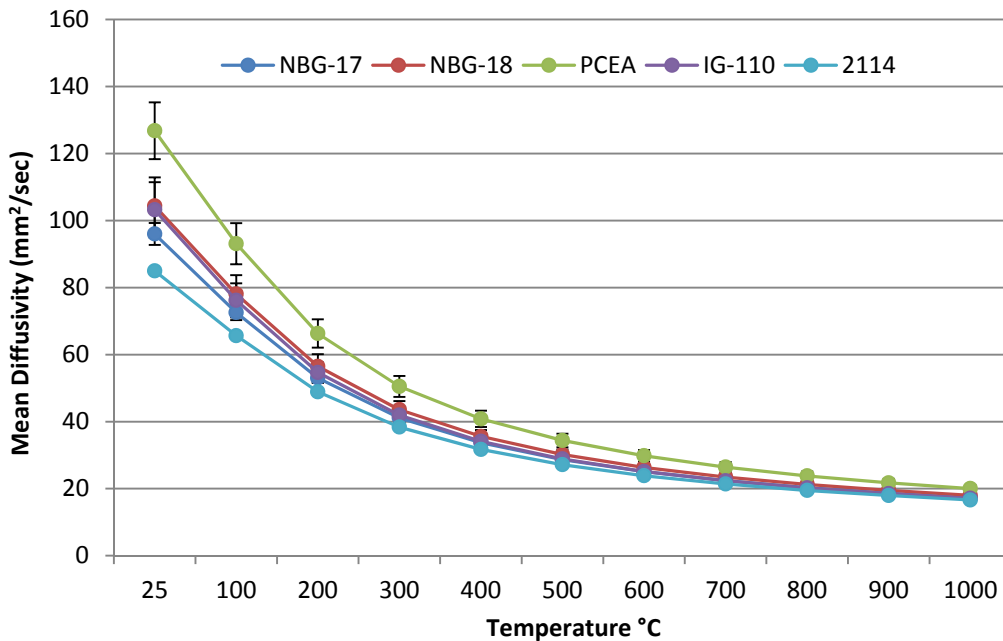


Figure 19. Thermal diffusivity for various graphite types as a function of temperature. Error bars represent ± 1 standard deviation.

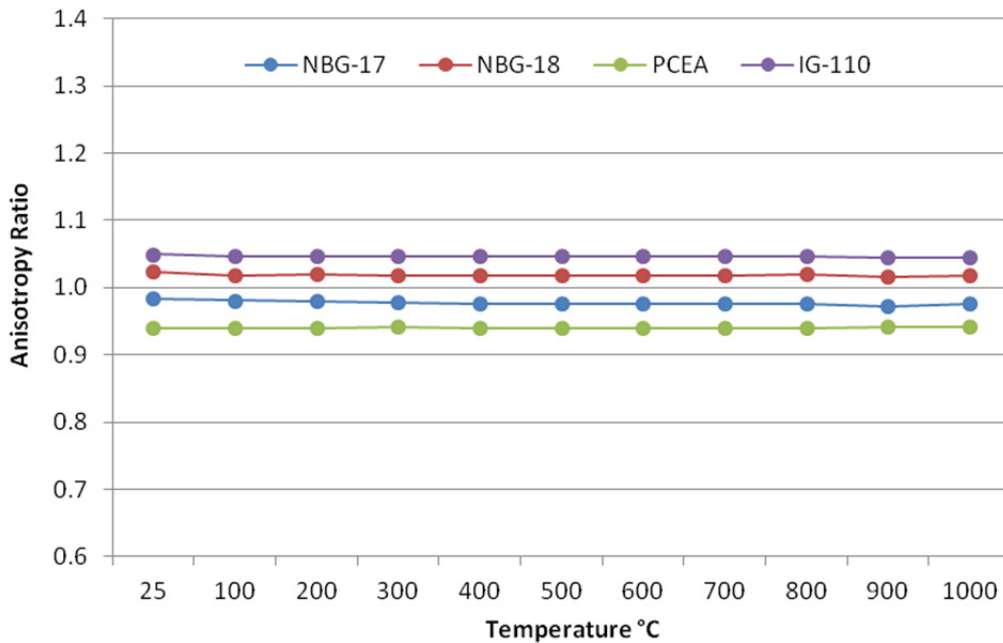


Figure 20. Thermal diffusivity anisotropy ratio for several types of nuclear grade graphite as a function of temperature.

6. REFERENCES

1. T. Burchell, R. Bratton, W. Windes, *NGNP Graphite Selection and Acquisition Strategy*, ORNL/TM-2007/153, September 2007.
2. W. Windes, T. Burchell, R. Bratton, "Graphite Technology Development Plan," PLN-2497, Rev. 1, October 2010.
3. R. L. Bratton and T. D. Burchell, *NGNP Graphite Testing and Qualification Specimen Selection Strategy*, INL/EXT-05-00269, May 2005.
4. M. Davenport, "AGC-4 Test Train Technical and Functional Requirements," TFR-875, July 2014.
5. TEV-2467, "AGC-4 Dose Rate and Shielding Evaluation," June 6, 2015.
6. DWG 778033, "ATR Advanced Graphite Capsule (AGC) AGC-4 Graphite Specimen Cutout Diagrams," October 06, 2014.
7. DWG 604554, "AGC-4 Test Train Facility Assembly," July 08, 2014.
8. DWG 603521, "AGC Graphite Specimen Holder Machining Details," Rev. 2, June 14, 2012.
9. DWG 604553, "AGC-4 Specimen Stack-up Arrangements," Rev. 1, April 21, 2015.
10. William Windes, W. David Swank, David Rohrbaugh, and Joseph Lord, *AGC-3 Graphite Preirradiation Data Analysis Report*, INL/EXT-13-30297, September 2013.
11. Y. S. Touloukian, *Thermophysical Properties of Matter - Thermal Diffusivity*, John Wiley & Sons Ltd., May 6, 1973.
12. PLN-2690, "Idaho National Laboratory Advanced Reactor Technologies Technology Development Office Quality Assurance Program Plan," Rev. 14, September 2015.
13. Form 241.21, "Records Transmittal," Rev. 6, June 19, 2014.

- 14 PLN-3319, "Records Management Plan for the INL Advanced Reactor Technologies Technology Development Office Program, Rev 4, May 6, 2015.
- 15 LWP-20000-01, "Conduct of Research Plan," Rev. 0, December 3, 2015.
- 16 PLN-4239, "AGC-4 Graphite Specimen Preirradiation Characterization Plan," Rev. 0, August 30, 2012.
- 17 MCP-1380, "Research and Development Test Control," Rev. 3, March 19, 2012.
- 18 NQA-1-2008; 1a-2009, "Quality Assurance Requirements for Nuclear Facility Applications," Requirement 11, Test Control, 2009.
- 19 LWP-21220, "Work Management," Rev. 12, July 17, 2014.
- 20 PLN-3319, "Records Management Plan for the INL Advanced Reactor Technologies Technology Development Office Program," Rev. 4, May 6, 2015.
- 21 LWP-12033, "Personnel Qualification and Certification," Rev. 7, February 24, 2016.
- 22 LWP-13455, "Control of Measuring and Test Equipment," Rev. 4, December 10, 2015.
- 23 ASTM C611-98(2010), "Standard Test Method for Electrical Resistivity of Manufactured Carbon and Graphite Articles at Room Temperature," ASTM International, 2010.
- 24 ASTM C769-98(2005), "Standard Test Method for Sonic Velocity in Manufactured Carbon and Graphite Materials for Use in Obtaining an Approximate Value of Young's Modulus," ASTM International, 2005.
- 25 ASTM C747-93(2010), "Standard Test Method for Moduli of Elasticity and Fundamental Frequencies of Carbon and Graphite Materials by Sonic Resonance," ASTM International, 2010.
- 26 ASTM C1259-08, "Standard Test Method for Dynamic Young's Modulus, Shear Modulus, and Poisson's Ratio for Advanced Ceramics by Impulse Excitation of Vibration," ASTM International, 2008.
- 27 ASTM E228-06, "Standard Test Method for Linear Expansion of Solid Materials with a Push-Rod Dilatometer," ASTM International, 2006.
- 28 R. D. Cowan, "Pulse Method of Measuring Thermal Diffusivity at High Temperatures," *Journal of Applied Physics*, Vol. 34, No. 4, 1963, p. 926.
- 29 Y. S. Touloukian, *Thermophysical Properties of Matter - Thermal Diffusivity*, John Wiley & Sons Ltd., May 6, 1973.

Appendix A

AGC-4 Post-Irradiation Data

Appendix A AGC-4 Post-Irradiation Data

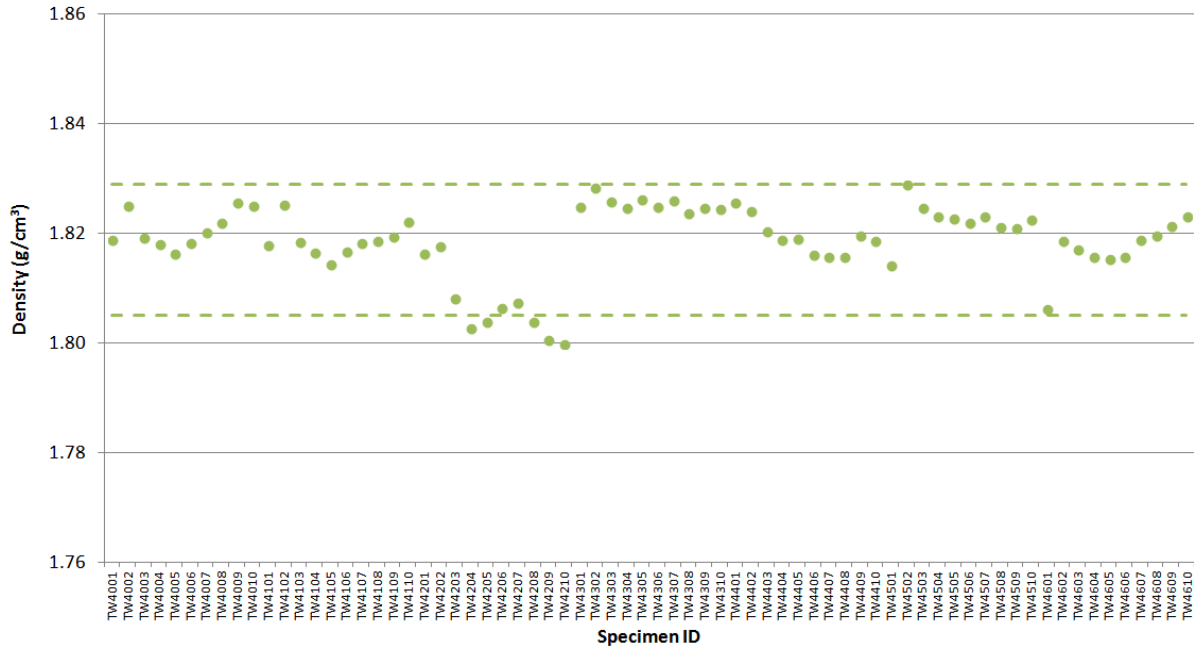


Figure A-1. 2114 Creep specimen density.

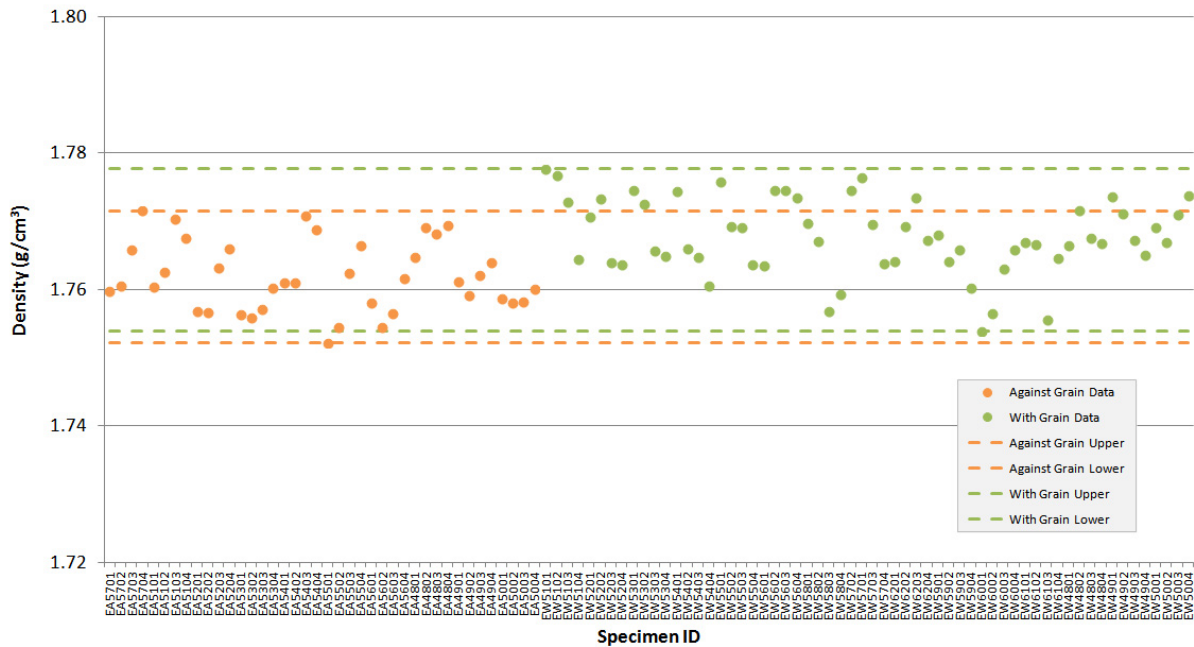


Figure A-2. IG-110 Creep specimen density.

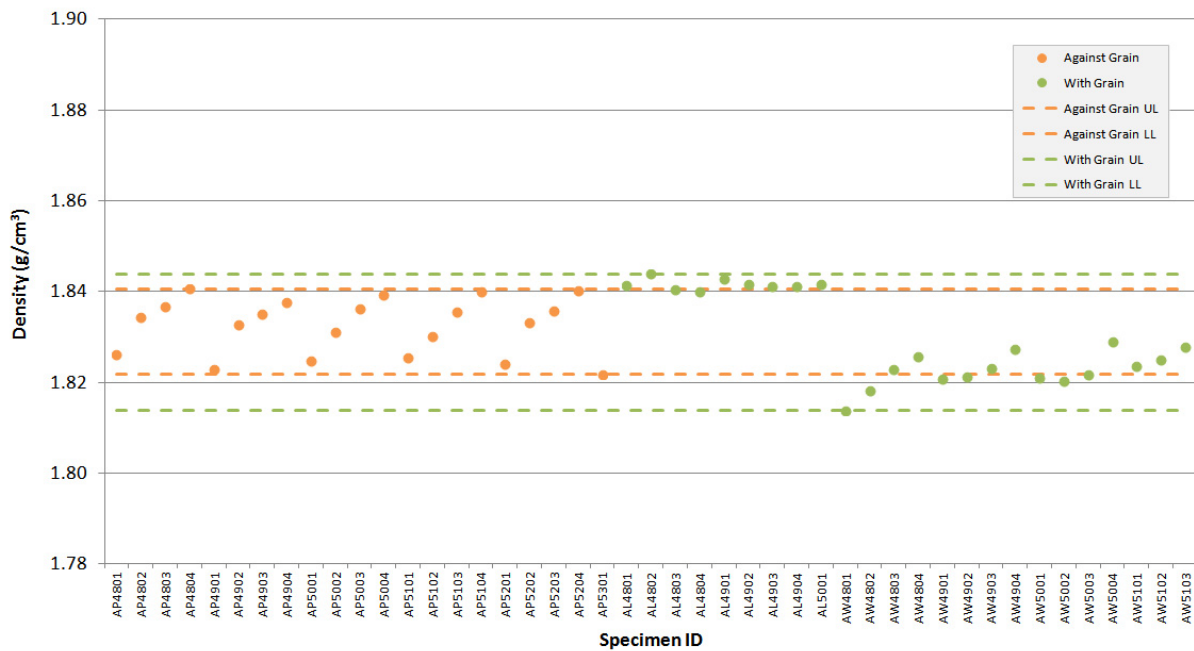


Figure A-3. NBG-17 creep specimen density.

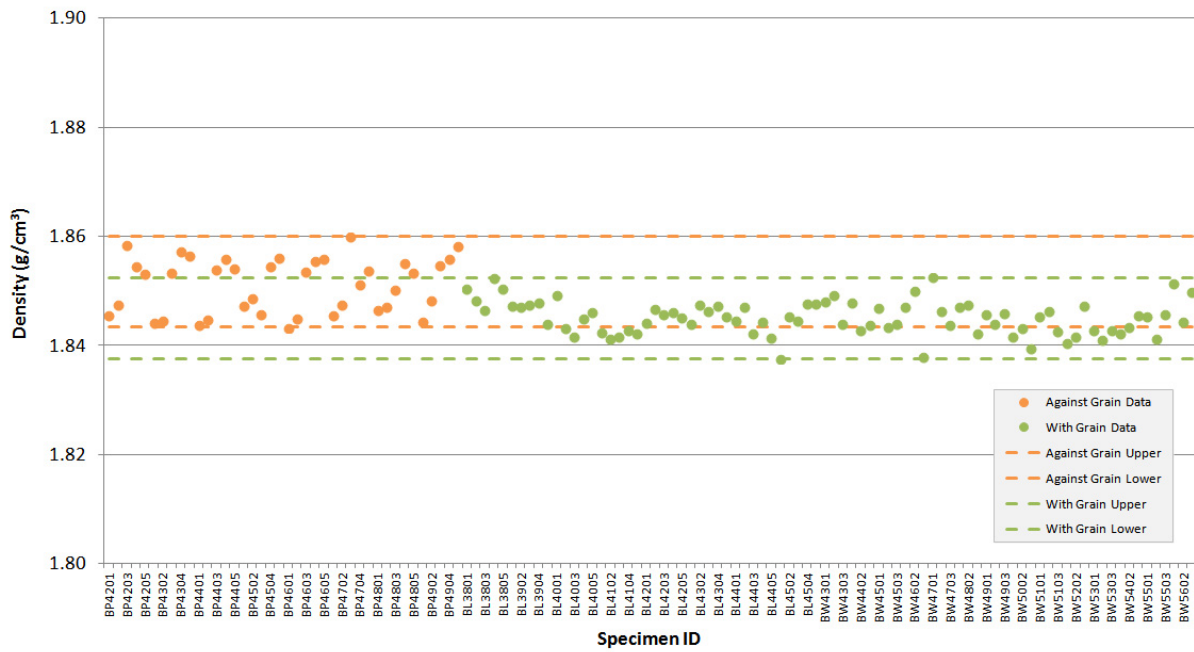


Figure A-4. NBG-18 creep specimen density.

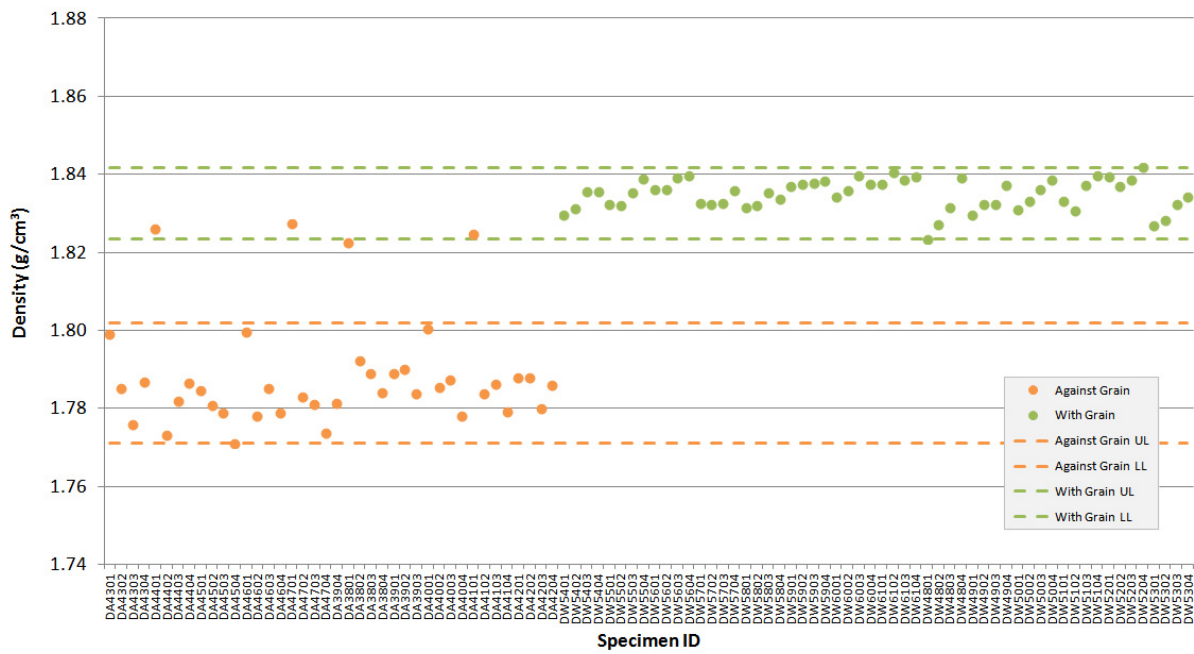


Figure A-5. PCEA creep specimen density.

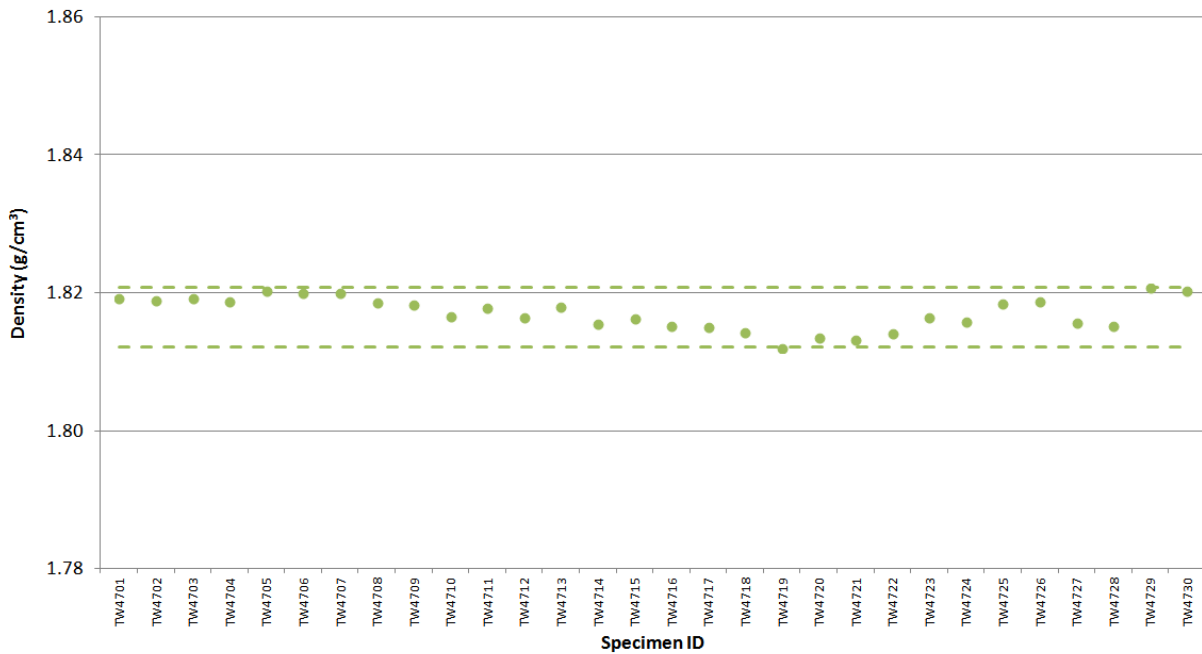


Figure A-6. 2114 piggyback specimen density.

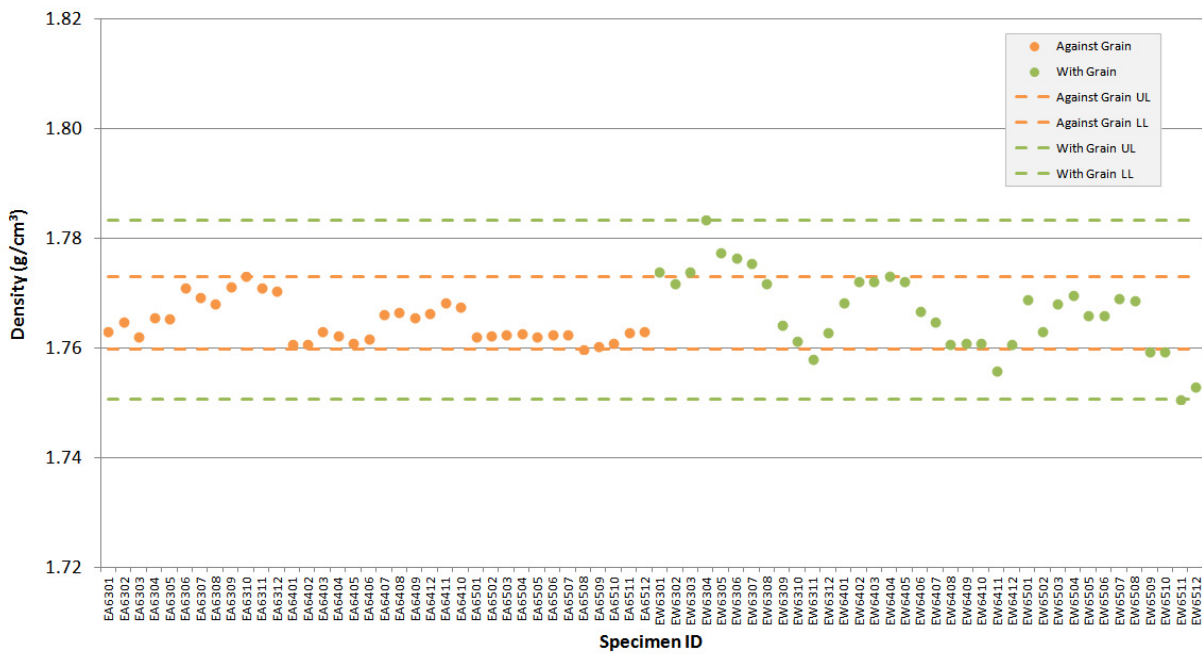


Figure A-7. IG-110 piggyback specimen density.

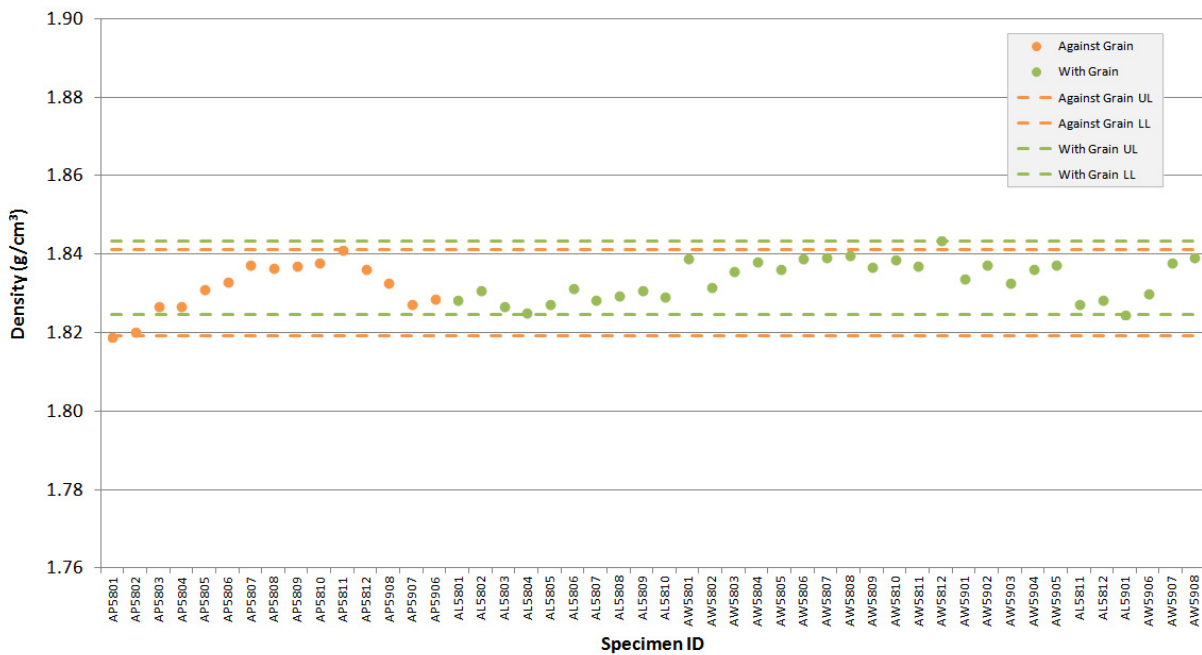


Figure A-8. NBG-17 piggyback specimen density.

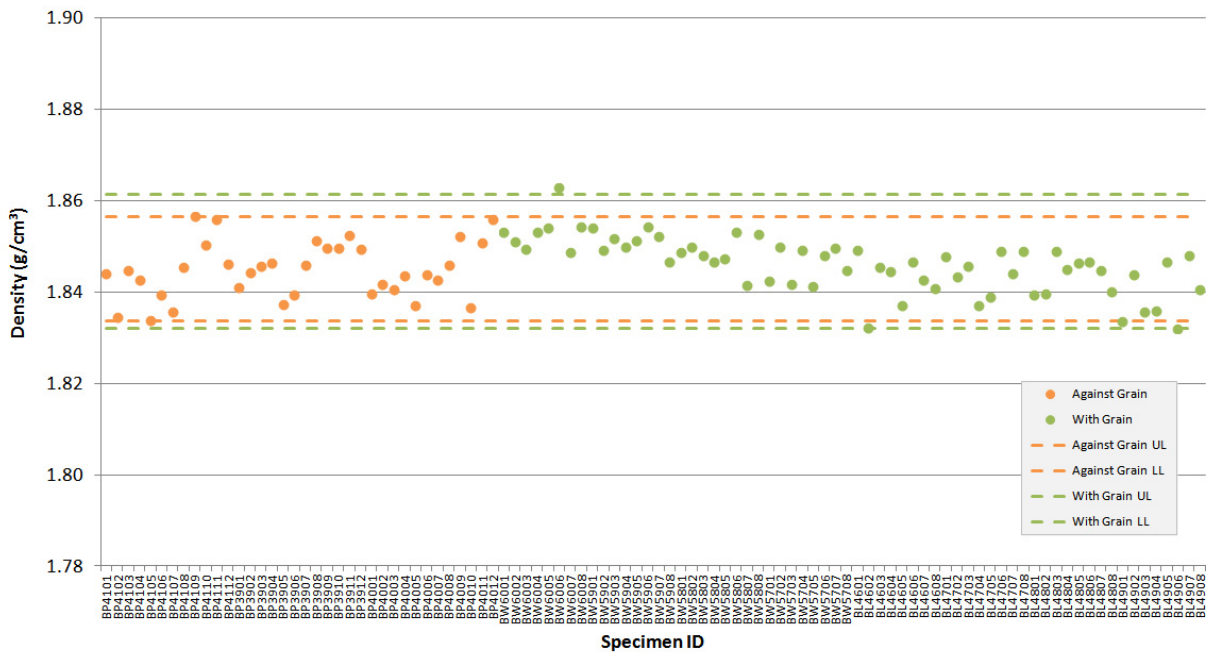


Figure A-9. NBG-18 piggyback specimen density.

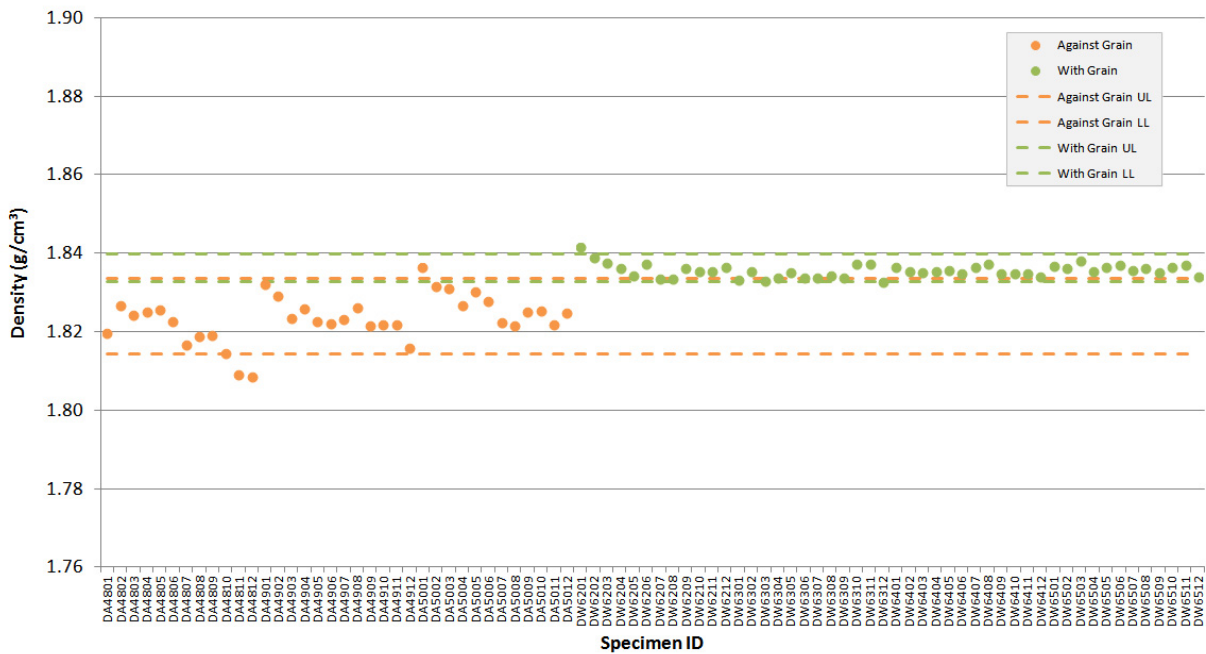


Figure A-10. PCEA piggyback specimen density.

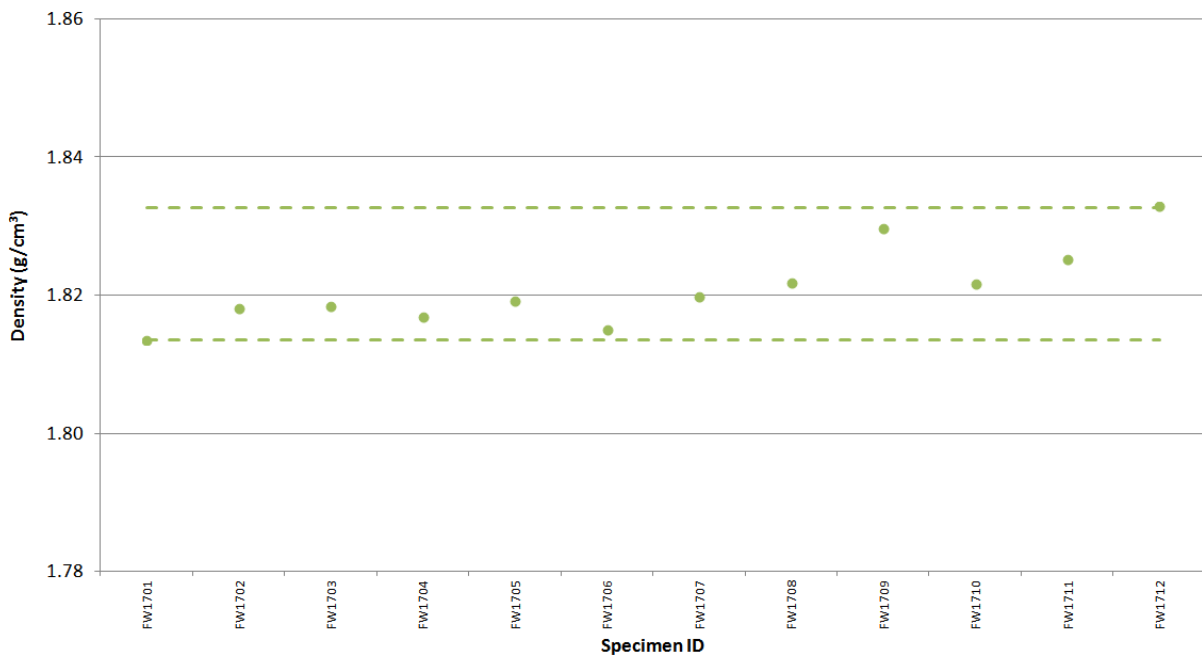


Figure A-11. IG-430 piggyback specimen density.

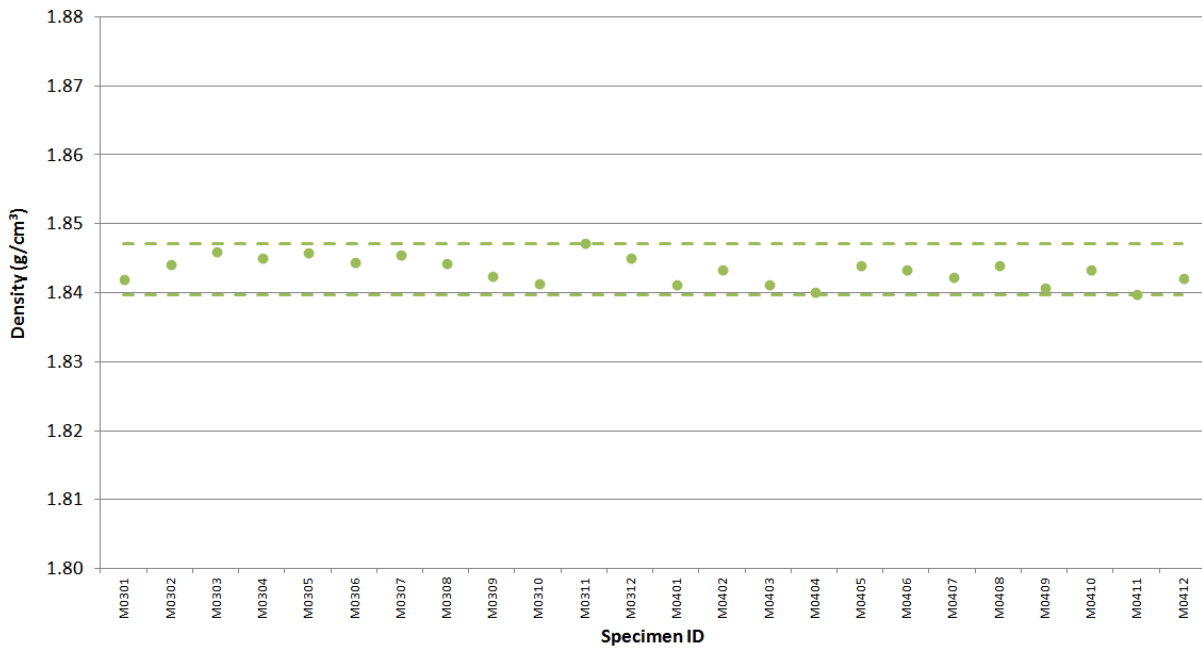


Figure A-12. NBG-25 piggyback specimen density.

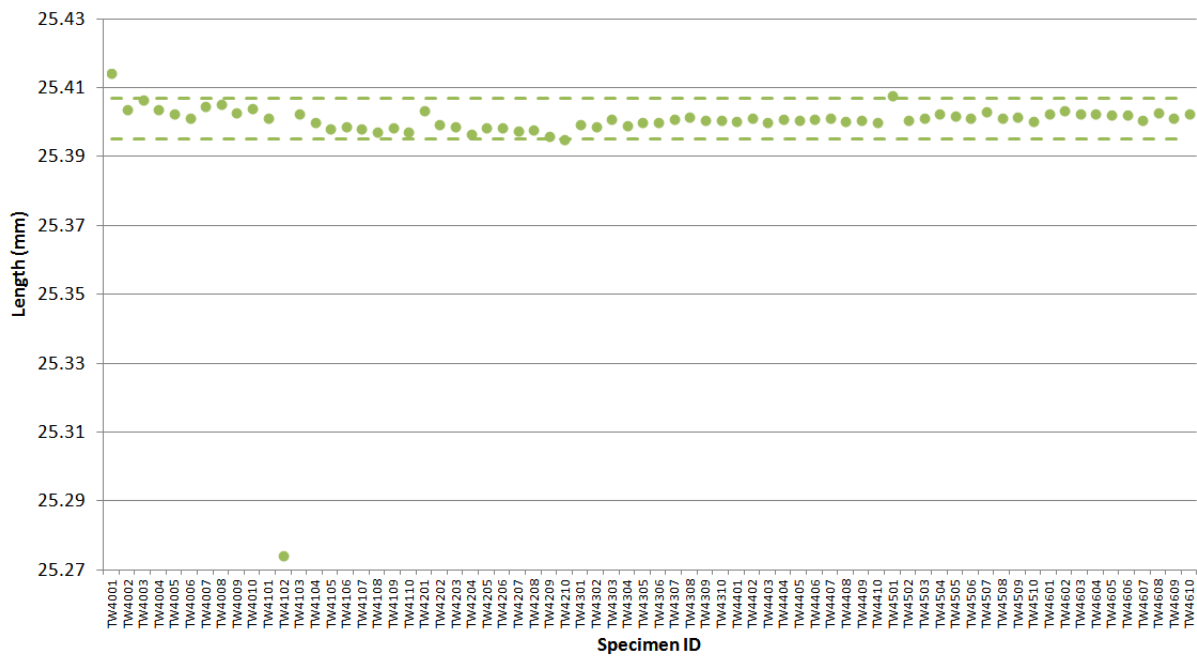


Figure A-13. 2114 creep specimen length.



Figure A-14. IG-110 creep specimen length.

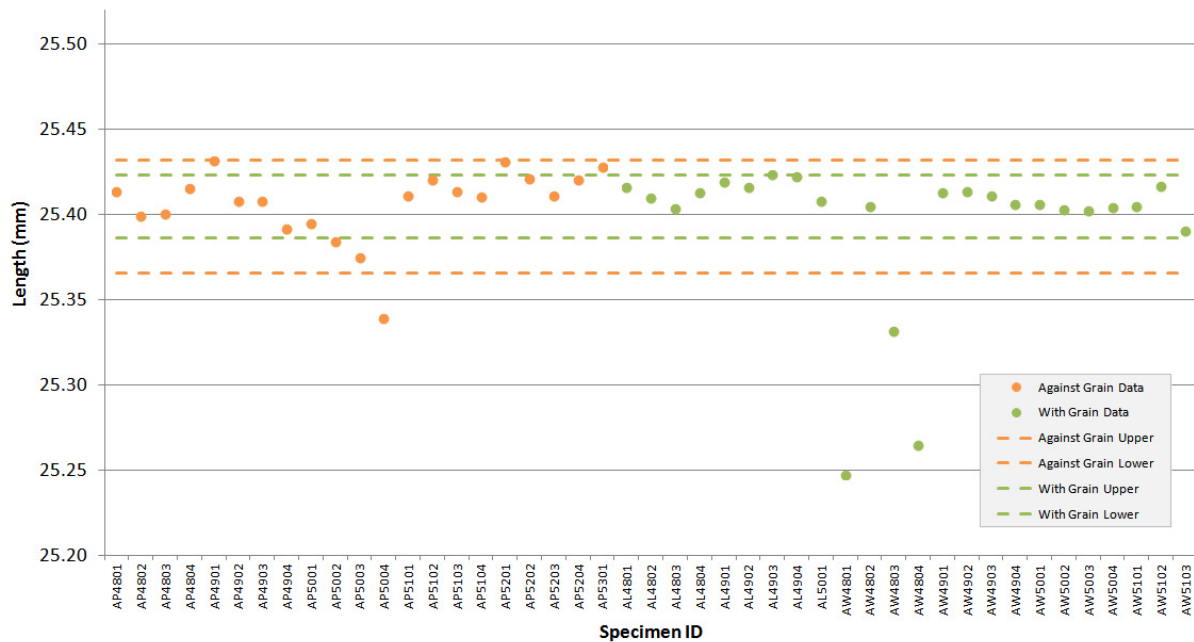


Figure A-15. NBG-17 creep specimen length.

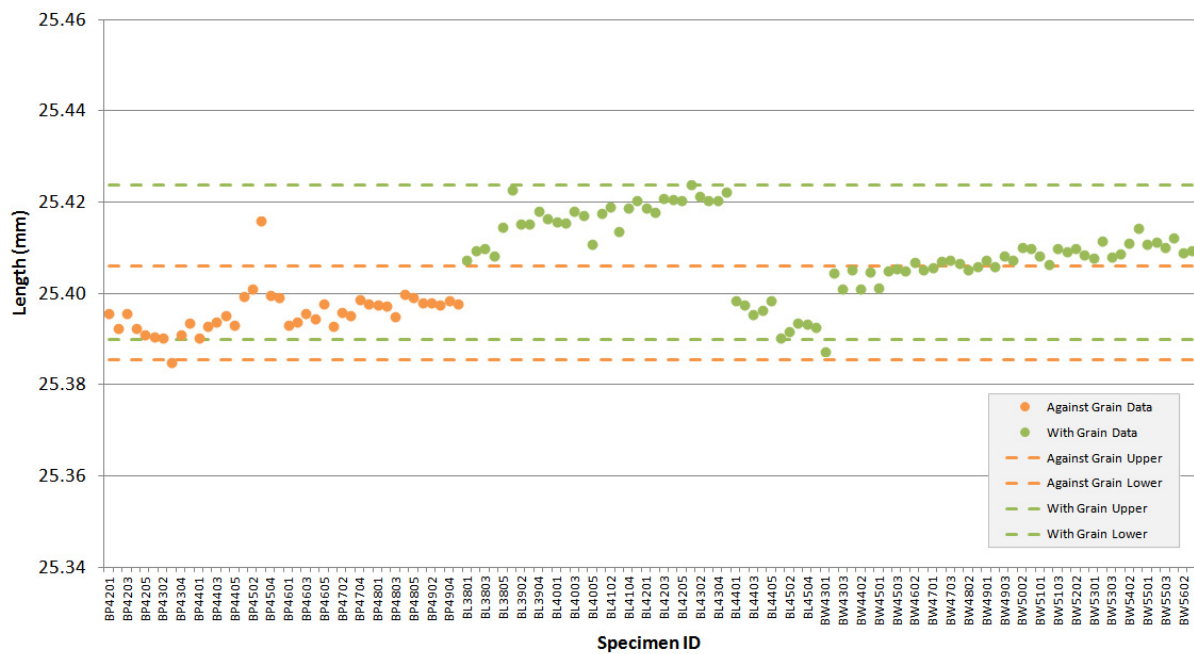


Figure A-16. NBG-18 creep specimen length.

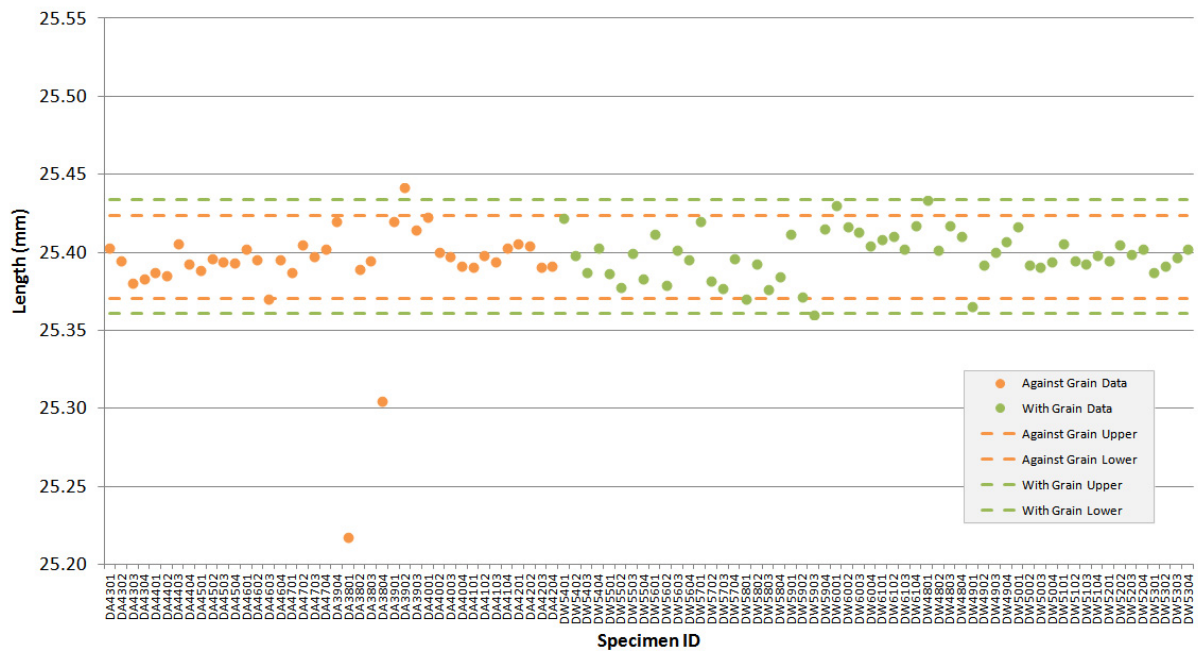


Figure A-17. PCEA creep specimen length.

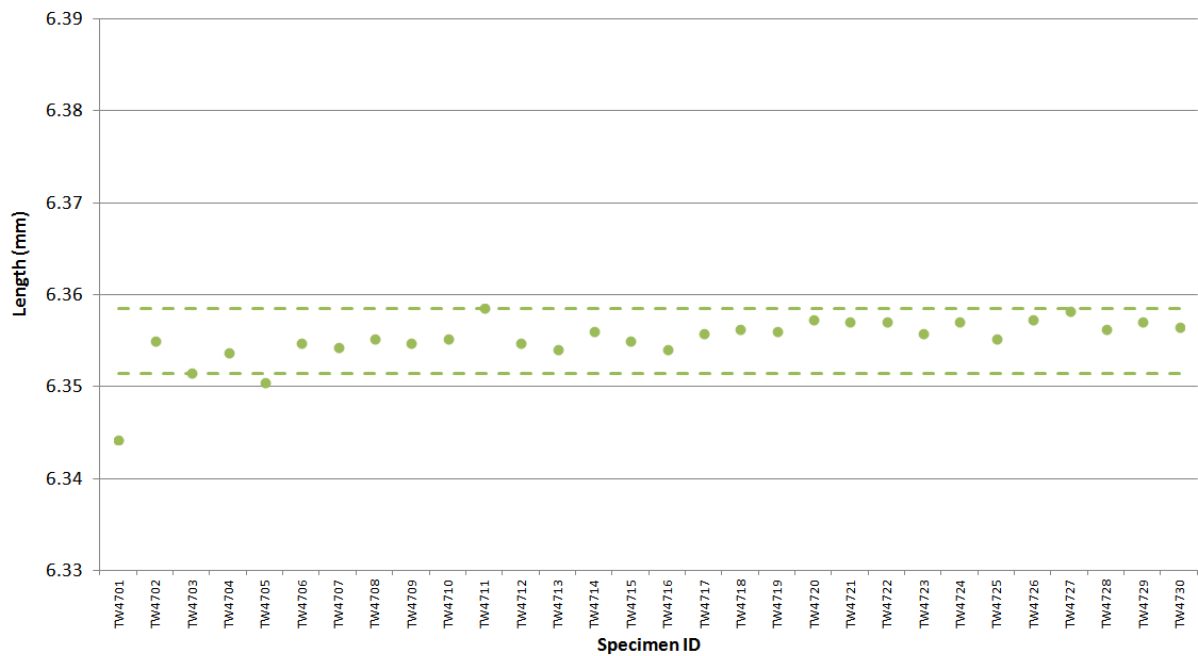


Figure A-18. 2114 piggyback specimen length.

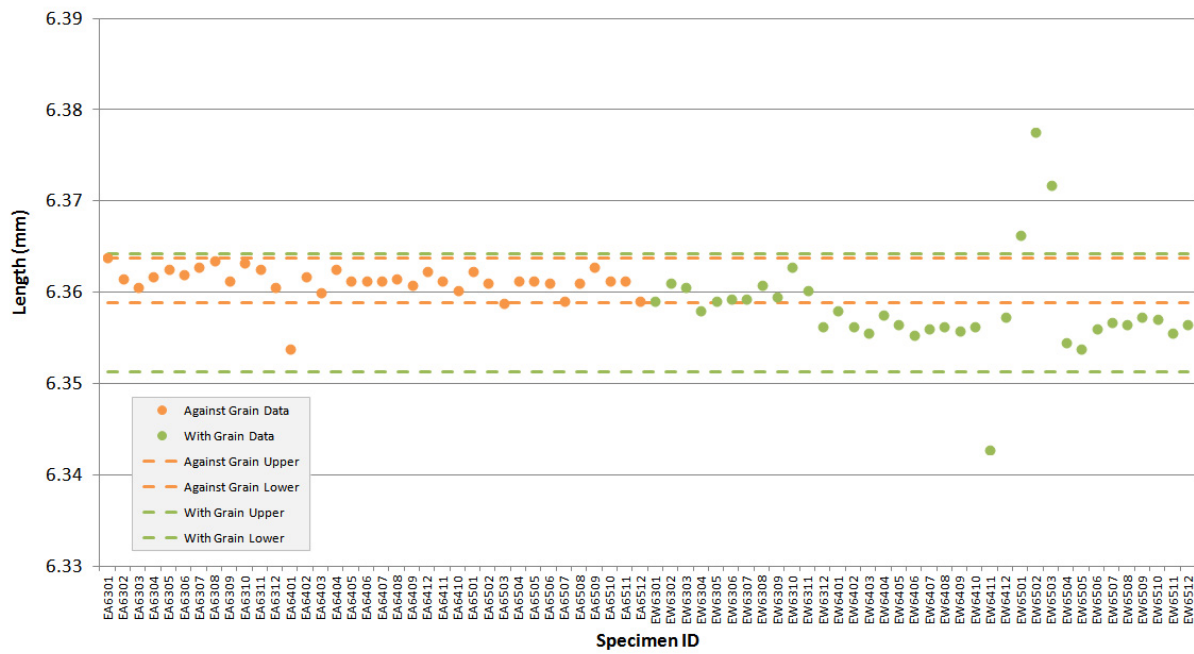


Figure A-19. IG-110 piggyback specimen length.

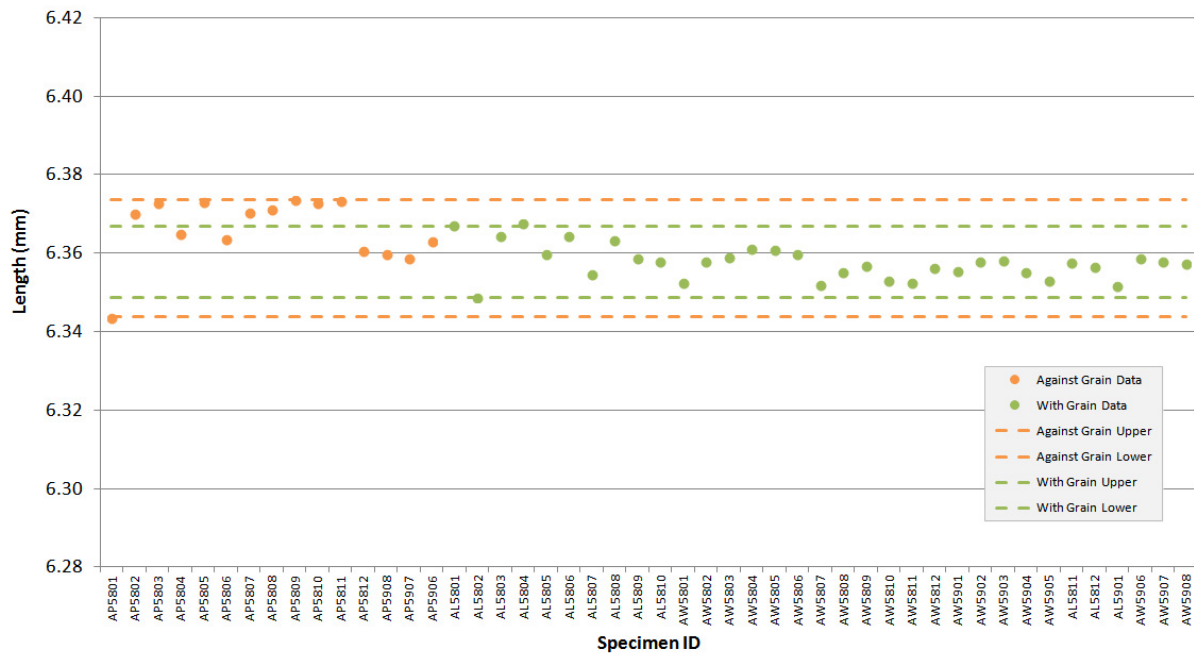


Figure A-20. NBG-17 piggyback specimen length.

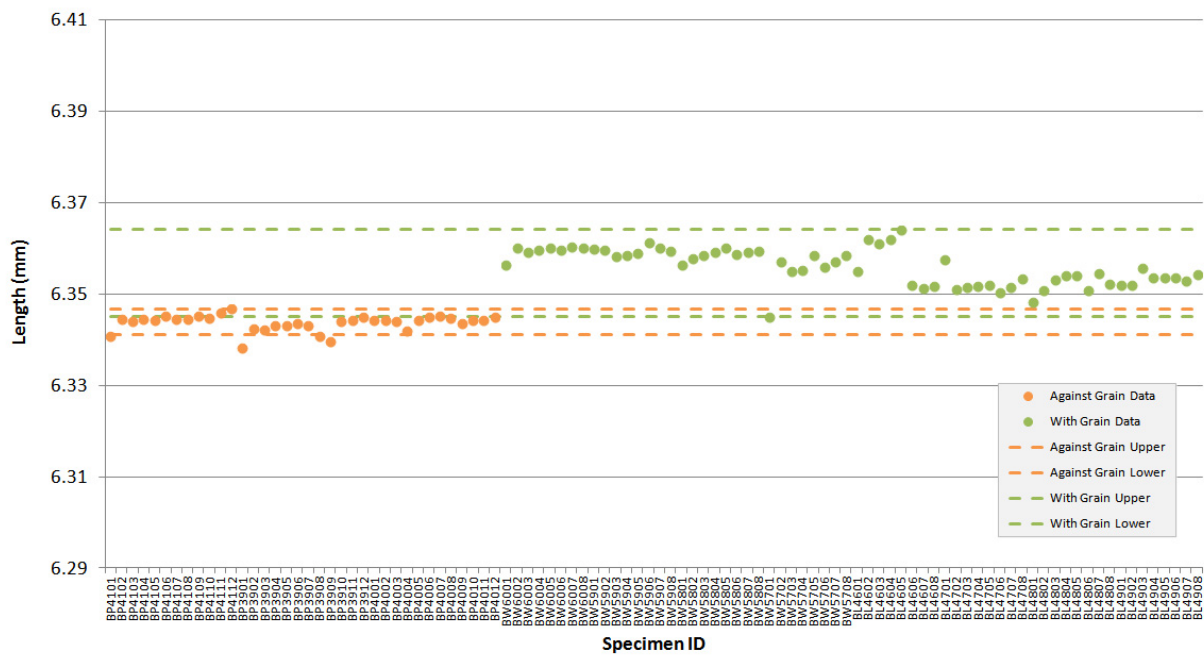


Figure A-21. NBG-18 piggyback specimen length.

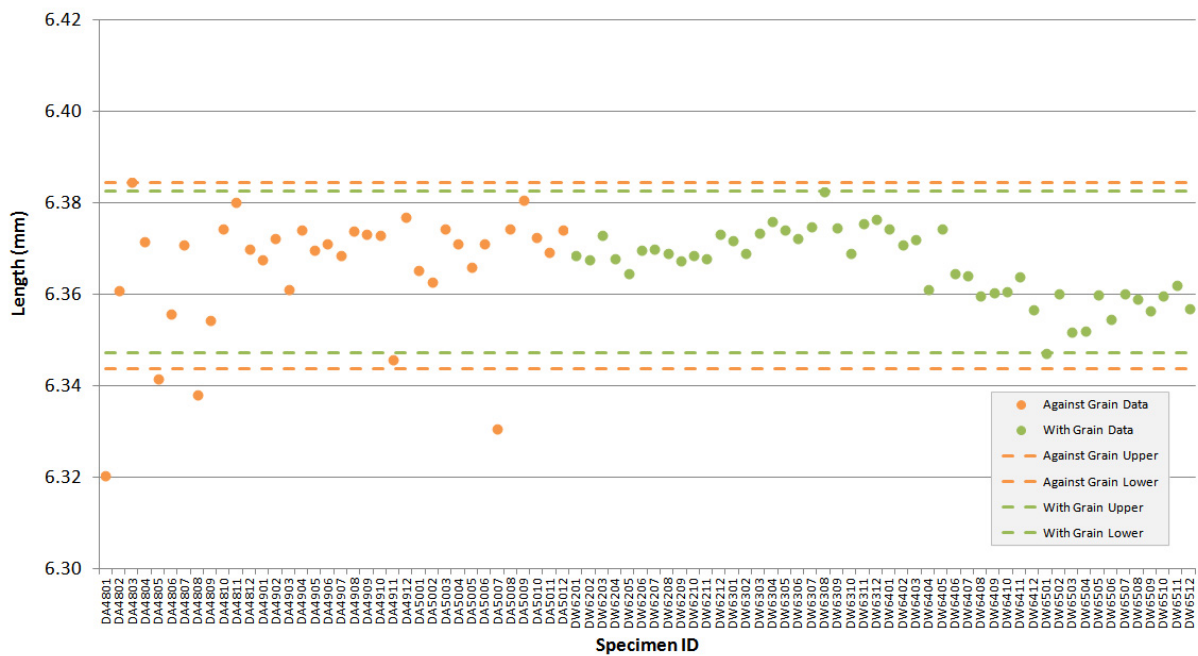


Figure A-22. PCEA piggyback specimen length.

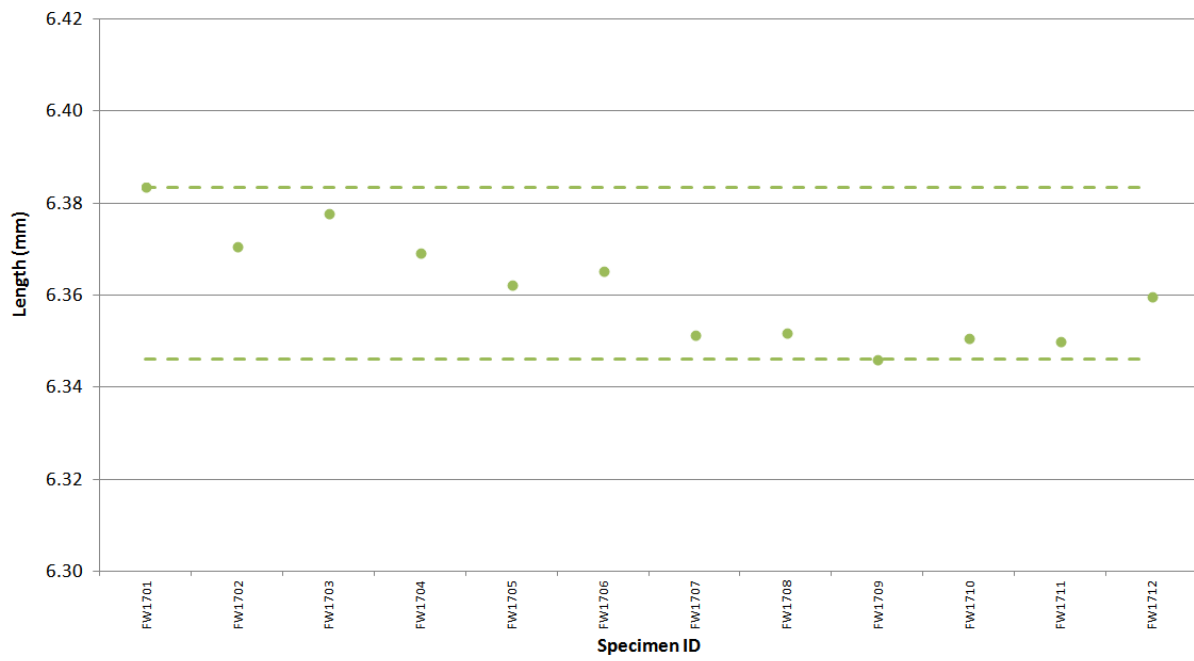


Figure A-23. IG-430 piggyback specimen length.

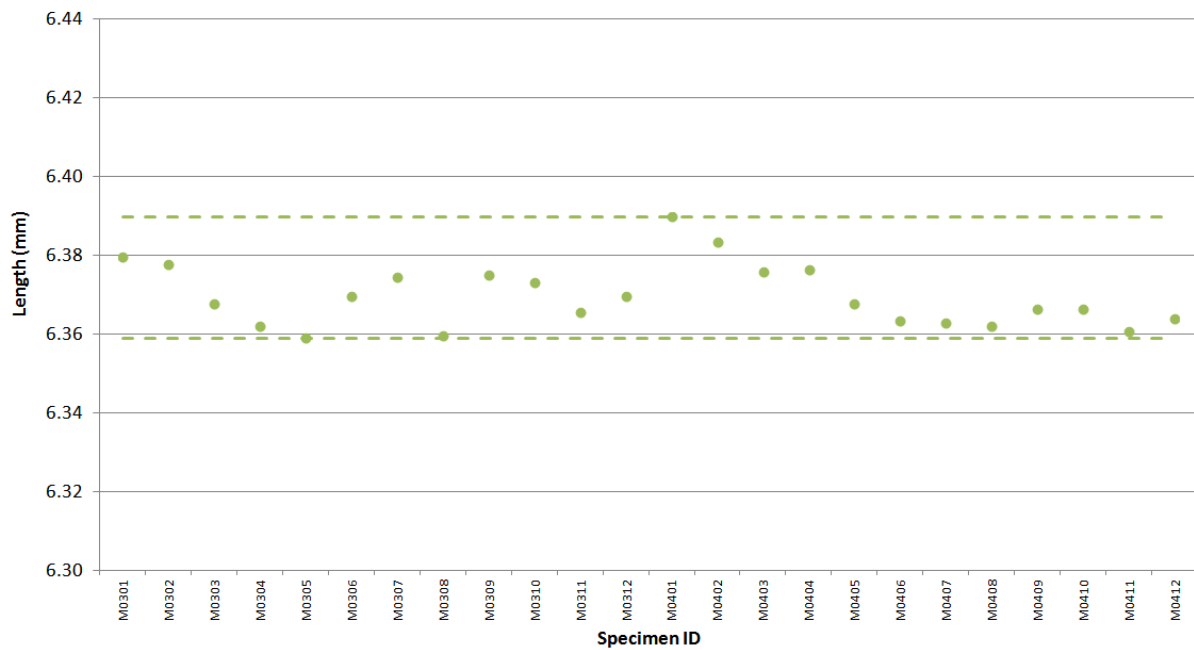


Figure A-24. NBG-25 piggyback specimen length.

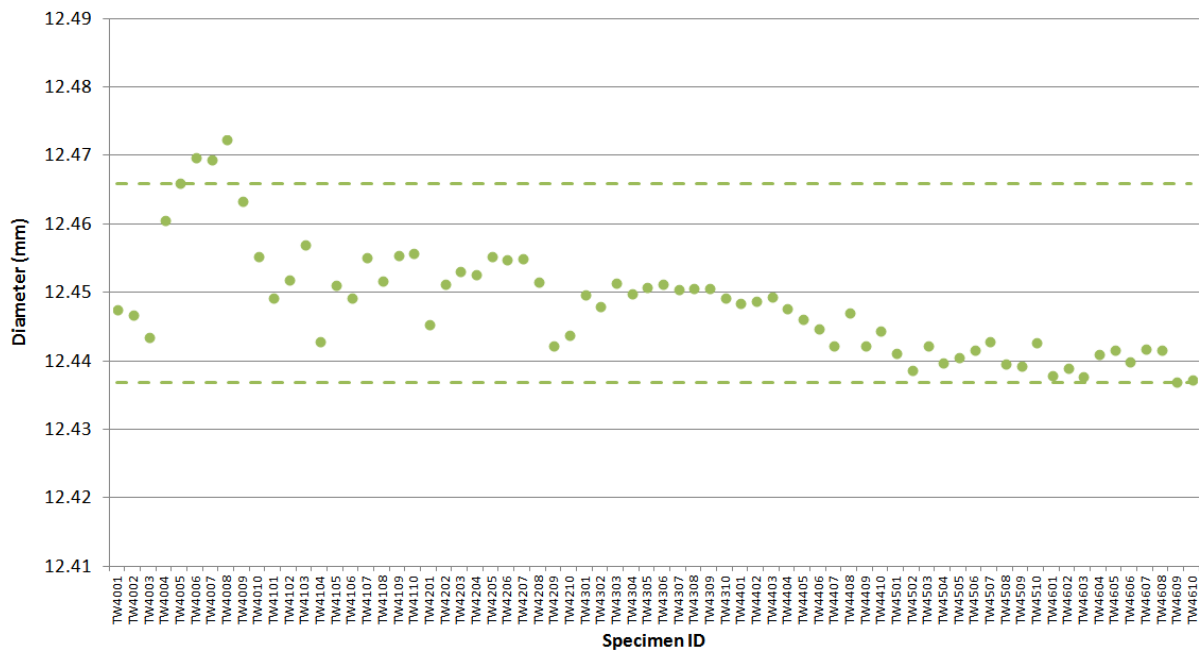


Figure A-25. 2114 creep specimen diameter.

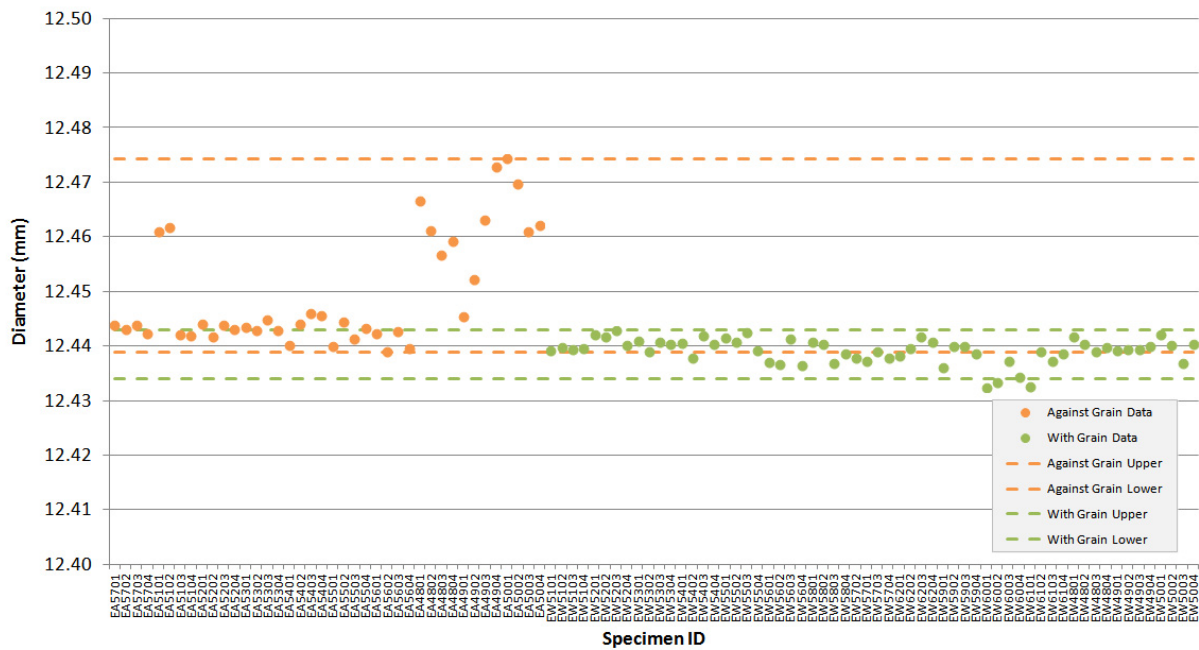


Figure A-26. IG-110 creep specimen diameter.

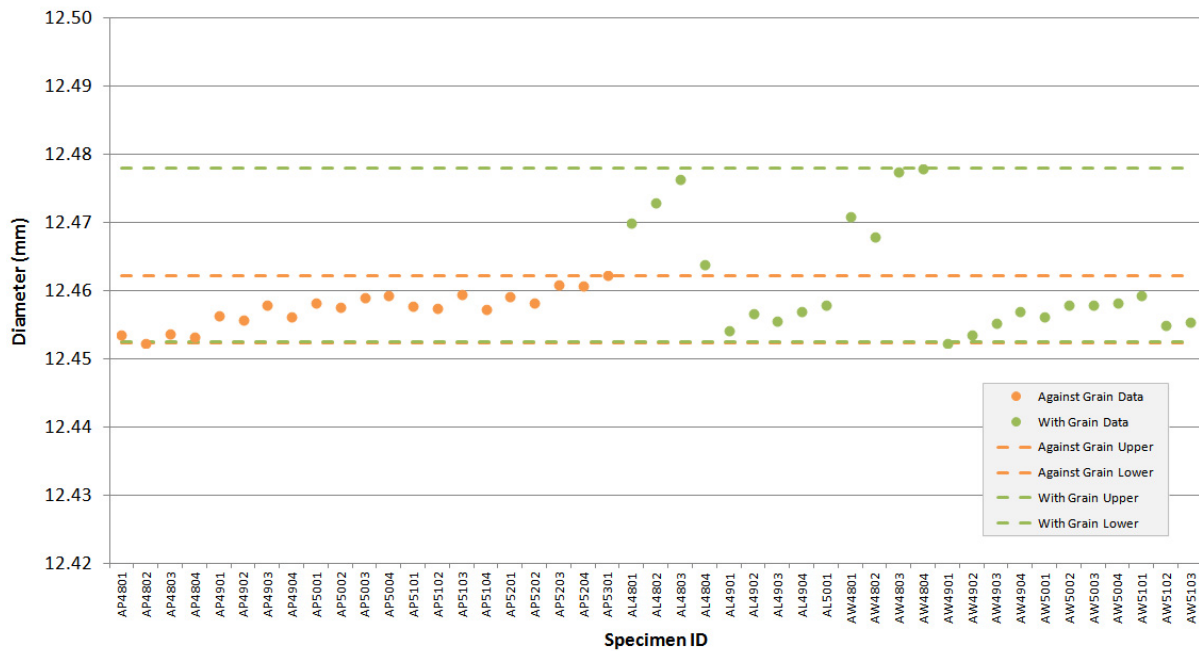


Figure A-27. NBG-17 creep specimen diameter.

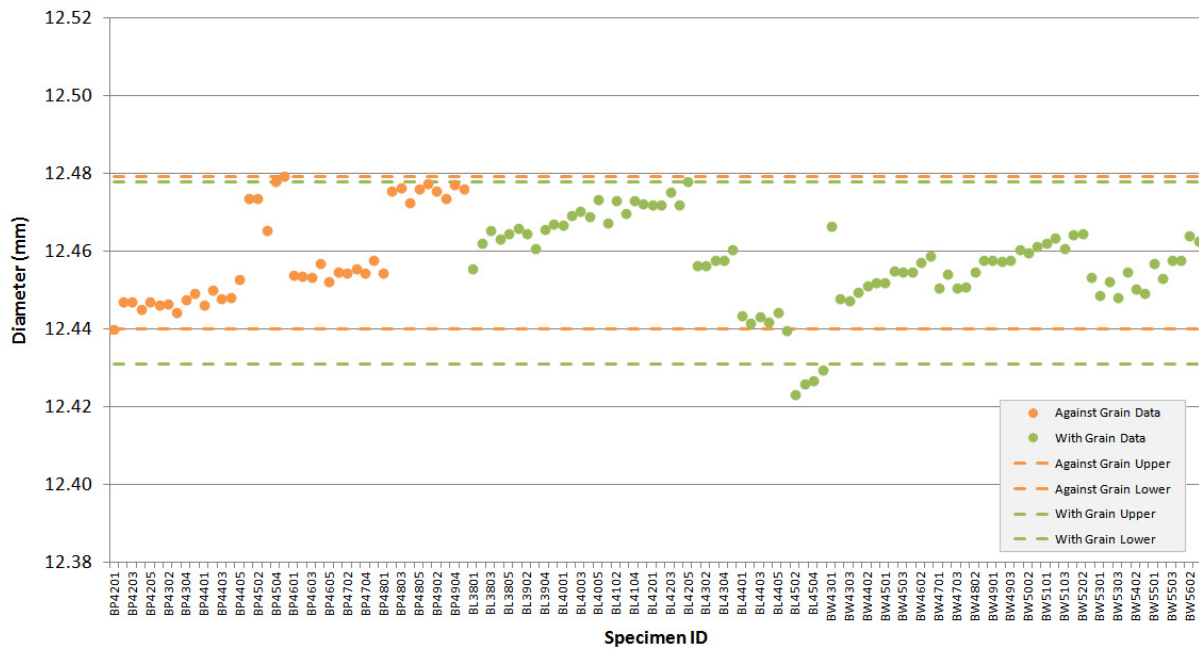


Figure A-28. NBG-18 creep specimen diameter.

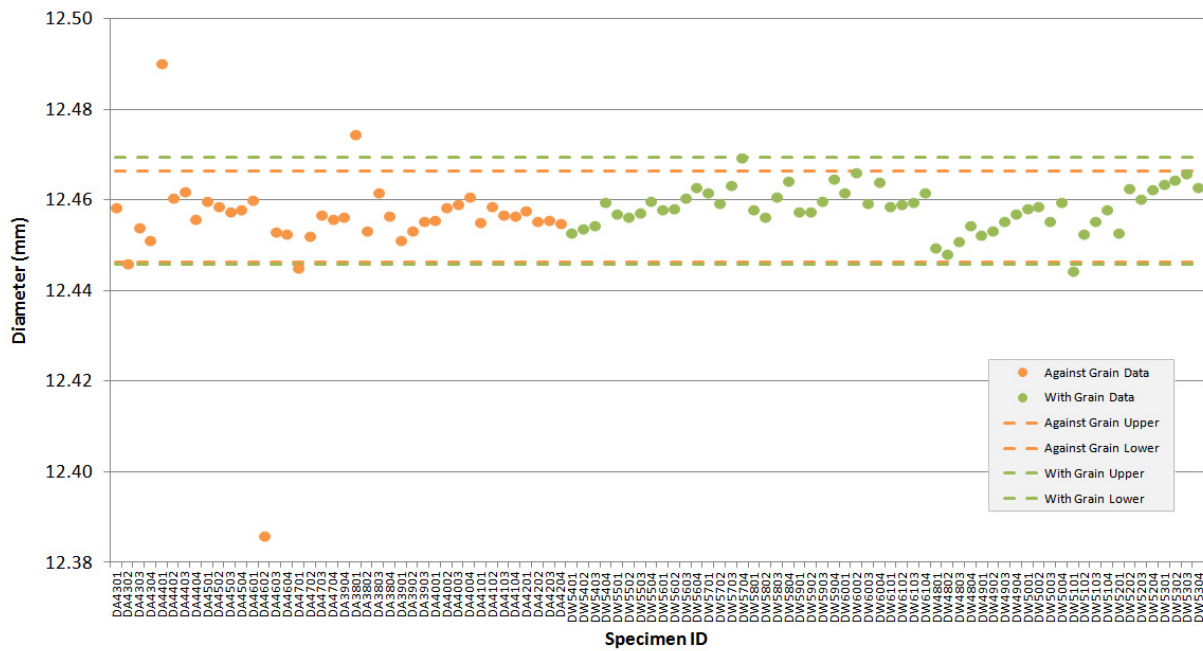


Figure A-29. PCEA creep specimen diameter.

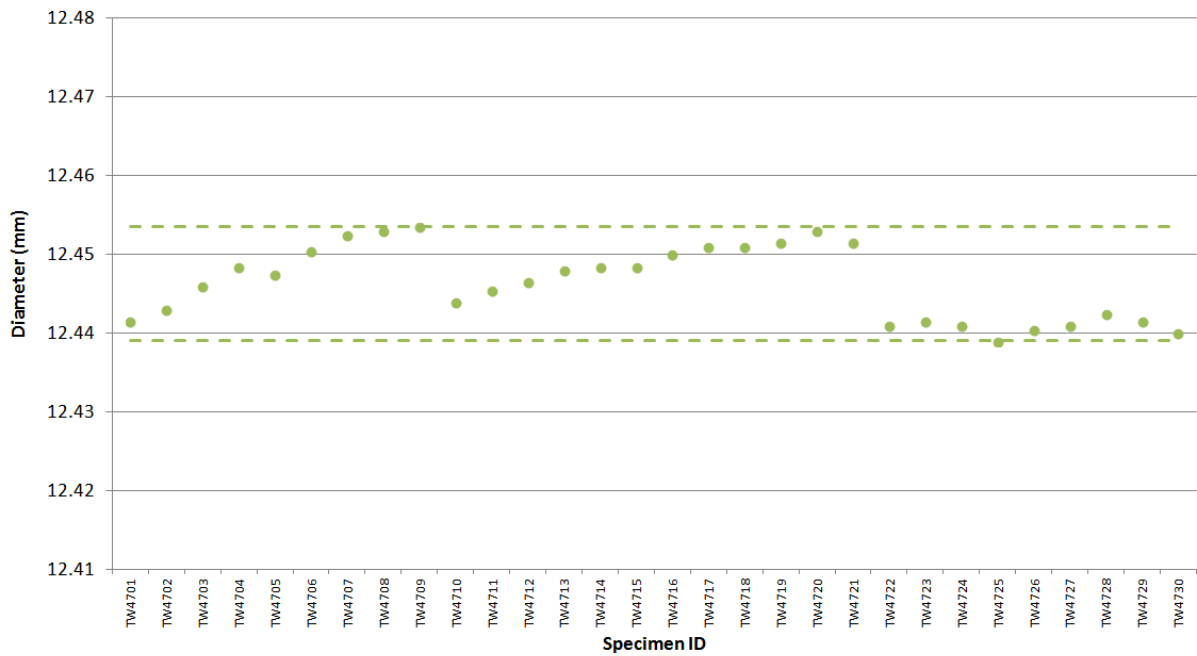


Figure A-30. 2114 piggyback specimen diameter.

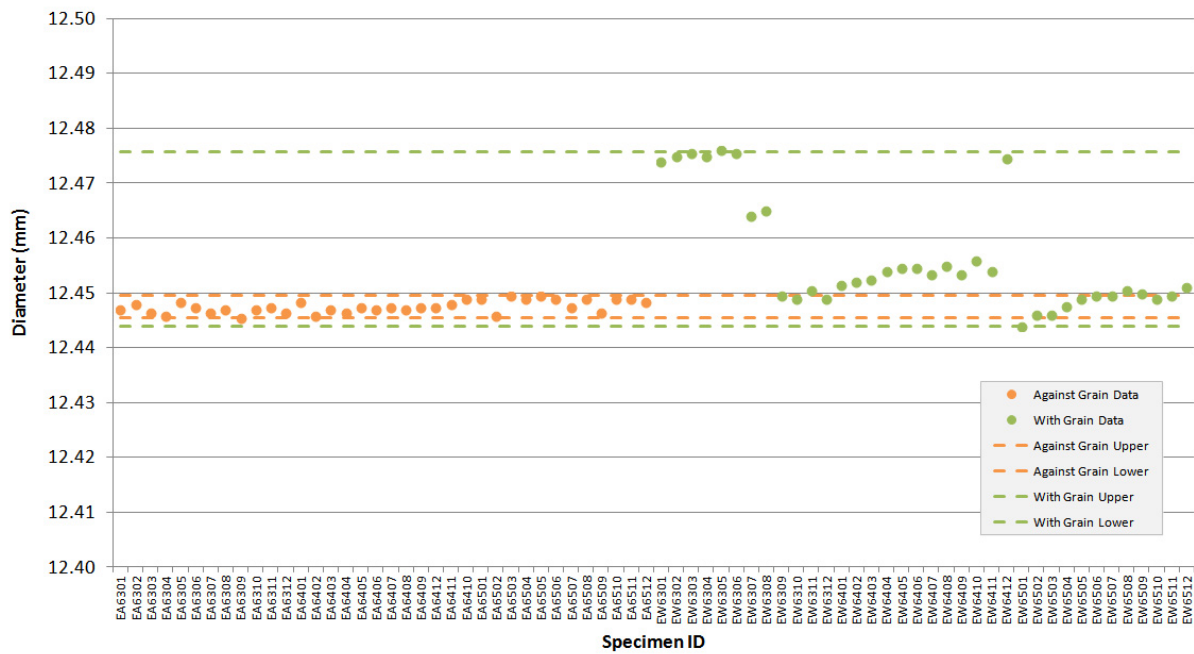


Figure A-31. IG-110 piggyback specimen diameter.

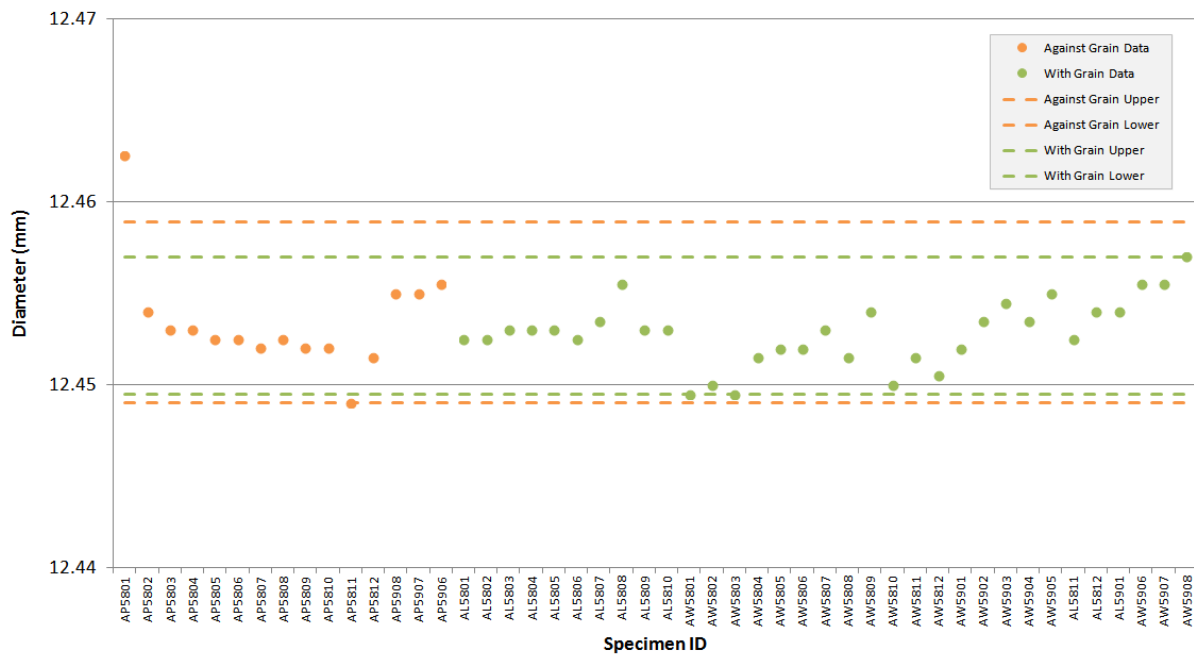


Figure A-32. NBG-17 piggyback specimen diameter.

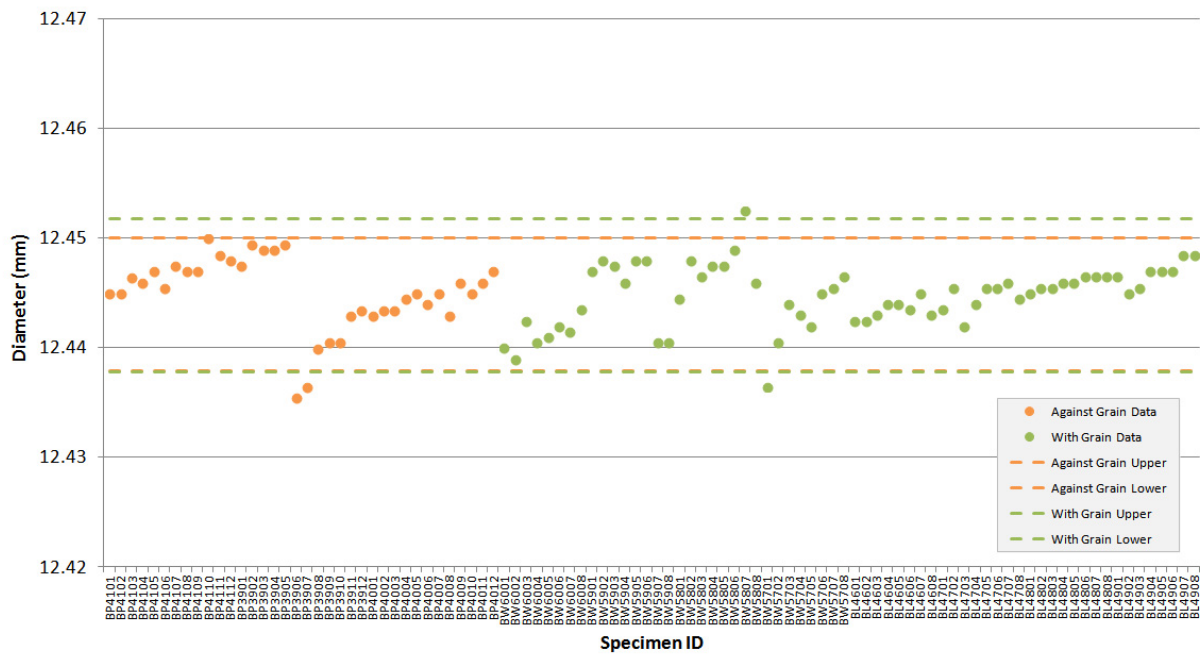


Figure A-33. NBG-18 piggyback specimen diameter.

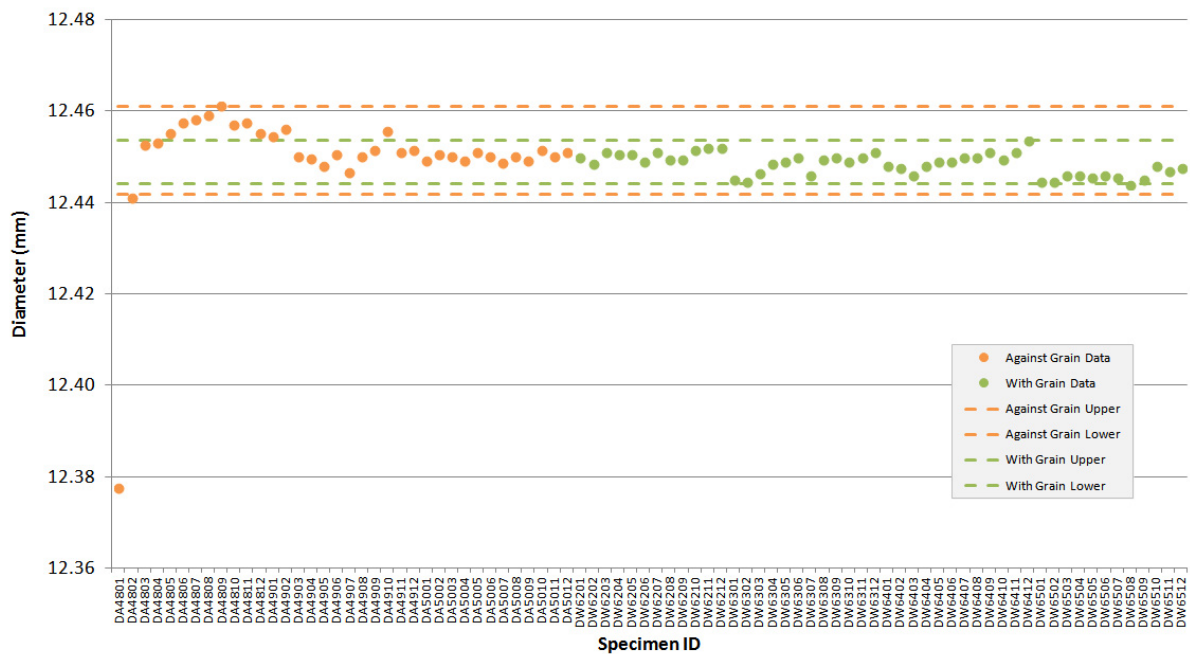


Figure A-34. PCEA piggyback specimen diameter.

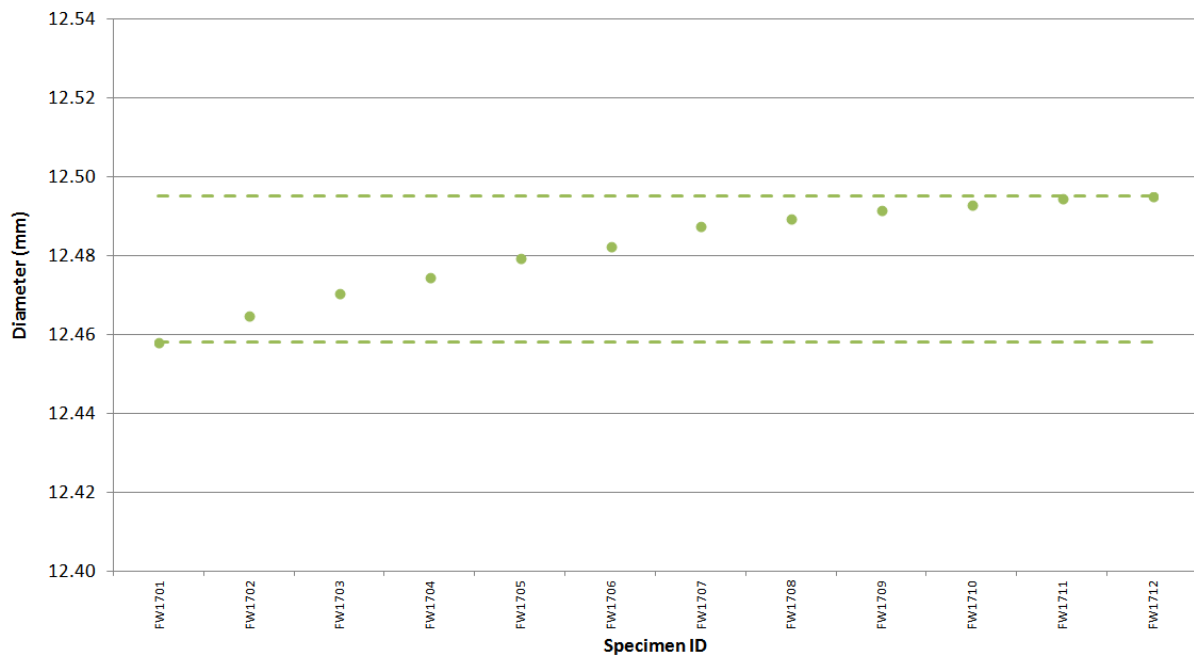


Figure A-35. IG-430 piggyback specimen diameter.

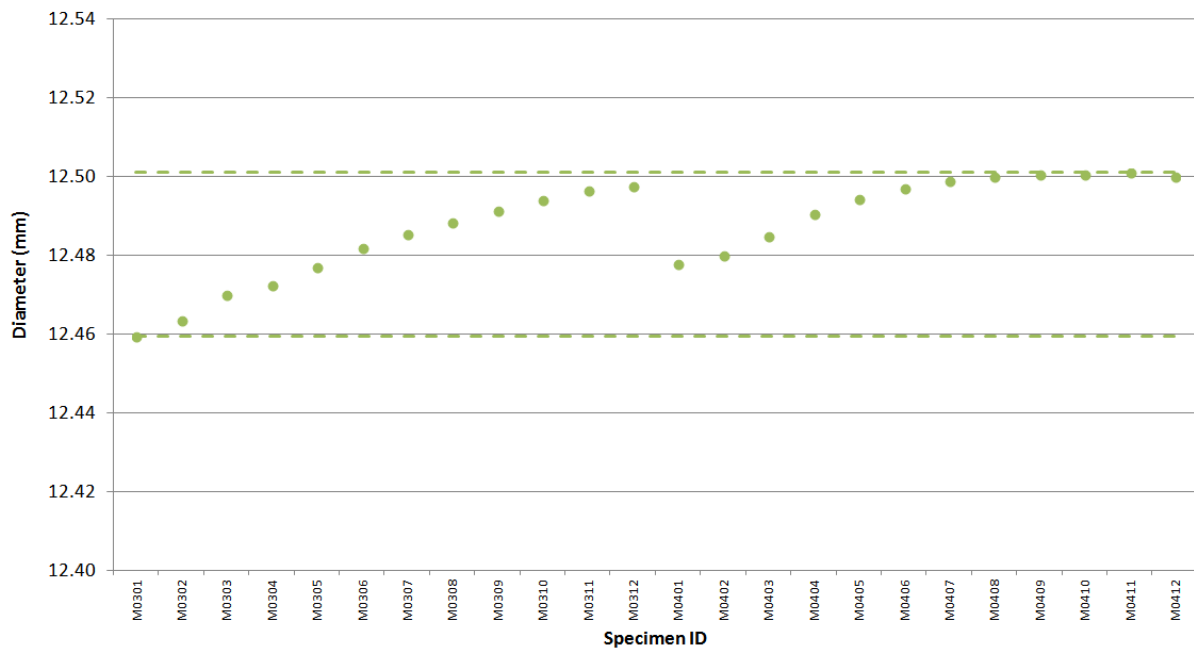


Figure A-36. NBG-25 piggyback specimen diameter.

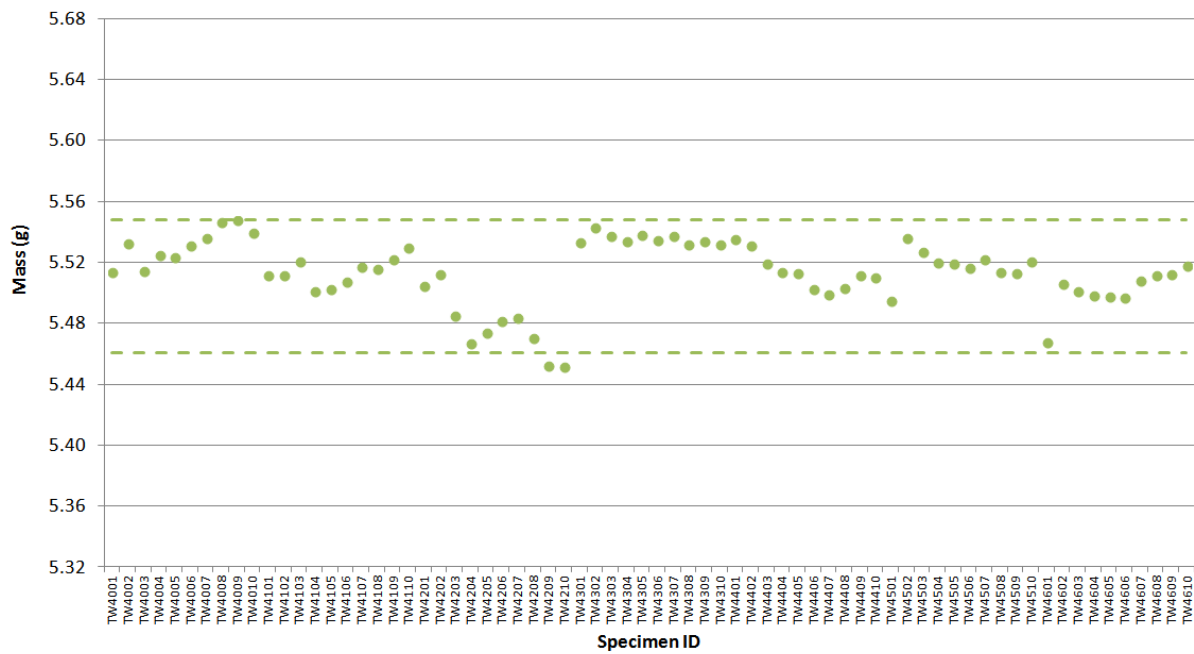


Figure A-37. 2114 creep specimen mass.

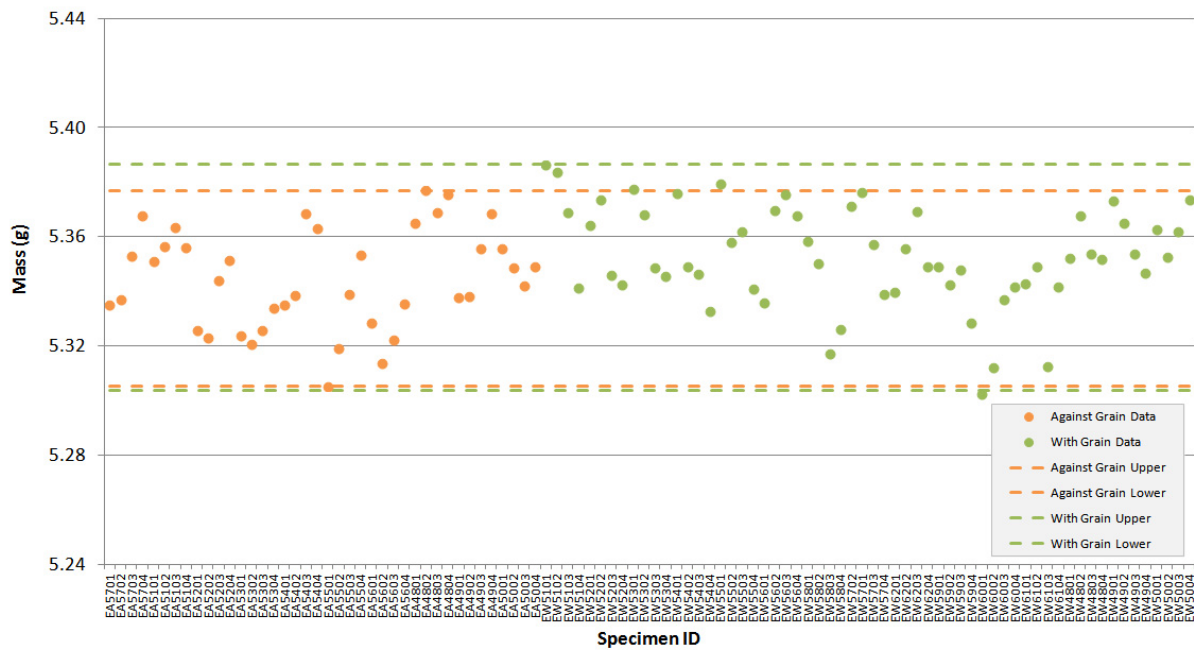


Figure A-38. IG-110 creep specimen mass.

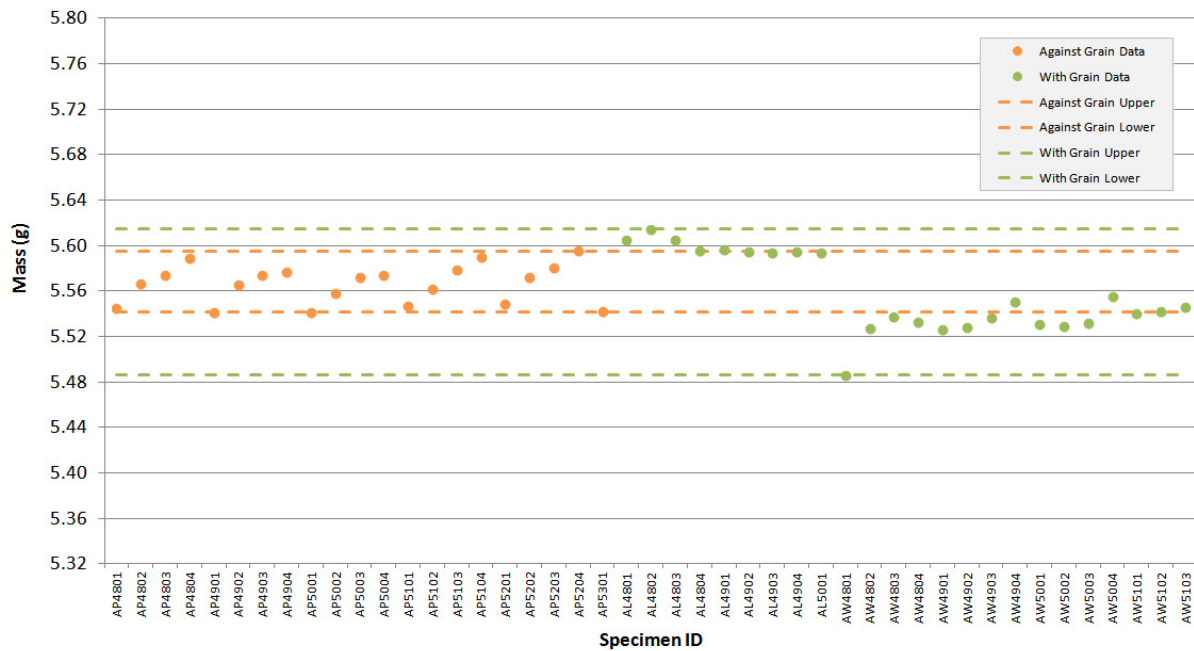


Figure A-39. NBG-17 creep specimen mass.

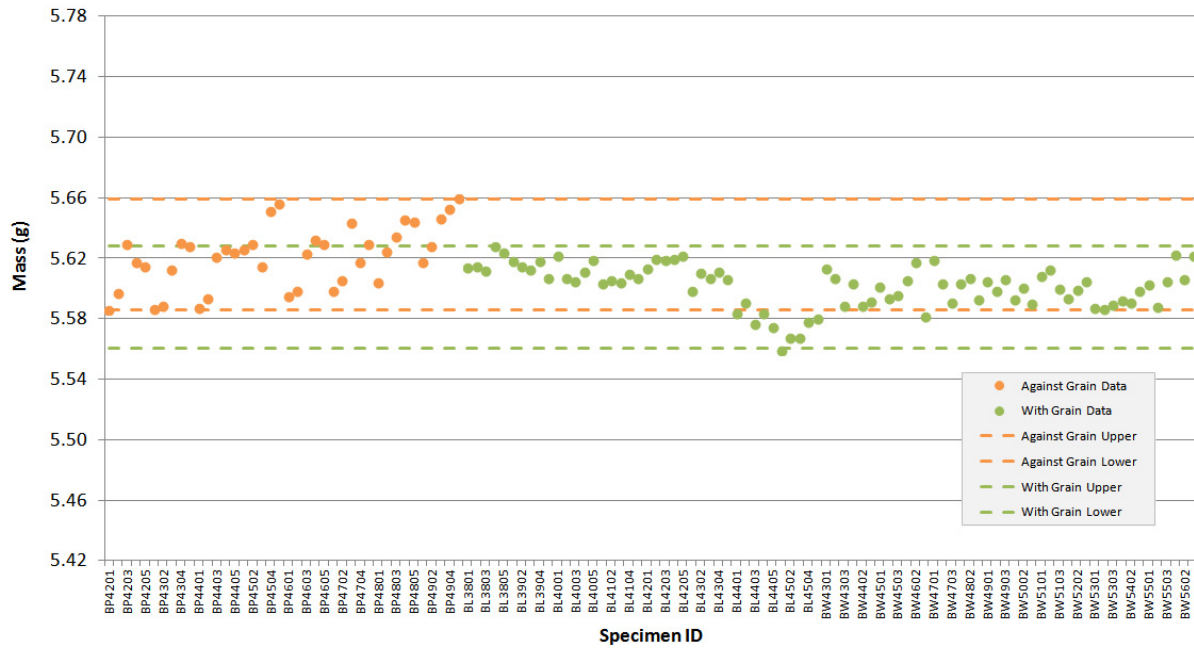


Figure A-40. NBG-18 creep specimen mass.

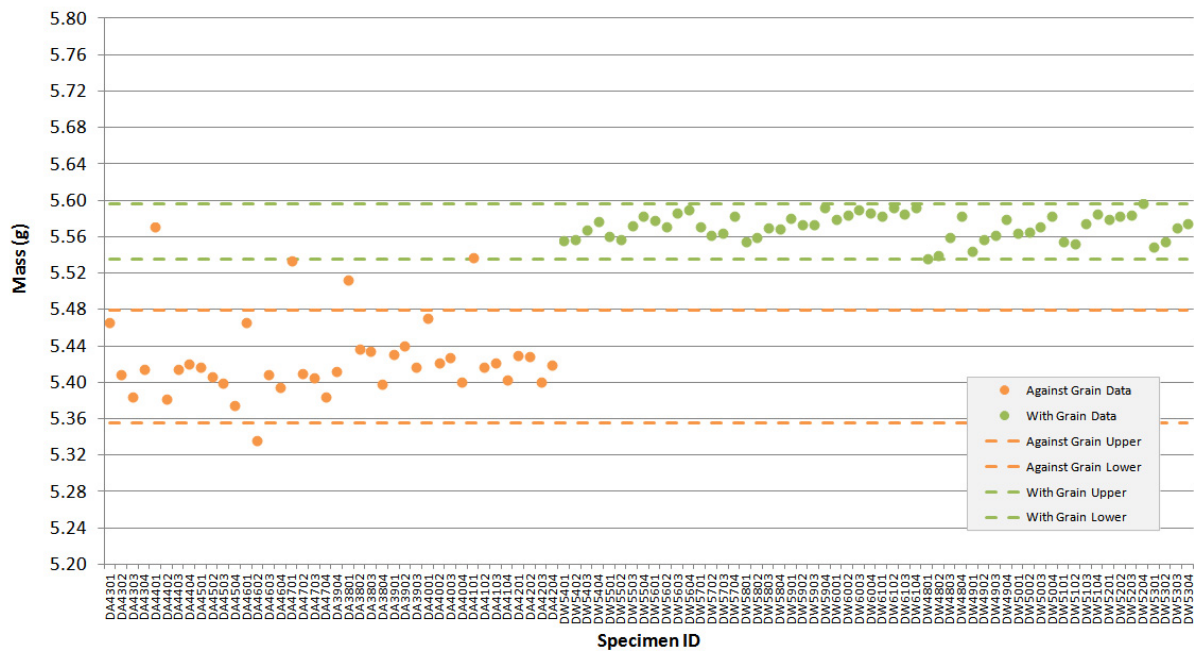


Figure A-41. PCEA creep specimen mass.

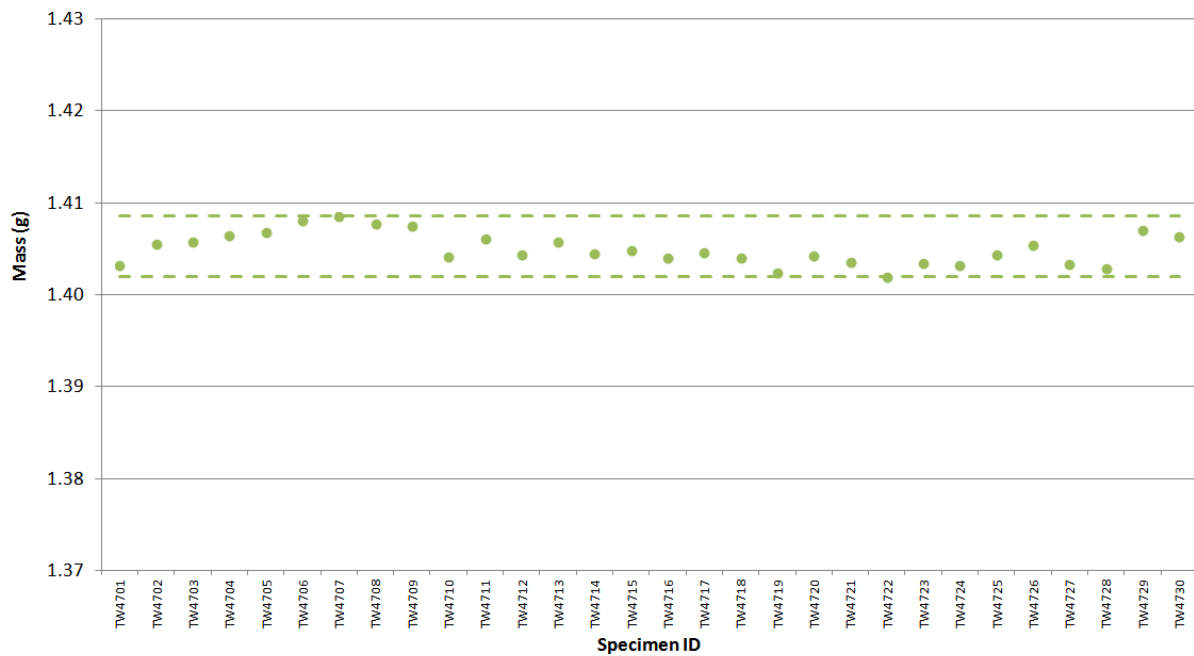


Figure A-42. 2114 piggyback specimen mass.

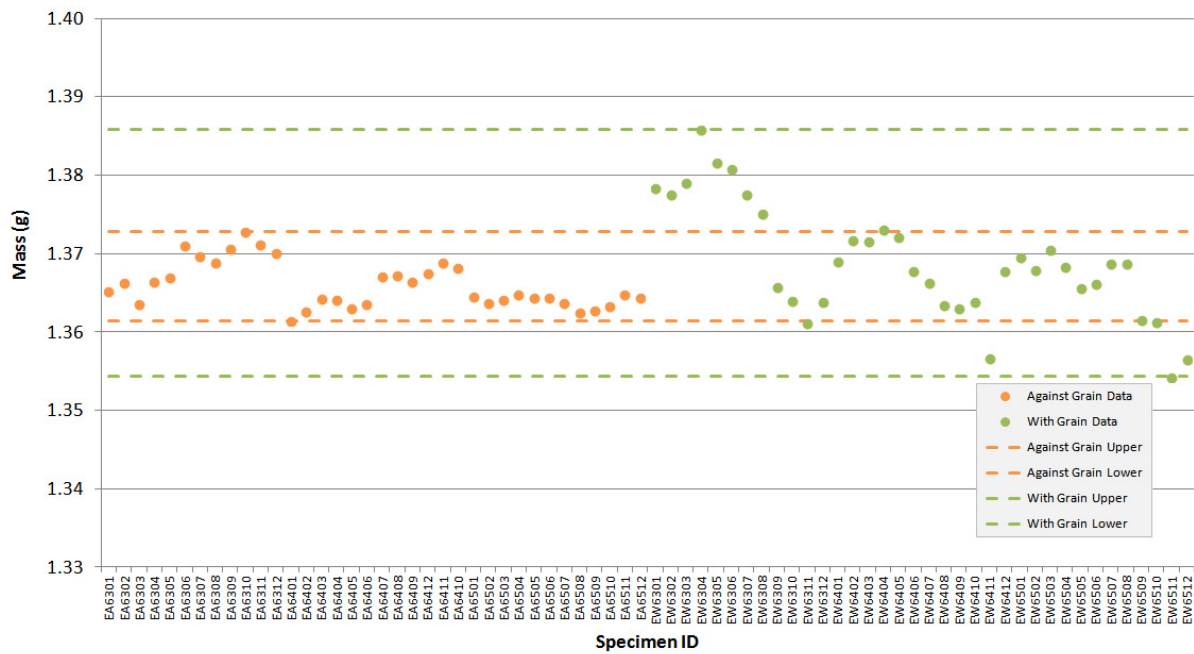


Figure A-43. IG-110 piggyback specimen mass.

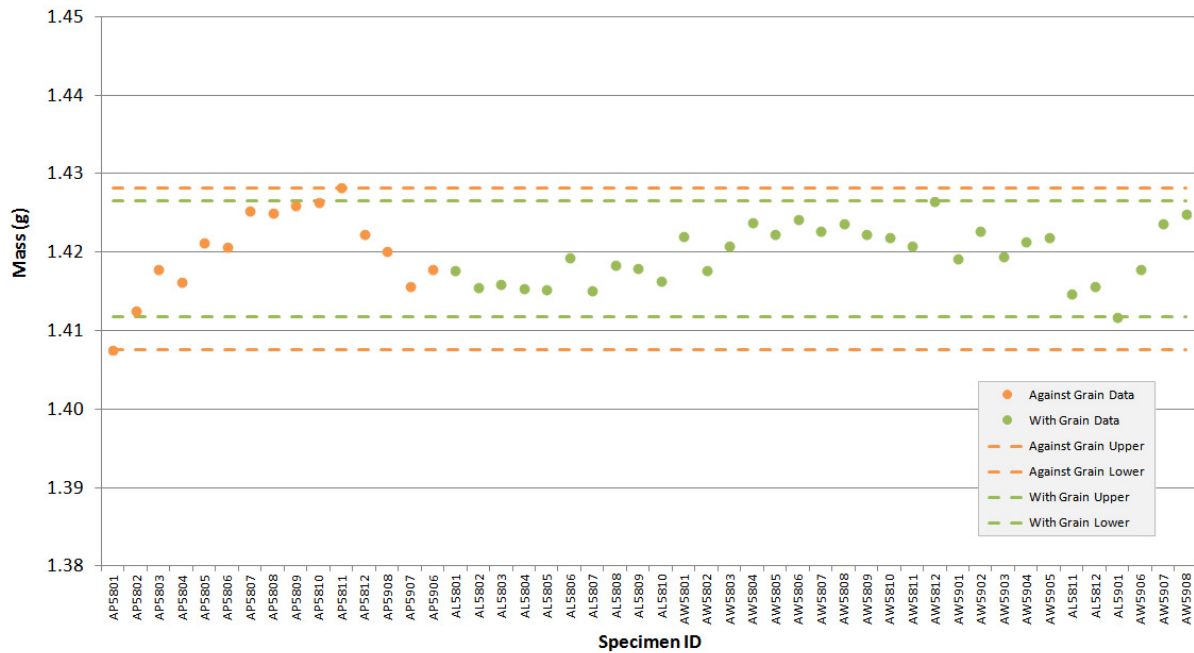


Figure A-44. NBG-17 piggyback specimen mass.

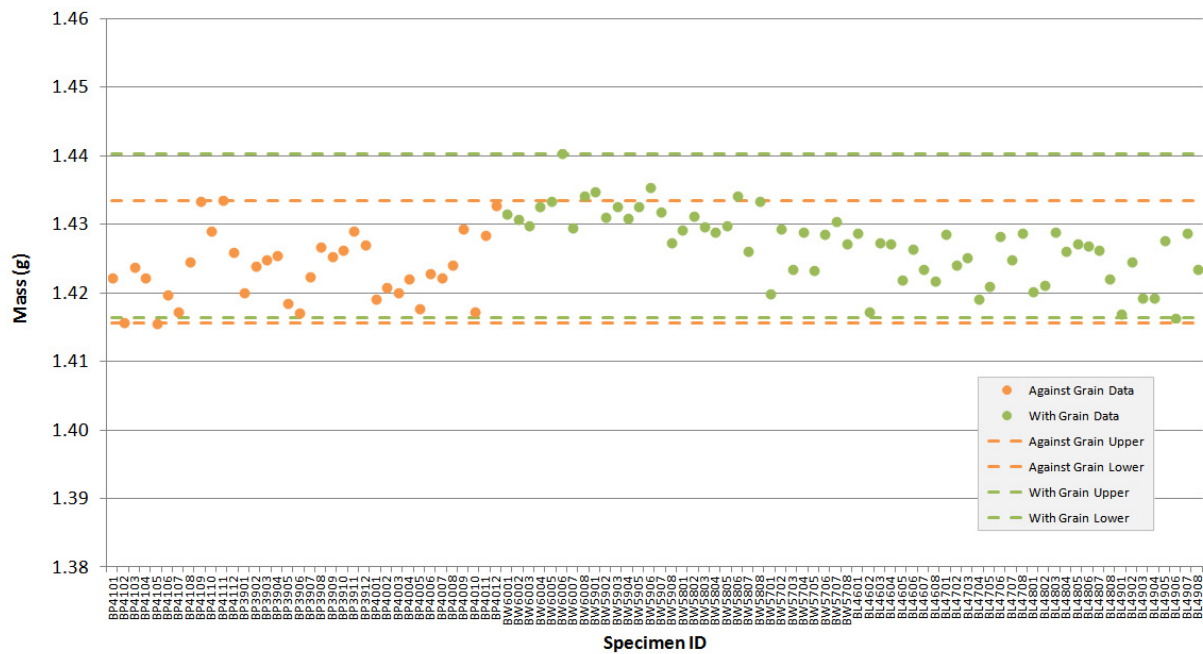


Figure A-45. NBG-18 piggyback specimen mass.

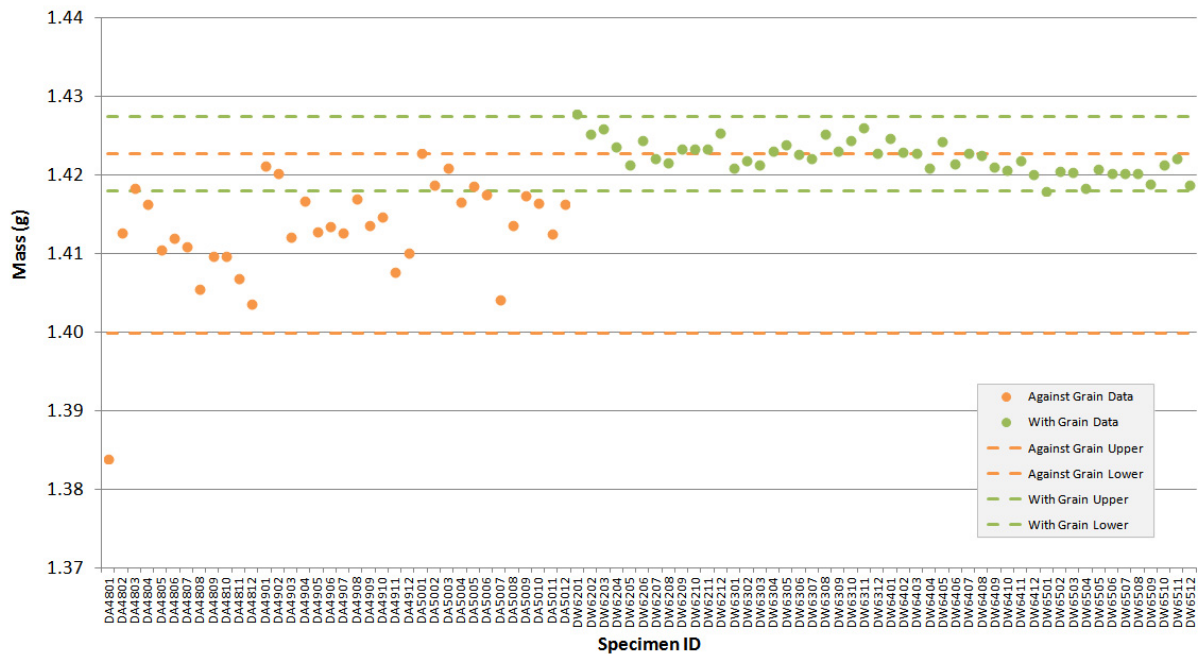


Figure A-46. PCEA piggyback specimen mass.

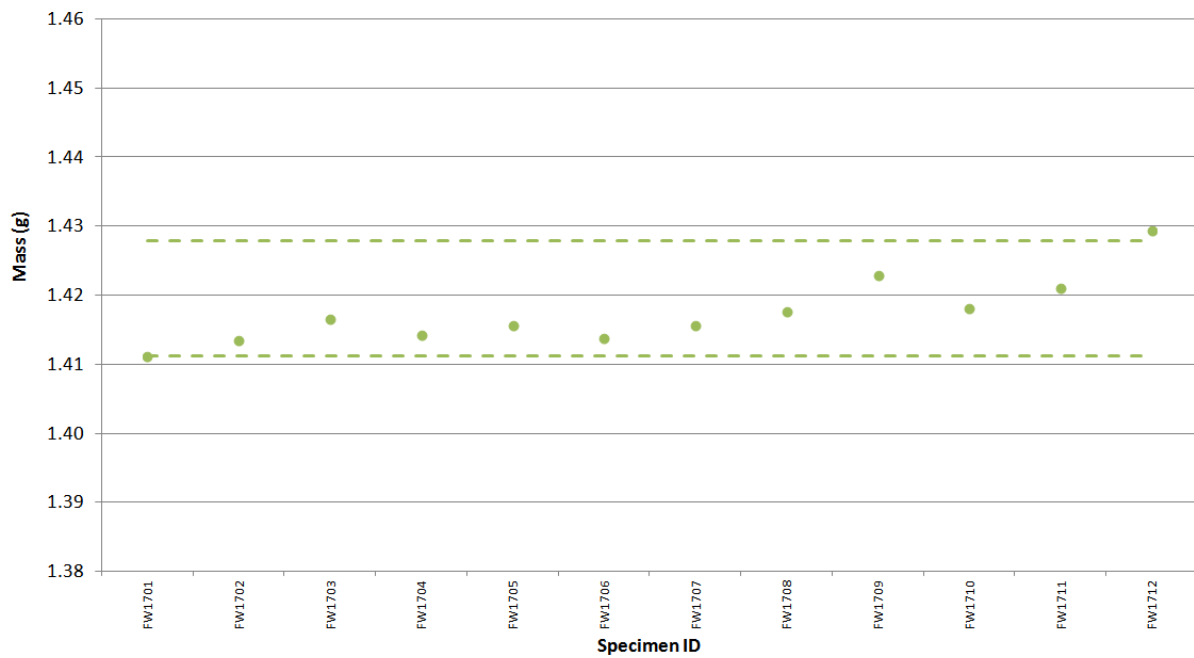


Figure A-47. IG-430 piggyback specimen mass.

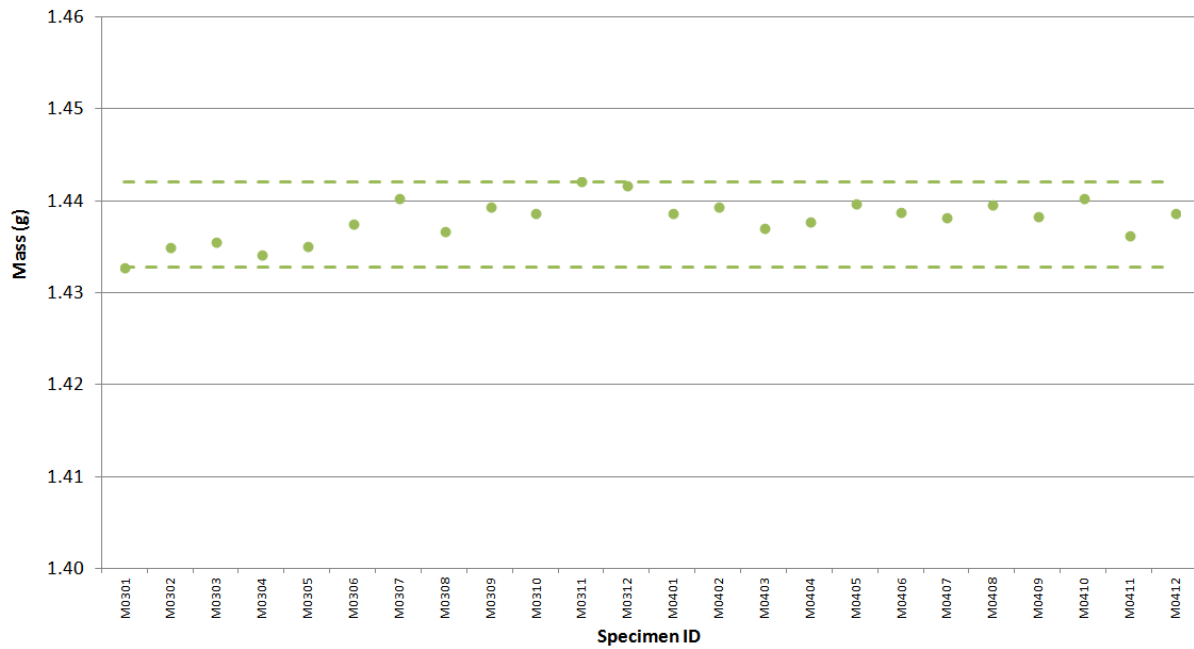


Figure A-48. NBG-25 piggyback specimen mass.

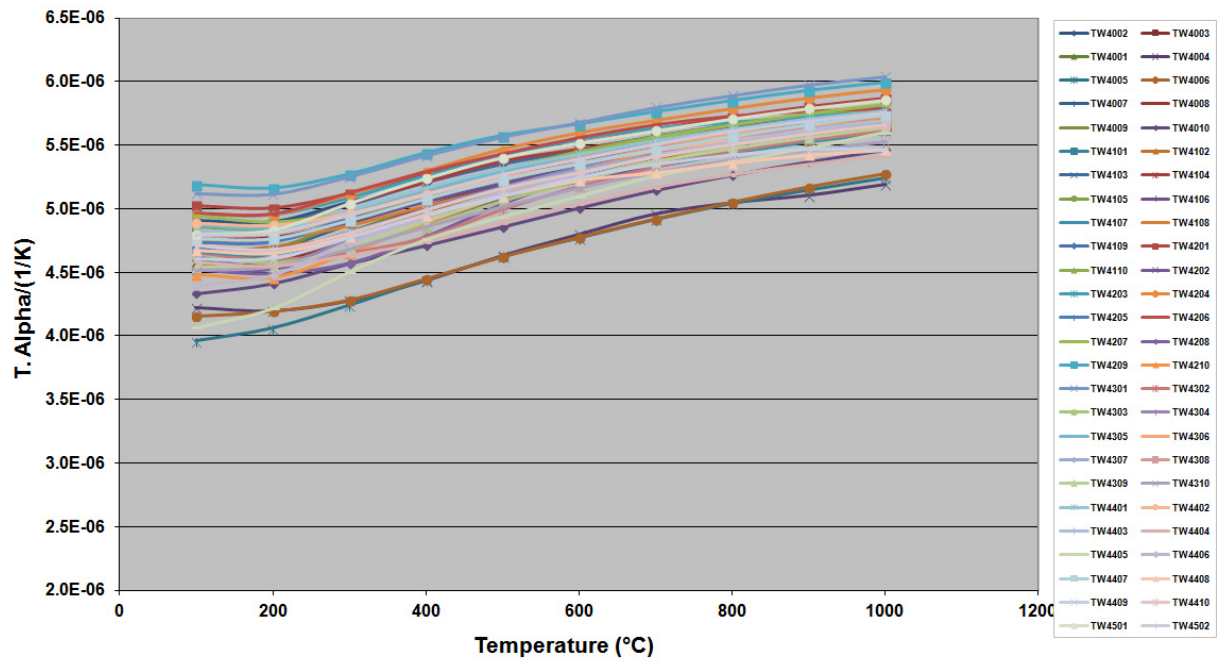


Figure A-49. 2114 Creep Specimen Coefficient of Thermal Expansion.

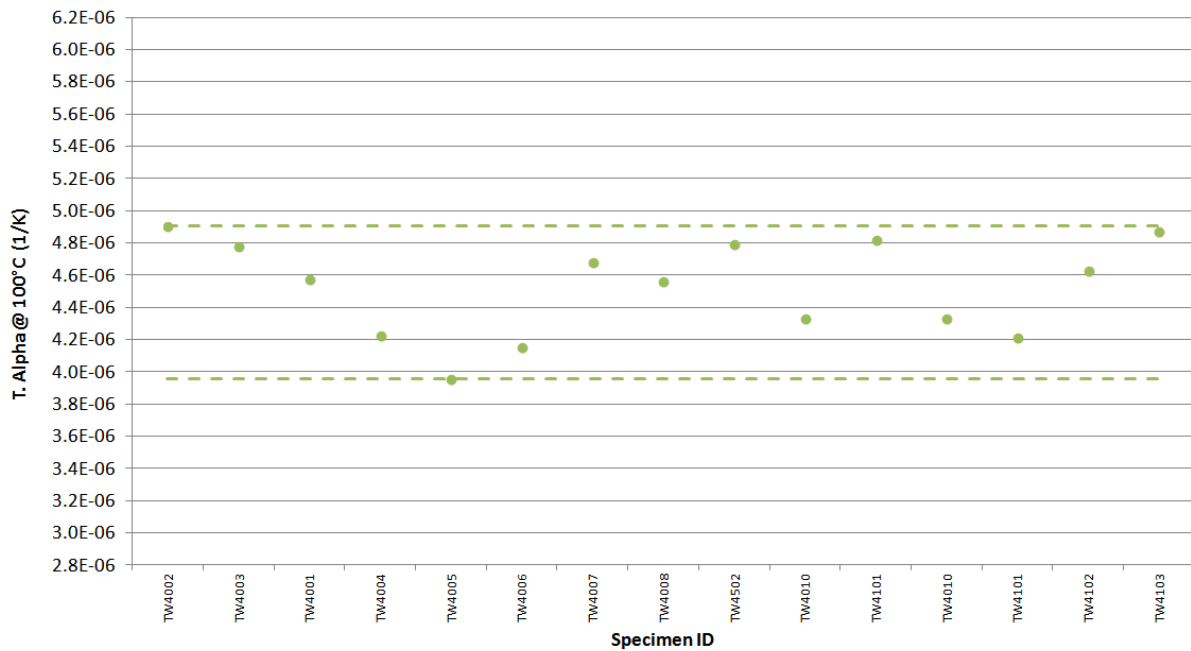


Figure A-50. 2114 creep specimen coefficient of thermal expansion @ 100 $^{\circ}C$.

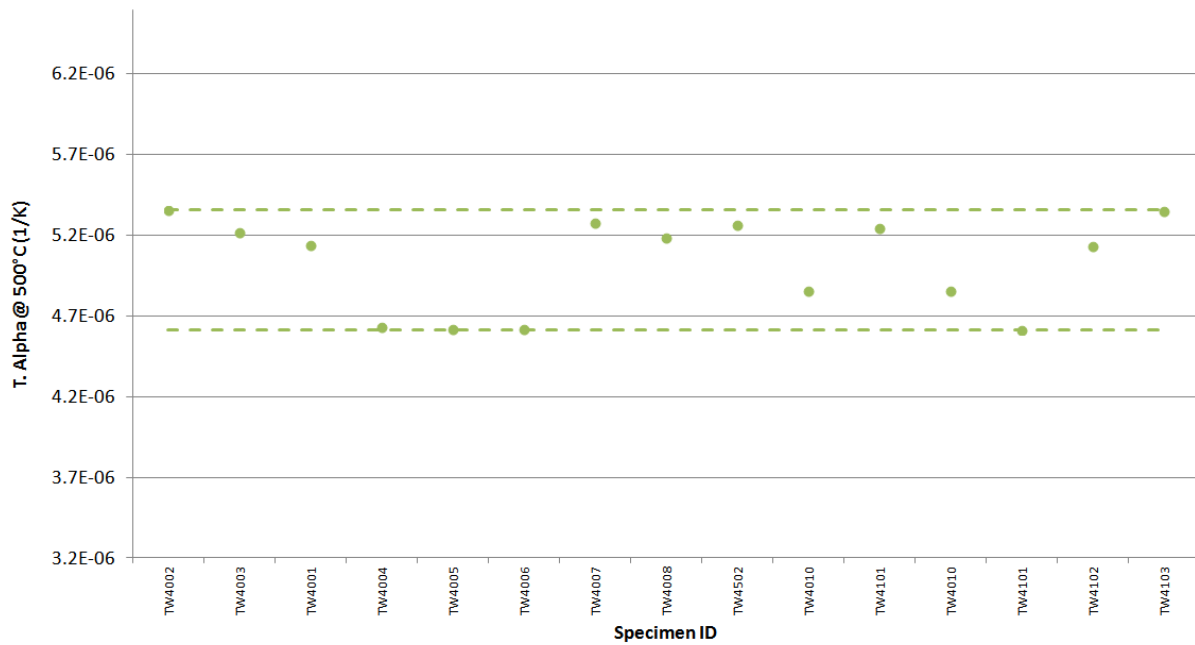


Figure A-51. 2114 creep specimen coefficient of thermal expansion @ 500°C.

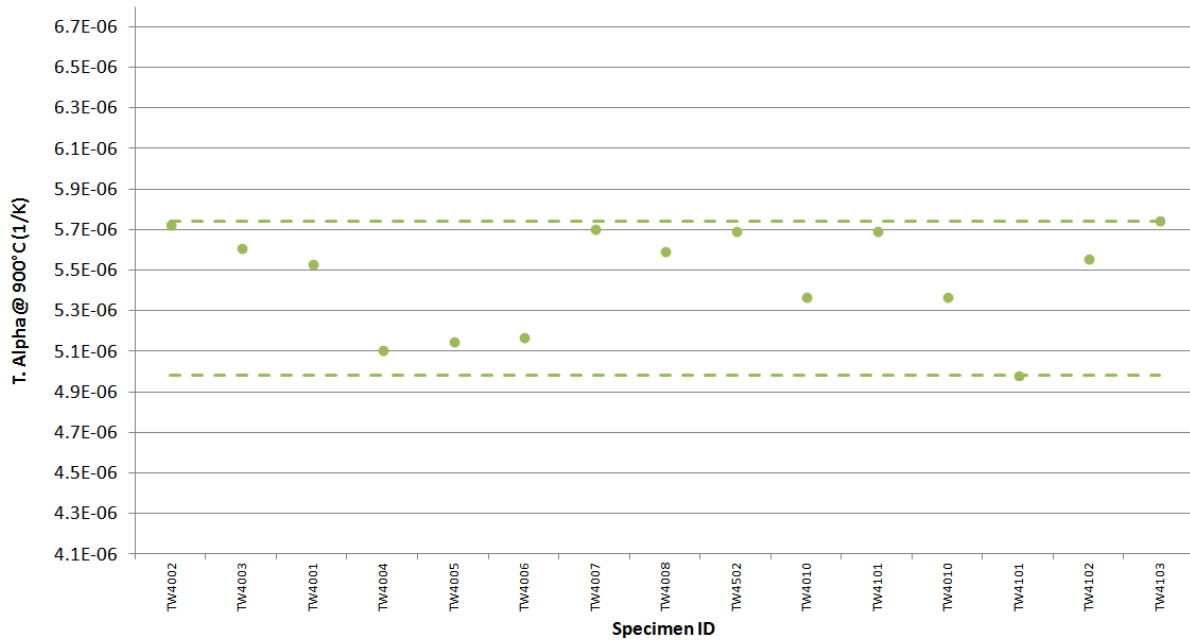


Figure A-52. 2114 creep specimen coefficient of thermal expansion @ 900°C.

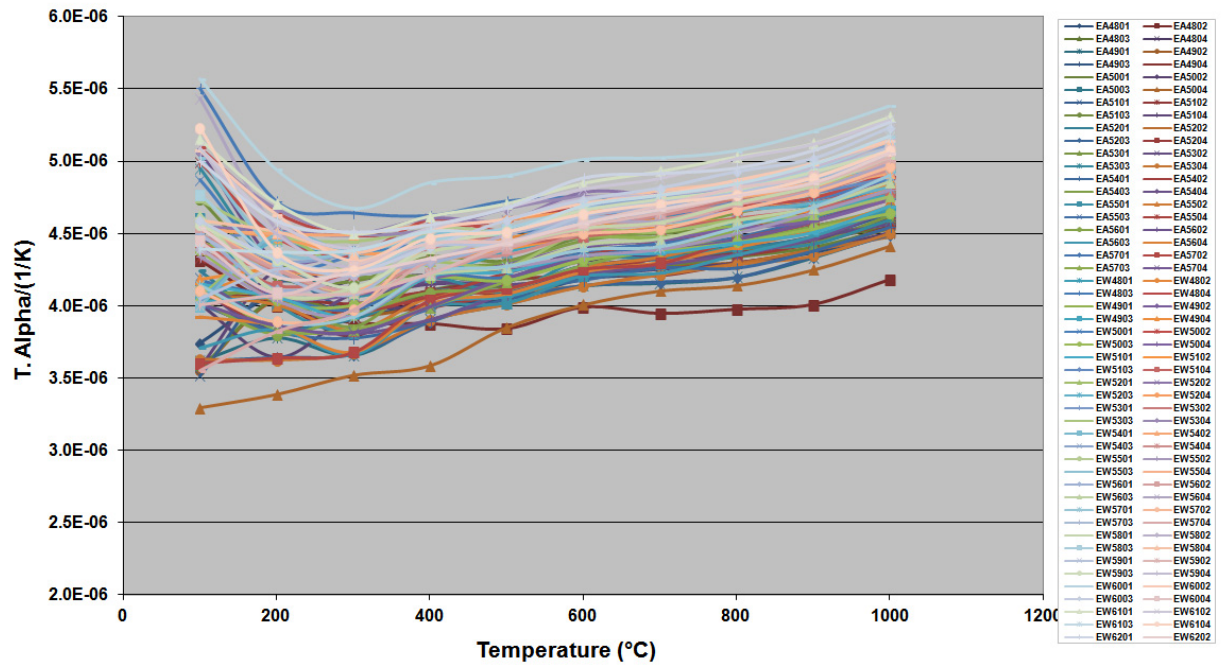


Figure A-53. IG-110 creep specimen coefficient of thermal expansion.

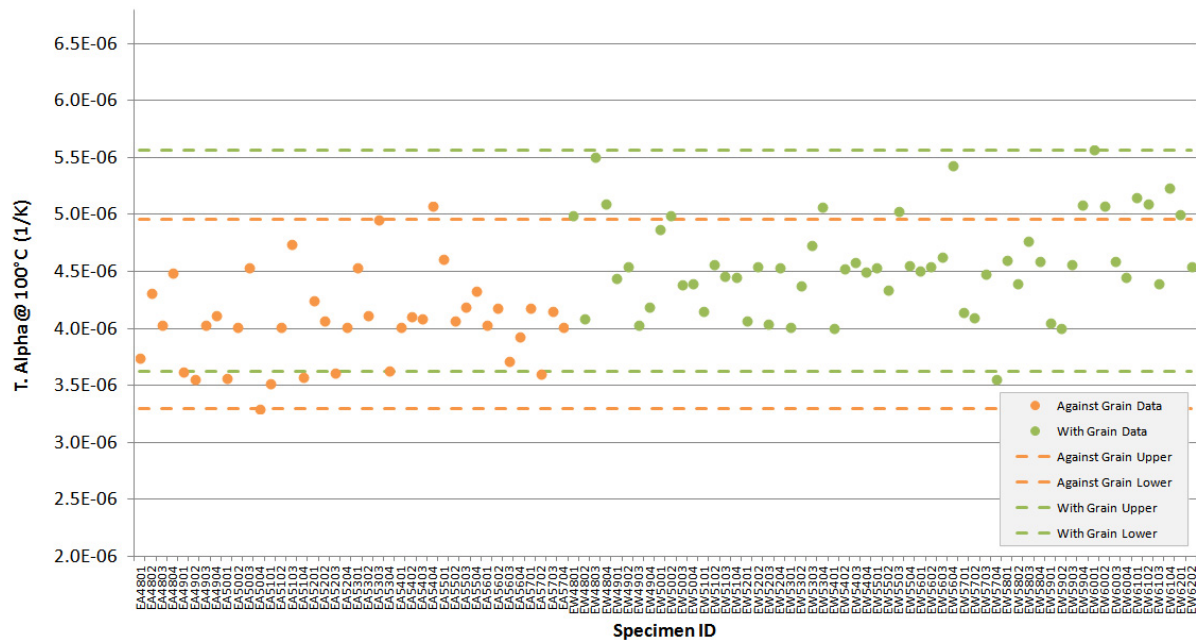


Figure A-54. IG-110 creep specimen coefficient of thermal expansion @ 100°C.

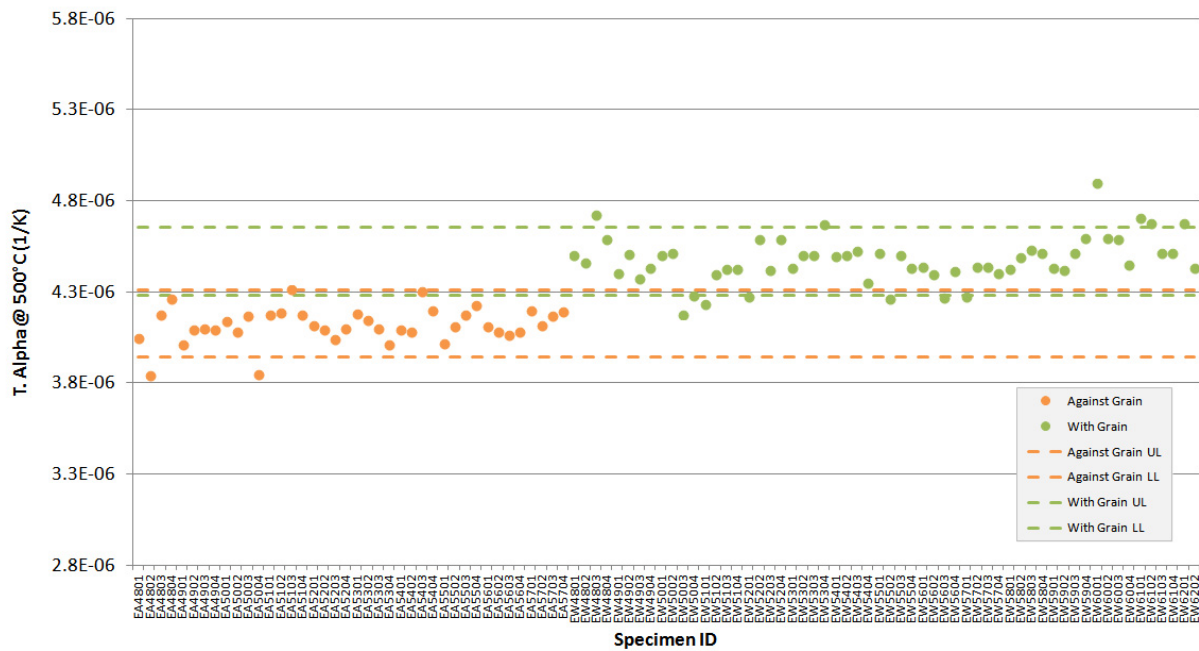


Figure A-55. IG-110 creep specimen coefficient of thermal expansion @ 500°C.

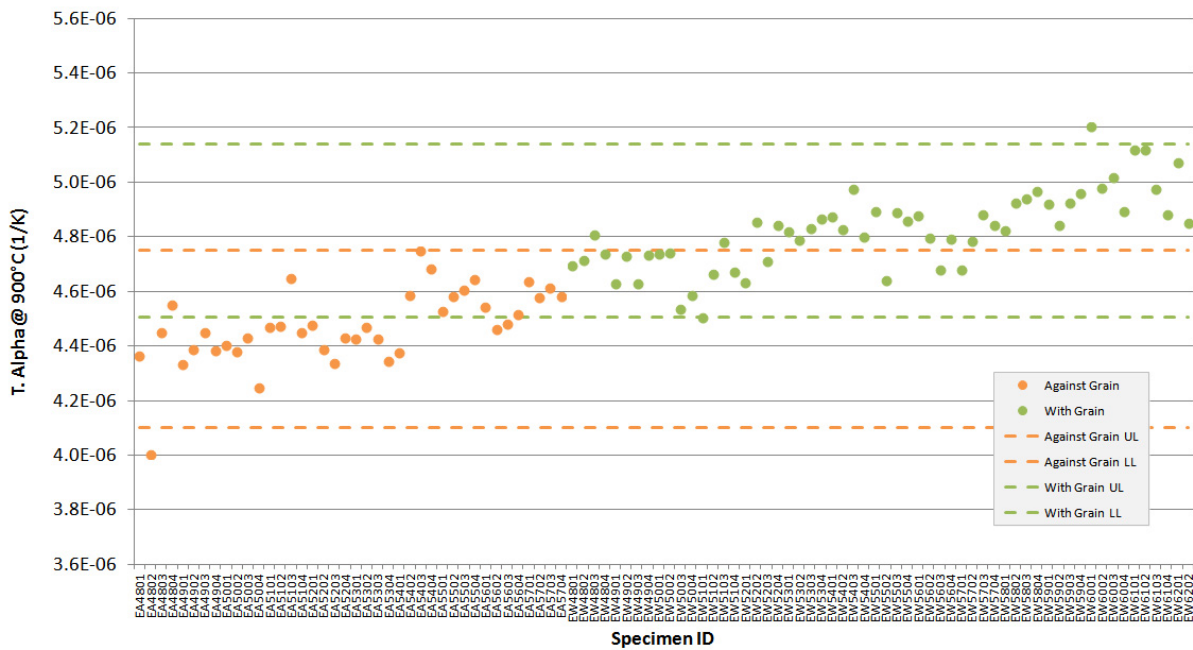


Figure A-56. IG-110 creep specimen coefficient of thermal expansion @ 900°C.

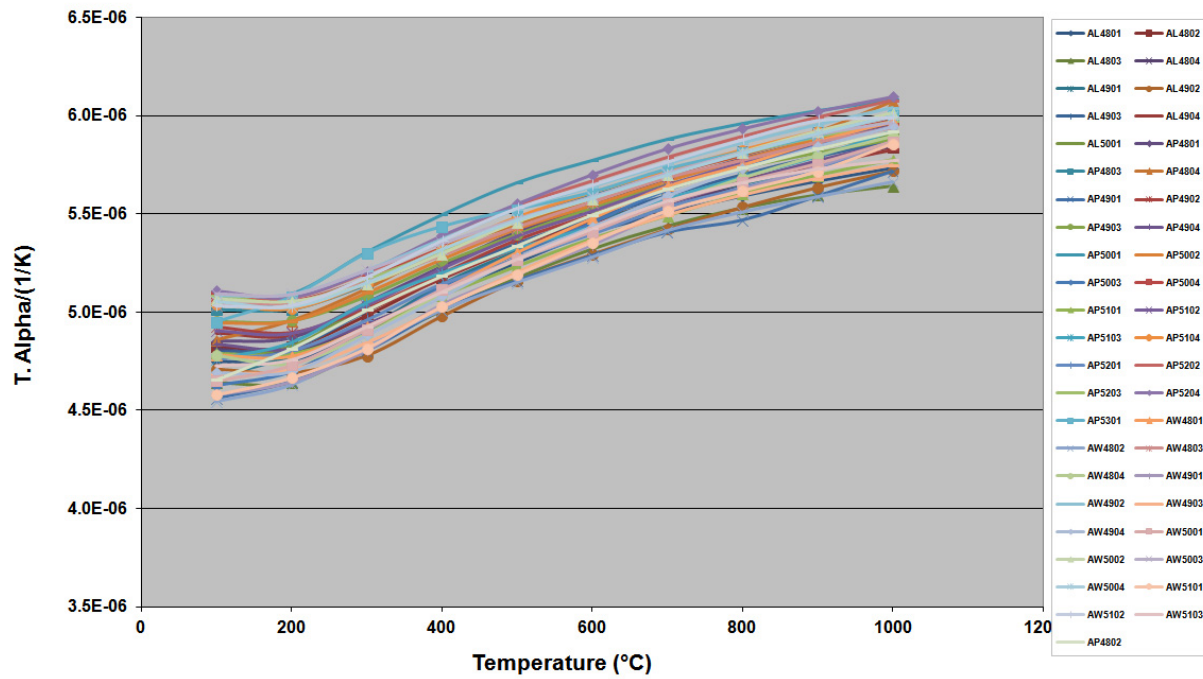


Figure A-57. NBG-17 creep specimen coefficient of thermal expansion.

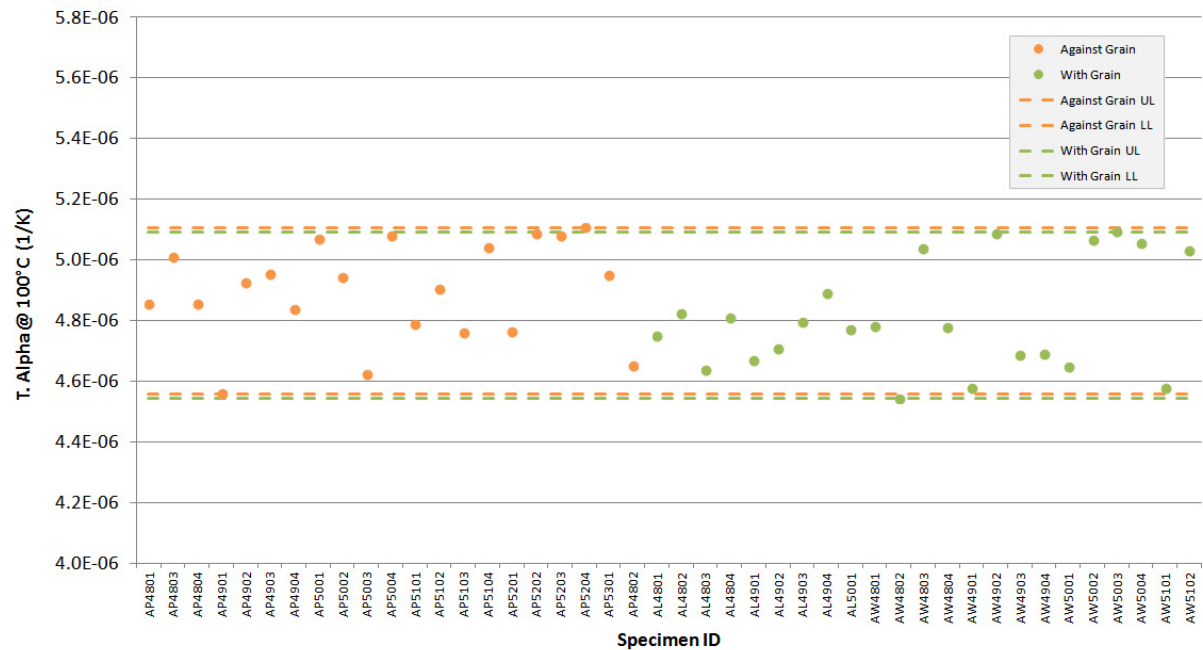


Figure A-58. NBG-17 creep specimen coefficient of thermal expansion @ 100°C.

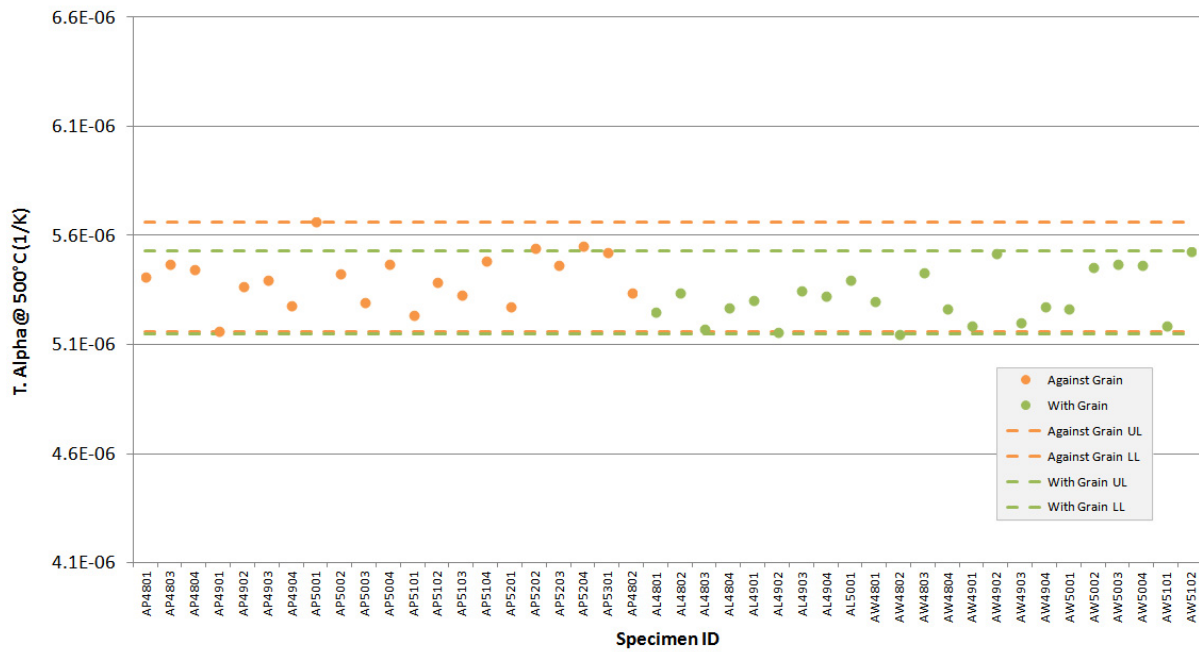


Figure A-59. NBG-17 creep specimen coefficient of thermal expansion @ 500°C.

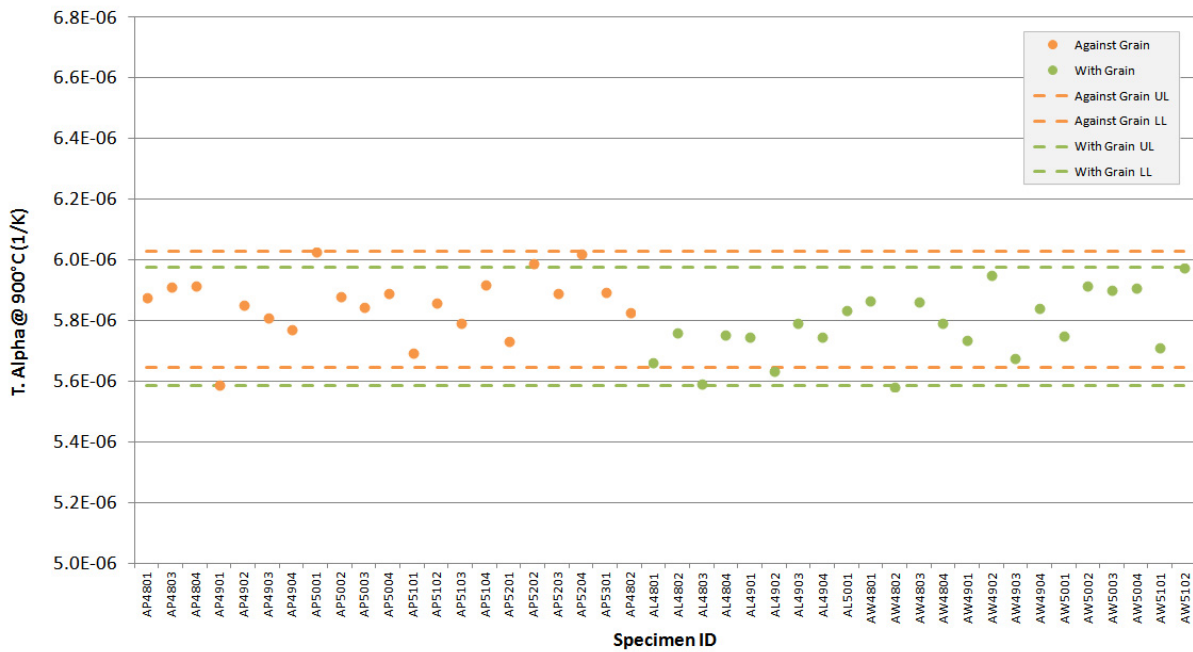


Figure A-60. NBG-17 creep specimen coefficient of thermal expansion @ 900°C.

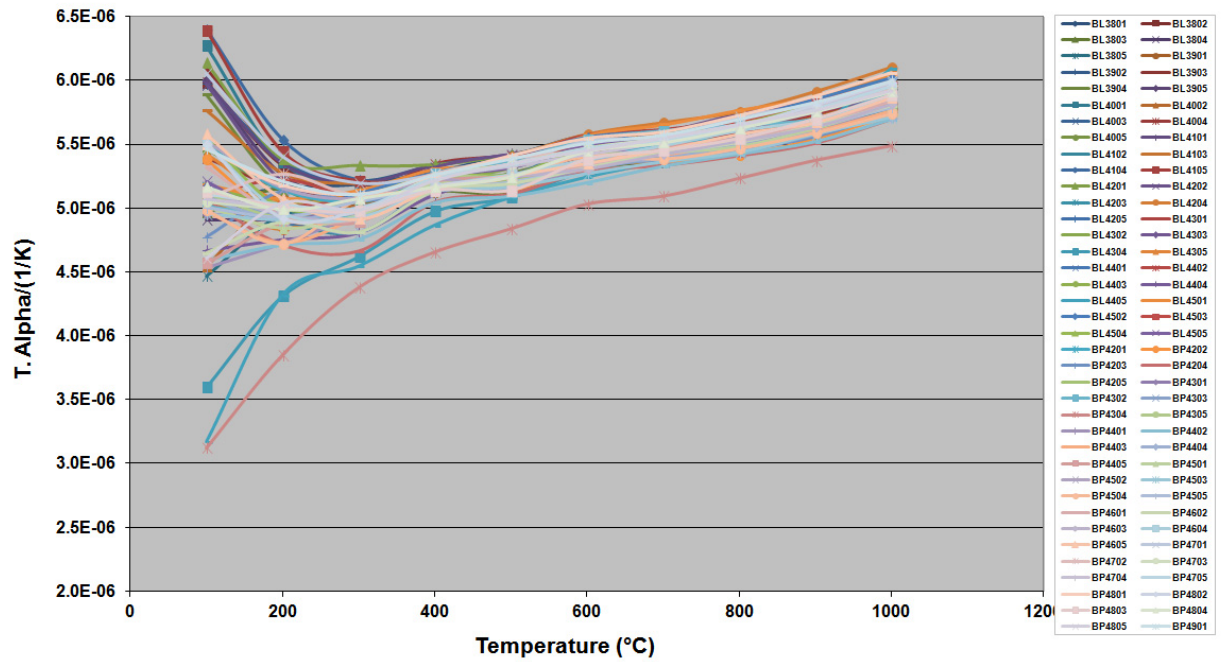


Figure A-61. NBG-18 creep specimen coefficient of thermal expansion.

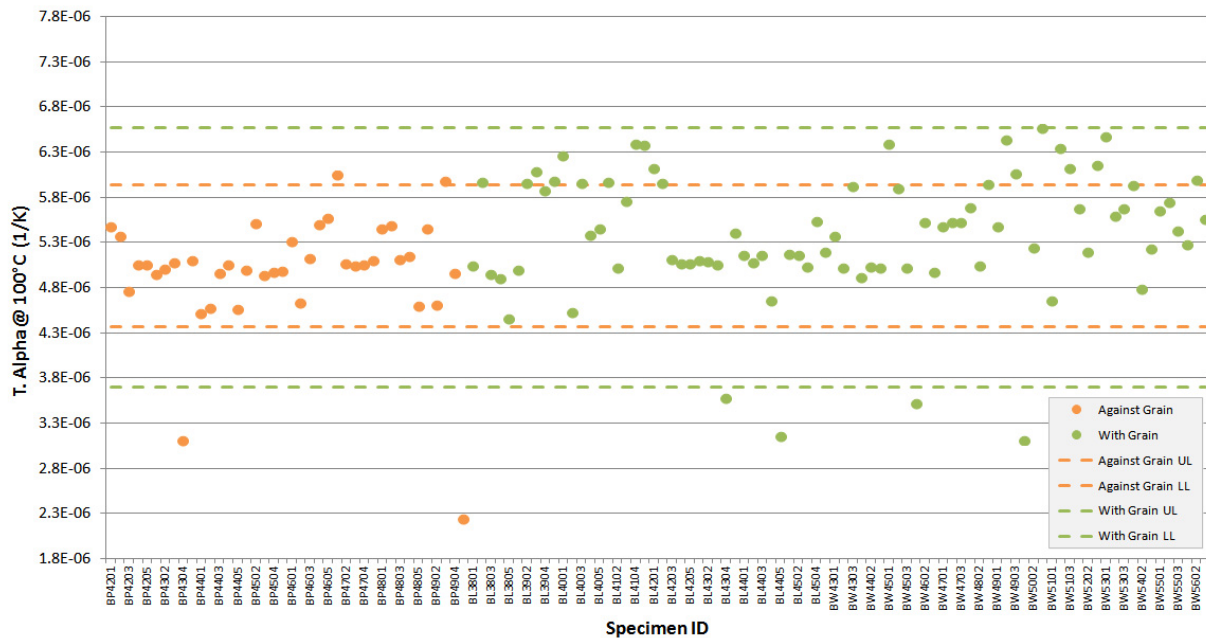


Figure A-62. NBG-18 creep specimen coefficient of thermal expansion @ 100°C.

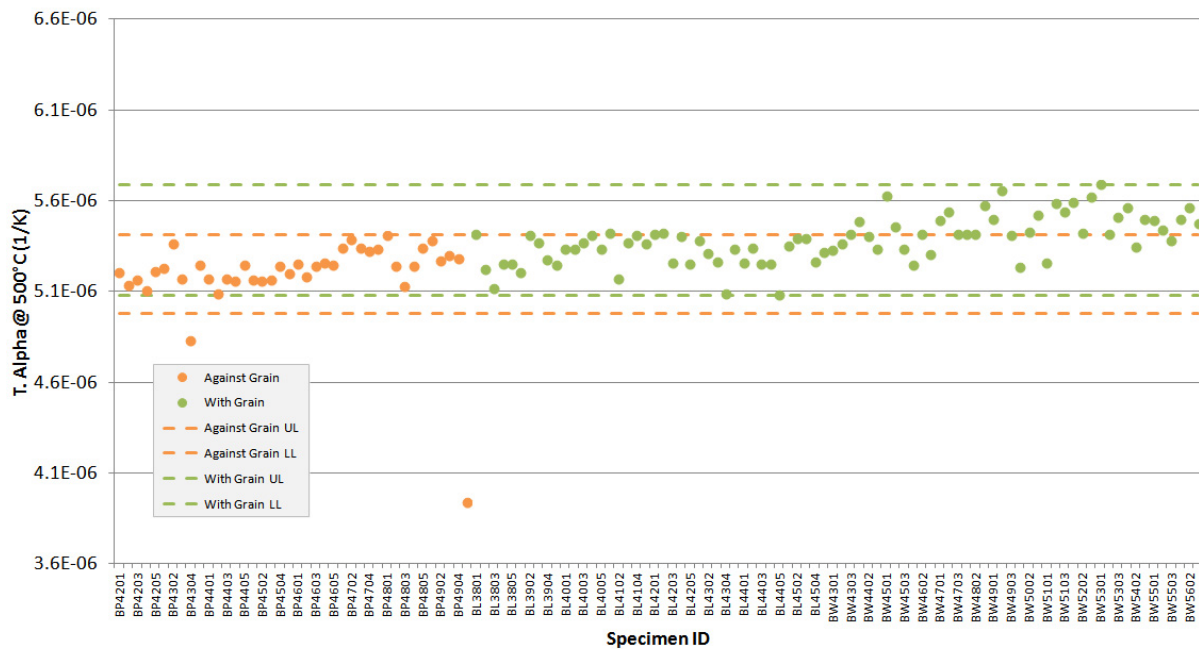


Figure A-63. NBG-18 creep specimen coefficient of thermal expansion @ 500°C.

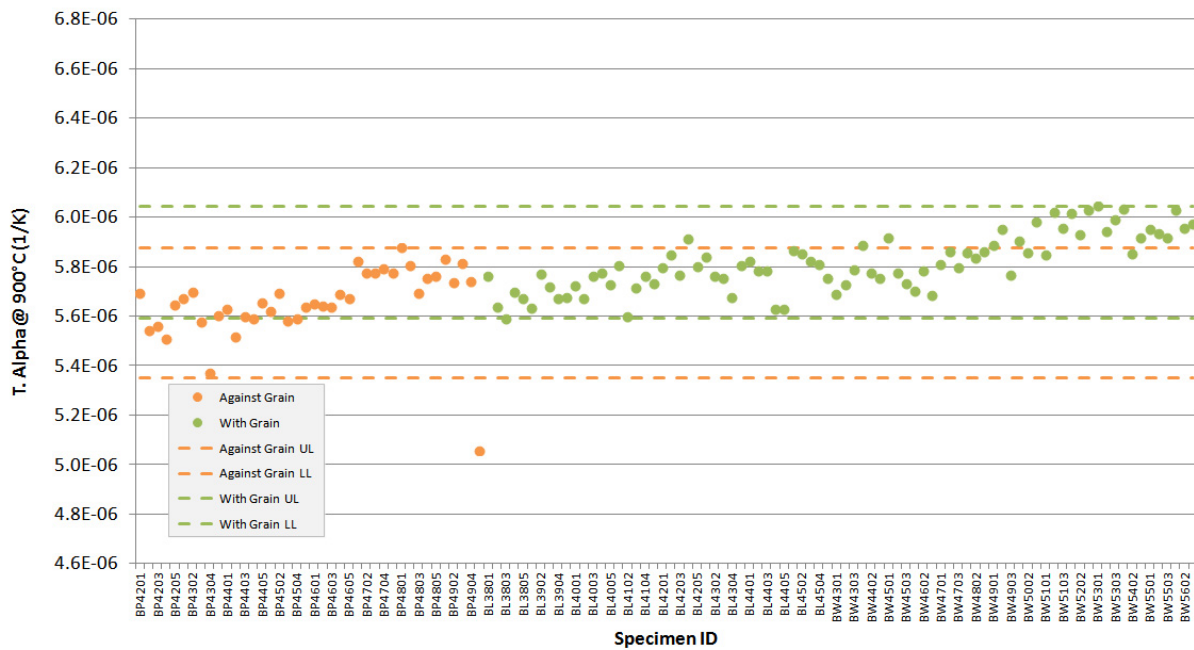


Figure A-64. NBG-18 creep specimen coefficient of thermal expansion @ 900°C.

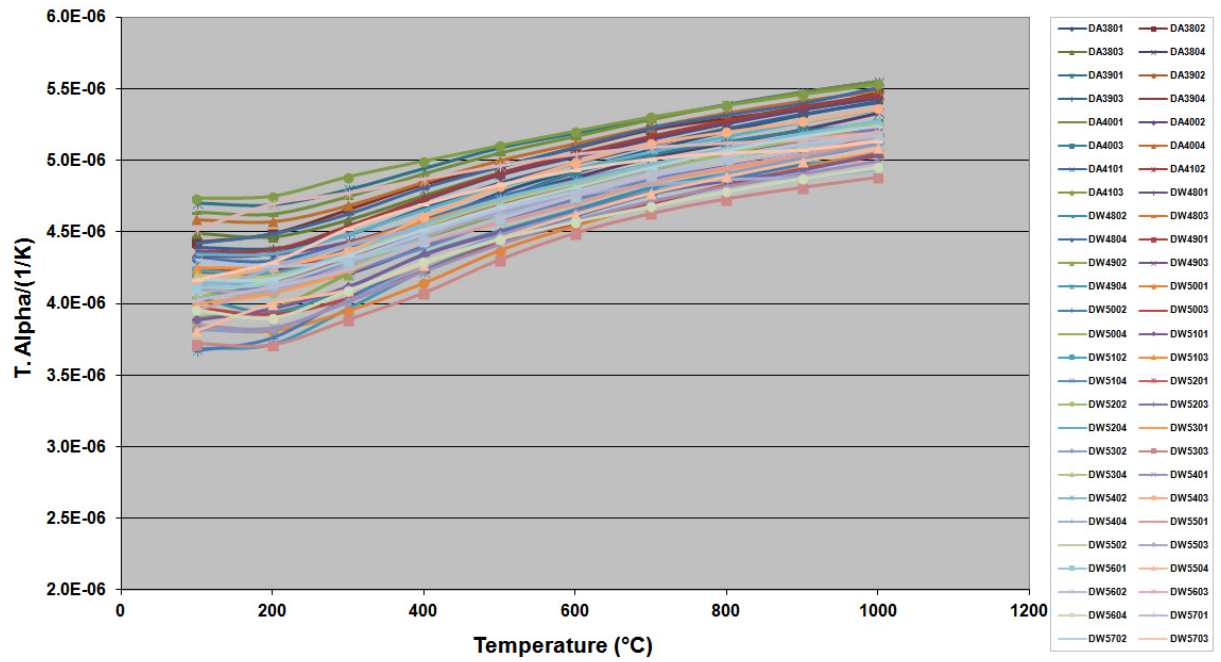


Figure A-65. PCEA creep specimen coefficient of thermal expansion.

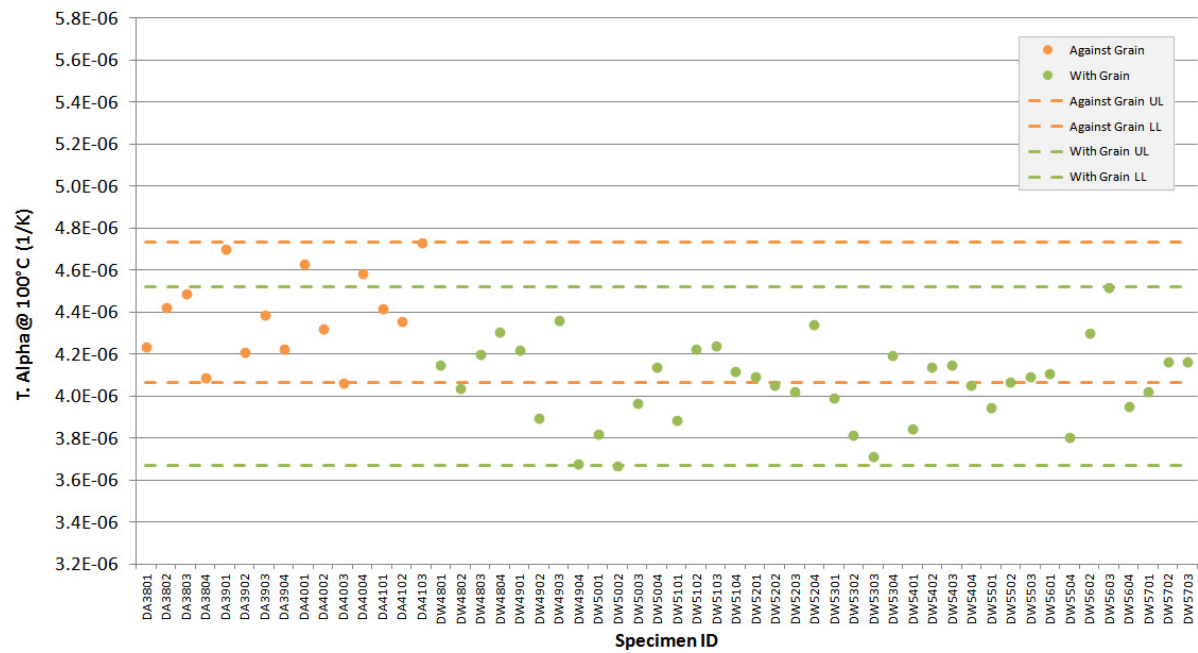


Figure A-66. PCEA creep specimen coefficient of thermal expansion @ 100°C.

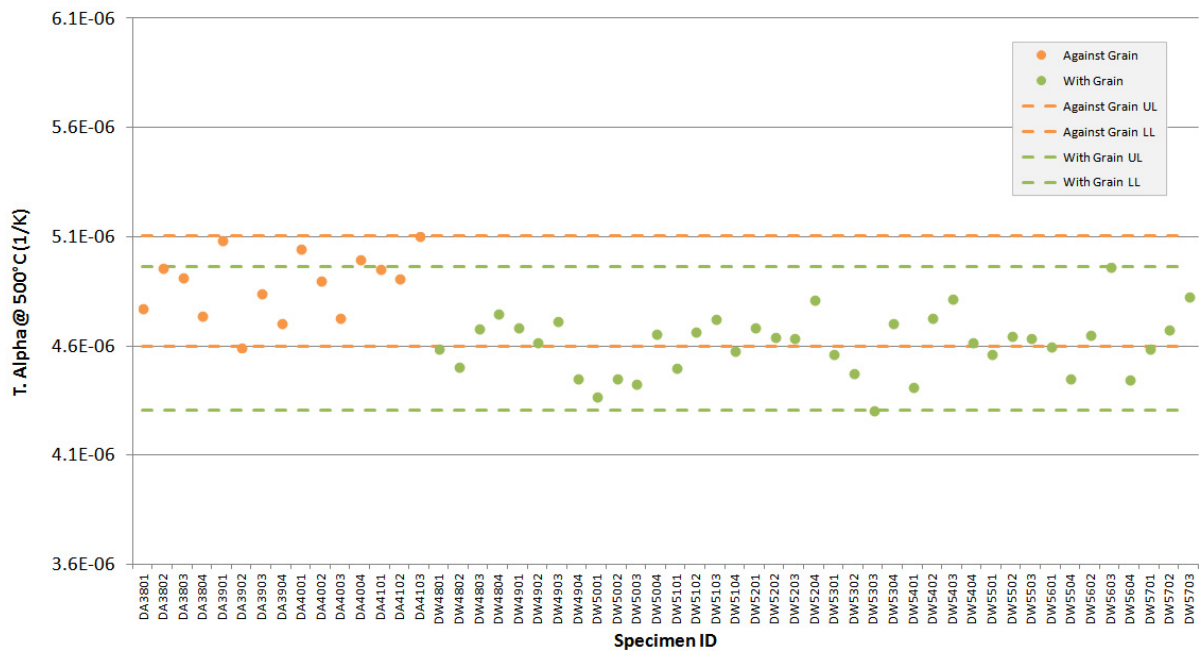


Figure A-67. PCEA creep specimen coefficient of thermal expansion @ 500°C.

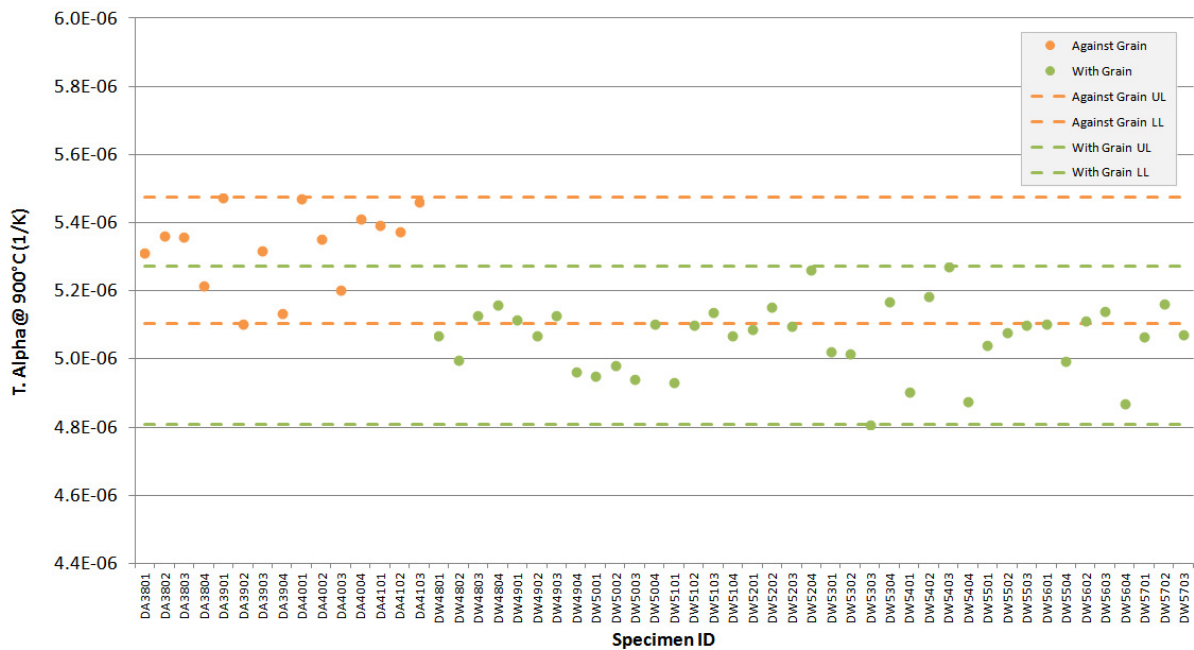


Figure A-68. PCEA creep specimen coefficient of thermal expansion @ 900°C.

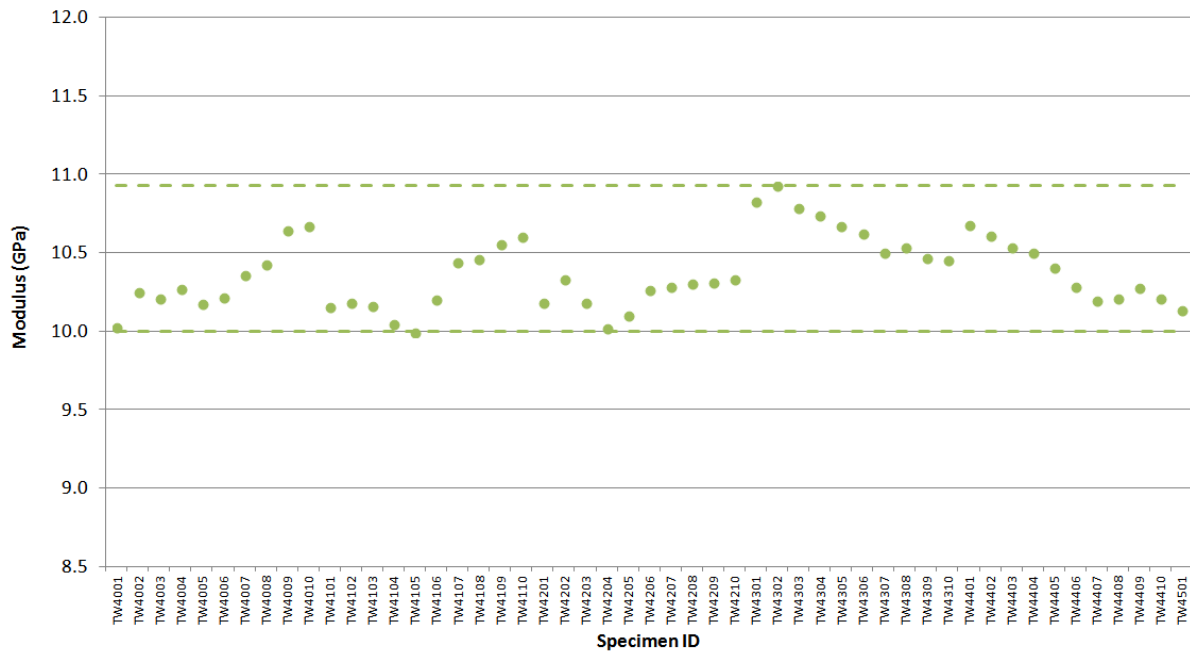


Figure A-69. 2114 creep specimen modulus by sonic resonance.

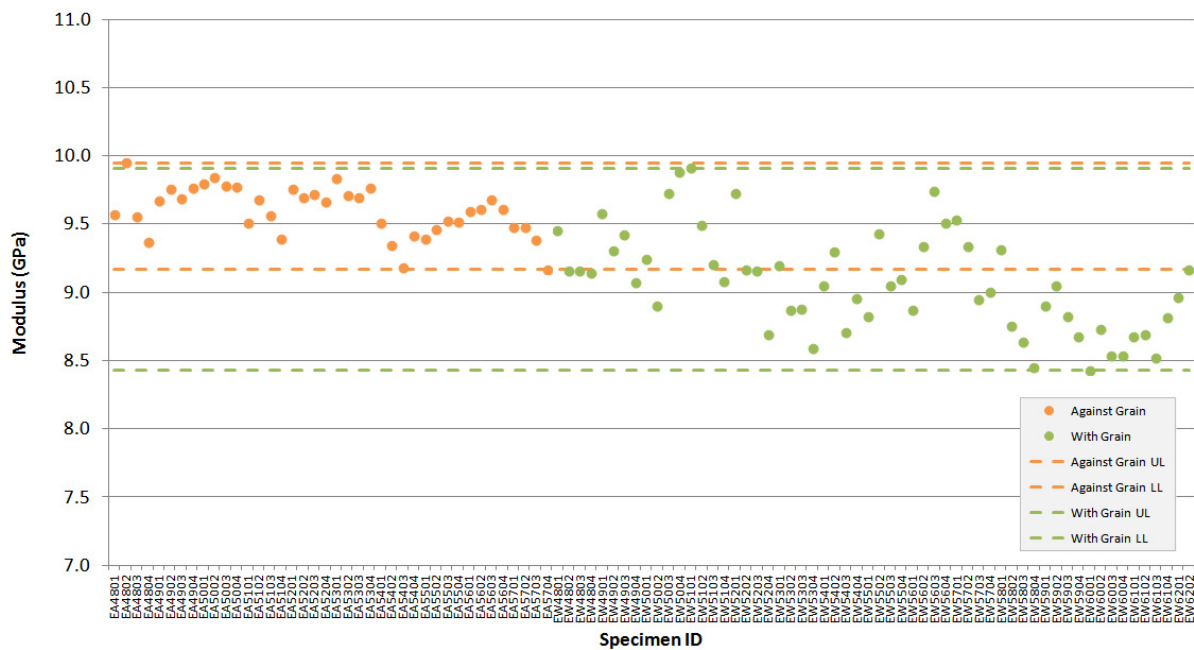


Figure A-70. IG-110 creep specimen modulus by sonic resonance.

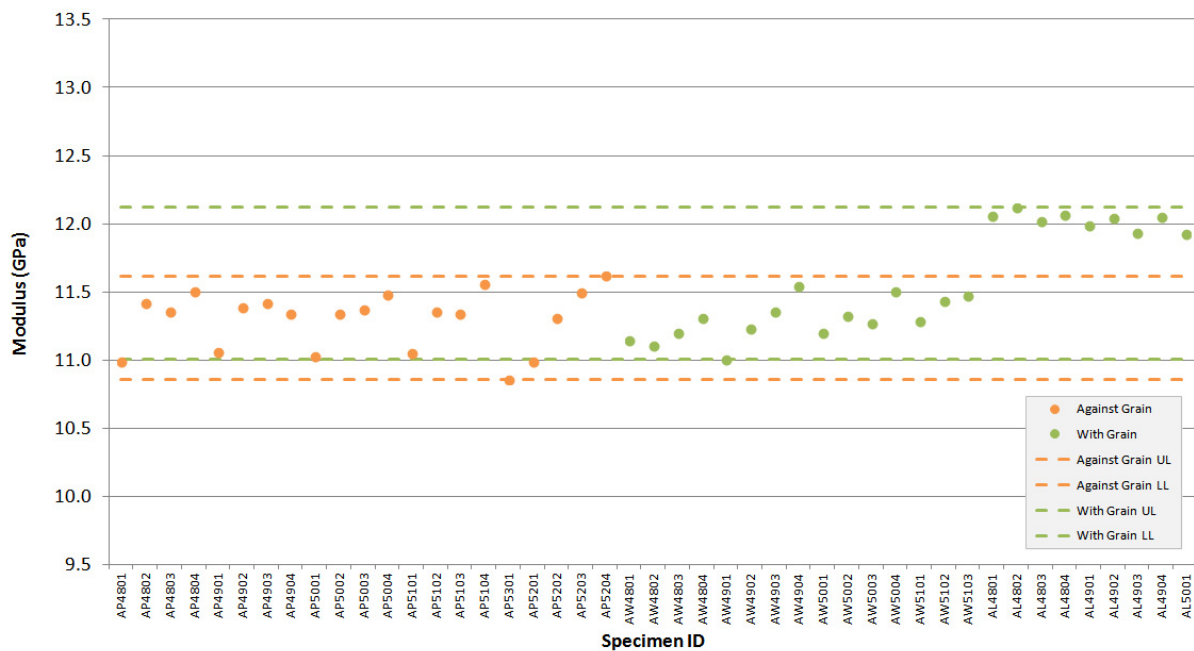


Figure A-71. NBG-17 creep specimen modulus by sonic resonance.

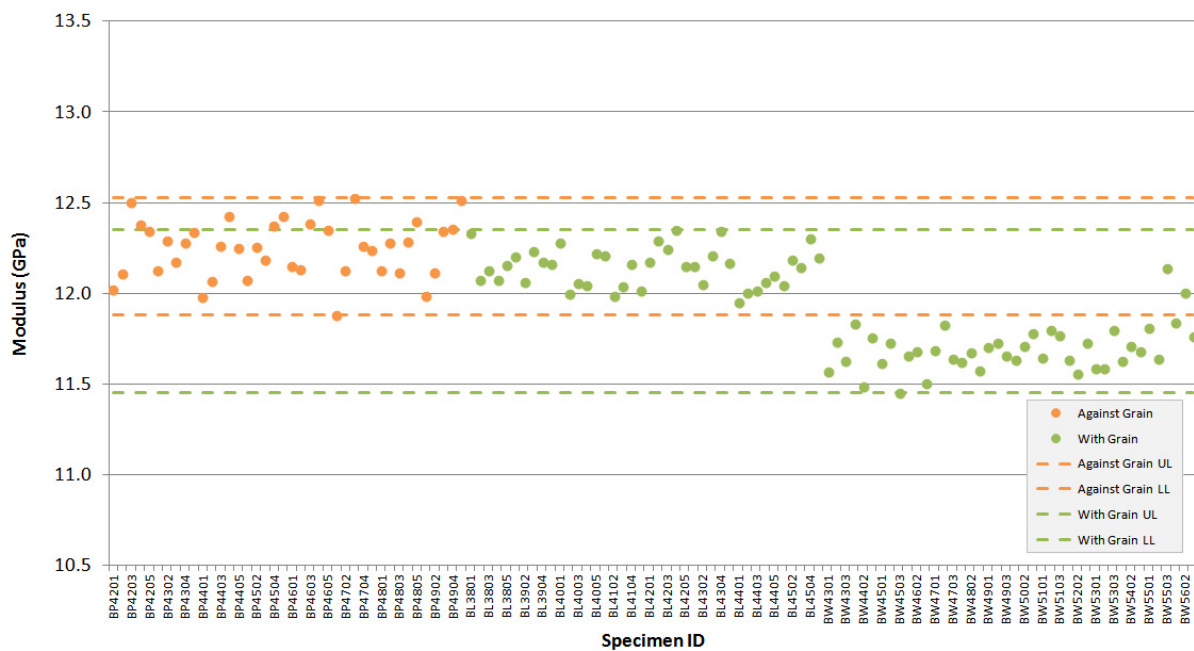


Figure A-72. NBG-18 creep specimen modulus by sonic resonance.

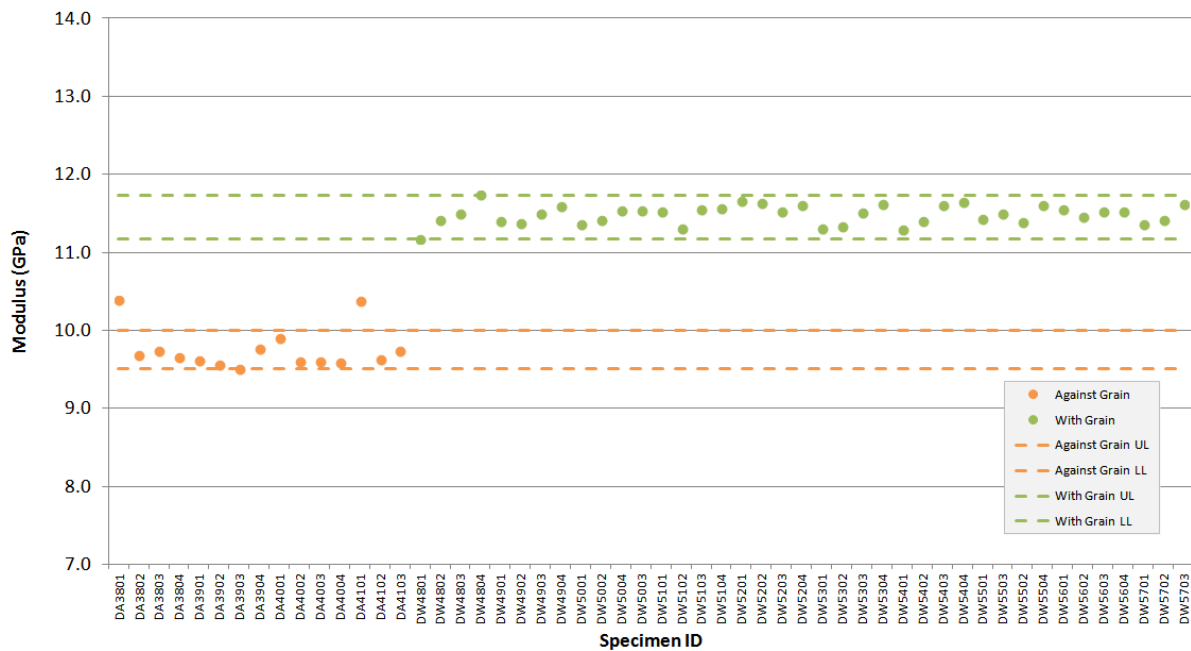


Figure A-73. PCEA creep specimen modulus by sonic resonance.

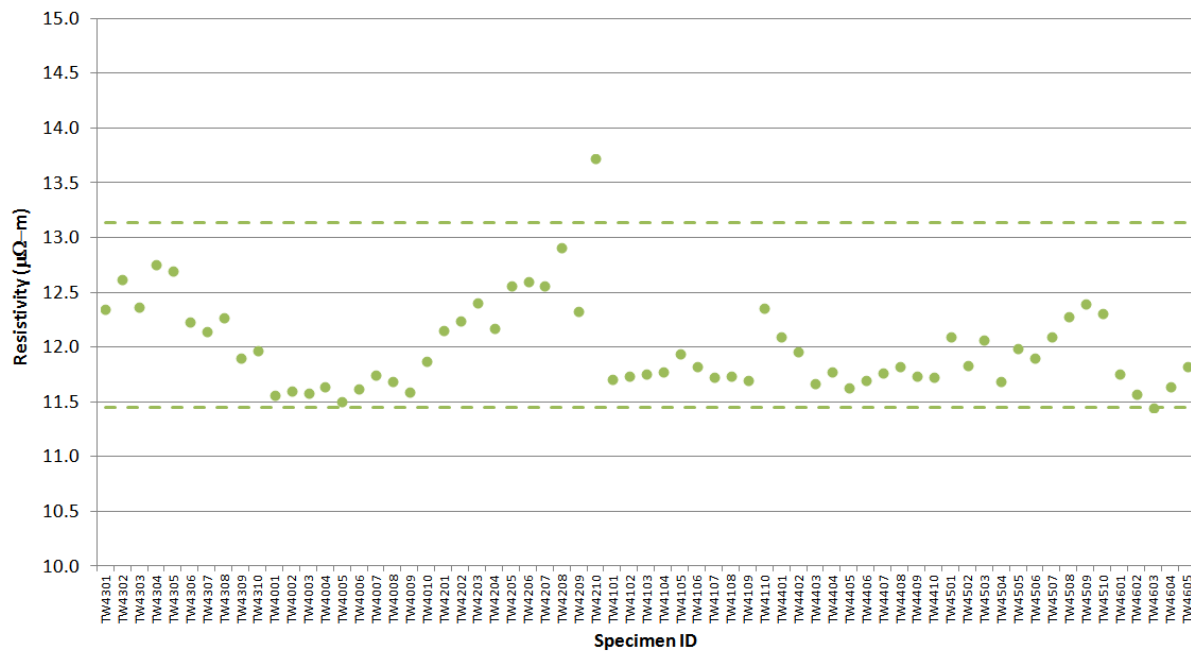


Figure A-74. 2114 creep specimen resistivity.

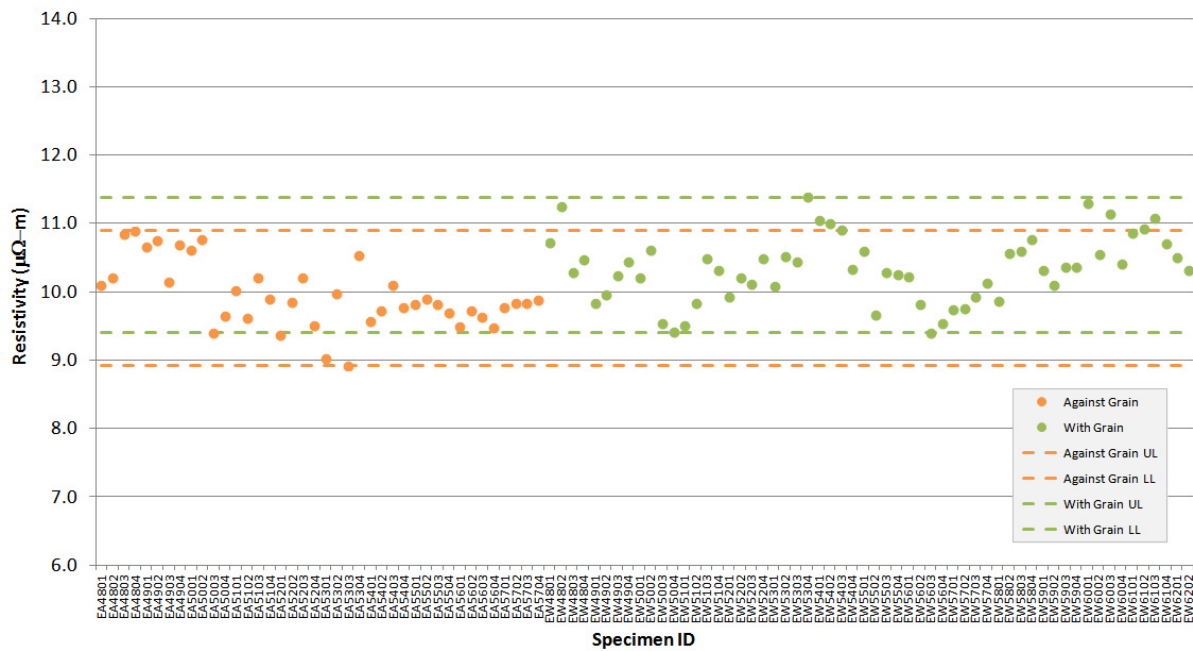


Figure A-75. IG-110 creep specimen resistivity.

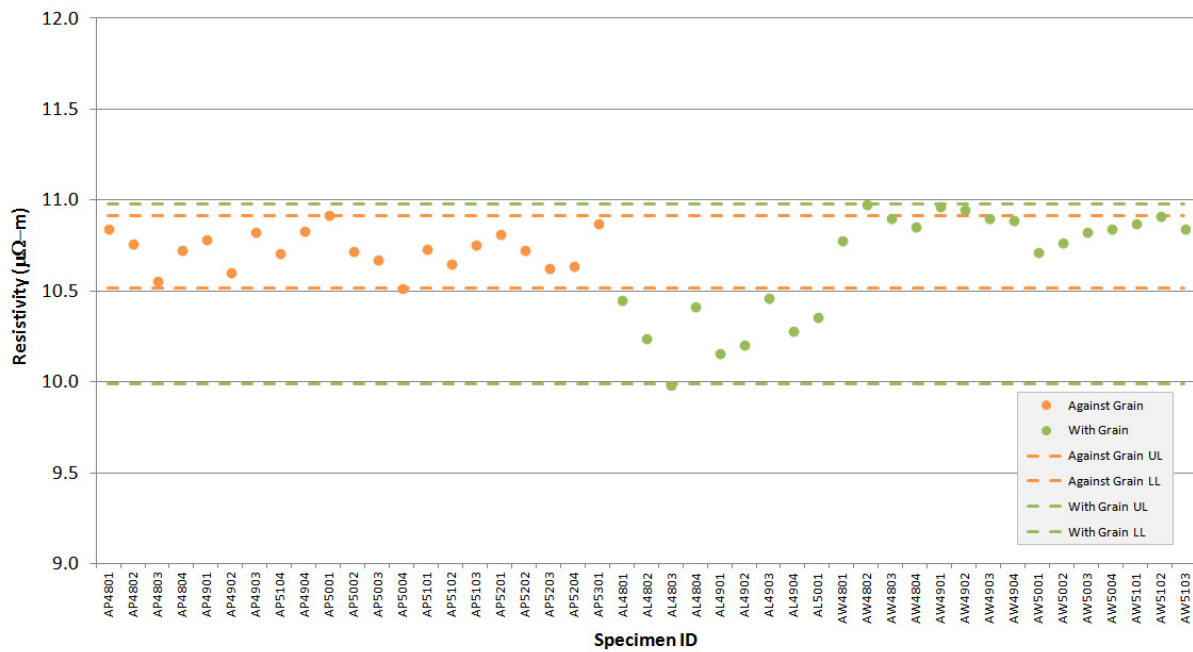


Figure A-76. NBG-17 creep specimen resistivity.

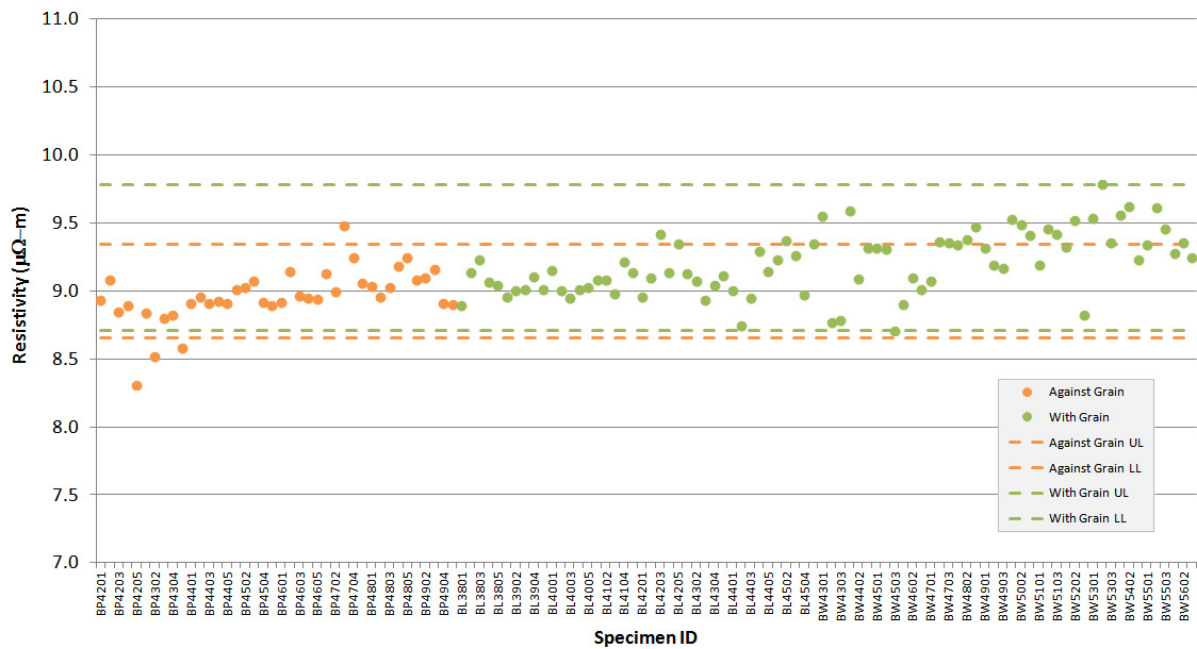


Figure A-77. NBG-18 creep specimen resistivity.

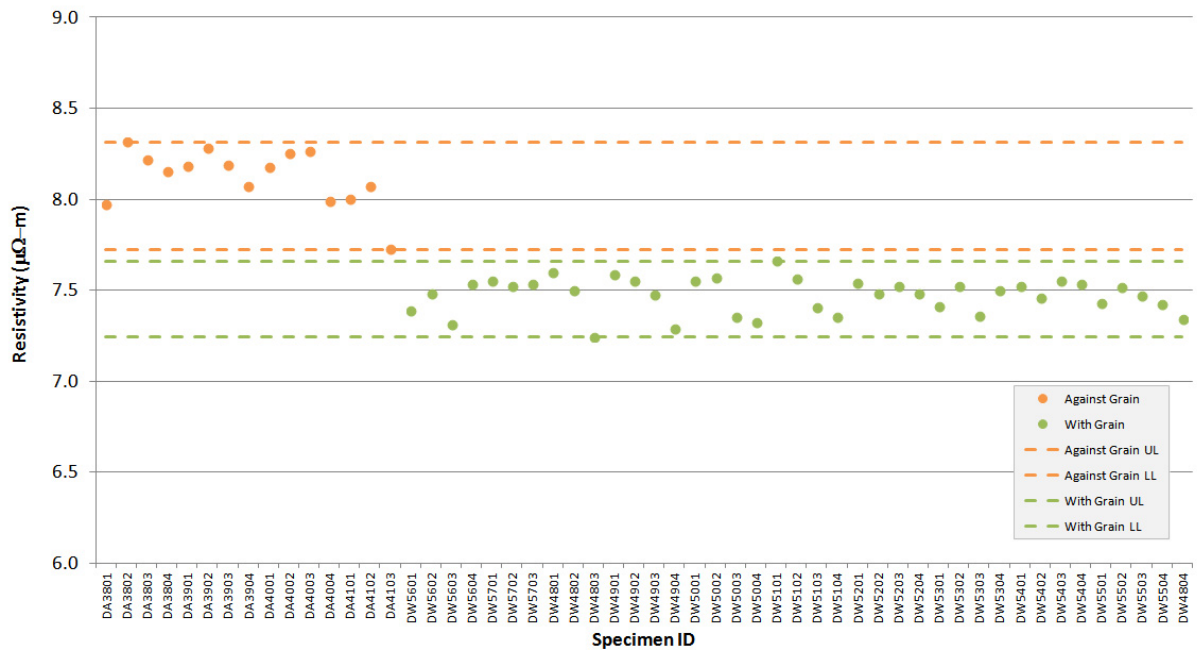


Figure A-78. PCEA creep specimen resistivity.

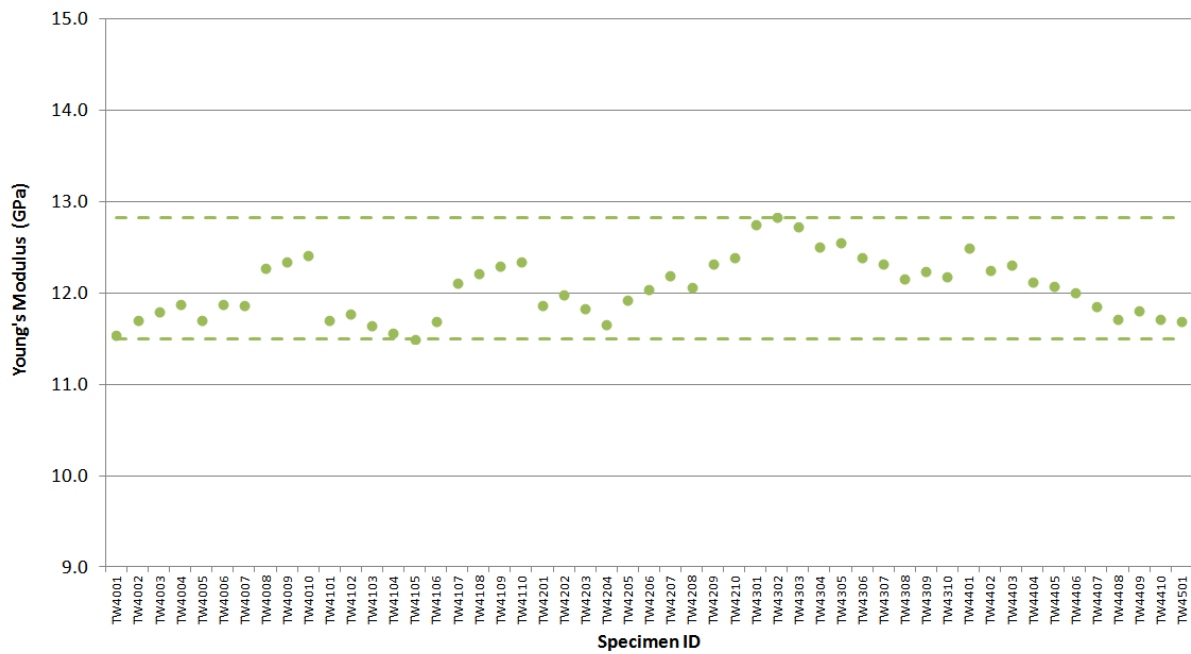


Figure A-79. 2114 creep specimen Young's Modulus by sonic velocity.

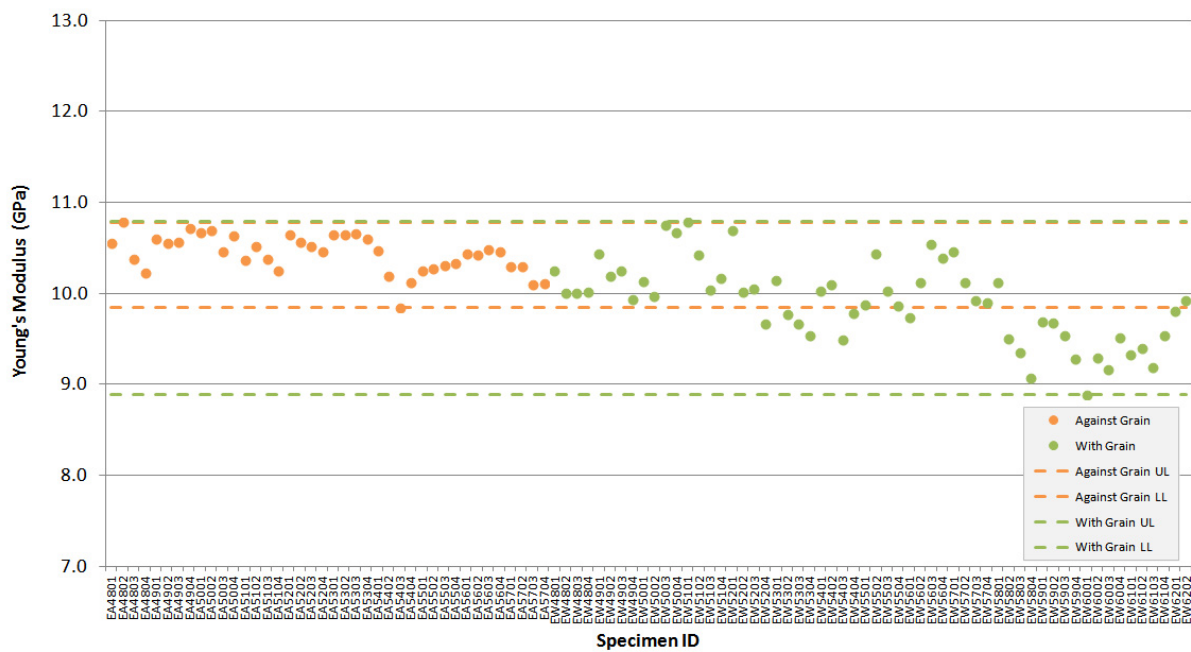


Figure A-80. IG-110 creep specimen Young's Modulus by sonic velocity.

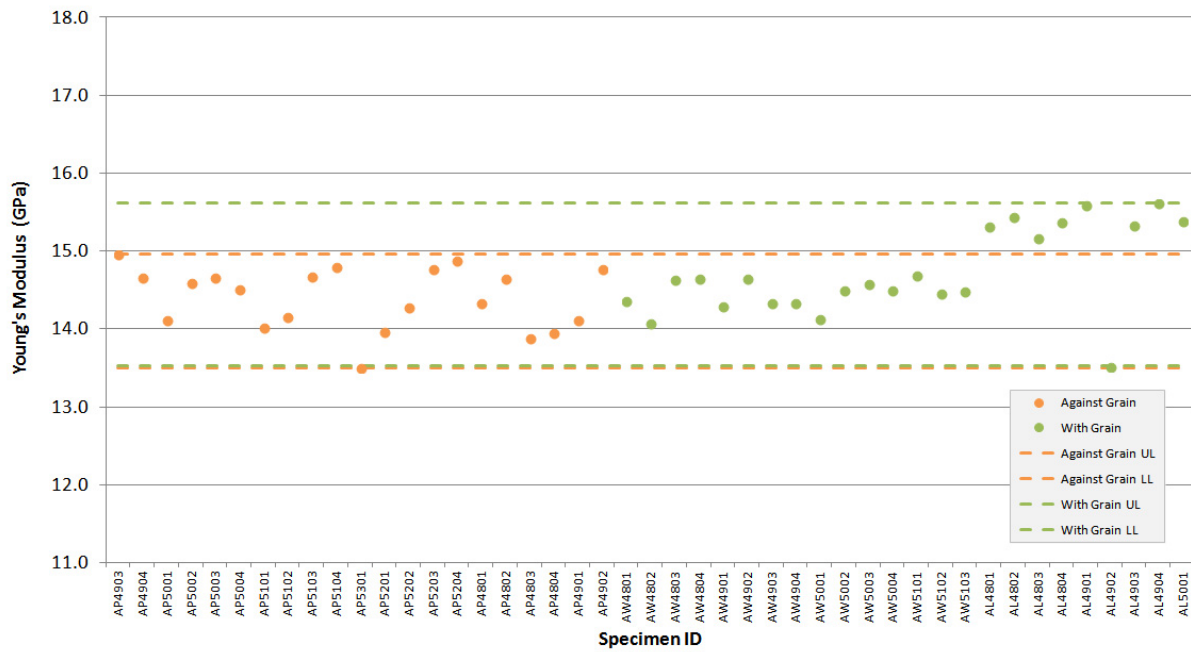


Figure A-81. NBG-17 creep specimen Young's Modulus by sonic velocity.

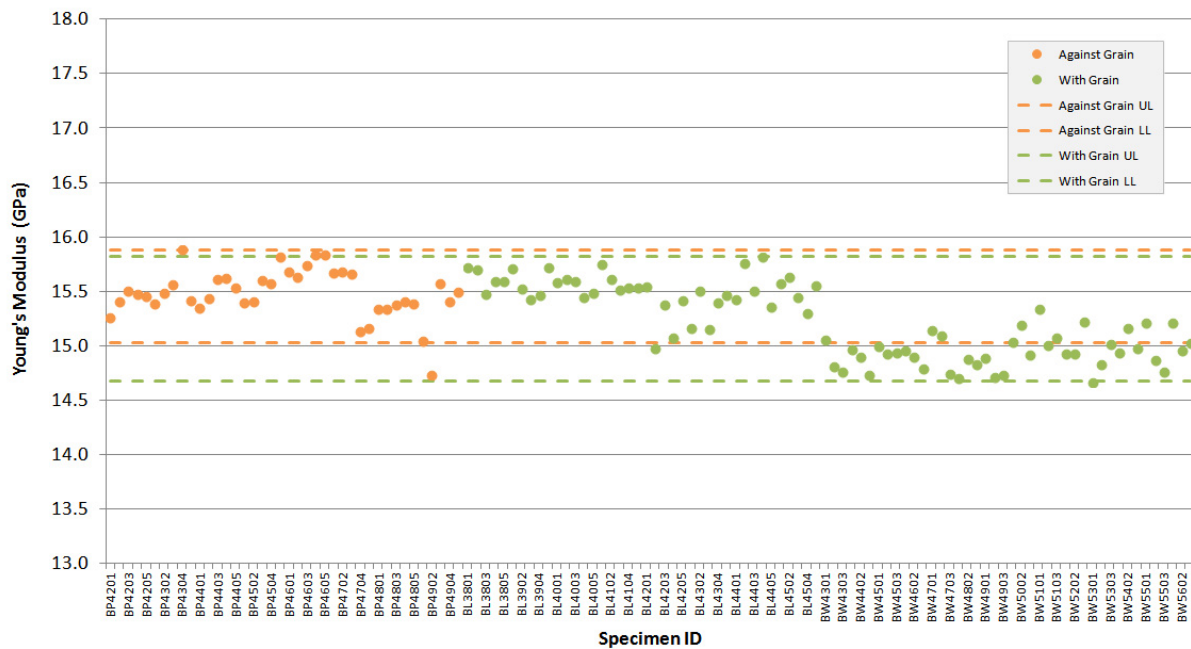


Figure A-82. NBG-18 creep specimen Young's Modulus by sonic velocity.

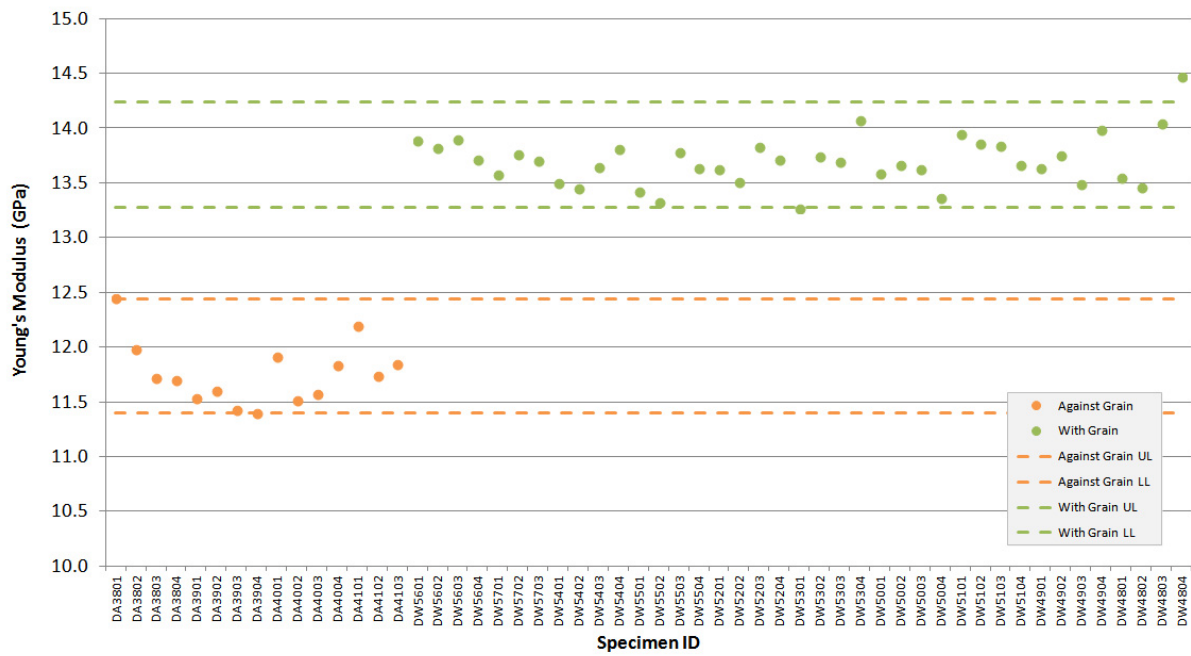


Figure A-83. PCEA creep specimen Young's Modulus by sonic velocity.

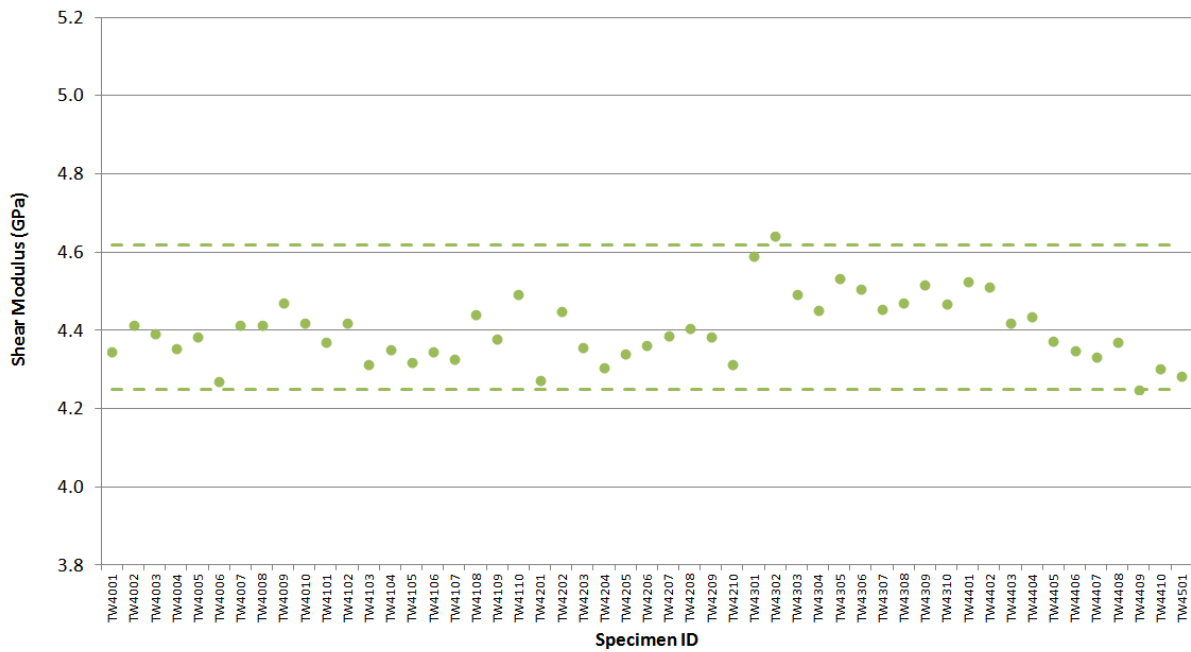


Figure A-84. 2114 creep specimen shear modulus by sonic velocity.

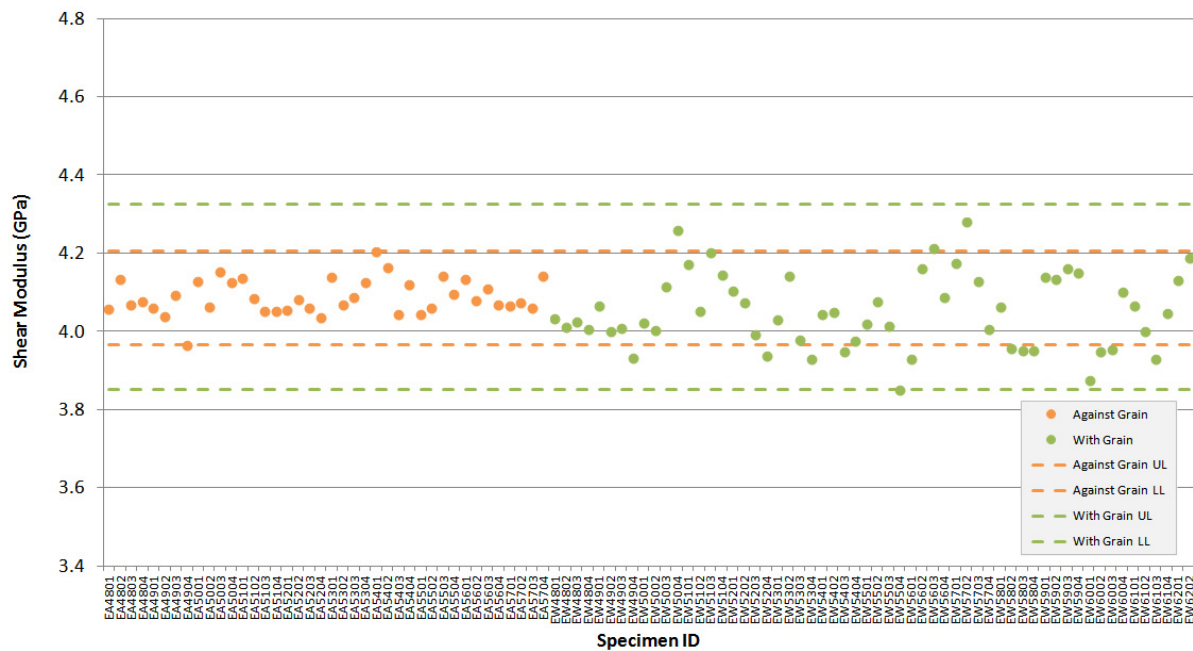


Figure A-85. IG-110 creep specimen shear modulus by sonic velocity.

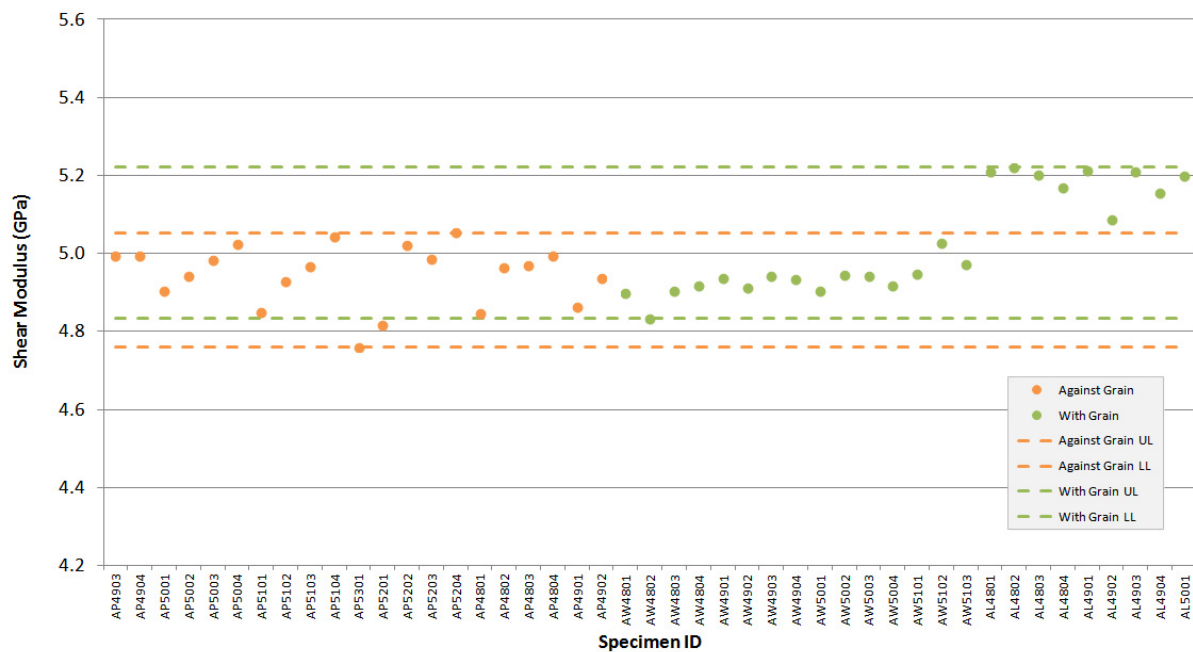


Figure A-86. NBG-17 creep specimen shear modulus by sonic velocity.

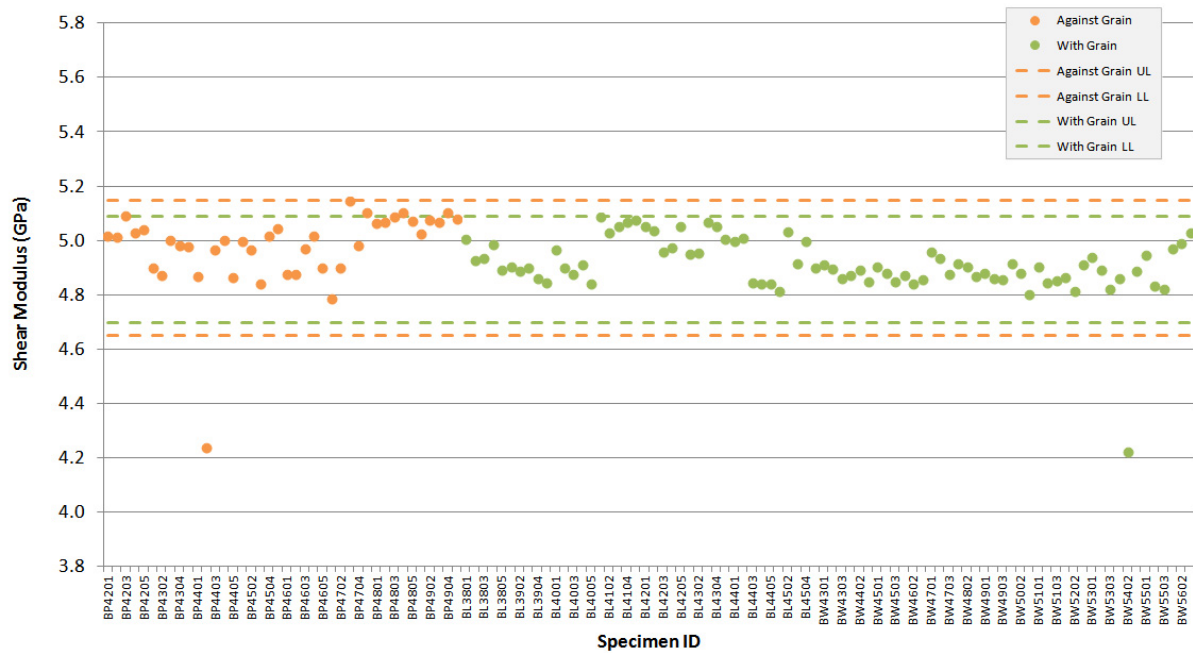


Figure A-87. NBG-18 creep specimen shear modulus by sonic velocity.

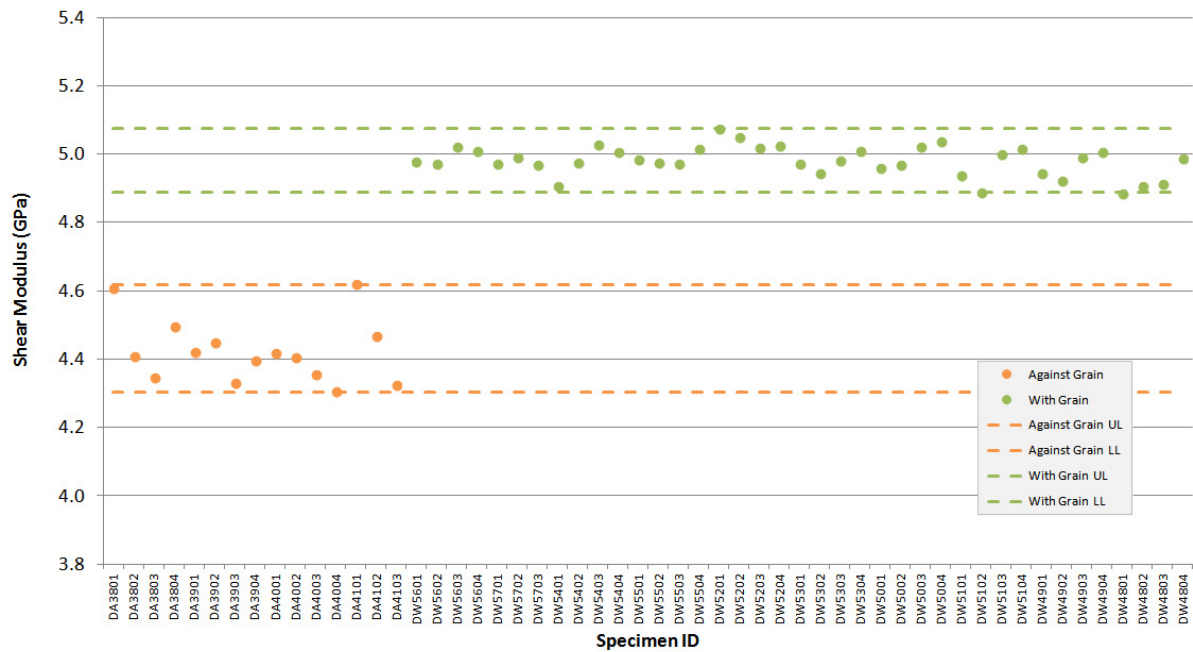


Figure A-88. PCEA creep specimen shear modulus by sonic velocity.

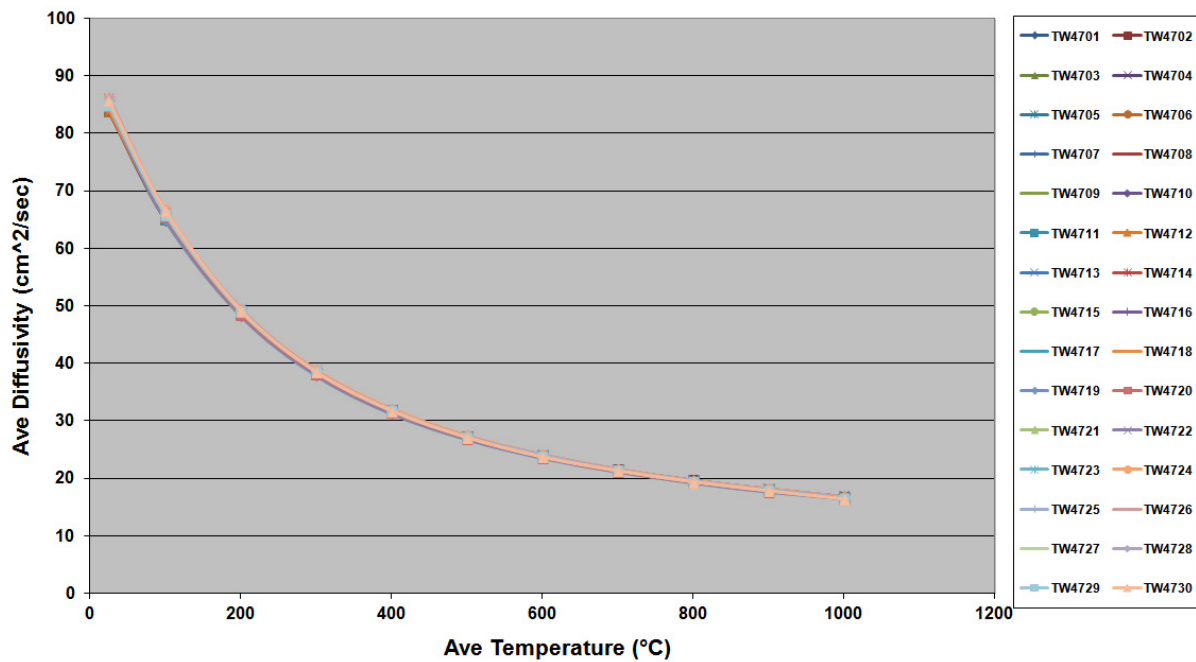


Figure A-89. 2114 piggyback specimen diffusivity.

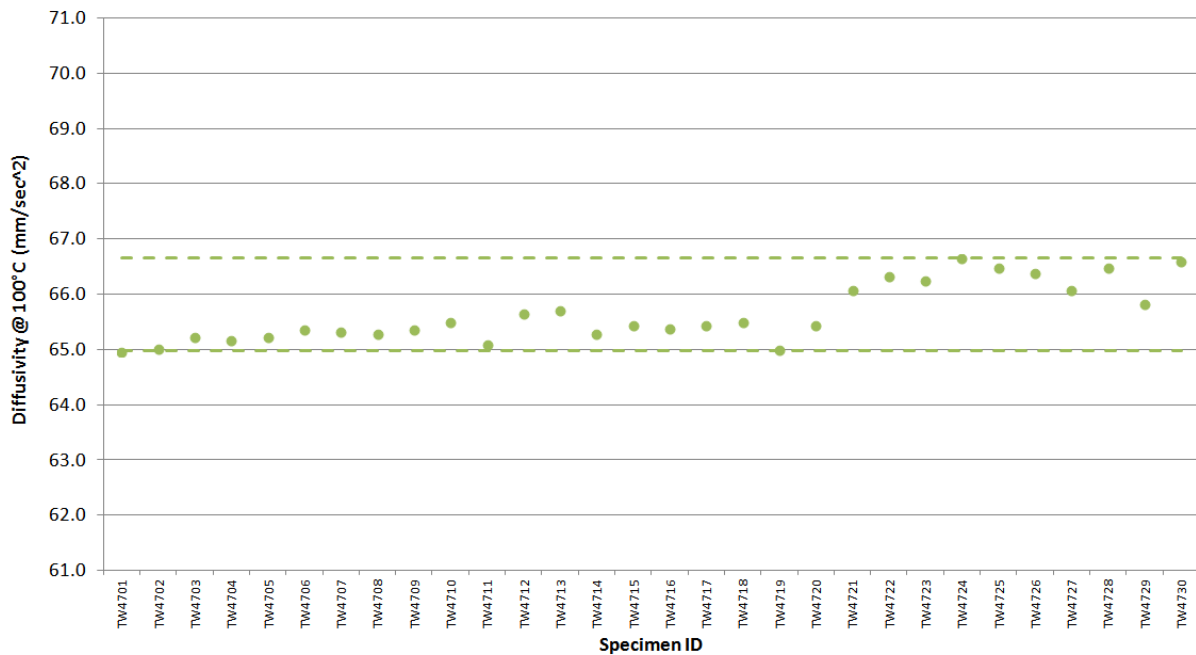


Figure A-90. 2114 piggyback specimen diffusivity @ 100°C.

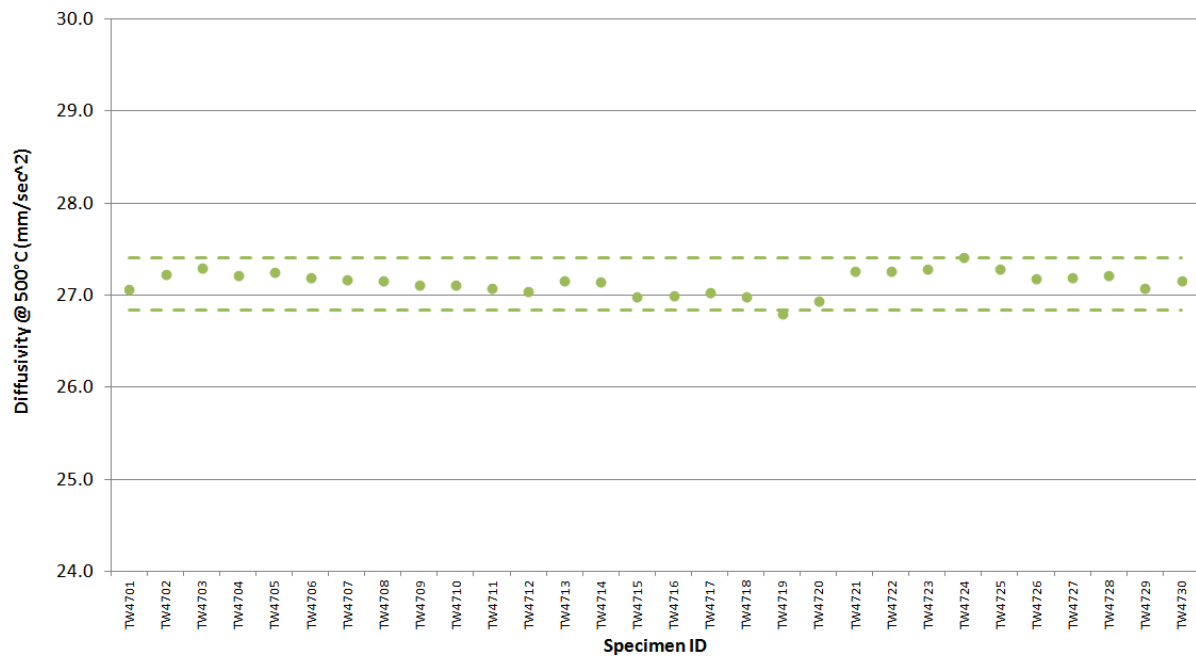


Figure A-91. 2114 piggyback specimen diffusivity @ 500°C.

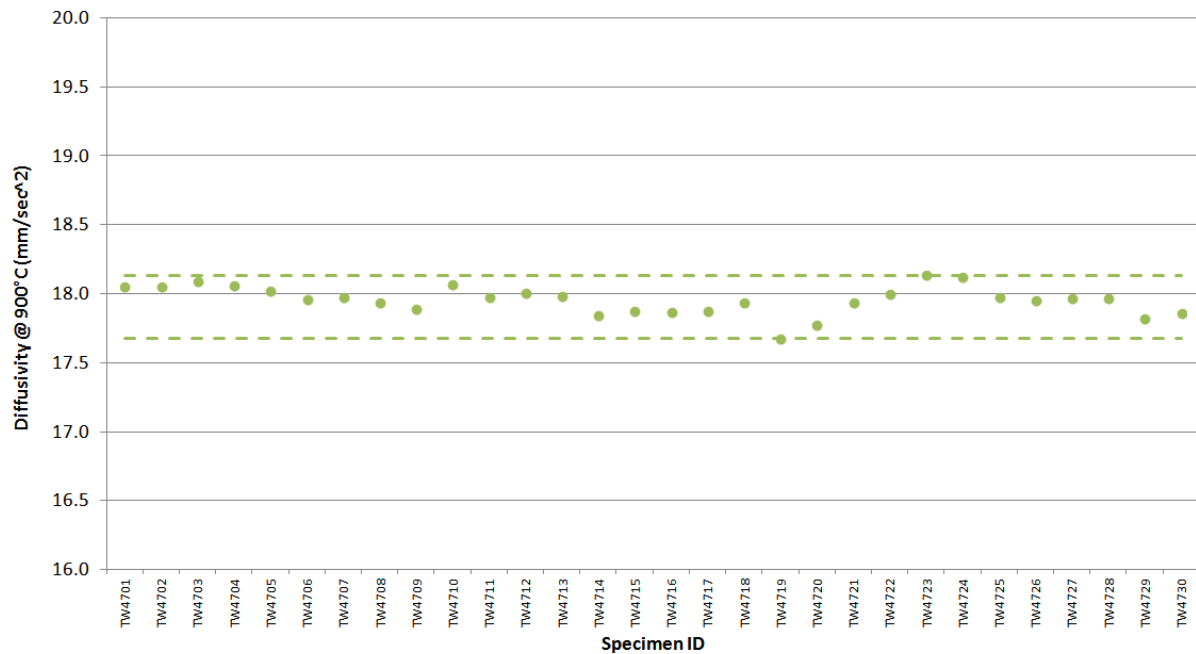


Figure A-92. 2114 piggyback specimen diffusivity @ 900°C.

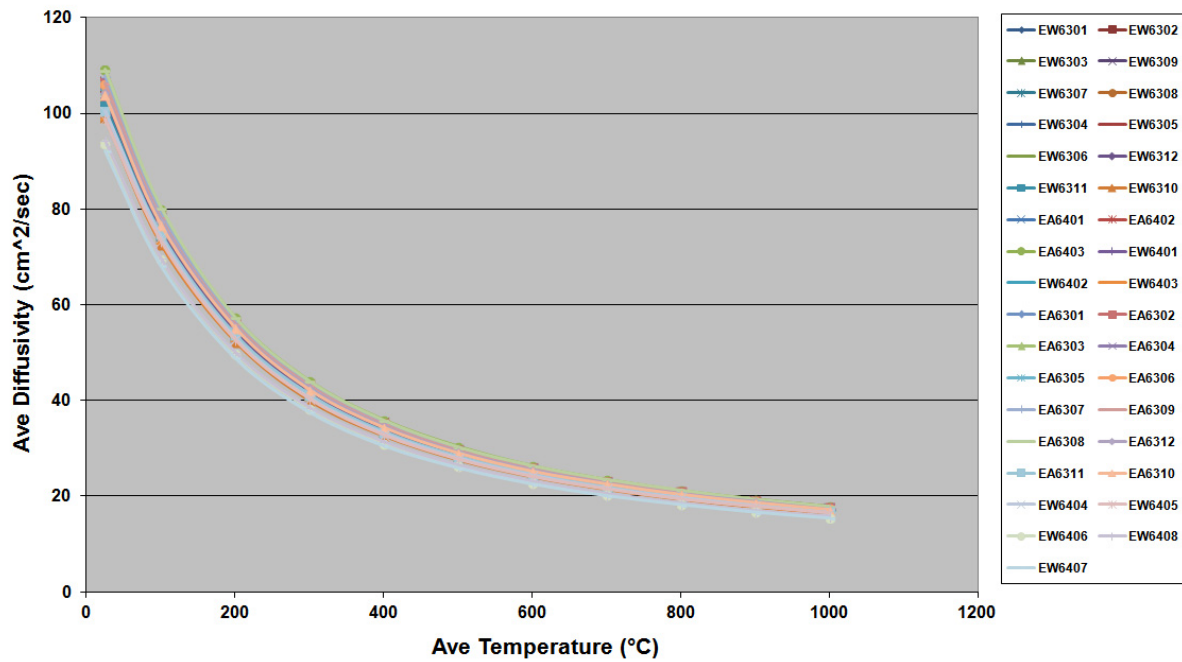


Figure A-93. IG-110 piggyback specimen diffusivity.

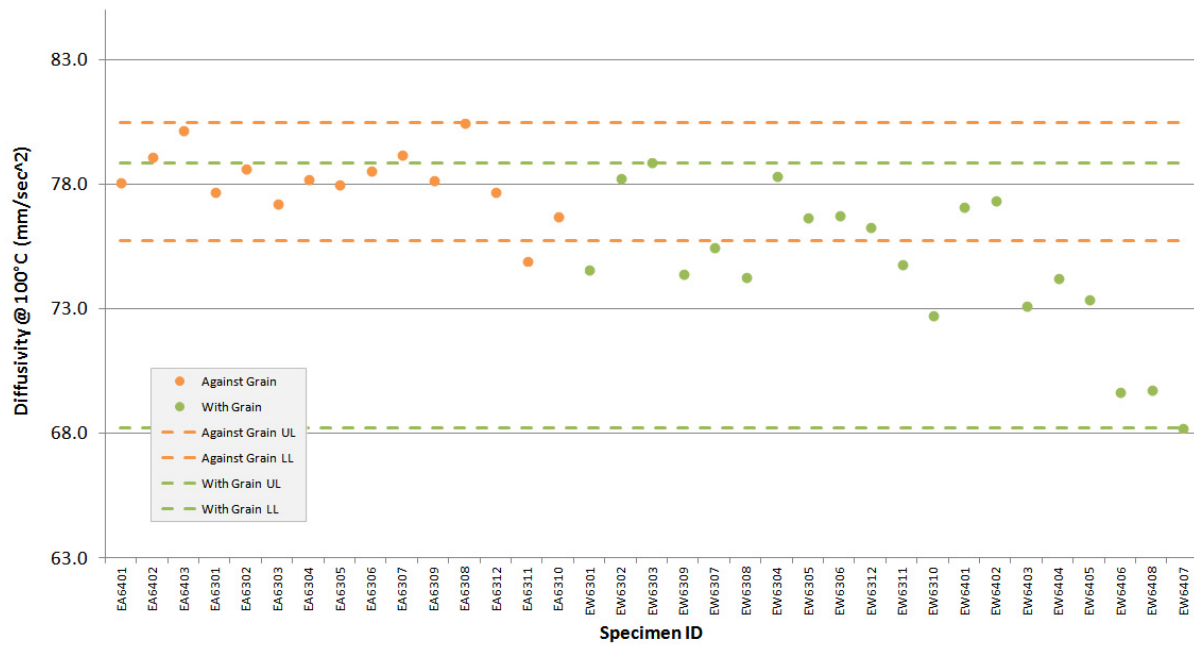


Figure A-94. IG-110 piggyback specimen diffusivity @ 100°C.

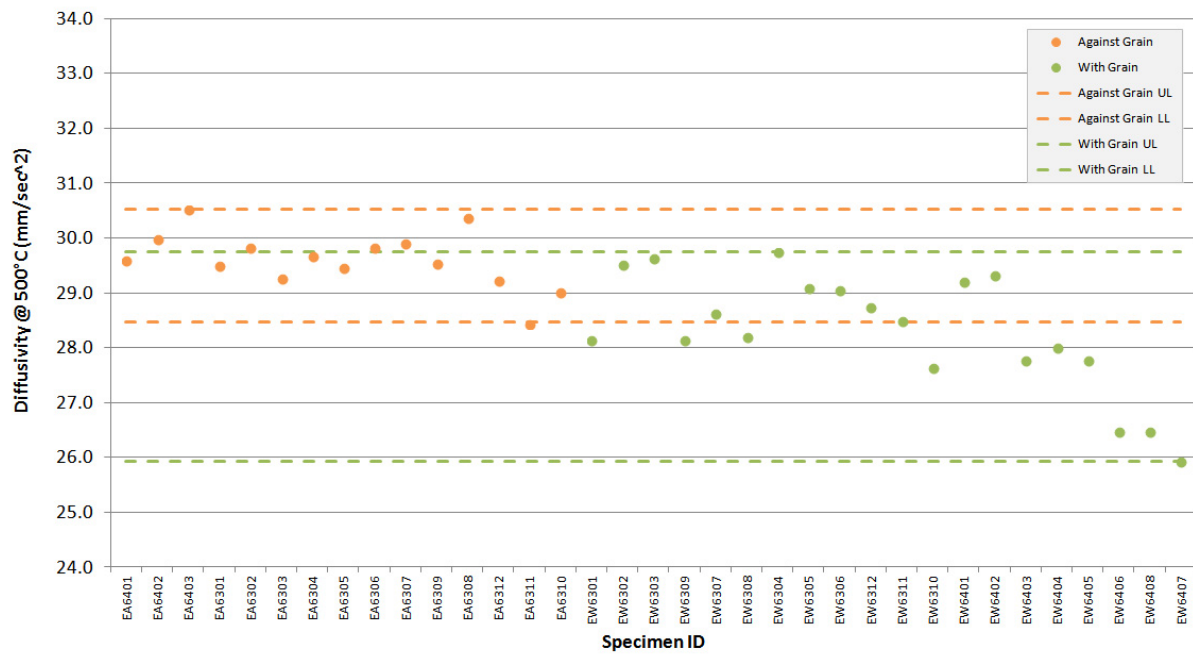


Figure A-95. IG-110 piggyback specimen diffusivity @ 500°C.

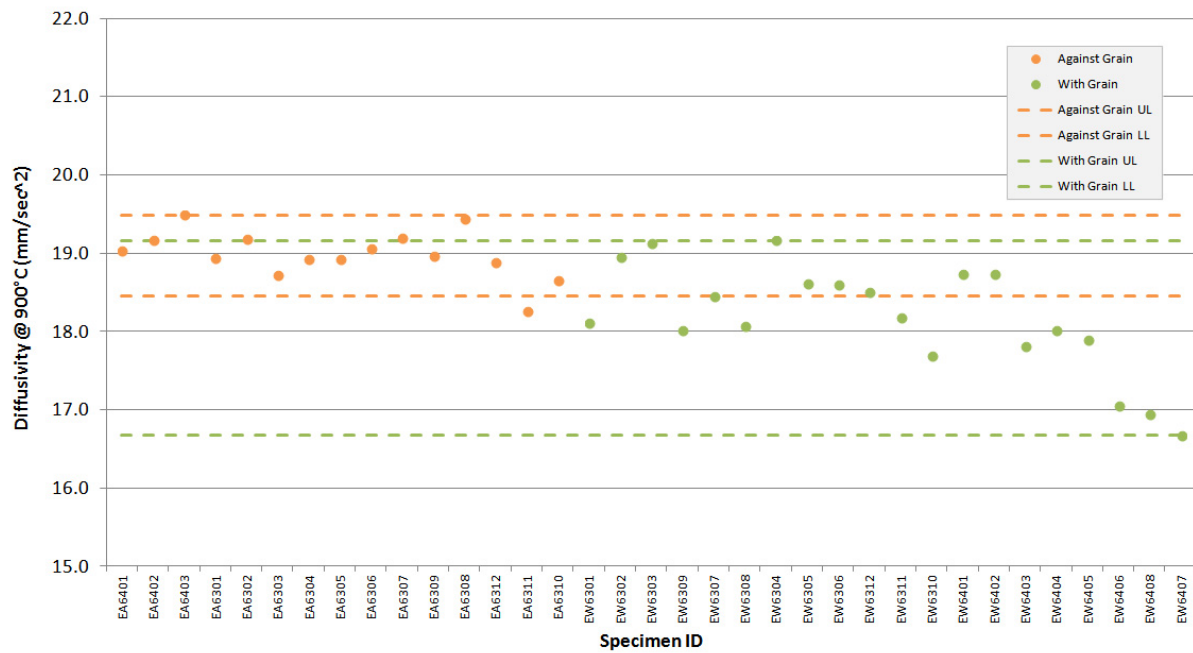


Figure A-96. IG-110 piggyback specimen diffusivity @ 900°C.

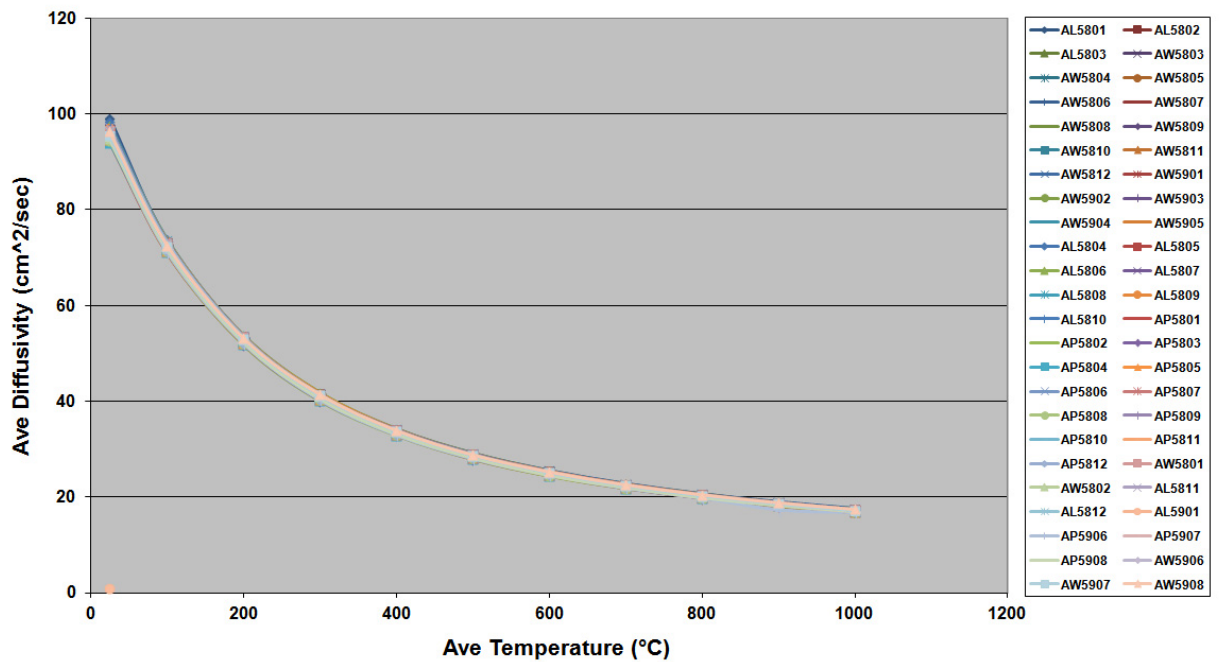


Figure A-97. NBG-17 piggyback specimen diffusivity.

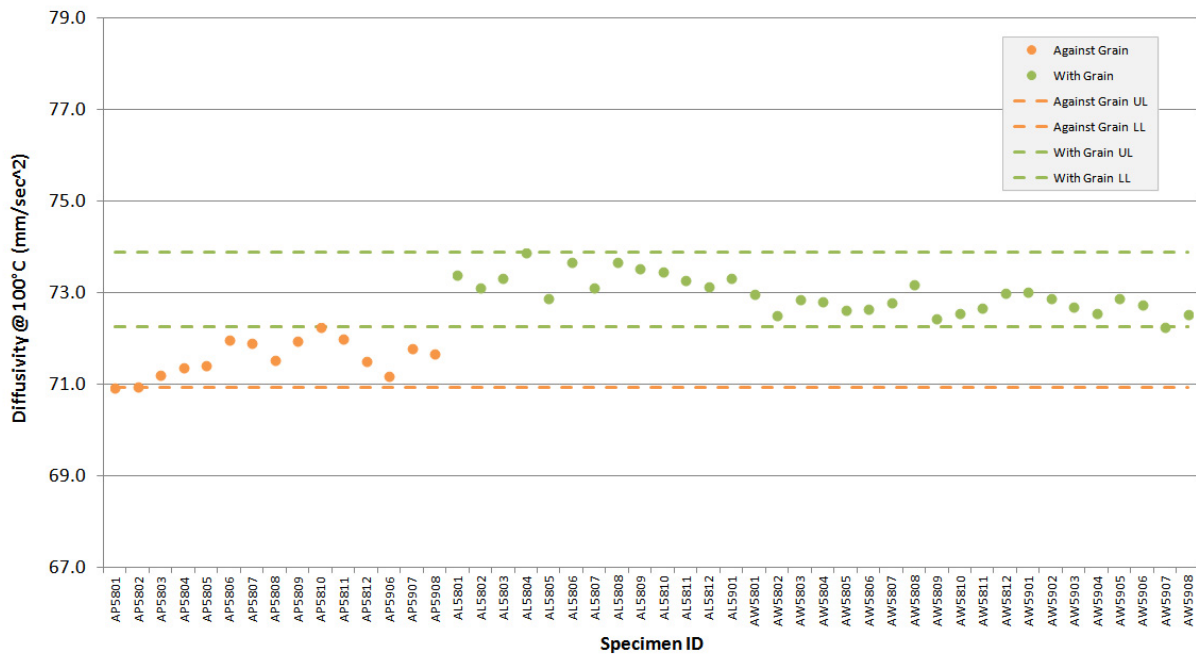


Figure A-98. NBG-17 piggyback specimen diffusivity @ 100°C.

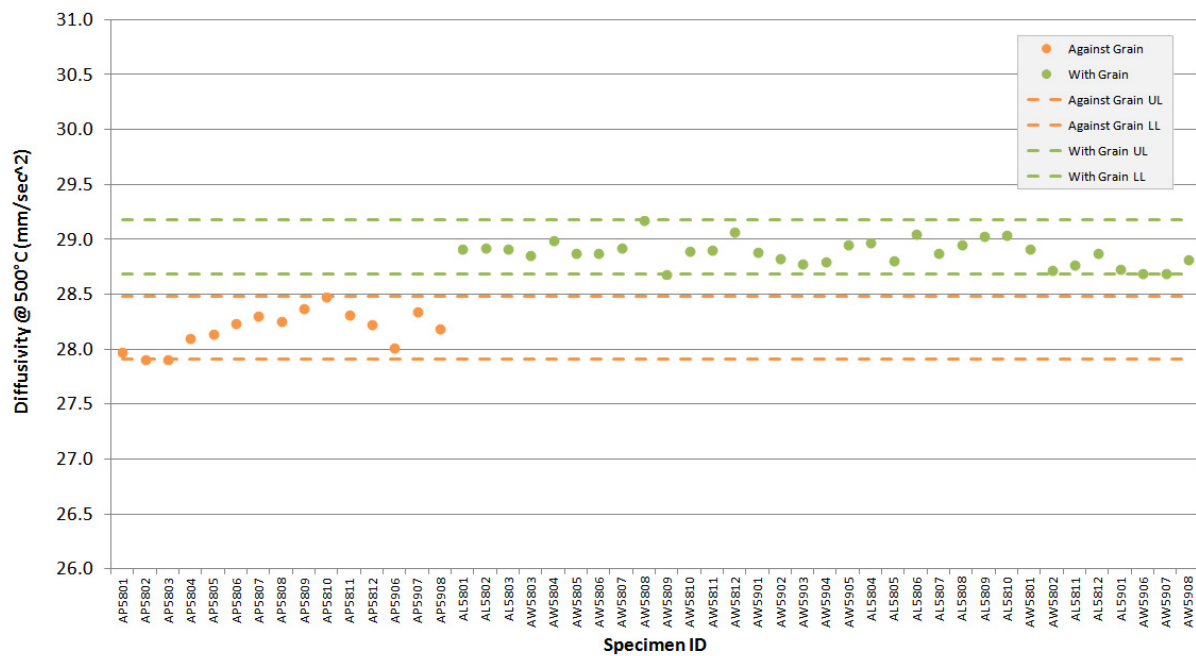


Figure A-99. NBG-17 piggyback specimen diffusivity @ 500°C.

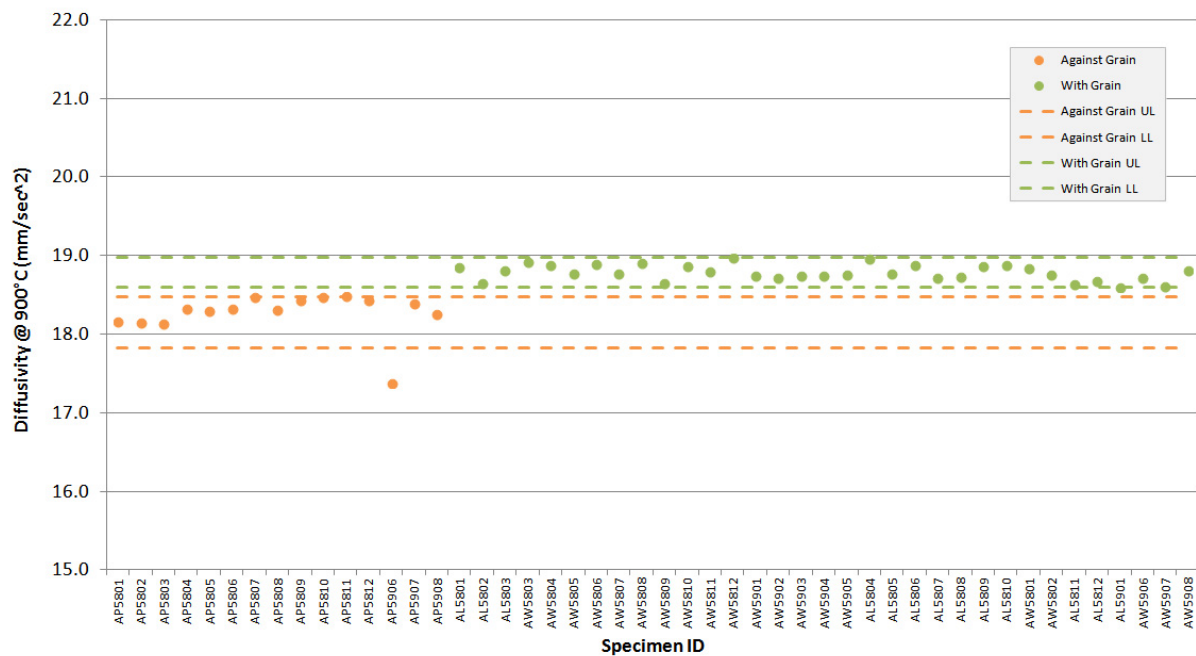


Figure A-100. NBG-17 piggyback specimen diffusivity @ 900°C.

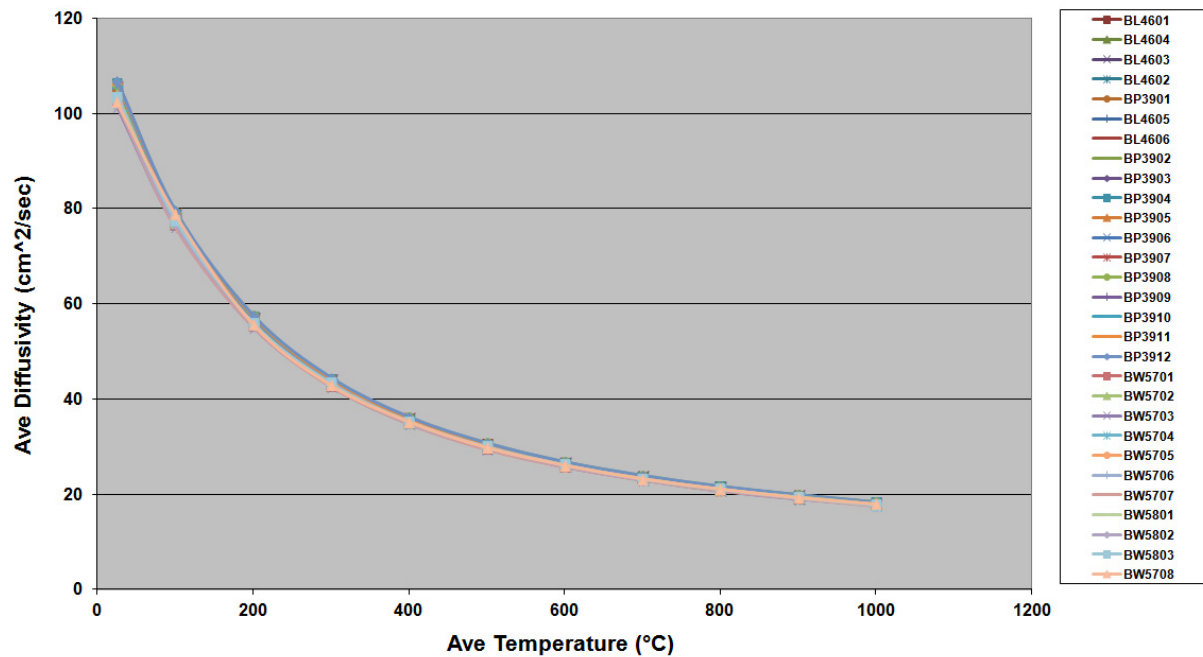


Figure A-101. NBG-18 piggyback specimen diffusivity.

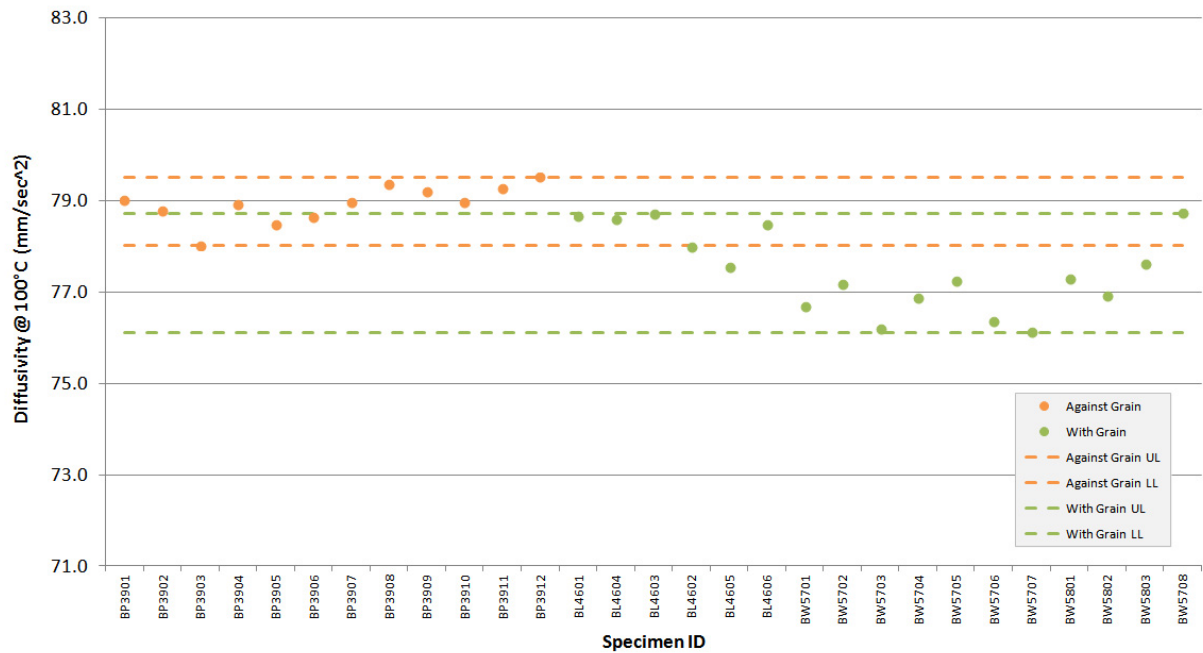


Figure A-102. NBG-18 piggyback specimen diffusivity @ 100°C.

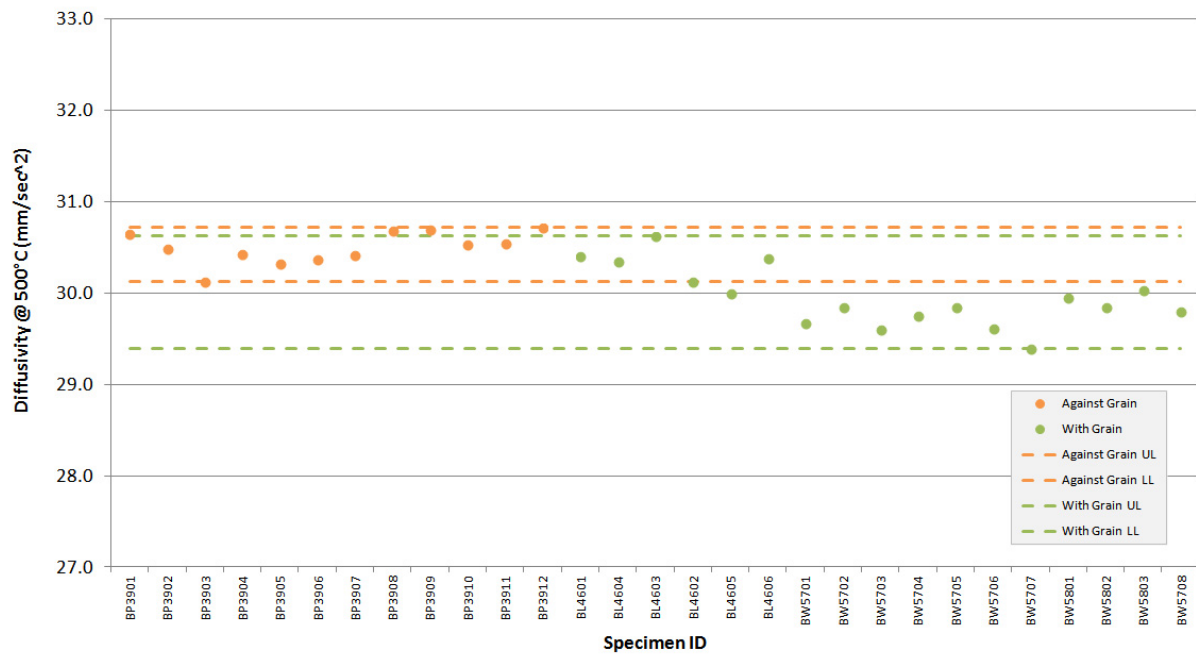


Figure A-103. NBG-18 piggyback specimen diffusivity @ 500°C.

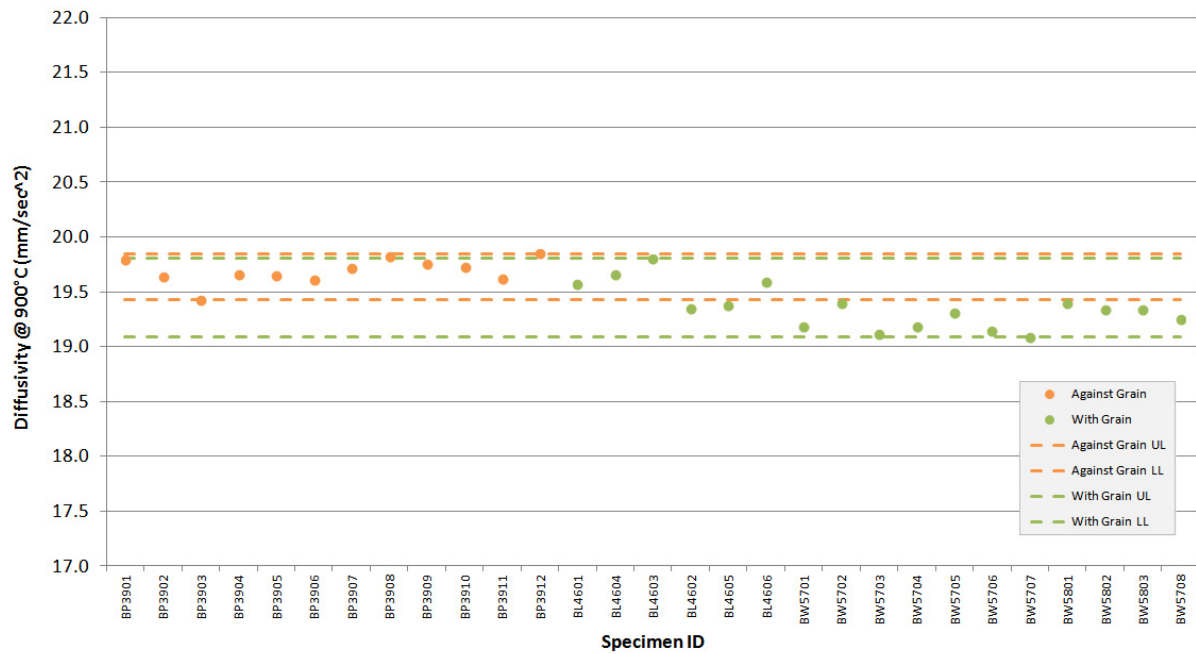


Figure A-104. NBG-18 piggyback specimen diffusivity @ 900°C.

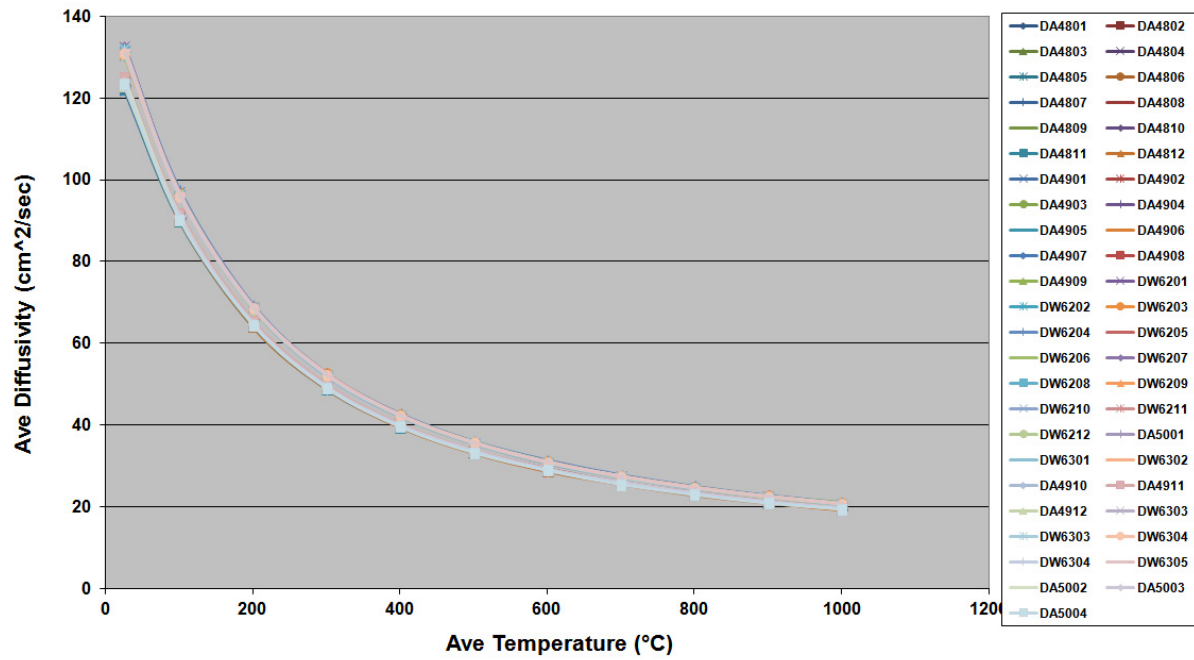


Figure A-105. PCEA piggyback specimen diffusivity.

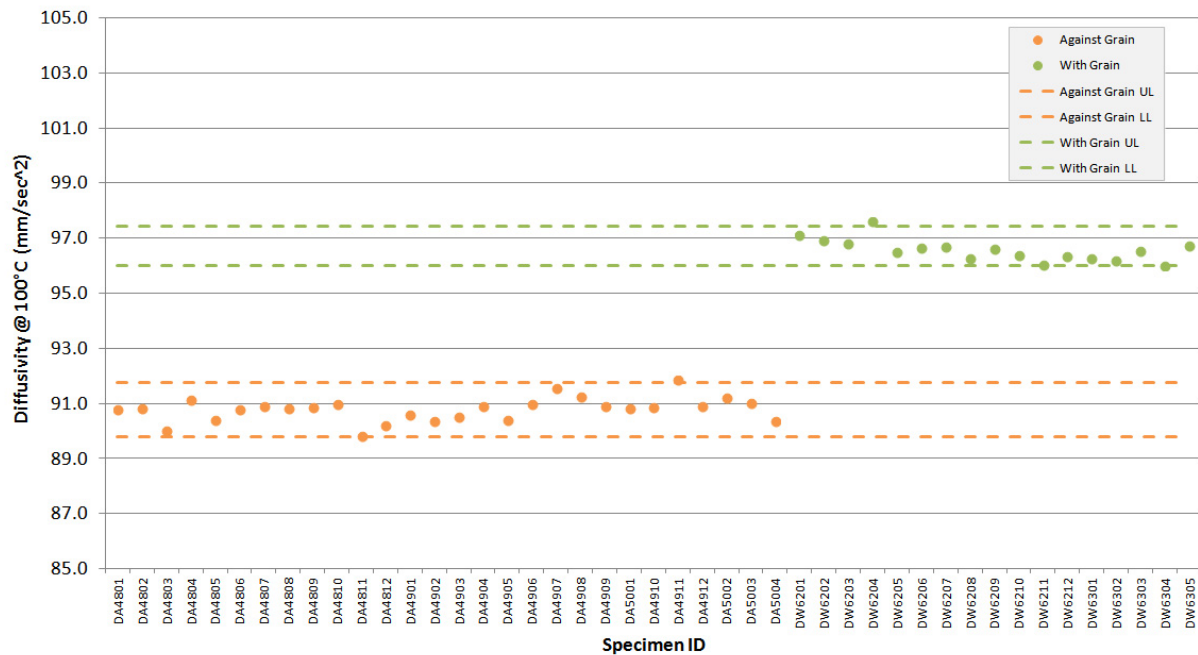


Figure A-106. PCEA piggyback specimen diffusivity @ 100°C.

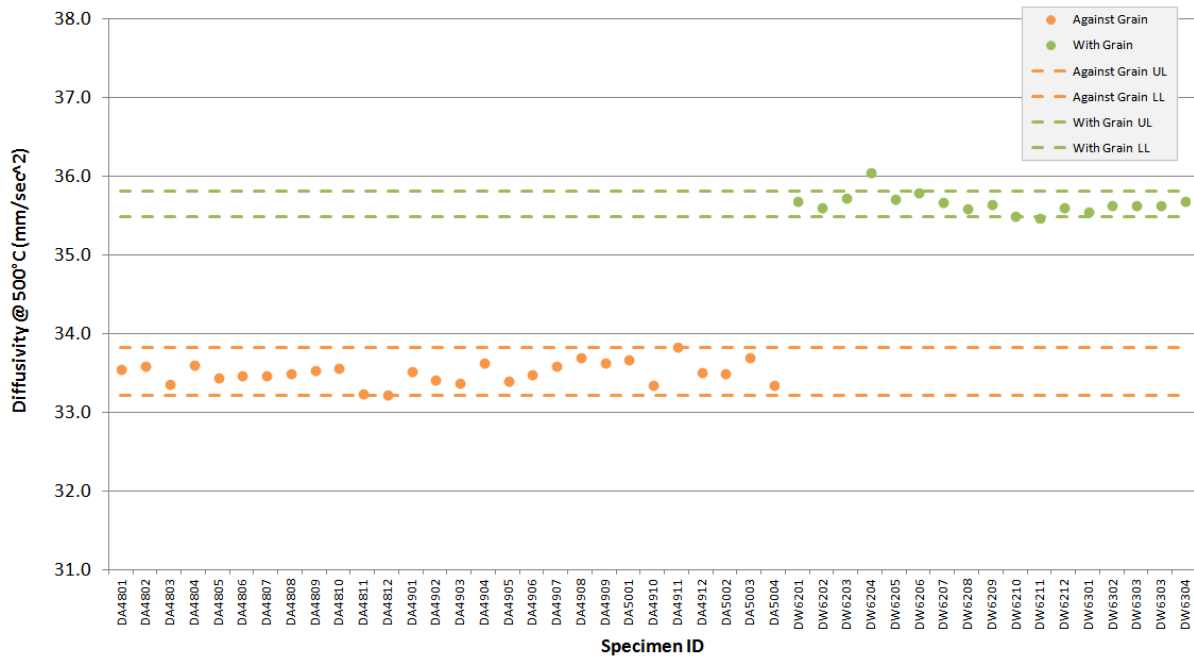


Figure A-107. PCEA piggyback specimen diffusivity @ 500°C.

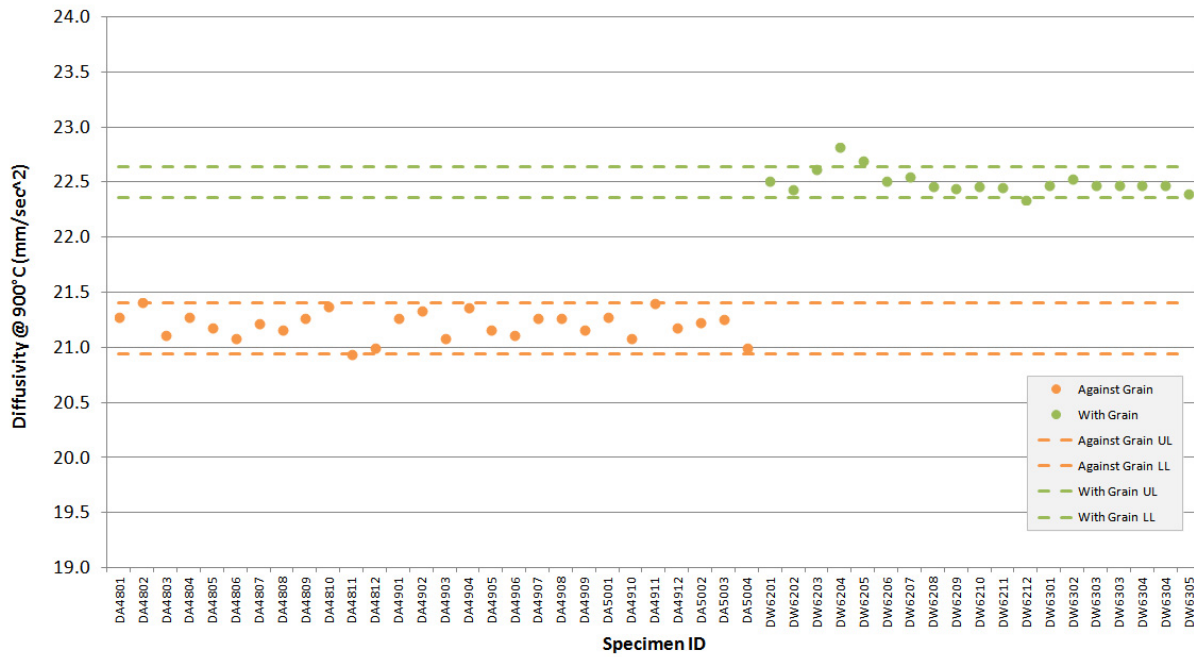


Figure A-108. PCEA piggyback specimen diffusivity @ 900°C.

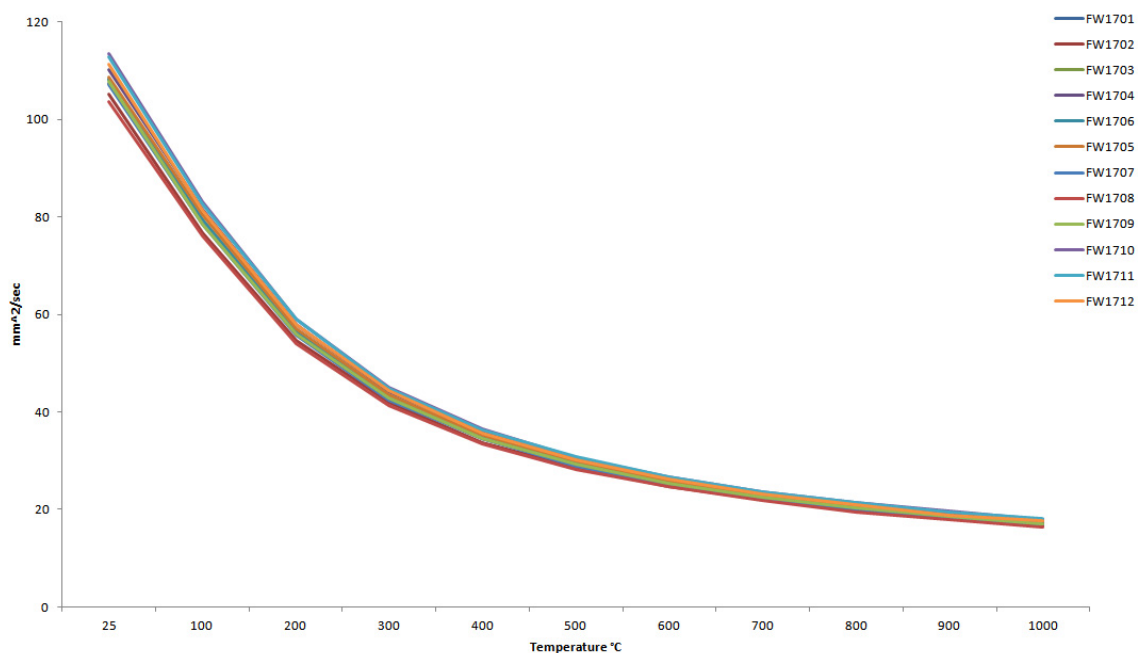


Figure A-109. IG-430 piggyback specimen diffusivity.

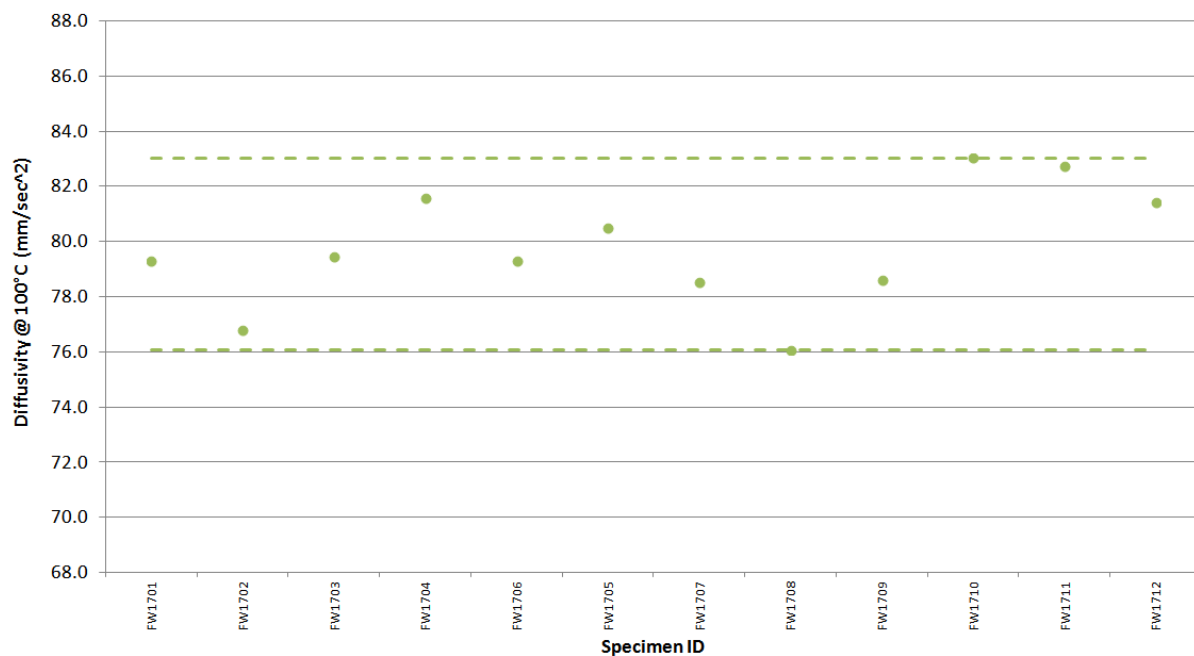


Figure A-110. IG-430 piggyback specimen diffusivity @ 100°C.

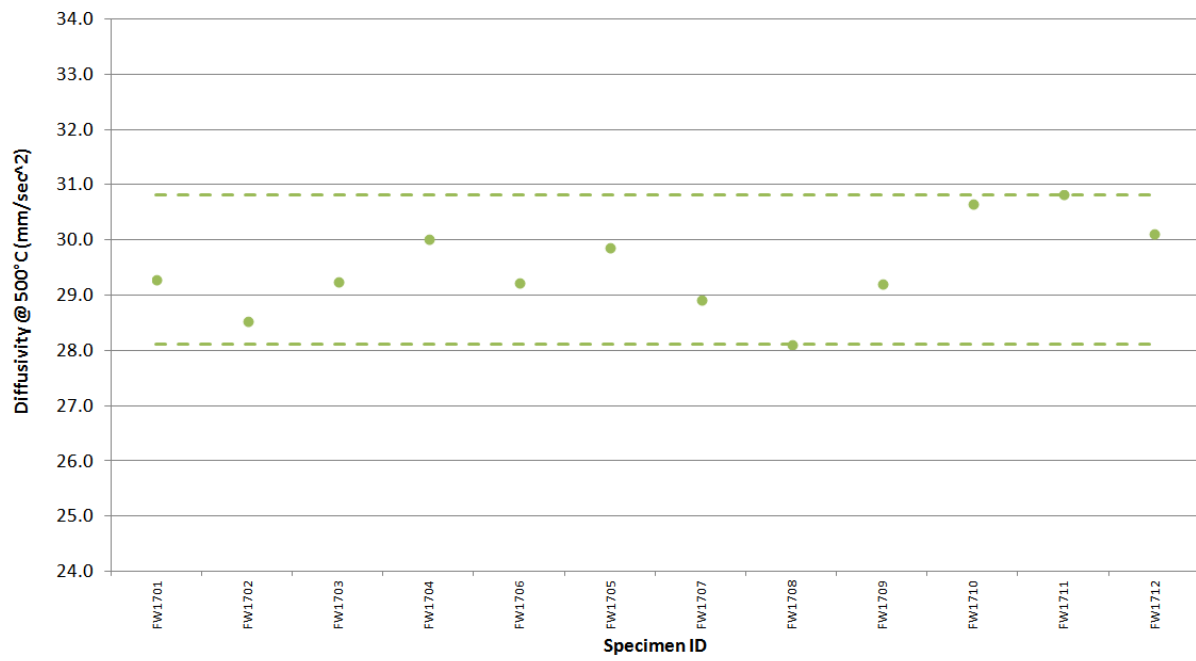


Figure A-111. IG-430 piggyback diffusivity @ 500°C.

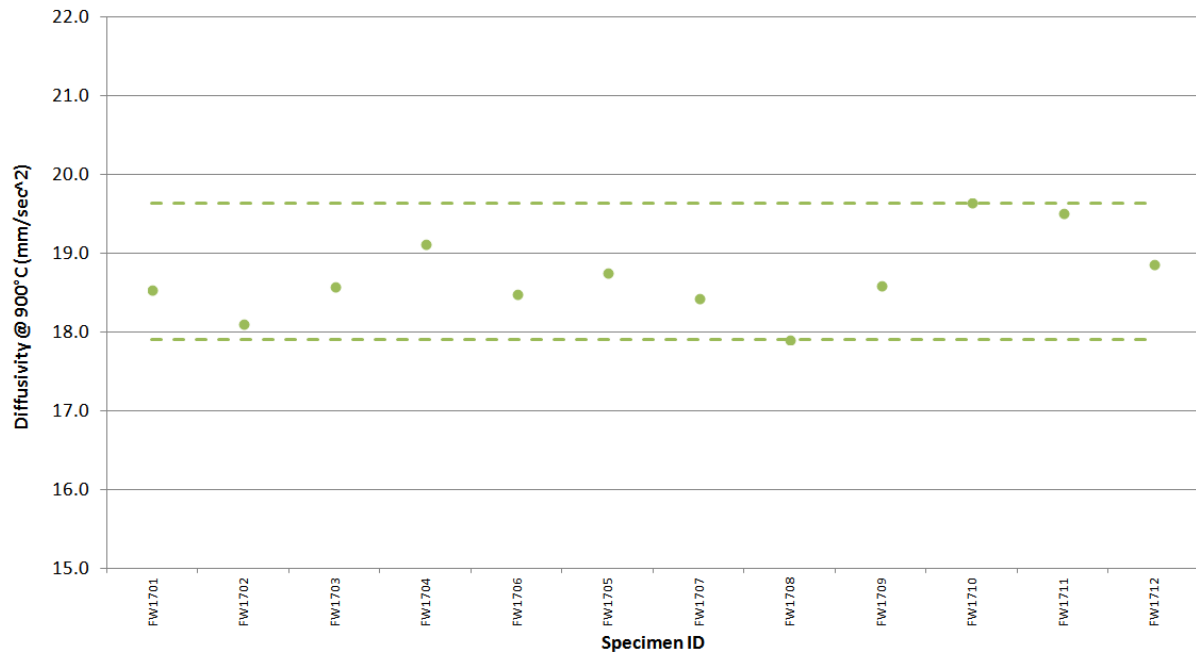


Figure A-112. IG-430 piggyback specimen diffusivity @ 900°C.

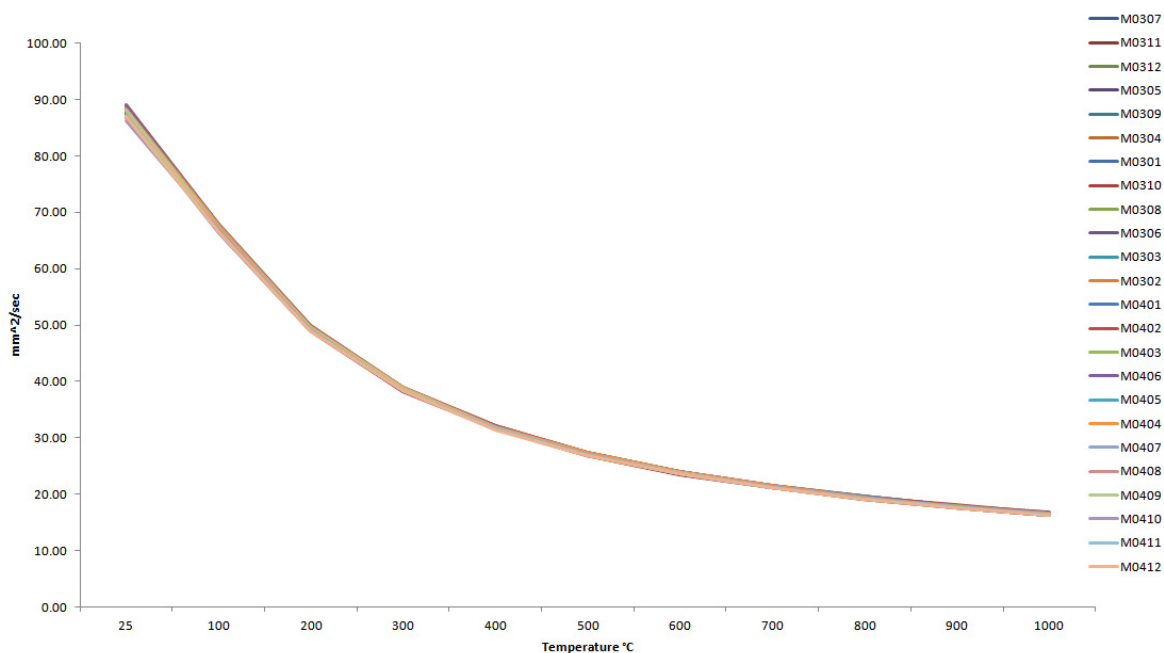


Figure A-113. NBG-25 piggyback specimen diffusivity.

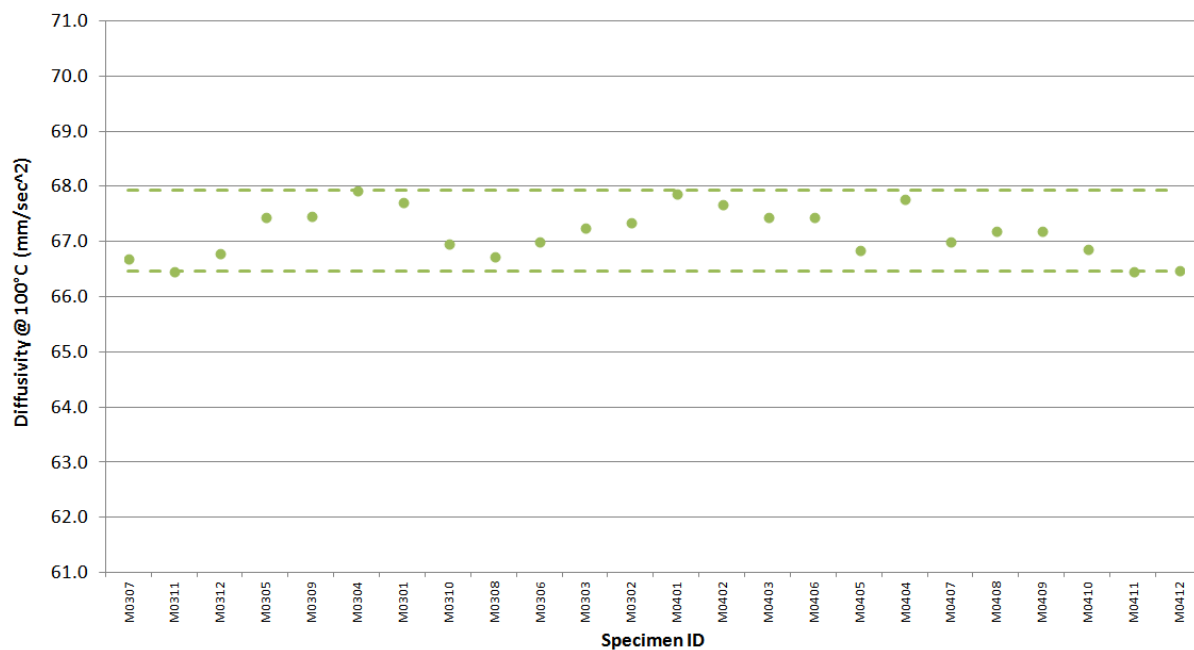


Figure A-114. NBG-25 piggyback specimen diffusivity @ 100°C .

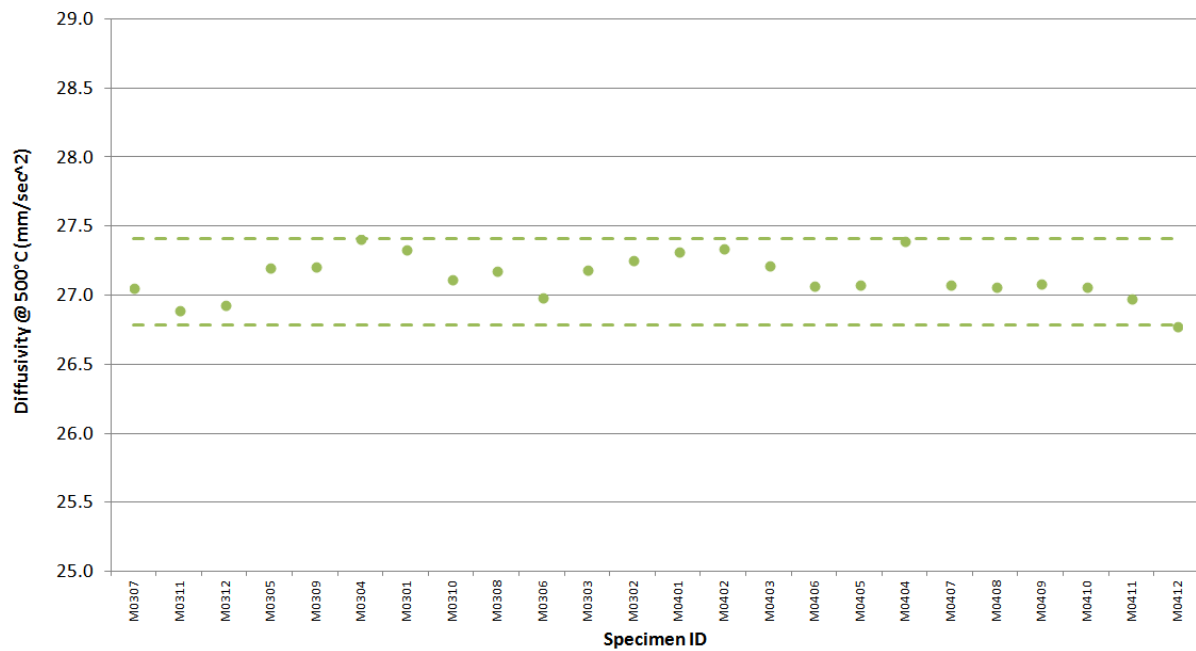


Figure A-115. NBG-25 piggyback specimen diffusivity @ 500°C.

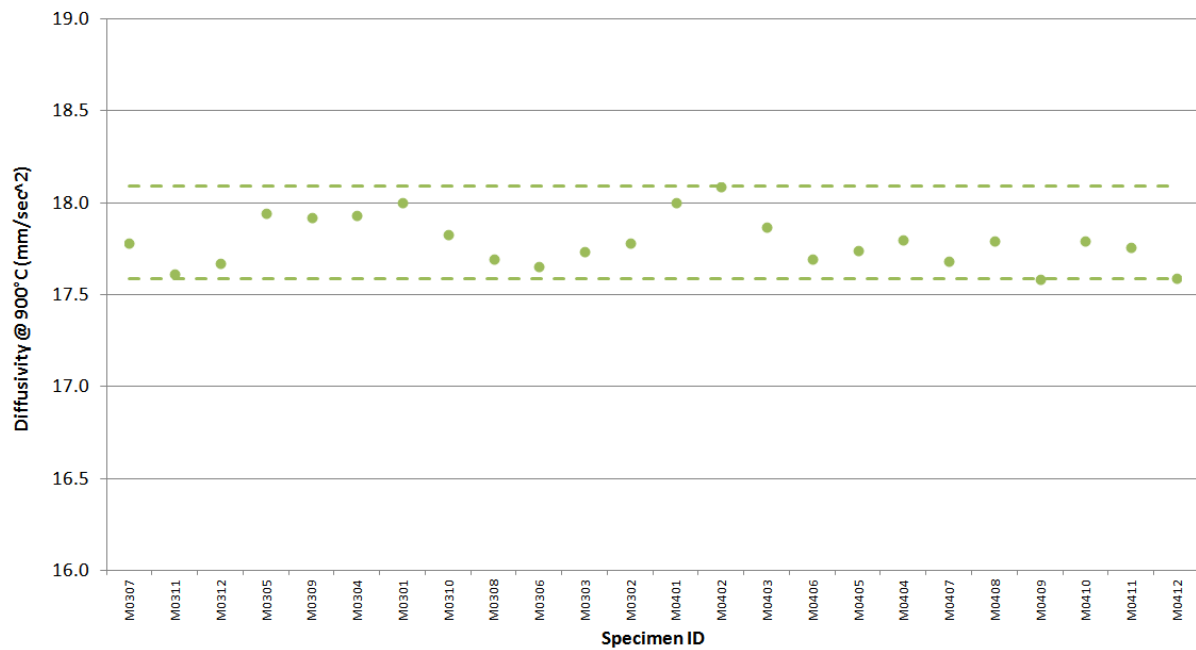


Figure A-116. NBG-25 piggyback specimen diffusivity @ 900°C.

Appendix B

Summary of Statistical Parameters

Appendix B

Summary of Statistical Parameters

Table B-1. Creep specimen length (mm) summary statistics.

Combined Specimens	Mean	Std Dev	CoV (%)	Median	Upper Limit	Lower Limit
NBG-17	25.400	0.037	0.14	25.410	25.432	25.381
NBG-18	25.405	0.010	0.04	25.406	25.424	25.385
PCEA	25.396	0.025	0.10	25.397	25.429	25.367
2114	25.399	0.015	0.06	25.401	25.407	25.395
IG-110	25.415	0.007	0.03	25.417	25.429	25.396

Against Grain Specimens	Mean	Std Dev	CoV (%)	Median	Upper Limit	Lower Limit
NBG-17	25.407	0.021	0.08	25.412	25.432	25.366
NBG-18	25.396	0.005	0.02	25.396	25.406	25.385
PCEA	25.392	0.034	0.13	25.395	25.423	25.370
2114	—	—	—	—	—	—
IG-110	25.416	0.006	0.02	25.418	25.424	25.401

With Grain Specimens	Mean	Std Dev	CoV (%)	Median	Upper Limit	Lower Limit
NBG-17	25.394	0.046	0.18	25.407	25.424	25.386
NBG-18	25.409	0.008	0.03	25.409	25.424	25.390
PCEA	25.399	0.016	0.06	25.399	25.434	25.361
2114	25.399	0.015	0.06	25.401	25.407	25.395
IG-110	25.414	0.008	0.03	25.415	25.429	25.396

Table B-2. Creep specimen diameter (mm) summary statistics.

Combined Specimens	Mean	Std Dev	CoV (%)	Median	Upper Limit	Lower Limit
NBG-17	12.460	0.007	0.05	12.458	12.466	12.452
NBG-18	12.458	0.012	0.09	12.457	12.479	12.427
PCEA	12.457	0.009	0.08	12.458	12.468	12.447
2114	12.448	0.008	0.06	12.448	12.466	12.437
IG-110	12.443	0.008	0.07	12.441	12.449	12.433

Against Grain Specimens	Mean	Std Dev	CoV (%)	Median	Upper Limit	Lower Limit
NBG-17	12.457	0.003	0.02	12.458	12.462	12.452
NBG-18	12.459	0.013	0.10	12.455	12.479	12.440
PCEA	12.456	0.013	0.11	12.456	12.466	12.446
2114	—	—	—	—	—	—
IG-110	12.449	0.010	0.08	12.444	12.474	12.439

With Grain Specimens	Mean	Std Dev	CoV (%)	Median	Upper Limit	Lower Limit
NBG-17	12.462	0.008	0.07	12.458	12.478	12.453
NBG-18	12.457	0.011	0.09	12.458	12.478	12.431
PCEA	12.458	0.005	0.04	12.459	12.469	12.446
2114	12.448	0.008	0.06	12.448	12.466	12.437
IG-110	12.439	0.002	0.02	12.440	12.443	12.434

Table B-3. Creep specimen mass (g) summary statistics.

Combined Specimens	Mean	Std Dev	CoV (%)	Median	Upper Limit	Lower Limit
NBG-17	5.562	0.028	0.505	5.562	5.615	5.486
NBG-18	5.608	0.019	0.333	5.607	5.658	5.560
PCEA	5.511	0.078	1.416	5.556	5.596	5.336
2114	5.514	0.021	0.388	5.515	5.548	5.460
IG-110	5.350	0.019	0.348	5.349	5.386	5.303

Against Grain Specimens	Mean	Std Dev	CoV (%)	Median	Upper Limit	Lower Limit
NBG-17	5.566	0.017	0.304	5.572	5.595	5.541
NBG-18	5.621	0.020	0.361	5.624	5.659	5.586
PCEA	5.427	0.046	0.839	5.417	5.479	5.356
2114	—	—	—	—	—	—
IG-110	5.344	0.018	0.340	5.343	5.377	5.305

With Grain Specimens	Mean	Std Dev	CoV (%)	Median	Upper Limit	Lower Limit
NBG-17	5.559	0.035	0.632	5.545	5.615	5.486
NBG-18	5.602	0.014	0.256	5.605	5.628	5.560
PCEA	5.571	0.014	0.256	5.572	5.596	5.536
2114	5.514	0.021	0.388	5.515	5.548	5.460
IG-110	5.353	0.018	0.340	5.352	5.386	5.304

Table B-4. Creep specimen density (g/cm³) summary statistics.

Combined Specimens	Mean	Std Dev	CoV (%)	Median	Upper Limit	Lower Limit
NBG-17	1.8311	0.0083	0.46	1.8311	1.8439	1.8138
NBG-18	1.8471	0.0048	0.26	1.8462	1.8574	1.8376
PCEA	1.8155	0.0249	1.37	1.8311	1.8417	1.7711
2114	1.8186	0.0066	0.37	1.8191	1.8288	1.8050
IG-110	1.7654	0.0061	0.34	1.7658	1.7776	1.7522

Against Grain Specimens	Mean	Std Dev	CoV (%)	Median	Upper Limit	Lower Limit
NBG-17	1.8325	0.0061	0.33	1.8343	1.8406	1.8218
NBG-18	1.8512	0.0050	0.27	1.8534	1.8600	1.8434
PCEA	1.7884	0.0140	0.78	1.7852	1.8019	1.7711
2114	—	—	—	—	—	—
IG-110	1.7618	0.0050	0.29	1.7610	1.7715	1.7522

With Grain Specimens	Mean	Std Dev	CoV (%)	Median	Upper Limit	Lower Limit
NBG-17	1.8298	0.0098	0.54	1.8265	1.8439	1.8138
NBG-18	1.8451	0.0031	0.17	1.8453	1.8524	1.8376
PCEA	1.8348	0.0039	0.21	1.8355	1.8417	1.8235
2114	1.8186	0.0066	0.37	1.8191	1.8288	1.8050
IG-110	1.7677	0.0055	0.31	1.7672	1.7776	1.7539

Table B-5. Creep specimen coefficient of thermal expansion (1/K) at 100 °C summary statistics.

Combined Specimens	Mean	Std Dev	CoV (%)	Median	Upper Limit	Lower Limit
NBG-17	4.85E-06	1.73E-07	3.57	4.82E-06	5.11E-06	4.54E-06
NBG-18	5.27E-06	7.00E-07	13.27	5.18E-06	6.57E-06	4.00E-06
PCEA	4.16E-06	2.46E-07	5.91	4.15E-06	4.73E-06	3.67E-06
2114	4.69E-06	2.42E-07	5.17	4.71E-06	5.19E-06	4.20E-06
IG-110	4.36E-06	4.78E-07	10.96	4.39E-06	5.42E-06	3.29E-06

Against Grain Specimens	Mean	Std Dev	CoV (%)	Median	Upper Limit	Lower Limit
NBG-17	4.90E-06	1.62E-07	3.30	4.93E-06	5.11E-06	4.56E-06
NBG-18	5.00E-06	6.49E-07	12.97	5.07E-06	5.94E-06	4.37E-06
PCEA	4.39E-06	2.08E-07	4.73	4.39E-06	4.73E-06	4.07E-06
2114	—	—	—	—	—	—
IG-110	4.06E-06	3.96E-07	9.74	4.05E-06	4.96E-06	3.29E-06

With Grain Specimens	Mean	Std Dev	CoV (%)	Median	Upper Limit	Lower Limit
NBG-17	4.80E-06	1.74E-07	3.61	4.78E-06	5.09E-06	4.54E-06
NBG-18	5.41E-06	6.88E-07	12.73	5.43E-06	6.57E-06	3.70E-06
PCEA	4.07E-06	1.94E-07	4.77	4.10E-06	4.52E-06	3.67E-06
2114	4.69E-06	2.42E-07	5.17	4.71E-06	5.19E-06	4.20E-06
IG-110	4.57E-06	4.19E-07	9.16	4.54E-06	5.57E-06	3.62E-06

Table B-6. Creep specimen coefficient of thermal expansion (1/K) at 500 °C summary statistics.

Combined Specimens	Mean	Std Dev	CoV (%)	Median	Upper Limit	Lower Limit
NBG-17	5.36E-06	1.25E-07	2.33	5.34E-06	5.66E-06	5.15E-06
NBG-18	5.32E-06	1.87E-07	3.51	5.34E-06	5.66E-06	5.00E-06
PCEA	4.69E-06	1.86E-07	3.97	4.67E-06	5.10E-06	4.30E-06
2114	5.18E-06	2.06E-07	3.97	5.19E-06	5.58E-06	4.79E-06
IG-110	4.33E-06	2.11E-07	4.88	4.38E-06	4.90E-06	3.84E-06

Against Grain Specimens	Mean	Std Dev	CoV (%)	Median	Upper Limit	Lower Limit
NBG-17	5.40E-06	1.20E-07	2.22	5.41E-06	5.66E-06	5.16E-06
NBG-18	5.20E-06	2.29E-07	4.40	5.24E-06	5.41E-06	4.98E-06
PCEA	4.88E-06	1.50E-07	3.08	4.91E-06	5.10E-06	4.60E-06
2114	—	—	—	—	—	—
IG-110	4.12E-06	9.52E-08	2.31	4.11E-06	4.31E-06	3.94E-06

With Grain Specimens	Mean	Std Dev	CoV (%)	Median	Upper Limit	Lower Limit
NBG-17	5.32E-06	1.16E-07	2.19	5.29E-06	5.53E-06	5.15E-06
NBG-18	5.38E-06	1.26E-07	2.34	5.39E-06	5.69E-06	5.08E-06
PCEA	4.61E-06	1.38E-07	2.99	4.64E-06	4.96E-06	4.30E-06
2114	5.18E-06	2.06E-07	3.97	5.19E-06	5.58E-06	4.79E-06
IG-110	4.48E-06	1.29E-07	2.88	4.48E-06	4.65E-06	4.28E-06

Table B-7. Creep specimen coefficient of thermal expansion (1/K) at 900 °C summary statistics.

Combined Specimens	Mean	Std Dev	CoV (%)	Median	Upper Limit	Lower Limit
NBG-17	5.82E-06	1.12E-07	1.92	5.84E-06	6.03E-06	5.59E-06
NBG-18	5.76E-06	1.44E-07	2.49	5.77E-06	6.05E-06	5.40E-06
PCEA	5.14E-06	1.61E-07	3.13	5.11E-06	5.47E-06	4.81E-06
2114	5.61E-06	1.68E-07	3.00	5.62E-06	5.91E-06	5.34E-06
IG-110	4.68E-06	2.22E-07	4.74	4.68E-06	5.20E-06	4.01E-06

Against Grain Specimens	Mean	Std Dev	CoV (%)	Median	Upper Limit	Lower Limit
NBG-17	5.86E-06	1.04E-07	1.78	5.88E-06	6.03E-06	5.65E-06
NBG-18	5.66E-06	1.42E-07	2.52	5.66E-06	5.88E-06	5.35E-06
PCEA	5.33E-06	1.17E-07	2.20	5.36E-06	5.47E-06	5.10E-06
2114	—	—	—	—	—	—
IG-110	4.47E-06	1.34E-07	2.99	4.47E-06	4.75E-06	4.10E-06

With Grain Specimens	Mean	Std Dev	CoV (%)	Median	Upper Limit	Lower Limit
NBG-17	5.78E-06	1.08E-07	1.88	5.76E-06	5.98E-06	5.59E-06
NBG-18	5.82E-06	1.13E-07	1.95	5.80E-06	6.05E-06	5.59E-06
PCEA	5.06E-06	1.04E-07	2.05	5.08E-06	5.27E-06	4.81E-06
2114	5.61E-06	1.68E-07	3.00	5.62E-06	5.91E-06	5.34E-06
IG-110	4.82E-06	1.43E-07	2.97	4.83E-06	5.14E-06	4.50E-06

Table B-8. Creep specimen modulus (GPa) by sonic resonance summary statistics.

Combined Specimens	Mean	Std Dev	CoV (%)	Median	Upper Limit	Lower Limit
NBG-17	11.44	0.34	2.97	11.36	12.03	10.86
NBG-18	12.03	0.28	2.29	12.08	12.53	11.45
PCEA	11.00	0.80	7.27	11.41	11.73	9.50
2114	10.37	0.23	2.19	10.31	10.93	10.00
IG-110	9.29	0.40	4.26	9.36	9.95	8.43

Against Grain Specimens	Mean	Std Dev	CoV (%)	Median	Upper Limit	Lower Limit
NBG-17	11.30	0.21	1.88	11.35	11.62	10.86
NBG-18	12.25	0.16	1.30	12.26	12.53	11.88
PCEA	9.76	0.27	2.78	9.65	10.00	9.50
2114	—	—	—	—	—	—
IG-110	9.60	0.18	1.86	9.61	9.95	9.17

With Grain Specimens	Mean	Std Dev	CoV (%)	Median	Upper Limit	Lower Limit
NBG-17	11.57	0.38	3.30	11.46	12.12	11.01
NBG-18	11.92	0.25	2.13	11.97	12.35	11.45
PCEA	11.48	0.12	1.06	11.51	11.73	11.17
2114	10.37	0.23	2.19	10.31	10.93	10.00
IG-110	9.09	0.37	4.05	9.08	9.91	8.43

Table B-9. Creep specimen resistivity ($\mu\Omega\text{-m}$) summary statistics.

Combined Specimens	Mean	Std Dev	CoV (%)	Median	Upper Limit	Lower Limit
NBG-17	10.69	0.24	2.22	10.76	10.98	10.20
NBG-18	9.13	0.24	2.67	9.09	9.78	8.42
PCEA	7.65	0.32	4.12	7.53	8.31	7.25
2114	12.01	0.41	3.44	11.87	13.13	11.45
IG-110	10.18	0.51	5.04	10.21	11.38	8.93

Against Grain Specimens	Mean	Std Dev	CoV (%)	Median	Upper Limit	Lower Limit
NBG-17	10.73	0.10	0.98	10.72	10.91	10.51
NBG-18	8.97	0.20	2.21	8.96	9.34	8.65
PCEA	8.12	0.16	1.91	8.18	8.31	7.73
2114	—	—	—	—	—	—
IG-110	9.95	0.48	4.84	9.85	10.89	8.93

With Grain Specimens	Mean	Std Dev	CoV (%)	Median	Upper Limit	Lower Limit
NBG-17	10.65	0.31	2.89	10.80	10.98	9.99
NBG-18	9.20	0.23	2.48	9.18	9.78	8.71
PCEA	7.47	0.10	1.28	7.50	7.66	7.25
2114	12.01	0.41	3.44	11.87	13.13	11.45
IG-110	10.33	0.48	4.64	10.32	11.38	9.40

Table B-10. Creep specimen Young's Modulus (GPa) by sonic velocity.

Combined Specimens	Mean	Std Dev	CoV (%)	Median	Upper Limit	Lower Limit
NBG-17	14.57	0.51	3.48	14.58	15.58	13.50
NBG-18	15.31	0.32	2.10	15.40	15.88	14.67
PCEA	13.16	0.91	6.90	13.61	14.47	11.40
2114	12.06	0.34	2.78	12.07	12.83	11.50
IG-110	10.13	0.44	4.34	10.16	10.79	8.98

Against Grain Specimens	Mean	Std Dev	CoV (%)	Median	Upper Limit	Lower Limit
NBG-17	14.39	0.40	2.75	14.52	14.96	13.50
NBG-18	15.48	0.23	1.46	15.48	15.88	15.03
PCEA	11.77	0.29	2.45	11.72	12.44	11.40
2114	—	—	—	—	—	—
IG-110	10.44	0.20	1.95	10.47	10.78	9.85

With Grain Specimens	Mean	Std Dev	CoV (%)	Median	Upper Limit	Lower Limit
NBG-17	14.73	0.55	3.73	14.61	15.61	13.52
NBG-18	15.22	0.33	2.15	15.18	15.82	14.67
PCEA	13.70	0.23	1.67	13.69	14.24	13.27
2114	12.06	0.34	2.78	12.07	12.83	11.50
IG-110	9.92	0.43	4.35	9.99	10.79	8.89

Table B-11. Creep specimen shear modulus (GPa) by sonic velocity.

Combined Specimens	Mean	Std Dev	CoV (%)	Median	Upper Limit	Lower Limit
NBG-17	4.99	0.12	2.35	4.96	5.21	4.76
NBG-18	4.93	0.12	2.53	4.92	5.15	4.66
PCEA	4.83	0.26	5.38	4.97	5.07	4.30
2114	4.40	0.08	1.91	4.39	4.62	4.25
IG-110	4.07	0.08	2.06	4.07	4.30	3.85

Against Grain Specimens	Mean	Std Dev	CoV (%)	Median	Upper Limit	Lower Limit
NBG-17	4.95	0.08	1.59	4.97	5.05	4.76
NBG-18	4.98	0.15	2.97	5.01	5.15	4.65
PCEA	4.42	0.09	2.13	4.41	4.62	4.30
2114	—	—	—	—	—	—
IG-110	4.09	0.05	1.10	4.08	4.20	3.97

With Grain Specimens	Mean	Std Dev	CoV (%)	Median	Upper Limit	Lower Limit
NBG-17	5.03	0.13	2.65	4.95	5.22	4.83
NBG-18	4.91	0.11	2.18	4.90	5.09	4.70
PCEA	4.98	0.04	0.89	4.98	5.07	4.89
2114	4.40	0.08	1.91	4.39	4.62	4.25
IG-110	4.06	0.10	2.47	4.05	4.33	3.85

Table B-12. Piggyback specimen length (mm) summary statistics.

Combined Specimens	Mean	Std Dev	CoV (%)	Median	Upper Limit	Lower Limit
NBG-17	6.360	0.007	0.11	6.359	6.374	6.344
NBG-18	6.352	0.007	0.11	6.352	6.364	6.338
PCEA	6.366	0.011	0.17	6.369	6.385	6.342
2114	6.355	0.003	0.04	6.356	6.359	6.351
IG-110	6.360	0.004	0.07	6.361	6.368	6.350

Against Grain Specimens	Mean	Std Dev	CoV (%)	Median	Upper Limit	Lower Limit
NBG-17	6.366	0.008	0.13	6.370	6.374	6.344
NBG-18	6.344	0.002	0.03	6.344	6.347	6.341
PCEA	6.366	0.014	0.22	6.371	6.385	6.344
2114	—	—	—	—	—	—
IG-110	6.361	0.002	0.03	6.361	6.364	6.359

With Grain Specimens	Mean	Std Dev	CoV (%)	Median	Upper Limit	Lower Limit
NBG-17	6.358	0.004	0.07	6.358	6.367	6.349
NBG-18	6.356	0.004	0.06	6.357	6.364	6.345
PCEA	6.366	0.008	0.12	6.368	6.383	6.347
2114	6.355	0.003	0.04	6.356	6.359	6.351
IG-110	6.358	0.005	0.08	6.357	6.364	6.351

Table B-13. Piggyback specimen diameter (mm) summary statistics.

Combined Specimens	Mean	Std Dev	CoV (%)	Median	Upper Limit	Lower Limit
NBG-17	12.453	0.002	0.02	12.453	12.457	12.449
NBG-18	12.445	0.003	0.02	12.446	12.453	12.437
PCEA	12.449	0.009	0.07	12.450	12.456	12.444
2114	12.446	0.005	0.04	12.447	12.454	12.439
IG-110	12.452	0.008	0.07	12.449	12.460	12.444

Against Grain Specimens	Mean	Std Dev	CoV (%)	Median	Upper Limit	Lower Limit
NBG-17	12.453	0.003	0.02	12.453	12.459	12.449
NBG-18	12.445	0.003	0.03	12.445	12.450	12.438
PCEA	12.450	0.013	0.10	12.451	12.461	12.442
2114	—	—	—	—	—	—
IG-110	12.448	0.001	0.01	12.448	12.450	12.446

With Grain Specimens	Mean	Std Dev	CoV (%)	Median	Upper Limit	Lower Limit
NBG-17	12.453	0.002	0.01	12.453	12.457	12.450
NBG-18	12.445	0.003	0.02	12.446	12.452	12.438
PCEA	12.448	0.002	0.02	12.449	12.454	12.444
2114	12.446	0.005	0.04	12.447	12.454	12.439
IG-110	12.456	0.010	0.08	12.452	12.476	12.444

Table B-14. Piggyback specimen mass (g) summary statistics.

Combined Specimens	Mean	Std Dev	CoV (%)	Median	Upper Limit	Lower Limit
NBG-17	1.420	0.004	0.30	1.420	1.428	1.408
NBG-18	1.426	0.005	0.37	1.426	1.440	1.416
PCEA	1.418	0.007	0.47	1.420	1.428	1.405
2114	1.405	0.002	0.12	1.405	1.409	1.402
IG-110	1.367	0.006	0.42	1.366	1.379	1.355

Against Grain Specimens	Mean	Std Dev	CoV (%)	Median	Upper Limit	Lower Limit
NBG-17	1.420	0.006	0.40	1.421	1.428	1.408
NBG-18	1.424	0.005	0.34	1.423	1.433	1.416
PCEA	1.413	0.007	0.49	1.414	1.423	1.400
2114	—	—	—	—	—	—
IG-110	1.366	0.003	0.21	1.365	1.373	1.361

With Grain Specimens	Mean	Std Dev	CoV (%)	Median	Upper Limit	Lower Limit
NBG-17	1.420	0.004	0.25	1.420	1.427	1.412
NBG-18	1.427	0.005	0.35	1.428	1.440	1.416
PCEA	1.422	0.002	0.15	1.422	1.427	1.418
2114	1.405	0.002	0.12	1.405	1.409	1.402
IG-110	1.369	0.007	0.54	1.368	1.386	1.354

Table B-15. Piggyback specimen density (g/cm³) summary statistics.

Combined Specimens	Mean	Std Dev	CoV (%)	Median	Upper Limit	Lower Limit
NBG-17	1.8329	0.0056	0.30	1.8330	1.8433	1.8190
NBG-18	1.8456	0.0060	0.33	1.8460	1.8622	1.8320
PCEA	1.8303	0.0073	0.40	1.8337	1.8414	1.8085
2114	1.8171	0.0024	0.13	1.8173	1.8207	1.8121
IG-110	1.7656	0.0058	0.33	1.7650	1.7808	1.7506
Against Grain Specimens	Mean	Std Dev	CoV (%)	Median	Upper Limit	Lower Limit
NBG-17	1.8315	0.0066	0.36	1.8329	1.8411	1.8190
NBG-18	1.8447	0.0061	0.33	1.8445	1.8565	1.8337
PCEA	1.8234	0.0058	0.32	1.8233	1.8335	1.8144
2114	—	—	—	—	—	—
IG-110	1.7646	0.0036	0.21	1.7629	1.7730	1.7597
With Grain Specimens	Mean	Std Dev	CoV (%)	Median	Upper Limit	Lower Limit
NBG-17	1.8335	0.0051	0.28	1.8338	1.8433	1.8246
NBG-18	1.8461	0.0060	0.32	1.8466	1.8612	1.8320
PCEA	1.8356	0.0017	0.09	1.8354	1.8398	1.8326
2114	1.8171	0.0024	0.13	1.8173	1.8207	1.8121
IG-110	1.7666	0.0072	0.41	1.7674	1.7832	1.7506

Table B-16. Piggyback specimen diffusivity (mm²/sec) at 100 °C summary statistics.

Combined Specimens	Mean	Std Dev	CoV (%)	Median	Upper Limit	Lower Limit
NBG-17	72.55	0.77	1.06	72.69	73.88	70.93
NBG-18	78.07	1.03	1.32	78.47	79.51	76.12
PCEA	93.11	2.89	3.10	91.13	97.60	89.80
2114	65.66	0.53	0.80	65.46	66.66	64.97
IG-110	76.20	2.96	3.88	77.08	80.45	68.80

Against Grain Specimens	Mean	Std Dev	CoV (%)	Median	Upper Limit	Lower Limit
NBG-17	71.58	0.40	0.56	71.53	72.25	70.93
NBG-18	78.92	0.41	0.52	78.95	79.51	78.01
PCEA	90.78	0.43	0.48	90.84	91.76	89.80
2114	—	—	—	—	—	—
IG-110	78.20	1.34	1.72	78.17	80.45	75.74

With Grain Specimens	Mean	Std Dev	CoV (%)	Median	Upper Limit	Lower Limit
NBG-17	72.99	0.40	0.54	72.89	73.88	72.25
NBG-18	77.48	0.91	1.17	77.29	78.72	76.12
PCEA	96.54	0.40	0.42	96.53	97.45	96.01
2114	65.66	0.53	0.80	65.46	66.66	64.97
IG-110	74.70	2.96	3.97	74.68	78.85	68.21

Table B-17. Piggyback specimen diffusivity (mm^2/sec) at 500 °C summary statistics.

Combined Specimens	Mean	Std Dev	CoV (%)	Median	Upper Limit	Lower Limit
NBG-17	28.67	0.35	1.24	28.82	29.18	27.91
NBG-18	30.18	0.39	1.28	30.33	30.72	29.39
PCEA	34.38	1.08	3.13	33.63	36.04	33.22
2114	27.14	0.13	0.47	27.16	27.41	26.83
IG-110	28.86	1.09	3.79	29.22	30.52	25.97

Against Grain Specimens	Mean	Std Dev	CoV (%)	Median	Upper Limit	Lower Limit
NBG-17	28.19	0.17	0.61	28.23	28.48	27.91
NBG-18	30.50	0.18	0.58	30.51	30.72	30.12
PCEA	33.50	0.14	0.42	33.50	33.83	33.22
2114	—	—	—	—	—	—
IG-110	29.61	0.52	1.75	29.59	30.52	28.47

With Grain Specimens	Mean	Std Dev	CoV (%)	Median	Upper Limit	Lower Limit
NBG-17	28.89	0.12	0.40	28.89	29.18	28.69
NBG-18	29.95	0.33	1.10	29.85	30.62	29.39
PCEA	35.66	0.12	0.34	35.65	35.80	35.49
2114	27.14	0.13	0.47	27.16	27.41	26.83
IG-110	28.30	1.08	3.82	28.35	29.74	25.93

Table B-18. Piggyback specimen diffusivity (mm^2/sec) at 900 °C summary statistics.

Combined Specimens	Mean	Std Dev	CoV (%)	Median	Upper Limit	Lower Limit
NBG-17	18.62	0.30	1.60	18.73	18.97	17.88
NBG-18	19.50	0.23	1.20	19.58	19.85	19.09
PCEA	21.73	0.66	3.03	21.33	22.82	20.94
2114	17.96	0.10	0.57	17.97	18.13	17.67
IG-110	18.52	0.69	3.74	18.73	19.49	16.68

Against Grain Specimens	Mean	Std Dev	CoV (%)	Median	Upper Limit	Lower Limit
NBG-17	18.26	0.27	1.50	18.33	18.48	17.82
NBG-18	19.69	0.12	0.59	19.69	19.85	19.42
PCEA	21.20	0.12	0.58	21.22	21.41	20.94
2114						
IG-110	18.99	0.31	1.61	18.97	19.49	18.46

With Grain Specimens	Mean	Std Dev	CoV (%)	Median	Upper Limit	Lower Limit
NBG-17	18.79	0.10	0.54	18.78	18.97	18.60
NBG-18	19.36	0.20	1.03	19.34	19.81	19.09
PCEA	22.51	0.11	0.48	22.48	22.63	22.36
2114	17.96	0.10	0.57	17.97	18.13	17.67
IG-110	18.17	0.70	3.84	18.15	19.17	16.67

Table B-19. HOPG specimen mass and dimensional data.

Specimen	Average Mass (g)	Avg Length (mm)	Length STD (mm)	Avg Width (mm)	Width STD (mm)	Avg Thickness (mm)	Thickness STD (mm)
001	0.06057	5.004	0.009	5.040	0.004	1.198	0.004
002	0.05708	5.003	0.010	5.037	0.003	1.141	0.004
003	0.04331	5.107	0.012	5.046	0.014	0.810	0.002
004	0.07546	5.138	0.006	5.164	0.016	1.359	0.002
005	0.04584	5.098	0.005	5.149	0.035	0.849	0.002
006	0.05822	5.316	0.007	5.252	0.003	1.015	0.002
007	0.04703	5.128	0.007	5.134	0.007	0.939	0.012
008	0.08073	5.096	0.011	5.163	0.042	1.532	0.004
009	0.05489	5.107	0.018	5.133	0.005	1.124	0.002
010	0.04429	5.177	0.034	5.241	0.030	0.849	0.002
011	0.04797	5.136	0.005	5.321	0.014	0.922	0.002
012	0.05893	5.087	0.005	5.003	0.005	1.204	0.005
013	0.06794	5.004	0.005	4.892	0.004	1.351	0.001
014	0.05080	5.102	0.006	5.057	0.013	0.982	0.001
015	0.04597	5.132	0.010	5.178	0.006	0.850	0.002
016	0.07211	5.402	0.009	5.369	0.009	1.273	0.002
017	0.05679	5.074	0.005	5.047	0.009	1.077	0.007
018	0.04273	5.112	0.008	5.014	0.005	0.806	0.002
019	0.05742	5.001	0.012	4.784	0.019	1.131	0.001
020	0.04424	5.394	0.007	5.091	0.007	0.793	0.007

Appendix C

Final Loading Configuration for AGC-4 Specimens

Appendix C

Final Loading Configuration for AGC-4 Specimens

Table C-1. Final loading configuration for AGC-4 specimens. The height (inches) is the distance from the reactor core centerline to the specimens center of mass.

Stack 1				
Orientation	Specimen Type	ID No.	Graphite	Height
	Stack end cap		NBG-25	20.125
AP	Stressed Creep	AP4801	NBG-17	19.500
	Flux Wire	57	Flux Monitor	18.875
DW	Stressed Creep	DW4801	PCEA	18.250
BW	Stressed Creep	BW4301	NBG-18	17.250
EW	Stressed Creep	EW4801	IG-110	16.250
TW	Stressed Creep	TW4001	2114	15.250
DW	Stressed Creep	DW4803	PCEA	14.250
	Flux Wire	A1	Flux Monitor	13.625
BP	Stressed Creep	BP4605	NBG-18	13.000
TW	Stressed Creep	TW4002	2114	12.000
EW	Stressed Creep	EW4802	IG-110	11.000
DW	Stressed Creep	DW4804	PCEA	10.000
BW	Stressed Creep	BW4302	NBG-18	9.000
TW	Stressed Creep	TW4003	2114	8.000
	Flux Wire	IH	Flux Monitor	7.375
AP	Stressed Creep	AP4802	NBG-17	6.750
EW	Stressed Creep	EW4803	IG-110	5.750
DW	Stressed Creep	DW4901	PCEA	4.750
BL	Stressed Creep	BL3801	NBG-18	3.750
TW	Stressed Creep	TW4004	2114	2.750
	Flux Wire	IR	Flux Monitor	2.125
AW	Stressed Creep	AW4801	NBG-17	1.500
	Top of Shuttle Piston			1.000
Core Centerline				0.000
TW	Unstressed Creep	TW4005	2114	-2.000
FW	Piggyback	FW1707	IG-430	-2.625
AW	Unstressed Creep	AW4802	NBG-17	-3.250
	Flux Wire	7J	Flux Monitor	-3.875
TW	Unstressed Creep	TW4006	2114	-4.500
BL	Unstressed Creep	BL3802	NBG-18	-5.500

Stack 1				
Orientation	Specimen Type	ID No.	Graphite	Height
DW	Unstressed Creep	DW4902	PCEA	-6.500
EW	Unstressed Creep	EW4804	IG-110	-7.500
AP	Unstressed Creep	AP4803	NBG-17	-8.500
	Piggyback	M0401	NBG-25	-9.125
TW	Unstressed Creep	TW4007	2114	-9.750
BW	Unstressed Creep	BW4303	NBG-18	-10.750
DW	Unstressed Creep	DW4903	PCEA	-11.750
EW	Unstressed Creep	EW4901	IG-110	-12.750
TW	Unstressed Creep	TW4008	2114	-13.750
BP	Unstressed Creep	BP4202	NBG-18	-14.750
	Flux Wire	7I	Flux Monitor	-15.375
DW	Unstressed Creep	DW4904	PCEA	-16.000
TW	Unstressed Creep	TW4009	2114	-17.000
EW	Unstressed Creep	EW4902	IG-110	-18.000
BW	Unstressed Creep	BW4401	NBG-18	-19.000
DW	Unstressed Creep	DW5001	PCEA	-20.000
	Flux Wire	SA	Flux Monitor	-20.625
AP	Unstressed Creep	AP4804	NBG-17	-21.250
TW	Unstressed Creep	TW4010	2114	-22.250
FW	Piggyback	FW1701	IG-430	-22.875
	SiC-G can	CAN121	NBG-25	-23.250

Stack 2				
Orientation	Specimen Type	ID No.	Graphite	Height
	Stack end cap			20.125
AP	Stressed Creep	AP4901	NBG-17	19.500
	Piggyback	M0402	NBG-25	18.875
DW	Stressed Creep	DW5002	PCEA	18.250
BW	Stressed Creep	BW4402	NBG-18	17.250
EW	Stressed Creep	EW4903	IG-110	16.250
TW	Stressed Creep	TW4101	2114	15.250
DW	Stressed Creep	DW5003	PCEA	14.250
	Flux Wire	1I	Flux Monitor	13.625
BP	Stressed Creep	BP4203	NBG-18	13.000
TW	Stressed Creep	TW4102	2114	12.000
EW	Stressed Creep	EW4904	IG-110	11.000
DW	Stressed Creep	DW5004	PCEA	10.000
BW	Stressed Creep	BW4403	NBG-18	9.000

Stack 2				
Orientation	Specimen Type	ID No.	Graphite	Height
TW	Stressed Creep	TW4103	2114	8.000
	Piggyback	M0403	NBG-25	7.375
AP	Stressed Creep	AP4902	NBG-17	6.750
EW	Stressed Creep	EW5001	IG-110	5.750
DW	Stressed Creep	DW5101	PCEA	4.750
BL	Stressed Creep	BL3803	NBG-18	3.750
TW	Stressed Creep	TW4104	2114	2.750
	Flux Wire	5Z	Flux Monitor	2.125
AW	Stressed Creep	AW4803	NBG-17	1.500
	Top of Shuttle Piston			1.000
Core Centerline				0.000
TW	Unstressed Creep	TW4105	2114	-2.000
FW	Piggyback	FW1708	IG-430	-2.625
AW	Unstressed Creep	AW4804	NBG-17	-3.250
	Piggyback	M0404	NBG-25	-3.875
TW	Unstressed Creep	TW4106	2114	-4.500
BL	Unstressed Creep	BL3804	NBG-18	-5.500
DW	Unstressed Creep	DW5102	PCEA	-6.500
EW	Unstressed Creep	EW5002	IG-110	-7.500
AP	Unstressed Creep	AP4903	NBG-17	-8.500
	Piggyback	M0405	NBG-25	-9.125
TW	Unstressed Creep	TW4107	2114	-9.750
BW	Unstressed Creep	BW4501	NBG-18	-10.750
DW	Unstressed Creep	DW5103	PCEA	-11.750
EW	Unstressed Creep	EW5003	IG-110	-12.750
TW	Unstressed Creep	TW4108	2114	-13.750
BP	Unstressed Creep	BP4204	NBG-18	-14.750
	Flux Wire	9E	Flux Monitor	-15.375
DW	Unstressed Creep	DW5104	PCEA	-16.000
TW	Unstressed Creep	TW4109	2114	-17.000
EW	Unstressed Creep	EW5004	IG-110	-18.000
BW	Unstressed Creep	BW4603	NBG-18	-19.000
DW	Unstressed Creep	DW5201	PCEA	-20.000
	Piggyback	M0406	NBG-25	-20.625
AP	Unstressed Creep	AP4904	NBG-17	-21.250
TW	Unstressed Creep	TW4110	2114	-22.250
FW	Piggyback	FW1702	IG-430	-22.875
	SiC-G can	CAN122	NBG-25	-23.250

Stack 3				
Orientation	Specimen Type	ID No.	Graphite	Height
	Stack end cap			20.125
AP	Stressed Creep	AP5001	NBG-17	19.500
	Piggyback	M0407	NBG-25	18.875
DW	Stressed Creep	DW5202	PCEA	18.250
BW	Stressed Creep	BW4502	NBG-18	17.250
EW	Stressed Creep	EW5101	IG-110	16.250
TW	Stressed Creep	TW4201	2114	15.250
DW	Stressed Creep	DW5203	PCEA	14.250
	Flux Wire	IB	Flux Monitor	13.625
BP	Stressed Creep	BP4205	NBG-18	13.000
TW	Stressed Creep	TW4202	2114	12.000
EW	Stressed Creep	EW5102	IG-110	11.000
DW	Stressed Creep	DW5204	PCEA	10.000
BW	Stressed Creep	BW4503	NBG-18	9.000
TW	Stressed Creep	TW4203	2114	8.000
	Piggyback	M0408	NBG-25	7.375
AP	Stressed Creep	AP5002	NBG-17	6.750
EW	Stressed Creep	EW5103	IG-110	5.750
DW	Stressed Creep	DW5301	PCEA	4.750
BL	Stressed Creep	BL3805	NBG-18	3.750
TW	Stressed Creep	TW4204	2114	2.750
	Flux Wire	IZ	Flux Monitor	2.125
AW	Stressed Creep	AW4901	NBG-17	1.500
	Top of Shuttle Piston			1.000
Core Centerline				0.000
TW	Unstressed Creep	TW4205	2114	-2.000
FW	Piggyback	FW1709	IG-430	-2.625
AW	Unstressed Creep	AW4902	NBG-17	-3.250
	Piggyback	M0409	NBG-25	-3.875
TW	Unstressed Creep	TW4206	2114	-4.500
BL	Unstressed Creep	BL3901	NBG-18	-5.500
DW	Unstressed Creep	DW5302	PCEA	-6.500
EW	Unstressed Creep	EW5104	IG-110	-7.500
AP	Unstressed Creep	AP5003	NBG-17	-8.500
	Flux Wire	SY	Flux Monitor	-9.125
TW	Unstressed Creep	TW4207	2114	-9.750
BW	Unstressed Creep	BW4601	NBG-18	-10.750

Stack 3				
Orientation	Specimen Type	ID No.	Graphite	Height
DW	Unstressed Creep	DW5303	PCEA	-11.750
EW	Unstressed Creep	EW5201	IG-110	-12.750
TW	Unstressed Creep	TW4208	2114	-13.750
BP	Unstressed Creep	BP4301	NBG-18	-14.750
	Piggyback	M0410	NBG-25	-15.375
DW	Unstressed Creep	DW5304	PCEA	-16.000
TW	Unstressed Creep	TW4209	2114	-17.000
EW	Unstressed Creep	EW5202	IG-110	-18.000
BW	Unstressed Creep	BW4602	NBG-18	-19.000
DW	Unstressed Creep	DW5401	PCEA	-20.000
	Piggyback	M0411	NBG-25	-20.625
AP	Unstressed Creep	AP5004	NBG-17	-21.250
TW	Unstressed Creep	TW4210	2114	-22.250
FW	Piggyback	FW1703	IG-430	-22.875
	SiC-G can	CAN123	NBG-25	-23.250

Stack 4				
Orientation	Specimen Type	ID No.	Graphite	Height
	Stack end cap			20.125
EW	Stressed Creep	EW5203	IG-110	19.500
	Flux Wire	IE	Flux Monitor	18.875
TW	Stressed Creep	TW4301	2114	18.250
DA	Stressed Creep	DA3801	PCEA	17.250
BP	Stressed Creep	BP4302	NBG-18	16.250
AL	Stressed Creep	AL4801	NBG-17	15.250
EW	Stressed Creep	EW5204	IG-110	14.250
	Flux Wire	SB	Flux Monitor	13.625
DW	Stressed Creep	DW5402	PCEA	13.000
BL	Stressed Creep	BL3902	NBG-18	12.000
TW	Stressed Creep	TW4302	2114	11.000
AW	Stressed Creep	AW4903	NBG-17	10.000
EA	Stressed Creep	EA4801	IG-110	9.000
DA	Stressed Creep	DA3802	PCEA	8.000
	Flux Wire	8R	Flux Monitor	7.375
BP	Stressed Creep	BP4604	NBG-18	6.750
TW	Stressed Creep	TW4303	2114	5.750
AP	Stressed Creep	AP5101	NBG-17	4.750
EA	Stressed Creep	EA4802	IG-110	3.750

Stack 4				
Orientation	Specimen Type	ID No.	Graphite	Height
DW	Stressed Creep	DW5403	PCEA	2.750
	Flux Wire	5L	Flux Monitor	2.125
BP	Stressed Creep	BP4303	NBG-18	1.500
	Top of Shuttle Piston			1.000
Core Centerline				0.000
AW	Piggyback	AW5801	NBG-17	-1.625
EW	Piggyback	EW6301	IG-110	-1.875
TW	Piggyback	TW4701	2114	-2.125
BP	Piggyback	BP3910	NBG-18	-2.375
FW	Piggyback	FW1704	IG-430	-2.625
BP	Unstressed Creep	BP4304	NBG-18	-3.250
	Flux Wire	9F	Flux Monitor	-3.875
DW	Unstressed Creep	DW5404	PCEA	-4.500
EA	Unstressed Creep	EA5004	IG-110	-5.500
AP	Unstressed Creep	AP5102	NBG-17	-6.500
TW	Unstressed Creep	TW4304	2114	-7.500
BP	Unstressed Creep	BP4305	NBG-18	-8.500
	Piggyback	M0412	NBG-25	-9.125
DA	Unstressed Creep	DA3803	PCEA	-9.750
EA	Unstressed Creep	EA4803	IG-110	-10.750
AW	Unstressed Creep	AW4904	NBG-17	-11.750
TW	Unstressed Creep	TW4305	2114	-12.750
BL	Unstressed Creep	BL3903	NBG-18	-13.750
DW	Unstressed Creep	DW5501	PCEA	-14.750
	Flux Wire	5R	Flux Monitor	-15.375
EW	Unstressed Creep	EW5302	IG-110	-16.000
AL	Unstressed Creep	AL4802	NBG-17	-17.000
BP	Unstressed Creep	BP4401	NBG-18	-18.000
DA	Unstressed Creep	DA3804	PCEA	-19.000
TW	Unstressed Creep	TW4306	2114	-20.000
	Flux Wire	2A	Flux Monitor	-20.625
EW	Unstressed Creep	EW5303	IG-110	-21.250
BL	Piggyback	BL4601	NBG-18	-21.875
AL	Piggyback	AL5801	NBG-17	-22.125
EW	Piggyback	EW6302	IG-110	-22.375
TW	Piggyback	TW4702	2114	-22.625
DW	Piggyback	DW6201	PCEA	-22.875
	SiC-G can	CAN124	NBG-25	-23.250

Stack 5				
Orientation	Specimen Type	ID No.	Graphite	Height
	Stack end cap			20.125
EW	Stressed Creep	EW5304	IG-110	19.500
	Piggyback	M0301	NBG-25	18.875
TW	Stressed Creep	TW4307	2114	18.250
DA	Stressed Creep	DA3901	PCEA	17.250
BP	Stressed Creep	BP4402	NBG-18	16.250
AL	Stressed Creep	AL4803	NBG-17	15.250
EW	Stressed Creep	EW5401	IG-110	14.250
	Flux Wire	I0	Flux Monitor	13.625
DW	Stressed Creep	DW5502	PCEA	13.000
BL	Stressed Creep	BL3904	NBG-18	12.000
TW	Stressed Creep	TW4308	2114	11.000
AW	Stressed Creep	AW5001	NBG-17	10.000
EA	Stressed Creep	EA4804	IG-110	9.000
DA	Stressed Creep	DA3902	PCEA	8.000
	Piggyback	M0302	NBG-25	7.375
BP	Stressed Creep	BP4403	NBG-18	6.750
TW	Stressed Creep	TW4309	2114	5.750
AP	Stressed Creep	AP5I03	NBG-17	4.750
EA	Stressed Creep	EA4901	IG-110	3.750
DW	Stressed Creep	DW5503	PCEA	2.750
	Flux Wire	7F	Flux Monitor	2.125
BP	Stressed Creep	BP4404	NBG-18	1.500
	Top of Shuttle Piston			1.000
Core Centerline				0.000
AW	Piggyback	AW5802	NBG-17	-1.625
EW	Piggyback	EW6303	IG-110	-1.875
TW	Piggyback	TW4703	2114	-2.125
BP	Piggyback	BP3911	NBG-18	-2.375
FW	Piggyback	FW1705	IG-430	-2.625
BP	Unstressed Creep	BP4405	NBG-18	-3.250
	Piggyback	M0303	NBG-25	-3.875
DW	Unstressed Creep	DW5504	PCEA	-4.500
EA	Unstressed Creep	EA4902	IG-110	-5.500
AP	Unstressed Creep	AP5104	NBG-17	-6.500
TW	Unstressed Creep	TW4310	2114	-7.500
BP	Unstressed Creep	BP4501	NBG-18	-8.500

Stack 5				
Orientation	Specimen Type	ID No.	Graphite	Height
	Piggyback	M0304	NBG-25	-9.125
DA	Unstressed Creep	DA3903	PCEA	-9.750
EA	Unstressed Creep	EA4903	IG-110	-10.750
AW	Unstressed Creep	AW5002	NBG-17	-11.750
TW	Unstressed Creep	TW4401	2114	-12.750
BL	Unstressed Creep	BL3905	NBG-18	-13.750
DW	Unstressed Creep	DW5601	PCEA	-14.750
	Flux Wire	7E	Flux Monitor	-15.375
EW	Unstressed Creep	EW5402	IG-110	-16.000
AL	Unstressed Creep	AL4804	NBG-17	-17.000
BP	Unstressed Creep	BP4502	NBG-18	-18.000
DA	Unstressed Creep	DA3904	PCEA	-19.000
TW	Unstressed Creep	TW4402	2114	-20.000
	Piggyback	M0305	NBG-25	-20.625
EW	Unstressed Creep	EW5403	IG-110	-21.250
BL	Piggyback	BL4602	NBG-18	-21.875
AL	Piggyback	ALS802	NBG-17	-22.125
EW	Piggyback	EW6304	IG-110	-22.375
TW	Piggyback	TW4704	2114	-22.625
DW	Piggyback	DW6202	PCEA	-22.875
	SiC-G can	CAN125	NBG-25	-23.250

Stack 6				
Orientation	Specimen Type	ID No.	Graphite	Height
	Stack end cap			20.125
EW	Stressed Creep	EW5404	IG-110	19.500
	Piggyback	M0306	NBG-25	18.875
TW	Stressed Creep	TW4403	2114	18.250
DA	Stressed Creep	DA4001	PCEA	17.250
BP	Stressed Creep	BP4503	NBG-18	16.250
AL	Stressed Creep	AL4901	NBG-17	15.250
EW	Stressed Creep	EW5501	IG-110	14.250
	Flux Wire	2L	Flux Monitor	13.625
DW	Stressed Creep	DW5602	PCEA	13.000
BL	Stressed Creep	BL4001	NBG-18	12.000
TW	Stressed Creep	TW4404	2114	11.000
AW	Stressed Creep	AW5003	NBG-17	10.000
EA	Stressed Creep	EA4904	IG-110	9.000

Stack 6				
Orientation	Specimen Type	ID No.	Graphite	Height
DA	Stressed Creep	DA4002	PCEA	8.000
	Piggyback	M0307	NBG-25	7.375
BP	Stressed Creep	BP4504	NBG-18	6.750
TW	Stressed Creep	TW4405	2114	5.750
AP	Stressed Creep	AP5201	NBG-17	4.750
EA	Stressed Creep	EA5001	IG-110	3.750
DW	Stressed Creep	DW5603	PCEA	2.750
	Flux Wire	8F	Flux Monitor	2.125
BP	Stressed Creep	BP4505	NBG-18	1.500
	Top of Shuttle Piston			1.000
Core Centerline				0.000
AW	Piggyback	AW5803	NBG-17	-1.625
EW	Piggyback	EW6305	IG-110	-1.875
TW	Piggyback	TW4705	2114	-2.125
BP	Piggyback	BP3912	NBG-18	-2.375
FW	Piggyback	FW1706	IG-430	-2.625
BP	Unstressed Creep	BP4601	NBG-18	-3.250
	Piggyback	M0308	NBG-25	-3.875
DW	Unstressed Creep	DW5604	PCEA	-4.500
EA	Unstressed Creep	EA5002	IG-110	-5.500
AP	Unstressed Creep	AP5202	NBG-17	-6.500
TW	Unstressed Creep	TW4406	2114	-7.500
BP	Unstressed Creep	BP4602	NBG-18	-8.500
	Flux Wire	87	Flux Monitor	-9.125
DA	Unstressed Creep	DA4003	PCEA	-9.750
EA	Unstressed Creep	EA5003	IG-110	-10.750
AW	Unstressed Creep	AW5004	NBG-17	-11.750
TW	Unstressed Creep	TW4407	2114	-12.750
BL	Unstressed Creep	BL4002	NBG-18	-13.750
DW	Unstressed Creep	DW5701	PCEA	-14.750
	Piggyback	M0309	NBG-25	-15.375
EW	Unstressed Creep	EW5502	IG-110	-16.000
AL	Unstressed Creep	AL4902	NBG-17	-17.000
BP	Unstressed Creep	BP4603	NBG-18	-18.000
DA	Unstressed Creep	DA4004	PCEA	-19.000
TW	Unstressed Creep	TW4408	2114	-20.000
	Piggyback	M0310	NBG-25	-20.625

Stack 6				
Orientation	Specimen Type	ID No.	Graphite	Height
EW	Unstressed Creep	EW5503	IG-110	-21.250
BL	Piggyback	BL4603	NBG-18	-21.875
AL	Piggyback	AL5803	NBG-17	-22.125
EW	Piggyback	EW6306	IG-110	-22.375
TW	Piggyback	TW4706	2114	-22.625
DW	Piggyback	DW6203	PCEA	-22.875
	SiC-G can	CAN126	NBG-25	-23.250

Stack 7				
Orientation	Specimen Type	ID No.	Graphite	Height
	SiC-G can	CAN127	SiC-G can	18.250
	SiC-G can	CAN128	SiC-G can	17.750
BP	Piggyback	BP3901	NBG-18	17.375
AL	Piggyback	AL5804	NBG-17	17.125
EA	Piggyback	EA6301	IG-110	16.875
TW	Piggyback	TW4707	2114	16.625
DA	Piggyback	DA4801	PCEA	16.375
	HOPG can	CAN101	HOPG can	16.125
	C-C can	CAN131	C-C can	15.750
BW	Piggyback	BW5701	NBG-18	15.375
AW	Piggyback	AW5804	NBG-17	15.125
EW	Piggyback	EW6405	IG-110	14.875
TW	Piggyback	TW4708	2114	14.625
DW	Piggyback	DW6301	PCEA	14.375
	Piggyback	Z-1	A3-27	14.125
	HOPG can	CAN102	HOPG can	13.875
BP	Piggyback	BP3902	NBG-18	13.625
AP	Piggyback	AP5801	NBG-17	13.375
EA	Piggyback	EA6303	IG-110	13.125
TW	Piggyback	TW4709	2114	12.875
DA	Piggyback	DA4803	PCEA	12.625
	Piggyback	Z-2	A3-27	12.375
	HOPG can	CAN103	HOPG can	12.125
	C-C can	CAN132	C-C can	11.750
BW	Piggyback	BW5702	NBG-18	11.375
AW	Piggyback	AW5805	NBG-17	11.125
EW	Piggyback	EW6307	IG-110	10.875
TW	Piggyback	TW4710	2114	10.625

Stack 7				
Orientation	Specimen Type	ID No.	Graphite	Height
DW	Piggyback	DW6204	PCEA	10.375
	Piggyback	Z-3	A3-27	10.125
	HOPG can	CAN104	HOPG can	9.875
BW	Piggyback	BW5703	NBG-18	9.625
AP	Piggyback	AP5802	NBG-17	9.375
EA	Piggyback	EA6304	IG-110	9.125
TW	Piggyback	TW4711	2114	8.875
DA	Piggyback	DA4804	PCEA	8.625
	Piggyback	Z-4	A3-27	8.375
	HOPG can	CAN105	HOPG can	8.125
	C-C can	CAN133	C-C can	7.750
BW	Piggyback	BW5803	NBG-18	7.375
AP	Piggyback	AP5803	NBG-17	7.125
EW	Piggyback	EW6308	IG-110	6.875
TW	Piggyback	TW4712	2114	6.625
DW	Piggyback	DW6205	PCEA	6.375
	Piggyback	Z-5	A3-27	6.125
	HOPG can	CAN106	HOPG can	5.875
BP	Piggyback	BP3904	NBG-18	5.625
AL	Piggyback	AL5805	NBG-17	5.375
EA	Piggyback	EA6305	IG-110	5.125
TW	Piggyback	TW4713	2114	4.875
DA	Piggyback	DA4805	PCEA	4.625
	Piggyback	Z-6	A3-27	4.375
	HOPG can	CAN107	HOPG can	4.125
	C-C can	CAN134	C-C can	3.750
BW	Piggyback	BW5704	NBG-18	3.375
AP	Piggyback	AP5804	NBG-17	3.125
EA	Piggyback	EA6306	IG-110	2.875
TW	Piggyback	TW4714	2114	2.625
DA	Piggyback	DA4806	PCEA	2.375
	Piggyback	Z-7	A3-27	2.125
	HOPG can	CAN108	HOPG can	1.875
BW	Piggyback	BW5705	NBG-18	1.625
AW	Piggyback	AW5806	NBG-17	1.375
EW	Piggyback	EW6309	IG-110	1.125
TW	Piggyback	TW4715	2114	0.875

Stack 7				
Orientation	Specimen Type	ID No.	Graphite	Height
DW	Piggyback	DW6206	PCEA	0.625
	Piggyback	Z-8	A3-27	0.375
	HOPG can	CAN109	HOPG can	0.125
	C-C can	CAN135	C-C can	-0.250
BP	Piggyback	BP3905	NBG-18	-0.625
AW	Piggyback	AW5807	NBG-17	-0.875
EA	Piggyback	EA6311	IG-110	-1.125
TW	Piggyback	TW4716	2114	-1.375
DA	Piggyback	DA4807	PCEA	-1.625
	Piggyback	Z-9	A3-27	-1.875
	HOPG can	CAN110	HOPG can	-2.125
	C-C can	CAN136	C-C can	-2.500
BW	Piggyback	BW5706	NBG-18	-2.875
AW	Piggyback	AW5808	NBG-17	-3.125
EW	Piggyback	EW6311	IG-110	-3.375
TW	Piggyback	TW4717	2114	-3.625
DW	Piggyback	DW6207	PCEA	-3.875
	Piggyback	Z-10	A3-27	-4.125
	HOPG can	CAN111	HOPG can	-4.375
	C-C can	CAN137	C-C can	-4.750
BP	Piggyback	BP3906	NBG-18	-5.125
AP	Piggyback	AP5805	NBG-17	-5.375
EA	Piggyback	EA6307	IG-110	-5.625
TW	Piggyback	TW4718	2114	-5.875
DA	Piggyback	DA4808	PCEA	-6.125
	Piggyback	Z-11	A3-27	-6.375
	HOPG can	CAN112	HOPG can	-6.625
BP	Piggyback	BP3907	NBG-18	-6.875
AW	Piggyback	AW5809	NBG-17	-7.125
EA	Piggyback	EA6308	IG-110	-7.375
TW	Piggyback	TW4719	2114	-7.625
DA	Piggyback	DA4809	PCEA	-7.875
	Piggyback	Z-12	A3-27	-8.125
	HOPG can	CAN113	HOPG can	-8.375
	C-C can	CAN138	C-C can	-8.750
BW	Piggyback	BW5707	NBG-18	-9.125
AW	Piggyback	AW5810	NBG-17	-9.375

Stack 7				
Orientation	Specimen Type	ID No.	Graphite	Height
EW	Piggyback	EW6312	IG-110	-9.625
TW	Piggyback	TW4720	2114	-9.875
DW	Piggyback	DW6208	PCEA	-10.125
	Piggyback	Z-13	A3-27	-10.375
	HOPG can	CAN114	HOPG can	-10.625
BP	Piggyback	BP3908	NBG-18	-10.875
AL	Piggyback	AL5806	NBG-17	-11.125
EA	Piggyback	EA6309	IG-110	-11.375
TW	Piggyback	TW4721	2114	-11.625
DA	Piggyback	DA4810	PCEA	-11.875
	Piggyback	Z-14	A3-27	-12.125
	HOPG can	CAN115	HOPG can	-12.375
	C-C can	CAN139	C-C can	-12.750
BW	Piggyback	BW5708	NBG-18	-13.125
AW	Piggyback	AW5811	NBG-17	-13.375
EW	Piggyback	EW6401	IG-110	-13.625
TW	Piggyback	TW4722	2114	-13.875
DW	Piggyback	DW6209	PCEA	-14.125
	Piggyback	Z-15	A3-27	-14.375
	HOPG can	CAN116	HOPG can	-14.625
BP	Piggyback	BP3909	NBG-18	-14.875
AW	Piggyback	AW5812	NBG-17	-15.125
EW	Piggyback	EW6402	IG-110	-15.375
TW	Piggyback	TW4723	2114	-15.625
DW	Piggyback	DW6210	PCEA	-15.875
	Piggyback	Z-16	A3-27	-16.125
	HOPG can	CAN117	HOPG can	-16.375
	C-C can	CAN140	C-C can	-16.750
BW	Piggyback	BW5801	NBG-18	-17.125
AW	Piggyback	AW5901	NBG-17	-17.375
EW	Piggyback	EW6403	IG-110	-17.625
TW	Piggyback	TW4724	2114	-17.875
DW	Piggyback	DW6211	PCEA	-18.125
	Piggyback	Z-17	A3-27	-18.375
	HOPG can	CAN118	HOPG can	-18.625
BW	Piggyback	BW5802	NBG-18	-18.875
AW	Piggyback	AW5902	NBG-17	-19.125

Stack 7				
Orientation	Specimen Type	ID No.	Graphite	Height
EW	Piggyback	EW6404	IG-110	-19.375
TW	Piggyback	TW4725	2114	-19.625
DW	Piggyback	DW6212	PCEA	-19.875
	Piggyback	Z-18	A3-27	-20.125
	HOPG can	CAN119	HOPG can	-20.375
	C-C can	CAN141	C-C can	-20.750
BL	Piggyback	BL4604	NBG-18	-21.125
AP	Piggyback	AP5806	NBG-17	-21.375
EA	Piggyback	EA6310	IG-110	-21.625
TW	Piggyback	TW4726	2114	-21.875
DA	Piggyback	DA4812	PCEA	-22.125
	HOPG can	CAN120	HOPG can	-22.375
	C-C can	CAN142	C-C can	-22.750
	Sic-G can	CAN129	Sic-G can	-23.250
	Sic-G can	CAN130	Sic-G can	-23.750

Appendix D

Analytical Report

Appendix D

Analytical Report



GDMS
ANALYTICAL REPORT

SHIVA Technologies
An Operating Unit of Evans Analytical Group LLC
6707 Brooklawn Parkway
Syracuse, New York 13211

Telephone (315) 431-9900
Fax (315) 431-9800
Email info.ny@eaglabs.com
www.eaglabs.com

Customer: Idaho National Laboratory
Date: 30-Mar-2010

P.O.# 100778803
Job # S0AAK828

Customer ID: Graphite

Shiva ID: S100324127

Grade 2114 Run # 357-09-17N Bullet # 84576

QA# AGC-10-02

Element	Concentration [ppm wt]	Element	Concentration [ppm wt]
Li	< 0.05	Pd	< 0.05
Be	< 0.05	Ag	< 0.05
B	2.5	Cd	< 0.05
C	Matrix	In	< 0.05
N	-	Sn	< 0.05
O	-	Sb	< 0.05
F	< 0.1	Te	< 0.05
Na	< 0.05	I	< 0.01
Mg	< 0.05	Cs	< 0.05
Al	< 0.05	Ba	< 0.05
Si	0.63	La	< 0.05
P	0.27	Ce	< 0.05
S	5.7	Pr	< 0.05
Cl	0.91	Nd	< 0.05
K	< 0.1	Sm	< 0.01
Ca	< 0.05	Eu	< 0.01
Sc	< 0.01	Gd	< 0.01
Ti	< 0.01	Tb	< 0.01
V	< 0.01	Dy	< 0.01
Cr	< 0.5	Ho	< 0.01
Mn	< 0.01	Er	< 0.01
Fe	< 0.01	Tm	< 0.01
Co	< 0.01	Yb	< 0.01
Ni	< 0.01	Lu	< 0.01
Cu	< 0.05	Hf	< 0.01
Zn	< 0.05	Ta	< 100
Ga	< 0.01	W	< 0.05
Ge	< 0.05	Re	< 0.01
As	< 0.05	Os	< 0.01
Se	< 0.05	Ir	< 0.01
Br	< 0.1	Pt	< 0.01
Rb	< 0.05	Au	< 0.1
Sr	< 0.05	Hg	< 0.1
Y	< 0.05	Tl	< 0.05
Zr	< 0.05	Pb	< 0.05
Nb	< 0.05	Bi	< 0.05
Mo	< 0.05	Th	< 0.05
Ru	< 0.05	U	< 0.05
Rh	< 0.01		

J. SCHIEBLER

Joseph Schiebler

Page 1 of 1 - GDMS

Reviewed by _____

This report shall not be reproduced except in full without written approval of the laboratory. The recording of false, fictitious, or fraudulent statements or entries on the document may be punished as a felony under federal law



GDMS
ANALYTICAL REPORT

Evans Analytical Group
103 Commerce Blvd
Liverpool, New York 13088

Telephone (315) 431-9900
Fax: (315) 431-9800
Email info.ny@eaglabs.com
www.eaglabs.com

Customer: **Idaho National Laboratory**
1765 N. Yellowstone Hwy, Idaho Falls, ID 83415
Date: 27-Oct-2014
Customer ID: **Graphite**
NOG-2013

P.O. # **PC5189472**
Job # **S0ENC057**
Sample ID: **S141022043**

[Rev: 2014-10-27 09:24:44]

Element	Concentration [ppm wt]	Element	Concentration [ppm wt]
Li	< 0.05	Pd	< 0.05
Be	< 0.05	Ag	< 0.05
B	0.05	Cd	< 0.05
C	Matrix	In	< 0.05
N	-	Sn	< 0.05
O	-	Sb	< 0.05
F	< 0.1	Te	< 0.05
Na	0.05	I	< 0.01
Mg	< 0.05	Cs	< 0.05
Al	33	Ba	0.42
Si	240	La	< 0.05
P	0.79	Ce	< 0.05
S	32	Pr	< 0.05
Cl	0.19	Nd	< 0.05
K	13	Sm	< 0.01
Ca	400	Eu	< 0.01
Sc	< 0.01	Gd	< 0.01
Ti	1.5	Tb	< 0.01
V	0.49	Dy	< 0.01
Cr	< 0.5	Ho	< 0.01
Mn	< 0.01	Er	< 0.01
Fe	44	Tm	< 0.01
Co	0.11	Yb	< 0.01
Ni	15	Lu	< 0.01
Cu	< 0.05	Hf	< 0.01
Zn	< 0.05	Ta	< 100
Ga	< 0.01	W	< 0.05
Ge	< 0.05	Re	< 0.01
As	< 0.05	Os	< 0.01
Se	< 0.05	Ir	< 0.01
Br	< 0.1	Pt	< 0.01
Rb	< 0.05	Au	< 0.1
Sr	2.9	Hg	< 0.1
Y	0.16	Tl	< 0.05
Zr	1.0	Pb	< 0.05
Nb	< 0.05	Bi	< 0.05
Mo	0.15	Th	< 0.05
Ru	< 0.05	U	< 0.05
Rh	< 0.01		

ISO 17025



Testing Cert. #2797.03

Page 1 of 1 - GDMS
Analyzed according to WI F rev. 12/06/12
Reviewed by _____

J.SCHIEBLER (Analyst)

Joseph Schiebler

Precision and bias typical of GDMS measurements are discussed under ASTM F1593.
This shall not be reproduced except in full without written approval of the laboratory.



GDMS
ANALYTICAL REPORT

Evans Analytical Group
103 Commerce Blvd
Liverpool, New York 13088

Telephone (315) 431-9900
Fax: (315) 431-9800
Email info.ny@eaglabs.com
www.eaglabs.com

Customer: **Carlisle Brake and Friction**
29001 Solon Rd., Solon, OH 44139 USA

Date: 28-Jul-2014

Customer ID: **C/C Composite**

CTP-446-CHOP CHOPPED-HD

P.O.# **CG000650**

Job # **S0EMF909**

Sample ID: **S140724088**

[Rev: 2014-07-28 10:58:24]

Element	Concentration [ppm wt]	Element	Concentration [ppm wt]
Li	< 0.05	Ag	< 0.1
Be	< 0.05	Cd	< 1
B	9.3	In	Binder
C	Matrix	Sn	< 1
F	=< 10	Sb	< 1
Na	6.5	Te	< 0.5
Mg	2.1	I	=< 100 *
Al	4.2	Cs	< 0.05
Si	630	Ba	< 0.05
P	220	La	=< 2 *
S	290	Ce	< 0.5
Cl	18	Pr	< 0.05
K	2.2	Nd	< 0.05
Ca	17	Sm	< 0.05
Sc	< 0.05	Eu	< 0.1
Ti	12	Gd	< 0.05
V	5.1	Tb	< 0.05
Cr	< 1	Dy	< 0.05
Mn	0.11	Ho	< 0.05
Fe	19	Er	< 0.05
Co	< 0.05	Tm	< 0.05
Ni	4.8	Yb	< 0.05
Cu	0.43	Lu	< 0.05
Zn	2.5	Hf	< 0.05
Ga	< 0.5	Ta	< 100
Ge	< 1	W	9.1
As	0.76	Re	< 0.05
Se	< 0.5	Os	< 0.05
Br	< 0.5	Ir	< 0.05
Rb	< 0.1	Pt	< 0.1
Sr	< 0.1	Au	< 0.5
Y	0.20	Hg	< 0.5
Zr	1.1	Tl	< 0.05
Nb	< 0.5	Pb	< 0.05
Mo	5.8	Bi	< 0.05
Ru	< 0.5	Th	< 0.05
Rh	< 0.1	U	< 0.05
Pd	< 0.5		

*Mass interference associated with Indium (binder) and Carbon



Page 1 of 1 - GDMS
Analyzed according to WI F rev. 12/06/12
Reviewed by _____

J.SCHIEBLER (Analyst)

Joseph Schiebeler

Precision and bias typical of GDMS measurements are discussed under ASTM F1593.
This shall not be reproduced except in full without written approval of the laboratory.



GDMS
ANALYTICAL REPORT

Evans Analytical Group
103 Commerce Blvd
Liverpool, New York 13088

Telephone (315) 431-9900
Fax: (315) 431-9800
Email info.ny@eaglabs.com
www.eaglabs.com

Customer: Carlisle Brake and Friction
29001 Solon Rd., Solon, OH 44139 USA
Date: 28-Jul-2014
Customer ID: C/C Composite
CTP-446-12K 12K-HD

P.O.# CG000650
Job # S0EMF909
Sample ID: S140724089

[Rev: 2014-07-28 10:56:37]

Element	Concentration [ppm wt]	Element	Concentration [ppm wt]
Li	< 0.05	Ag	< 0.1
Be	< 0.05	Cd	< 1
B	1.5	In	Binder
C	Matrix	Sn	< 1
F	=< 10	Sb	< 1
Na	1.9	Te	< 0.5
Mg	1.3	I	=< 50 *
Al	0.43	Cs	< 0.05
Si	530	Ba	< 0.05
P	81	La	=< 1 *
S	47	Ce	< 0.5
Cl	17	Pr	< 0.05
K	0.71	Nd	< 0.05
Ca	4.3	Sm	< 0.05
Sc	< 0.05	Eu	< 0.1
Ti	0.15	Gd	< 0.05
V	0.18	Tb	< 0.05
Cr	55	Dy	< 0.05
Mn	2.1	Ho	< 0.05
Fe	210	Er	< 0.05
Co	0.87	Tm	< 0.05
Ni	32	Yb	< 0.05
Cu	340	Lu	< 0.05
Zn	200	Hf	< 0.05
Ga	< 0.5	Ta	< 100
Ge	< 1	W	8.2
As	0.64	Re	< 0.05
Se	< 0.5	Os	< 0.05
Br	< 0.5	Ir	< 0.05
Rb	< 0.1	Pt	< 0.1
Sr	< 0.1	Au	< 0.5
Y	< 0.05	Hg	< 0.5
Zr	< 0.05	Tl	< 0.05
Nb	< 0.5	Pb	< 0.05
Mo	0.18	Bi	< 0.05
Ru	< 0.5	Th	< 0.05
Rh	=< 1 **	U	< 0.05
Pd	=< 2 **		

*Mass interference associated with Indium (binder) and Carbon

**Mass interference associated with Argon and high levels of Cu and Zn



Page 1 of 1 - GDMS
Analyzed according to WI F rev. 12/06/12
Reviewed by _____

J.SCHIEBLER (Analyst)

Joseph Schiebeler

Precision and bias typical of GDMS measurements are discussed under ASTM F1593.
This shall not be reproduced except in full without written approval of the laboratory.



GDMS
ANALYTICAL REPORT

SHIVA Technologies
An Operating Unit of Evans Analytical Group LLC
6707 Brooklawn Parkway
Syracuse, New York 13211

Telephone (315) 431-9900
Fax: (315) 431-9800
Email: info.eag@eaglabs.com
www.eaglabs.com

Customer: **Idaho National Laboratory**
1765 N. Yellowstone Hwy., Idaho Falls, ID 83415-3779
Date: 23-Nov-2010
Customer ID: **Graphite**
IG-110 Lot 08-9-052

P.O.#
Job # S0ABZ738
Sample ID: S101119114

QA# A6C-11-001

Element	Concentration [ppm wt]	Element	Concentration [ppm wt]
Li	< 0.05	Pd	< 0.05
Be	< 0.05	Ag	< 0.05
B	< 0.05	Cd	< 0.05
C	Matrix	In	< 0.05
N	-	Sn	< 0.05
O	-	Sb	< 0.05
F	< 0.1	Te	< 0.05
Na	< 0.05	I	< 0.01
Mg	< 0.05	Cs	< 0.05
Al	< 0.05	Ba	< 0.05
Si	1.2	La	< 0.05
P	< 0.1	Ce	< 0.05
S	8.5	Pr	< 0.05
Cl	0.09	Nd	< 0.05
K	< 0.1	Sm	< 0.01
Ca	< 0.05	Eu	< 0.01
Sc	< 0.01	Gd	< 0.01
Ti	< 0.01	Tb	< 0.01
V	< 0.01	Dy	< 0.01
Cr	< 0.5	Ho	< 0.01
Mn	< 0.01	Er	< 0.01
Fe	< 0.01	Tm	< 0.01
Co	< 0.01	Yb	< 0.01
Ni	0.14	Lu	< 0.01
Cu	< 0.05	Hf	< 0.01
Zn	< 0.05	Ta	< 100
Ga	< 0.01	W	< 0.05
Ge	< 0.05	Re	< 0.01
As	< 0.05	Os	< 0.01
Se	< 0.05	Ir	< 0.01
Br	< 0.1	Pt	< 0.01
Rb	< 0.05	Au	< 0.1
Sr	< 0.05	Hg	< 0.1
Y	< 0.05	Tl	< 0.05
Zr	< 0.05	Pb	< 0.05
Nb	< 0.05	Bi	< 0.05
Mo	< 0.05	Th	< 0.05
Ru	< 0.05	U	< 0.05
Rh	< 0.01		

N. BOYEA (Analyst)

Nicholas Boyea

Page 1 of 1 - GDMS

Reviewed by _____

This report shall not be reproduced except in full without written approval of the laboratory. The recording of false, fictitious, or fraudulent statements or entries on the document may be punished as a felony under federal law.

Evans Analytical Group/Shiva

P.O. # 3400075184

Job # UP4897

QA# AGC-09-004

Customer ID	Graphite IG-430
Shiva ID	U060802020

Element	Concentration ppm wt	Element	Concentration ppm wt
Li	< 0.01	Aq	< 0.1
Be	< 0.01	Cd	< 0.1
B	0.08	In	< 0.1
c	Matrix	Sn	< 0.5
N	-	Sb	< 0.5
O	-	Te	< 0.1
F	< 1	I	< 0.1
Na	< 0.05	Cs	< 0.1
Mg	< 0.5	Ba	< 0.1
Al	< 0.05	La	< 0.5
Si	1.9	Ce	< 0.05
p	< 0.1	Pr	< 0.05
s	0.25	Nd	< 0.05
Cl	0.22	Sm	< 0.05
K	< 0.1	Eu	< 0.05
Ca	< 0.05	Gd	< 0.05
Sc	< 0.05	Tb	< 0.05
Ti	< 0.01	Dy	< 0.05
v	< 0.01	Ho	< 0.05
Cr	< 0.5	Er	< 0.05
Mn	< 0.05	Tm	< 0.05
Fe	< 0.01	Yb	< 0.05
Co	< 0.05	Lu	< 0.05
Ni	< 0.1	Hf	< 0.05
Cu	< 0.1	Ta	< 5
Zn	< 0.1	w	0.35
Ga	< 0.1	Re	< 0.05
Ge	< 0.1	Os	< 0.05
As	< 0.1	Ir	< 0.05
Se	< 0.1	Pt	< 0.05
Br	< 0.1	Au	< 0.1
Rb	< 0.05	Hg	< 0.5
Sr	< 0.05	Tl	< 0.1
Y	< 0.05	Pb	< 0.5
Zr	< 0.05	Bi	< 0.1
Nb	< 0.1	Th	< 0.05
Mo	< 0.05	u	< 0.05
Ru	< 0.1		
Rh	< 0.1		
Pd	< 0.1		

Note: analyzed by GDMS except as noted by ""**"

* analyzed by ICP-OES



GDMS
ANALYTICAL REPORT

Evans Analytical Group
103 Commerce Blvd
Liverpool, New York 13088

Telephone (315) 431-9900
Fax: (315) 431-9800
Email info.ny@eaglabs.com
www.eaglabs.com

Customer: Idaho National Laboratory
1765 N. Yellowstone Hwy, Idaho Falls, ID 83415
Date: 4-Nov-2014
Customer ID: Graphite
KAERI #14

P.O.# CC
Job # S0END717
Sample ID: S141031049

[Rev: 2014-11-04 07:46:30]

Element	Concentration [ppm wt]	Element	Concentration [ppm wt]
Li	< 0.05	Pd	< 0.05
Be	< 0.05	Ag	< 0.05
B	5.4	Cd	< 0.5
C	Matrix	In	Binder
N	-	Sn	< 0.1
O	-	Sb	< 0.1
F	=< 20	Te	< 0.05
Na	0.67	I	=< 30
Mg	0.71	Cs	< 0.05
Al	4.3	Ba	0.57
Si	800	La	=< 1
P	0.49	Ce	0.65
S	7.5	Pr	< 0.1
Cl	0.94	Nd	0.17
K	1.4	Sm	< 0.05
Ca	28	Eu	< 0.05
Sc	< 0.01	Gd	0.16
Ti	5.3	Tb	< 0.05
V	120	Dy	0.18
Cr	< 0.5	Ho	< 0.05
Mn	0.35	Er	< 0.05
Fe	32	Tm	< 0.05
Co	0.35	Yb	< 0.05
Ni	18	Lu	< 0.05
Cu	0.10	Hf	< 0.05
Zn	0.09	Ta	< 100
Ga	< 0.01	W	1.3
Ge	< 0.05	Re	< 0.05
As	< 0.05	Os	< 0.05
Se	< 0.05	Ir	< 0.05
Br	< 0.1	Pt	< 0.1
Rb	< 0.05	Au	< 0.5
Sr	0.19	Hg	< 0.1
Y	0.54	Tl	< 0.05
Zr	1.7	Pb	< 0.05
Nb	< 0.05	Bi	< 0.05
Mo	2.2	Th	< 0.05
Ru	< 0.05	U	< 0.05
Rh	< 0.01		

ISO 17025



Testing Cert. #2797.03

Page 1 of 1 - GDMS
Analyzed according to WLF rev. 12/06/12
Reviewed by _____

J. SCHIEBLER (Analyst)

Joseph Schiebler

Precision and bias typical of GDMS measurements are discussed under ASTM F1593.
This shall not be reproduced except in full without written approval of the laboratory.



Customer: **Idaho National Laboratory**
1765 N. Yellowstone Hwy, Idaho Falls, ID 83415
Date: 24-Feb-2016
Customer ID: **Graphite**
AW5201 QA-AGC-11-004

P.O.# **PC 5211613**
Job # **S0GTE622**
Sample ID: **S160218106**

[Rev: 2016-02-24 14:41:46]

Element	Concentration [ppm wt]	Element	Concentration [ppm wt]
Li	0.21	Pd	< 0.05
Be	< 0.05	Ag	< 0.05
B	0.97	Cd	< 0.05
C	Matrix	In	< 0.05
N	-	Sn	< 0.05
O	-	Sb	< 0.05
F	< 0.1	Te	< 0.05
Na	< 0.05	I	< 0.01
Mg	< 0.05	Cs	< 0.05
Al	< 0.05	Ba	0.12
Si	120	La	< 0.05
P	1.4	Ce	< 0.05
S	39	Pr	< 0.05
Cl	0.33	Nd	< 0.05
K	< 0.1	Sm	< 0.01
Ca	9.2	Eu	< 0.01
Sc	< 0.01	Gd	< 0.01
Ti	20	Tb	< 0.01
V	4.3	Dy	< 0.01
Cr	0.93	Ho	< 0.01
Mn	< 0.01	Er	< 0.01
Fe	14	Tm	< 0.01
Co	0.14	Yb	< 0.01
Ni	2.3	Lu	< 0.01
Cu	< 0.05	Hf	< 0.01
Zn	< 0.05	Ta	< 100
Ga	< 0.01	W	< 0.05
Ge	< 0.05	Re	< 0.01
As	< 0.05	Os	< 0.01
Se	< 0.05	Ir	< 0.01
Br	< 0.1	Pt	< 0.01
Rb	< 0.05	Au	< 0.1
Sr	0.15	Hg	< 0.1
Y	< 0.05	Tl	< 0.05
Zr	1.1	Pb	< 0.05
Nb	0.08	Bi	< 0.05
Mo	0.19	Th	< 0.05
Ru	< 0.05	U	< 0.05
Rh	< 0.01		



Page 1 of 1 - GDMS
Analyzed according to WI F rev. 12/06/12
Reviewed by _____

J.SCHIEBLER (Analyst)

Precision and bias typical of GDMS measurements are discussed under ASTM F1593.
This shall not be reproduced except in full without written approval of the laboratory.



GDMS
ANALYTICAL REPORT

Evans Analytical Group
6707 Brookdown Parkway
Syracuse, New York 13211

Telephone (315) 431-9800
Fax (315) 431-9800
Email info.my@eaglabs.com
www.eaglabs.com

Customer: **Idaho National Laboratory**
1765 N. Yellowstone Hwy., Idaho Falls, ID 83415-3779
Date: 17-Jan-2011
Customer ID: **Graphite**
NBG 18 QA#150280

P.O.#
Job # S0BCG688
Sample ID: S110113091

Element	Concentration [ppm wt]	Element	Concentration [ppm wt]
Li	< 0.05	Pd	< 0.05
Be	< 0.05	Ag	< 0.05
B	0.49	Cd	< 0.05
C	Matrix	In	< 0.05
N	-	Sn	< 0.05
O	-	Sb	< 0.05
F	< 0.1	Te	< 0.05
Na	< 0.05	I	< 0.01
Mg	< 0.05	Cs	< 0.05
Al	< 0.05	Ba	< 0.05
Si	75	La	< 0.05
P	0.65	Ce	< 0.05
S	6.9	Pr	< 0.05
Cl	0.21	Nd	< 0.05
K	0.12	Sm	< 0.01
Ca	0.16	Eu	< 0.01
Sc	< 0.01	Gd	< 0.01
Ti	1.4	Tb	< 0.01
V	0.34	Dy	< 0.01
Cr	< 0.5	Ho	< 0.01
Mn	< 0.01	Er	< 0.01
Fe	2.8	Tm	< 0.01
Co	< 0.01	Yb	< 0.01
Ni	0.91	Lu	< 0.01
Cu	< 0.05	Hf	< 0.01
Zn	< 0.05	Ta	< 100
Ga	< 0.01	W	0.06
Ge	< 0.05	Re	< 0.01
As	< 0.05	Os	< 0.01
Se	< 0.05	Ir	< 0.01
Br	< 0.1	Pt	< 0.01
Rb	< 0.05	Au	< 0.1
Sr	< 0.05	Hg	< 0.1
Y	< 0.05	Tl	< 0.05
Zr	< 0.05	Pb	< 0.05
Nb	< 0.05	Bi	< 0.05
Mo	< 0.05	Th	< 0.05
Ru	< 0.05	U	< 0.05
Rh	< 0.01		

J. SCHIEBLER (Analyst)

Accreditations: ISO/IEC 17025, Nadcap

Page 1 of 1 - GDMS

Reviewed by _____

This report shall not be reproduced except in full without written approval of the laboratory. The recording of false, fictitious, or fraudulent statements or entries on the document may be punished as a felony under federal law.

Evans Analytical Group/Shiva

P.O. # 3400075184

Job # UP4897

QA# AGC-09-011

Customer ID	Graphite
Shiva ID	NBG-25 U060802025

Element	Concentration ppm wt	Element	Concentration ppm wt
Li	< 0.01	Ag	< 0.1
Be	< 0.01	Cd	< 0.1
B	0.01	In	< 0.1
c	Matrix	Sn	< 0.5
N	-	Sb	< 0.5
O	-	Te	< 0.1
F	< 1	I	< 0.1
Na	< 0.05	Cs	< 0.1
Mq	< 0.5	Ba	< 0.1
Al	< 0.05	La	< 0.5
Si	2.5	Ce	< 0.05
P	< 0.1	Pr	< 0.05
s	1.6	Nd	< 0.05
Cl	11	Sm	< 0.05
K	< 0.1	Eu	< 0.05
Ca	< 0.05	Gd	< 0.05
Sc	< 0.05	Tb	< 0.05
Ti	0.02	Dy	< 0.05
v	< 0.01	Ho	< 0.05
Cr	< 0.5	Er	< 0.05
Mn	< 0.05	Tm	< 0.05
Fe	< 0.01	Yb	< 0.05
Co	< 0.05	Lu	< 0.05
Ni	< 0.1	Hf	< 0.05
Cu	< 0.1	Ta	< 5
Zn	< 0.1	w	< 0.05
Ga	< 0.1	Re	< 0.05
Ge	< 0.1	Os	< 0.05
As	< 0.1	Ir	< 0.05
Se	< 0.1	Pt	< 0.05
Br	< 0.1	Au	< 0.1
Rb	< 0.05	Hq	< 0.5
Sr	< 0.05	TI	< 0.1
Y	< 0.05	Pb	< 0.5
Zr	< 0.05	Bi	< 0.1
Nb	< 0.1	Th	< 0.05
Mo	< 0.05	u	< 0.05
Ru	< 0.1		
Rh	< 0.1		
Pd	< 0.1		

Note: analyzed by GDMS except as noted by ***

* analyzed by ICP-OE



GDMS
ANALYTICAL REPORT

Evans Analytical Group
103 Commerce Blvd
Liverpool, New York 13088

Telephone (315) 431-9900
Fax: (315) 431-9800
Email info.ny@eag.com
www.eag.com

Customer: **Idaho National Laboratory**
1765 N. Yellowstone Hwy, Idaho Falls, ID 83415
Date: 24-Feb-2016
Customer ID: **Graphite**
DA4404 QA153718

P.O.# **PC 5211613**
Job # **S0GTE622**
Sample ID: **S160218107**

[Rev: 2016-02-24 14:41:51]

Element	Concentration [ppm wt]	Element	Concentration [ppm wt]
Li	< 0.05	Pd	< 0.05
Be	< 0.05	Ag	< 0.05
B	2.8	Cd	< 0.05
C	Matrix	In	< 0.05
N	-	Sn	< 0.05
O	-	Sb	< 0.05
F	< 0.1	Te	< 0.05
Na	< 0.05	I	< 0.01
Mg	< 0.05	Cs	< 0.05
Al	< 0.05	Ba	< 0.05
Si	3.1	La	< 0.05
P	0.30	Ce	< 0.05
S	0.72	Pr	< 0.05
Cl	0.50	Nd	< 0.05
K	< 0.1	Sm	< 0.01
Ca	< 0.05	Eu	< 0.01
Sc	< 0.01	Gd	< 0.01
Ti	0.05	Tb	< 0.01
V	8.1	Dy	< 0.01
Cr	< 0.5	Ho	< 0.01
Mn	< 0.01	Er	< 0.01
Fe	< 0.01	Tm	< 0.01
Co	< 0.01	Yb	< 0.01
Ni	0.31	Lu	< 0.01
Cu	< 0.05	Hf	< 0.01
Zn	< 0.05	Ta	< 100
Ga	< 0.01	W	< 0.05
Ge	< 0.05	Re	< 0.01
As	< 0.05	Os	< 0.01
Se	< 0.05	Ir	< 0.01
Br	< 0.1	Pt	< 0.01
Rb	< 0.05	Au	< 0.1
Sr	< 0.05	Hg	< 0.1
Y	< 0.05	Tl	< 0.05
Zr	< 0.05	Pb	< 0.05
Nb	< 0.05	Bi	< 0.05
Mo	2.4	Th	< 0.05
Ru	< 0.05	U	< 0.05
Rh	< 0.01		



Page 1 of 1 - GDMS
Analyzed according to WI F rev. 12/06/12
Reviewed by _____

J. SCHIEBLER (Analyst)

Precision and bias typical of GDMS measurements are discussed under ASTM F1593.
This shall not be reproduced except in full without written approval of the laboratory.